



Groundwater Flow Model of Corrective Action Units 101 and 102: Central and Western Pahute Mesa, Nevada Test Site, Nye County, Nevada



Revision No.: 0

June 2006

Prepared for U.S. Department of Energy under Contract No. DE-AC52-03NA99205.

Approved for public release; further dissemination unlimited.

Uncontrolled When Printed

In this report, thermal conductivities for individual volcanic HSUs were estimated by considering the percentages of different rock types that are typically present in the HSU, as indicated by borehole stratigraphic logs. First, arithmetic averages of thermal conductivity were calculated for different rock types (e.g., welded devitrified tuff, lava, nonwelded zeolitic tuff) using data reported for those rock types (Gillespie, 2003; Sass and Lachenbruch, 1982; Sass et al., 1987) (see [Attachment A, Table B1](#)). Second, the borehole stratigraphic logs were examined and the thickness-weighted harmonic means of thermal conductivity were calculated for each HSU in individual boreholes using the saturated thickness of different rock types present in the HSU at that borehole (see [Attachment A, Table B2](#)). Lastly, the harmonic mean thermal conductivities for an HSU at individual boreholes were arithmetically averaged to produce the final estimate of the thermal conductivity for the HSU ([Attachment A, Table B3](#)). In general, these last estimates constitute the base-case thermal conductivity value for different HSUs used in this report. However, in some cases, other factors were also considered, as described in the following sections.

C.5.4.1 Extra-Caldera Volcanic Rocks

The thermal conductivities compiled by Gillespie et al. (2003) were based on measurements of extra-caldera volcanic rocks near Yucca Mountain, and are assumed to be representative of thermal conductivity values for similar rock types within the extra-caldera HSUs of the PM/OV flow domain. The methodology for estimating the thermal conductivity of individual HSUs was outlined previously in [Section C.5.4](#).

C.5.4.2 Intra-Caldera Volcanic Rocks

The intra-caldera HSUs in the PM/OV model domain are by definition within the structural margins of calderas and include the PBRCM, BRA, BFCU, and TMCM HSUs (BN, 2002). These HSUs contain lavas, welded tuffs, bedded and nonwelded tuffs, debris flows and dikes (Byers et al., 1976; Sawyer et al., 1994). The thermal conductivities compiled by Gillespie et al. (2003) were based on measurements of extra-caldera volcanic rocks near Yucca Mountain, which may be less indurated and hence have lower thermal conductivities than rocks found within the calderas of the PM/OV model. This hypothesis is supported by laboratory data from Morgan et al. (1996) that indicate the thermal conductivities of indurated intra-caldera volcanic rocks in the Jemez Mountains, New Mexico, are typically 1.7 to 2.9 times higher than the thermal conductivities of their extra-caldera counterparts.

Based on these data, it is assumed that the constituent rock types of intra-caldera HSUs within the PM/OV domain have thermal conductivities that are 1.7 times higher than the values reported by Gillespie (2003) for their extra-caldera analogs ([Attachment A, Tables B1 and B2](#)).

C.5.5 Alluvium

Thermal conductivity measurements for alluvium (AA) in the NTS area were not available in the literature. However, because of its high porosity at Yucca Mountain, the nonwelded and bedded Calico Hills Formation (CHZCM) was considered suitable as an analog for alluvium. Thermal conductivity measurements reported in Sass et al. (1987) from Yucca Mountain indicate that the Calico Hills Formation has thermal conductivities that range from 0.8 to 1.3 W/m•°K at ambient saturations above the water table, and from 1.1 to 1.6 W/m•°K in the saturated zone. An average unsaturated-zone thermal conductivity of 1.2 W/m•°K is reported for these tuffs at Yucca Mountain (Bodvarsson et al., 2003). The thermal conductivity of all types of tuff at Yucca Mountain increases by an average factor of 1.2 as the tuffs go from unsaturated to saturated conditions ([Attachment A, Table B3](#)). Based on these values, the base-case saturated thermal conductivity of alluvium derived from rocks like the Calico Hills Formation is estimated to be 1.44 W/m•°K with a lower bound of 1.2 W/m•°K. For comparison, an average saturated thermal conductivity of 1.5 W/m•°K was reported for Basin and Range tuffaceous alluvium (Wollenberg et al., 1983) and Olmsted and Rush (1987) reported that the saturated thermal conductivity of tuffaceous alluvium at a site in northern Nevada varies between 1.33 to 1.83 W/m•°K based on laboratory measurements of clay-, sand-, and gravel-sized alluvium.

The thermal conductivity of alluvium in the PM/OV heat conduction model was initially allowed to vary in the inverse model calibration, but was later fixed at 1.44 W/m•°K after determining that simulated temperatures at the observation points were insensitive to this parameter. Temperatures were probably insensitive to the assumed thermal conductivity of the alluvium because of its relatively small volume in the model and proximity of the alluvium to the upper boundary where temperatures were held constant.

C.5.6 Summary of Thermal Conductivity Estimates

The range in thermal conductivity estimates for HSUs in the PM/OV flow domain and sources for these estimates are summarized in [Table C.5-1](#). These estimates are based primarily on a thermal conductivity data measured on extra-caldera tuffs and lavas at Yucca Mountain (Sass et al., 1982; 1987), supplemented by measurements made elsewhere in the vicinity of the NTS (Sass et al., 1980; Sass et al., 1995) and values for analogous rocks reported in the literature (Morgan, 1996; Gillespie, 2003).

In the vicinity of the NTS, the thermal conductivities of volcanic rocks in the NTS depend on the degree of welding and alteration of the rock. Because volcanic HSUs in the PM/OV flow domain often contain multiple rock types, a methodology was developed to estimate representative thermal conductivities that considered variability in rock types within an HSU. In this methodology, the thickness-weighted harmonic mean thermal conductivities of different rock types in the HSU at individual boreholes were first calculated. These harmonic means were then averaged arithmetically across the multiple boreholes to estimate a representative thermal conductivity for the HSU that could be used throughout the model domain.

Other adjustments to the measured thermal conductivity values were made to provide estimates for HSUs in which measurements are lacking. To compensate for the lack of thermal conductivity measurements on intra-caldera tuffs, this study relies on observations from other sites (Morgan, 1996) which indicate that intra-caldera tuffs have thermal conductivities at least 1.7 times those of their extra-caldera analogs because of their greater alteration and induration. For alluvium, saturated thermal conductivity was estimated by analogy with porous bedded and nonwelded tuffs in the unsaturated zone at Yucca Mountain and by noting typical increases in thermal conductivity that accompany the transition from unsaturated to saturated conditions.

Although anisotropy in thermal conductivity was not explicitly analyzed as part of this study, its affect on heat transport may be less important than anisotropy of permeability is to groundwater flow (Phillips, 1991, p. 34). For this reason, together with the absence of anisotropic measurements, thermal conductivities were assumed isotropic in simulations.

C.6.0 BOUNDARY CONDITION ESTIMATES

C.6.1 Upper Boundary Condition

The upper boundary of the model coincides with the potentiometric surface, which in this report is taken to be synonymous with the water table. Constant, but spatially variable temperatures were estimated at the water table using borehole measurements of shallow groundwater temperature. These temperatures were kriged onto a uniform grid with 100 x 100 m cells using a linear variogram to approximate the covariance structure (Figure C.6-1). The kriged temperatures were then mapped onto the top nodes of the PM/OV CAU model grid using a nearest neighbor approach. By using measured temperatures to estimate temperatures along the upper boundary of the heat conduction model, the effects of unsaturated-zone hydrologic processes and variable unsaturated-zone thickness on water-table temperatures are implicitly taken into account.

In developing the dataset used to construct the map of water table temperatures, temperatures measured near the water table were evaluated against deeper temperature data and other nearby water table temperature measurements to determine their reliability as indicators of water table temperature. For example, the water table temperature for well UE-20e#1 measured on 6/2/1964 (immediately after drilling) was discarded due to possible upwelling in the borehole (Attachment A, Figure C6) and because it was anomalously warm temperatures relative to other wells in the area (Table C.6-1). By similar reasoning, the water table temperature at well U-19t measured on 9/27/1993 was included because a deeper, linear segment of the temperature profile at this well projected upward to this temperature, whereas a temperature measured on 6/7/1978 was discarded because it was anomalously cool for the area. An average of unpublished USGS temperatures measured 5 ft below the water table in various boreholes between the years 2000 and 2002 were used where available (Table C.6-1). Between the Handley Fault and the Purse Fault, the water table temperature from well U-20m was chosen as representative of this area because the water table temperature at nearby well UE-20j varied over time (Table C.6-1).

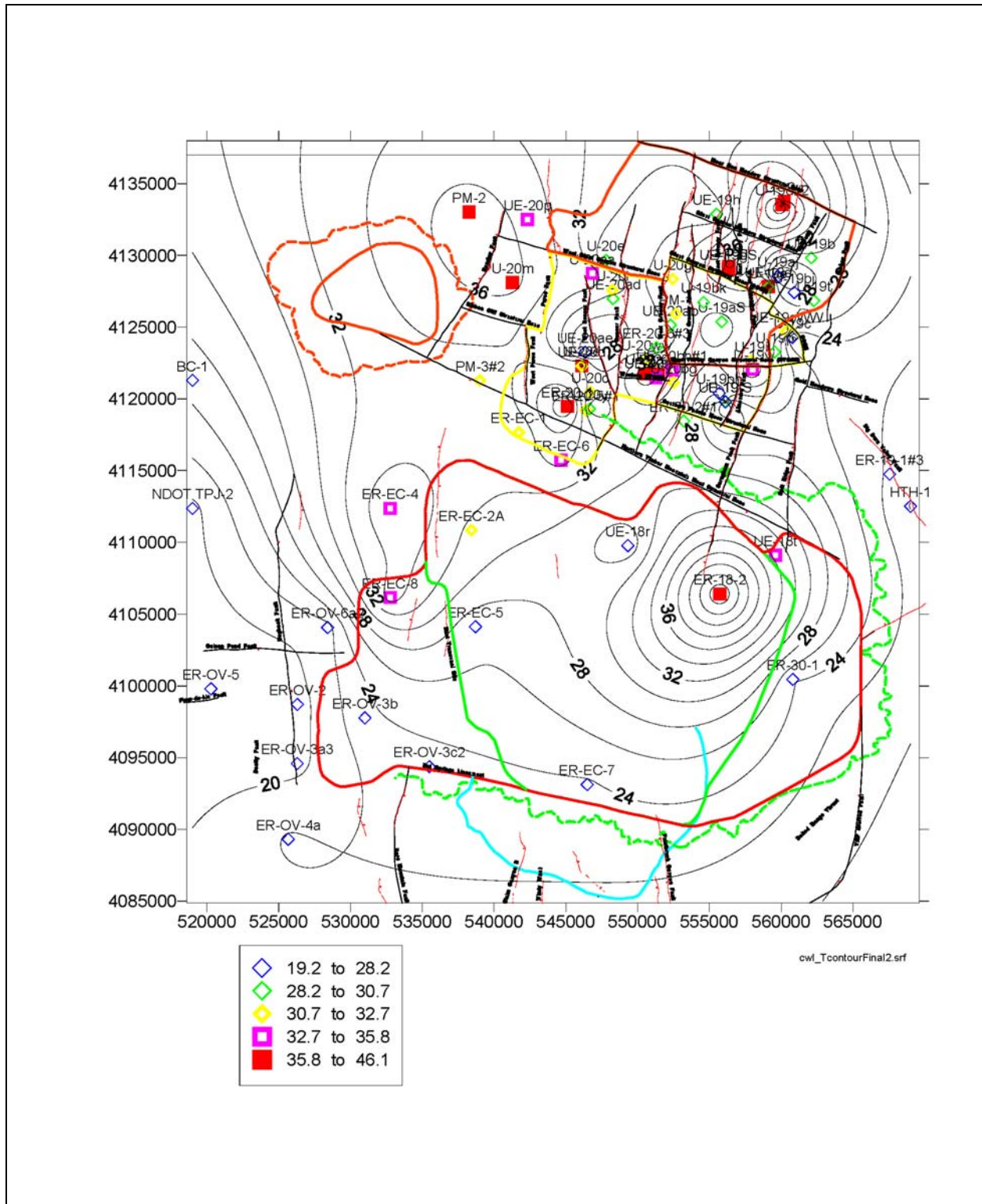


Figure C.6-1
Contour Map of Water Table Temperatures (°C) Used as Upper Boundary Conditions
 See [Table C.6-1](#).

Table C.6-1**Depth and Elevation Range, Hydrostratigraphic Unit, and Temperature of Borehole Composite Water Levels**

Depth, Temperature, and Elevation of Composite Water Levels are Shown in Bold

(Page 1 of 5)

Eastings	Northing	Composite Water Level Temperature (°C)	Standard Deviation (°C)	Borehole	Composite Water Level ^a Depth (m)	Standard Deviation (m)	Lower Depth (m)	Composite Water Level Elevation (m)	Lower Elevation (m)	Stratigraphic ^b	Class/Rock Type ^b	HGU ^b	HSU ^b	Temperature Log (Date)
Purse Fault-W. Boxcar Fault (1)														
545113.1	4119468	39.9	0.2	ER-20-1	606.2	0.0	623.0	1,277.8	1,261.0	Tpcm	MWT	WTA	TCA	2000-2002
546385.9	4119208	32.7		ER-20-5#1	626.4			1,276.1		Tp	BED	TCU	LPCU	11/3/1995
546698.7	4120478	31.2		U-20c	643.1			1,271.3		Tpcm	tuf	unk	TCA	4/5/1965
546102.6	4122301	35.8		U-20d	634.0			1,271.6		Tpb	LA	LFA	BA	1/31/1967
546651.3	4119291	28.8		U-20y	630.9			1,276.2		Tp	BED	TCU	LPCU	1/2/1975
546339.7	4123244	23.9		UE-20ae	609.6			1,276.8		unk	BED	unk	PVTA/TCVA	7/19/1978
546102.7	4122275	32.0		UE-20d	624.8			1,281.4		Tpb	LA	LFA	BA	7/28/1964
W. Boxcar Fault-Boxcar Fault (2)														
546837.4	4128745	33.3		U-20aa	570.0			1,361.5		Thp	FB	LFA	CHZCM	8/18/1975
547789.2	4129655	28.2		U-20e	566.9			1,358.2		Thp	LA	LFA	CHZCM	12/20/1968
548242.9	4127581	31.2		U-20i	582.2			1,359.4		Thp	PL	unk	CHZCM	10/20/1967
548286.2	4126975	28.9		UE-20ad	582.2			1,358.2		Thp	LA	LFA	CHZCM	8/4/1978
Boxcar Fault-W. Greeley Fault (3)														
551362.9	4123692	29.1		ER-20-6#1 ^c	618.4		633.7	1,355.1	1,339.8	Tpd	BED	TCU	UPCU	2002
551328	4123662	28.7		ER-20-6#2 ^d	618.6		633.9	1,355.0	1,339.7	Tpd	BED	TCU	UPCU	2002
551295.7	4123579	28.2		ER-20-6#3 ^e	615.9		631.1	1,354.9	1,339.7	Thp	LA	LFA	CHZCM	2002
550480.6	4121740	35.9		U-20a	563.9			1,423.4		Thp	LA	LFA	CHZCM	4/29/1964
551424.4	4121743	36.3		U-20n	634.0			1,340.2		Thp	LA	LFA	CHZCM	8/25/1968
550614	4122712	31.5	0.2	U-20ww	626.2	0.4	643.0	1,345.3	1,328.5	Thp	LA	LFA	CHZCM	2000-2002
551273.2	4121484	33.9	0.1	UE-20n#1	622.2	0.1	637.5	1,347.1	1,331.8	Thp	LA	LFA	CHZCM	2000-2002
S of Silent Canyon Caldera Structural Margin-N of Timber Mountain Caldera Topographic Margin (4)														
541729.8	4117660	32.3		ER-EC-1	565.6		580.9	1,271.1	1,255.9	Tmrf	NWT	TCU	FCCU	2000-2002
544673.5	4115729	34.6		ER-EC-6	434.6		449.8	1,273.5	1,258.3	Tmrf	BED	TCU	FCCU	2000-2002

Table C.6-1
Depth and Elevation Range, Hydrostratigraphic Unit, and Temperature of Borehole Composite Water Levels
Depth, Temperature, and Elevation of Composite Water Levels are Shown in Bold
 (Page 2 of 5)

Eastings	Northing	Composite Water Level Temperature (°C)	Standard Deviation (°C)	Borehole	Composite Water Level ^a Depth (m)	Standard Deviation (m)	Lower Depth (m)	Composite Water Level Elevation (m)	Lower Elevation (m)	Stratigraphic ^b	Class/Rock Type ^b	HGU ^b	HSU ^b	Temperature Log (Date)
Handley Fault-Purse Fault (5)														
539011.8	4121281	32.3	0.2	PM-3#1	444.2	0.02	461.0	1,330.6	1,313.9		NWT	TCU	UPCU	2000-2002
539011.8	4121281	32.7	0.1	PM-3#2	443.6	0.02	458.9	1,331.2	1,316.0		NWT	TCU	UPCU	2000-2002
541289.6	4128104	36.6		U-20m	381.0			1,418.2		Tmrp	DWT	WTA	TMA	10/24/1968
541285.3	4128082	30.8-32.7-37.89 ^c		UE-20j	390.1			1,409.1		Tmrp	MWT	WTA	TMA	9/5/1964 - 10/21/1964
NW of Handley Fault (6)														
538256.7	4133028	36.9	0.2	PM-2	261.7	0.03		1,440.9		Tqu	BED	unk	PBRCM	2000-2002
542331.4	4132503	35.4		UE-20p	277.4			1,415.2		Tmr	MWT	WTA	TMA	2/10/1968
W. Greeley Fault-E. Greeley Fault (7)														
553210.6	4118447	29.5	0.00	ER-20-2#1	692.6	0.1	709.4	1,340.4	1,323.6	Thp	BED	TCU	CHZCM	2000-2002
552668.1	4125925	31.6	0.1	PM-1	639.2	0.2	656.0	1,359.6	1,342.9	Thp	FB	LFA	CHZCM	2000-2002
552511.9	4121139	32.1	0.1	U-20bg	651.5	0.03	666.8	1,350.1	1,334.8	Thp	BED	TCU	CHZCM	2000-2002
552440.2	4128344	31.2		U-20g	615.7			1,356.4		Thp	LA	LFA	CHZCM	10/15/1964
552284.5	4125130	30.1		UE-20ab	652.3			1,353.6		Thp	FB	LFA	CHVCM	6/5/1978
552402.2	4122007	33.6	0.1	UE-20bh#1	674.6	0.1	689.9	1,321.8	1,306.6	Thp	BED	TCU	CHZCM	2000-2002
Silent Canyon Structural Zone-W and E Estuary Faults (8)														
559768.3	4128539	22.8		U-19aj	667.5			1,432.9		Tcblp	TB	TCU	BFCU	12/9/1980
555856.8	4125371	29.0		U-19aS	673.6			1,387.1		Thp	NWT	VTA	CHVTA	10/4/1964
554585.6	4126723	30.7	0.1	U-19bk	604.9	0.03	620.1	1,428.1	1,412.9	unk	unk	unk	unk	2000-2002
559100.9	4127775	30.7	3.4	U-19e	678.2	29.0		1,430.7		Tcblp	NWT	TCU	BFCU	1966-1968
556340.5	4129244	39.0		U-19g	627.9			1,424.6		Tcps	BED	TCU	CFCU	11/19/1965
556975.7	4125473	13.1	1.7	U-19yS	627.9	6.1		1,412.1		Tpr	LA/PL/FB	LFA	PLFA	1978
559100.4	4127836	37.5		UE-19e	698.0			1,410.9		Tcblp	NWT	TCU	BFCU	8/23/1964
556306.1	4129057	36.9	1.6	UE-19gS	695.1	55.0		1,352.9		Tcblp	NWT	TCU	BFCU	1965

Table C.6-1**Depth and Elevation Range, Hydrostratigraphic Unit, and Temperature of Borehole Composite Water Levels**

Depth, Temperature, and Elevation of Composite Water Levels are Shown in Bold

(Page 3 of 5)

Eastings	Northing	Composite Water Level Temperature (°C)	Standard Deviation (°C)	Borehole	Composite Water Level ^a Depth (m)	Standard Deviation (m)	Lower Depth (m)	Composite Water Level Elevation (m)	Lower Elevation (m)	Stratigraphic ^b	Class/Rock Type ^b	HGU ^b	HSU ^b	Temperature Log (Date)
E. Greeley Fault-Almendo Fault (9)														
555683.6	4120389	26.1	0.1	U-19bh	636.7	0.4	651.9	1,426.2	1,411.0	Tpe	NWT	TCU	PLFA	2000-2002
556107.4	4119811	29.4		U-19f	759.3			1,293.3		Thp	BED	TCU	CHCU	7/5/1968
556107.5	4119781	19.8		UE-19fS	731.5			1,321.3		Tpe	NWT	TCU	CHCU	7/28/1965
Halfbeak Fault-Moor Hen Meadow-Silent Canyon Northern Structure Zones (10)														
560056.3	4133535	44.8		U-19d#2	664.5			1,426.8		Tbds	LA	LFA	BRA	6/25/1964
560207.3	4133751	37.8		U-19u	661.4			1,433.5		Tbdb	LA	LFA	BRA	5/6/1969
555488.4	4132882	28.5	0.05	UE-19h	643.4	0.1	658.7	1,423.1	1,407.9	Tbdl	LA	LFA	BRA	2000-2002
Almendo Fault-Scrugham Peak Fault (11)														
557922.1	4122638	31.1		U-19i	728.5			1,355.1		Tcps	NWT	VTA	CFCU	8/24/1967
558003.1	4122055	33.8		U-19v	661.4			1,434.4		Thp	NWT	VTA	CHVTA	5/27/1969
Scrugham Peak Fault-Split Ridge Fault (12)														
559541.6	4123267	29.9		U-19p	670.6			1,432.3		Tcbip	NWT	TCU	BFCU	10/29/1975
Halfbeak Fault-Rickey Fault-Moor Hen Meadow Structure Zone (13)														
560900.4	4127416	26.3	0.1	U-19bj	650.9	0.1	666.1	1,493.4	1,478.1	Tcpk	LA	LFA	KA	2000-2002
560769.4	4124277	21.5	9.4	U-19c	454.2	40.6		1,689.2		Tmt	BS	LFA	PVTA	1965
562271.5	4126843	20.7		U-19t	588.3			1,542.6		Tcbk	FB	LFA	KA	6/7/1978
562271.5	4126843	29.5		U-19t	721.0			1,409.8		Tcbk	FB	LFA	KA	9/27/1993
562088.5	4129826	29.4	2.7	UE-19b	646.2	0.0		1,427.1		Tbdl	LA	LFA	BRA	1964
		34.6		UE-19c	716.3			1,427.4		Tcbr	NWT	TCU	BFCU	5/2/1964
560338.9	4124702	31.2	0.2	UE-19cWW	713.1	0.1	728.4	1,430.5	1,415.3		NWT	TCU	BFCU	2000-2002
Split Ridge Fault-Rainier Mesa/Ammonia Tanks Caldera Topographic Margin (14)														
567541.6	4114743	26.8	0.2	ER-19-1#1 ⁱ	544.1	0.7	559.3	1,327.4	1,312.1	Tor	BED	TCU	PBRCM	2000-2002
567541.6	4114743	22.5	0.2	ER-19-1#27 ^g	359.7	3.6	374.9	1,511.8	1,496.6	Ton2	NWT	TCU	PBRCM	2000-2002
567541.6	4114743	21.7	0.3	ER-19-1#3 ^h	306.7	0.0	321.9	1,564.8	1,549.6	Ton2	BED	TCU	PBRCM	2000-2002
569000.3	4112499	19.9	1.5	HTH-1	165.1	0.1	180.4	1,711.2	1,696.0	Tn	BED	unk	PBRCM	2001-2002

Table C.6-1

Depth and Elevation Range, Hydrostratigraphic Unit, and Temperature of Borehole Composite Water Levels

Depth, Temperature, and Elevation of Composite Water Levels are Shown in Bold

(Page 4 of 5)

Eastings	Northing	Composite Water Level Temperature (°C)	Standard Deviation (°C)	Borehole	Composite Water Level ^a Depth (m)	Standard Deviation (m)	Lower Depth (m)	Composite Water Level Elevation (m)	Lower Elevation (m)	Stratigraphic ^b	Class/Rock Type ^b	HGU ^b	HSU ^b	Temperature Log (Date)
E of Thirst Canyon Lineament-S of Silent Canyon Caldera Structural Margin (15)														
538420.8	4110841	31.5		ER-EC-2A	230.0		245.2	1,264.2	1,248.9	Tfbw	BED	TCU	FCCM	2000-2002
538701.8	4104137	26.5	0.5	ER-EC-5	309.9	0.1	325.2	1,237.5	1,222.3	Tmar	DWT-VT	WTA	TMCM	2000-2002
Ammonia Tanks Caldera Structure Margin-W of Scrugham Peak Fault (16)														
549322	4109762	26.5	0.2	UE-18r	415.8	0.02	431.0	1,272.2	1,257.0	Tma	PWT	WTA	TMCM	2000-2002
Ammonia Tanks Caldera Structural Margin-E of Scrugham Peak Fault (17)														
555724.6	4106389	46.1	0.3	ER-18-2	369.3	0.1	384.6	1,287.9	1,272.6	Tmar	NWT	TCU	TMCM	2000-2002
E of Ammonia Tanks Caldera Structure Margin-Within Rainier Mesa Caldera Structure Margin (18)														
560804.7	4100463	24.2		ER-30-1	137.5			1,279.0		Tfdb	BS	LFA	FCCM	3/22/1994
559591	4109095	33.5	0.2	UE-18t	278.7	0.02		1,306.6		Tfbw	BED	TCU	FCCM	2000-2002
E of Thirst Canyon Lineament-Hogback Fault-Ammonia Tanks Caldera Structure Margin (19)														
532763.8	4106142	34.8	0.1	ER-EC-8	98.3	0.1	113.6	1,222.4	1,207.1	Tfb	BED	TCU	FCCM	2000-2002
W of Thirst Canyon Lineament-SW of Silent Canyon Caldera Structure Margin (20)														
532759.6	4112356	35.7	0.1	ER-EC-4	228.3	0.04	243.5	1,222.6	1,207.3	Ttr	BED	VTA	TCVA	2000-2002
Claim Canyon Caldera Structure Margin (21)														
546483.5	4093127	23.8	0.4	ER-EC-7	228.0	0.1	243.2	1,236.6	1,221.3	Tfbw	LA	LFA	FCCM	2000-2002
Oasis Valley (22)														
528416.7	4104084	21.0	0.3	ER-OV-1(?)	5.5	0.0	20.8	1,235.9	1,220.6	Tf	LA	LFA	FCCM	2000-2002
526310.0	4098716	19.3	0.2	ER-OV-2	8.7	0.02	23.9	1,174.1	1,158.8	Tgs	AL	AA	AA	2000-2002
526298.8	4094587	19.8	0.1	ER-OV-3a	17.5	0.03	32.7	1,154.3	1,139.0	Tf	PWT-MWT	WTA	DVCM	2000-2002
526298.8	4094587	21.3	0.2	ER-OV-3a2	48.7	0.1	64.0	1,122.9	1,107.6	Tf	MWT	WTA	DVCM	2000-2002
526298.8	4094587	19.5	0.1	ER-OV-3a3	17.4	0.03	32.7	1,154.1	1,138.9	Tf	PWT-MWT	WTA	DVCM	2000-2002
531007.6	4097777	23.5	0.2	ER-OV-3b	105.6	0.03	120.8	1,184.5	1,169.3	Tgs	AL	AA	AA	2000-2002
535494.2	4094374	23.3	0.1	ER-OV-3c	65.3	0.02	80.5	1,212.3	1,197.1	Tma	NWT-PWT	VTA	TMA	2000-2002
535494.2	4094374	23.3	0.2	ER-OV-3c2	65.4	0.02	80.6	1,212.3	1,197.1	Tma	NWT-PWT	VTA	TMA	2000-2002
525671.4	4089316	22.2	0.1	ER-OV-4a	7.3	0.1	21.8	1,056.9	1,042.4	Tgs	AL	AA	AA	2000-2002
520280.1	4099809	19.3	0.2	ER-OV-5	9.7	0.01	24.2	1,190.5	1,176.0	Tgs	AL	AA	AA	2000-2002
528416.9	4104085	20.5	0.1	ER-OV-6a	4.9	0.5	19.4	1,236.6	1,222.1	Tf	LA	LFA	FCCM	2000-2002
528416.9	4104085	21.3	0.1	ER-OV-6a2	5.7	0.01	17.9	1,235.6	1,223.4	Tf	LA	LFA	FCCM	2000-2002

Table C.6-1
Depth and Elevation Range, Hydrostratigraphic Unit, and Temperature of Borehole Composite Water Levels
Depth, Temperature, and Elevation of Composite Water Levels are Shown in Bold
 (Page 5 of 5)

Eastings	Northing	Composite Water Level Temperature (°C)	Standard Deviation (°C)	Borehole	Composite Water Level ^a Depth (m)	Standard Deviation (m)	Lower Depth (m)	Composite Water Level Elevation (m)	Lower Elevation (m)	Stratigraphic ^b	Class/Rock Type ^b	HGU ^b	HSU ^b	Temperature Log (Date)
----------	----------	--	-------------------------	----------	--	------------------------	-----------------	-------------------------------------	---------------------	----------------------------	------------------------------	------------------	------------------	------------------------

^a USGS - Temperature collected by USGS in 2000, 2001, and 2002 at 5 ft below composite water level in well.

^b Explanation of abbreviations can be found at the end of [Attachment A](#)

^c Casing perforated and gravel packed over two intervals between depths of 742.8 to 843.4 m and 858 to 898.2 m.

^d Casing perforated and gravel packed over two intervals between depths of 735.8 to 840.3 m and 851.3 to 897.6 m.

^e Casing perforated and gravel packed between 755.9 to 855.6 m depth.

^f Casing set to 1,090.4 m depth; gravel packed and casing perforated 988.5 to 1,008.5 m and 1,051.7 to 1,069.9 m depth.

^g Casing set to 829.1 m depth; gravel packed and casing perforated 785.5 to 834.5 m depth.

^h Casing set to 420.8 m depth; gravel packed and casing perforated 405.7 to 433.4 m depth.

ⁱ Temperature of composite water level increased as warmer water rose in open borehole due to artificial breaching of confining units by borehole.

C.6.2 Lower Boundary Condition

The PM/OV flow domain is located in an area with a long and complex thermal history. Local igneous activity or tectonism has affected the geothermal regime in this area of the NTS since at least the Mesozoic, when granitic plutons were intruded (HSU MGPU). In the Cenozoic, thrust faulting re-arranged the distribution of rocks and probably redirected heat flow through thickened sections of high thermal conductivity rock like the lower carbonate aquifer. These events were followed by the development of the southwestern Nevada volcanic field (SWNVF) and the extrusion of hundreds of cubic kilometers of tuff and related lavas, caldera collapse and resurgence by new infusions of magma, and basin-and-range normal faulting (Sawyer et al., 1994; Grauch et al., 1999; BN, 2002). The residual effect of past igneous and tectonic events on the present-day geothermal regime is uncertain and it is possible that geothermal heat fluxes remain spatially variable to this day. This conclusion is supported by recent work has indicated that the Timber Mountain caldera complex is located within an inherent structural weakness in the upper crust that has a higher than average regional heat flow (Faulds and Varga, 1998, Figure 1).

Due to the great depth of the lower model boundary relative to boreholes in the area, considerable uncertainty exists regarding thermal conditions at the base of the model. Because of this uncertainty and the expected influence of the lower boundary conditions on model results, several different approaches were used to assign thermal conditions along the base of the model. The first approach assumes that heat flux is uniform along the base of the model, and that temperatures are free to vary in response to variations in thermal conductivity and overburden thickness. The second approach assumes that temperatures along the base of the model are uniform, and that heat flux along the base of the model is free to vary in response to the same factors. The third approach subdivides the base of the model into a number of different intra- and extra-caldera areas and allows heat fluxes (and, indirectly, temperatures) to vary between these areas.

C.6.2.1 Specified Heat Flux Lower Boundary Conditions

Sass et al. (1995) reported that deep groundwater flow through the LCA and faults may influence the shallow geothermal regime in the NTS area. Because estimates of heat flow in many boreholes at the NTS may have been influenced by groundwater flow in the LCA, the value of 84 mW/m² measured in the LCCU beneath the LCA at well TW-5 (Rock Valley) was considered by Sass et al. (1995) to be

most representative of deep regional heat fluxes in the NTS area. The use of this relatively high value as representative of the deep regional heat flux is supported by data from other non-Pahute-Mesa wells where shallow heat fluxes are similarly high, such as TW-3 (Frenchman Flat) and TW-4 (Indian Springs Valley) (Sass et al., 1987, Table 7).

Based on these considerations, a uniform heat flux value of 85 mW/m² was initially applied to the base of the PM/OV heat-conduction model. Subsequent analyses used uniform heat fluxes of 45, 65 and 105 mW/m² as lower boundary conditions to investigate the sensitivity of simulated temperatures to the assumed heat fluxes. Additionally, one inverse model allowed heat fluxes at six different intra-caldera and extra-caldera areas to be estimated independently as part of the calibration process.

C.6.2.2 Specified Temperature Lower Boundary Conditions

The elevation of the lower boundary of the PM/OV CAU model domain is 3,500 m below sea level (bsl). Because no boreholes have been drilled deep enough to measure temperatures at this elevation, it is necessary to estimate temperatures at the base of the model by using borehole temperatures measured at shallower depths and extrapolating these temperatures to greater depths using Fourier's Law ($q=kdt/dz$) and assumptions about deeper thermal conductivity values and heat fluxes. These estimates (Table C.6-1) were made in three different structural zones using bottom-hole temperature data from boreholes UE-20f (121°C), PM-2 (83.8°C) and UE-19gs (61.6°C) (Blankennagel and Weir, 1973, Table 8). The calculations assume conductive vertical heat flow and a regional heat flux of 85 mW/m² and rely on structure contour maps for the PBRCM, LCA, and UCCU (BN, 2002), and thermal conductivity estimates for different rock types (summarized in Table C.5-1) to estimate the distribution of thermal conductivity values below the bottoms of these boreholes.

The estimated temperature at the base of the model for the three structural zones is ~172 to 179°C, assuming a range in the temperature gradient for the PBRCM (Table C.6-1). For comparison, the simulated temperatures at the base of the model using a specified heat flux of 85 mW/m² range from 107 to 204°C and average ~162°C (see Section C.7.1) (As described below, specification of a heat flux boundary condition generates spatially variable temperatures at the base of the PM/OV model domain.). For different assumed heat fluxes, temperatures along the lower boundary are, of course, also different.

The estimated temperatures at the base of the model are sensitive to the assumed thermal properties between the depth of the temperature measurement and the base of the model. The deep thermal properties, in turn, depend on the type of rocks interpreted to exist at depth, which can differ among alternative HFMs because of limited information at depth. As an example, BN (2002) reported an alternative structural interpretation (Alternative #6) for the eastern part of the PM/OV domain near borehole ER-19-1. Lower model boundary temperatures were estimated for both the base case and the Alternative #6 structural interpretations using a measured temperature of 31.5°C at ER-19-1, a range of thermal properties for the LCCU1, the UCCU and the LCA, and an assumed a regional heat flux of 85 mW/m². The average temperature estimated at the base of the model at well ER-19-1 is 112°C for the Alternative #6 structural interpretation and 131°C for the base-case structural interpretation (Table C.6-2). This comparison highlights the sensitivity of estimated bottom boundary temperatures to uncertainties in the HFM in this part of the model domain.

Table C.6-2
Temperature Estimates at the Base of the PM/OV Model (3.5 km Below Sea Level)
Assuming Dominantly Conductive 1D Heat Flow and Background Regional Heat Flux of 85 mW/m²
 (Page 1 of 2)

Borehole	Area	Measured or Estimated Temperature ^a (°C)	HSU	Measured or Estimated Gradient Temperature ^b (°C/km)	Estimated Thickness (km)	Estimated Temperature at HSU Base (°C)	Estimated Temperature Increase (°C)	Estimated Elevation at HSU Base (km)	Estimated Heat Flux (Low λ) (mW/m ²)	Estimated Heat Flux (Base λ) (mW/m ²)	Average Estimated Temperature (mW/m ²)	Estimated Temperature Using 3-D FEHM (85 mW/m ²)
UE-20f	W. Boxcar Fault-Purse Fault (1)	121.0	PBRCM	22.2	0.73	137.2	16.2	-2.61	37.96	47.29		
		121.0	PBRCM	38.6	0.73	149.2	28.2	-2.61	66.01	82.22		
		121.0	PBRCM	58.2	0.73	163.5	42.5	-2.61	99.52	123.97		
UE-20f	W. Boxcar Fault-Purse Fault (1)	137.2	SCICU	32.7	0.89	166.3	29.1	-3.50		85.00	179.1	195.9
		149.2	SCICU	32.7	0.89	178.3	29.1	-3.50		85.00		
		163.5	SCICU	32.7	0.89	192.6	29.1	-3.50		85.00		
PM-2	NW of Handley Fault (6)	83.8	PBRCM	38.6	0.87	117.4	33.6	-0.82	66.01	82.22		
		83.8	PBRCM	40.4	0.87	118.9	35.1	-0.82	69.08	86.05		
		83.8	PBRCM	41.8	0.87	120.2	36.4	-0.82	71.48	89.03		
PM-2	NW of Handley Fault (6)	117.4	LCA	17.2	1.20	138.0	20.6	-2.02		85.00		
		118.9	LCA	17.2	1.20	139.6	20.6	-2.02		85.00		
		120.2	LCA	17.2	1.20	140.8	20.6	-2.02		85.00		
PM-2	NW of Handley Fault (6)	138.0	LCCU	21.8	1.48	170.2	32.3	-3.50		85.00	171.7	161.7
		139.6	LCCU	21.8	1.48	171.8	32.3	-3.50		85.00		
		140.8	LCCU	21.8	1.48	173.0	32.3	-3.50		85.00		
UE-19gS	SCStrucZone-W-E Estuary Faults (8)	61.6	PBRCM	22.2	1.26	89.7	28.1	-1.50	37.96	47.29		
		61.6	PBRCM	38.6	1.26	110.4	48.8	-1.50	66.01	82.22		
		61.6	PBRCM	58.2	1.26	135.2	73.6	-1.50	99.52	123.97		
UE-19gS	SCStrucZone-W-E Estuary Faults (8)	89.7	SCICU	32.7	2.00	154.9	65.2	-3.50		85.00	177.0	194.7
		110.4	SCICU	32.7	2.00	175.6	65.2	-3.50		85.00		
		135.2	SCICU	32.7	2.00	200.4	65.2	-3.50		85.00		

Table C.6-2

Temperature Estimates at the Base of the PM/OV Model (3.5 km Below Sea Level)
Assuming Dominantly Conductive 1D Heat Flow and Background Regional Heat Flux of 85 mW/m²
 (Page 2 of 2)

Borehole	Area	Measured or Estimated Temperature ^a (°C)	HSU	Measured or Estimated Gradient Temperature ^b (°C/km)	Estimated Thickness (km)	Estimated Temperature at HSU Base (°C)	Estimated Temperature Increase (°C)	Estimated Elevation at HSU Base (km)	Estimated Heat Flux (Low λ) (mW/m ²)	Estimated Heat Flux (Base λ) (mW/m ²)	Average Estimated Temperature (mW/m ²)	Estimated Temperature Using 3-D FEHM (85 mW/m ²)
ER-19-1	Split Ridge Fault-RM/AT Caldera Topo Margin (14)	31.5	LCCU1	40.5		31.5		0.93	90.32	157.95		
		31.5	LCCU1	21.8		31.5		0.93	48.60	85.00		
		31.5	LCCU1	38.1		31.5		0.93	85.00	148.65		
ER-19-1	Split Ridge Fault-RW/AT Caldera Topo Margin (14)	31.5	UCCU	18.8	2.43	77.2	45.6	-1.50	46.44	58.28		
		31.5	UCCU	27.4	2.43	98.1	66.6	-1.50	67.73	85.00		
		31.5	UCCU	34.4	2.43	115.1	83.6	-1.50	85.00	106.68		
ER-19-1	Split Ridge Fault-RM/AT Caldera Topo Margin (14)	77.2	LCA	17.2	2.00	111.5	34.3	-3.50	80.19	85.00	131.1	147.0
		98.1	LCA	17.2	2.00	132.5	34.3	-3.50	80.19	85.00		
		115.1	LCA	17.2	2.00	149.4	34.3	-3.50	80.19	85.00		
ER-19-1 ^c Alternative #6	Split Ridge Fault-RM/AT Caldera Topo Margin (14)	31.5	LCCU1	40.5		31.5		0.93	90.32	157.94		
		31.5	LCCU1	21.8		31.5		0.93	48.60	85.00		
		31.5	LCCU1	38.1		31.5		0.93	85.00	148.65		
ER-19-1 ^c Alternative #6	Split Ridge Fault-RM/AT Caldera Topo Margin (14)	31.5	UCCU	18.8	0.43	39.6	8.0	0.50	46.44	58.28		
		31.5	UCCU	27.4	0.43	43.3	11.7	0.50	67.73	85.00		
		31.5	UCCU	34.4	0.43	46.3	14.7	0.50	85.00	106.68		
ER-19-1 ^c Alternative #6	Split Ridge Fault-RM/AT Caldera Topo Margin (14)	39.6	LCA	17.2	4.00	108.3	68.7	-3.50	80.19	85.00	111.7	
		43.3	LCA	17.2	4.00	112.0	68.7	-3.50	80.19	85.00		
		46.3	LCA	17.2	4.00	114.9	68.7	-3.50	80.19	85.00		

^a Measured temperatures from [Attachment A](#) or Blankennagel and Weir (1973).

^b Estimated gradient temperature taken from range in temperature gradients for HSU reported in [Attachment A](#).

^c Structural interpretation alternative #6 (BN, 2002, Figure 6-14).

Table C.6-3
Temperature Estimates in ER-19-1 from Base of the PM/OV Model
(3.5 km Below Sea Level)

Assuming Dominantly Conductive Heat Flow, Background Regional Heat Flow of 85 mW/m²
 Base Temperature of 147°C, and Two Structural Interpretations

PM/OV Model	HSU	Elevation at HSU Base (m)	Estimated Temperature at HSU Base (°C)	λ (W/m °C)	Estimated Gradient Temperature (°C/km)	Estimated Heat Flow (mW/m ²)	Estimated Thickness (km)	Measured Temperature at HSU Base (°C)
Grid g (base λ)	PBRCM	999	44.5	2.13	39.9	85		
	LCCU1	928	46.1	3.9	21.8	85	0.07	31.5
	UCCU	-1,500	112.7	3.1	27.4	85	2.43	
	LCA	-3,500	147.0	4.95	17.2	85	2.00	
Grid g (low λ)	PBRCM	999	24.3	1.71	49.7	85		
	LCCU1	928	27.0	2.23	38.1	85	0.07	31.5
	UCCU	-1,500	110.6	2.47	34.4	85	2.43	
	LCA	-3,500	147.0	4.67	18.2	85	2.00	
Grid g (best λ)	PBRCM	999	27.6	2.13	39.9	85		
	LCCU1	928	29.1	3.9	21.8	85	0.07	31.5
	UCCU	-1,500	112.7	2.47	34.4	85	2.43	
	LCA	-3,500	147.0	4.95	17.2	85	2.00	
Alt #6 (base λ)	PBRCM	999	65.0	2.13	39.9	85		
	LCCU1	928	66.6	3.9	21.8	85	0.07	31.5
	UCCU	500	78.3	3.1	27.4	85	0.43	
	LCA	-3,500	147.0	4.95	17.2	85	4.00	
Alt #6 (low λ)	PBRCM	999	56.8	1.71	49.7	85		
	LCCU1	928	59.5	2.23	38.1	85	0.07	31.5
	UCCU	500	74.2	2.47	34.4	85	0.43	
	LCA	-3,500	147.0	4.67	18.2	85	4.00	
Alt #6 (high λ)	PBRCM	999	71.0	2.71	31.4	85		
	LCCU1	928	72.1	5.8	14.7	85	0.07	31.5
	UCCU	500	82.0	3.66	23.2	85	0.43	
	LCA	-3,500	147.0	5.23	16.3	85	4.00	

C.6.2.3 Summary of Lower Boundary Conditions

Different boundary conditions were used at the base of the model in the models described in this report, including specified uniform heat fluxes and specified uniform temperatures. Specified uniform heat fluxes used in forward heat-conduction models ranged from 45 to 105 mW/m² and encompassed the average deep heat flux of 85 mW/m² estimated for the vicinity of the NTS by Sass et al. (1995). Temperatures at the base of the model were calculated from Fourier's Law using measured bottom-hole temperatures reported in Blankennagel and Weir (1973, Table 8) and thermal properties estimated from the HFM (BN, 2002) and thermal conductivity data summarized in Gillespie (2003). Estimates of the temperature at the base of the PM/OV model (-3,500 m elevation) indicate an average temperature of at least 160°C. Simulation results discussed later in this report show that temperature distributions within the model domain are similar for models that use specified lower boundary temperatures of 160°C or specified lower heat fluxes of 65 mW/m². Inverse heat-conduction models were also done that consider variable intra- and extra-caldera heat fluxes. In these inverse models, heat fluxes are optimized by matching match model results with borehole temperature measurements.

C.7.0 MODEL RESULTS

This section describes the results of both forward models of steady-state heat conduction done with various thermal conductivity estimates and lower boundary conditions, and inverse models of heat conduction that optimize either thermal conductivities or deep heat flux at the base of the model. The forward models were used to determine if a uniform heat flux value at the base of the model, combined with the estimated thermal conductivities of the 46 HSUs, would be able to match the temperature observations or if a more complex distribution of heat flux along the lower boundary might be necessary. The inverse models investigated whether (1) grouped thermal conductivities could be optimized for a uniform heat flux to match the temperature data or (2) a simple, spatially variable distribution of heat flux could be found that, combined with the original 46 estimates of thermal conductivities, would provide an adequate match to the temperature data.

C.7.1 Forward Heat Conduction Models

Forward models of heat conduction in the PM/OV model domain were developed to investigate the sensitivity of simulated temperatures to thermal conductivity estimates and boundary conditions. Simulations considered upper, lower, and base-case thermal conductivity estimates ([Table C.5-1](#)) and either specified temperature (160°C) or specified heat flux (45, 65, 85 or 105 mW/m²) conditions at the base of the model. In addition to using the base-case thermal conductivities, the simulations run with a lower boundary temperature of 160°C also considered cases where the thermal conductivities were set at their upper or lower limits. For all models, the upper boundary was determined by interpolating borehole temperatures measured near the water table onto the top nodes in the model ([Figure C.6-1](#)). The simulated and measured temperatures are compared on a borehole-by-borehole basis for different model runs in ([Attachment A, Figures C1 to C-30](#)). Only summary results and overall conclusions are presented in the paragraphs and figures that follow.

Based on estimates of deep regional heat flux by Sass et al. (1995), the initial forward models assumed a uniform heat flux of 85 mW/m². The results from this model are presented to illustrate the

three-dimensional nature of heat transport in the PM/OV model domain. Simulated temperatures at the base of the model (Figure C.7-1) vary from less than 120°C to over 200°C as a consequence of the spatial variability in thermal conductivity associated with the distribution of HSUs in the model. Generally, temperatures at the base of the model are highest beneath the calderas and lowest in areas adjacent to the calderas. Beneath the Timber Mountain caldera complex and the Black Mountain caldera, the high temperatures simulated at the base of the model may be related to the great thickness of low-thermal conductivity rocks such as the intra-caldera intrusive confining units (BN, 2002, Figure 4-43) and the absence of high thermal conductivity HSUs like the LCA and LCCU (BN, 2002, Figures 4-49 and 4-51). Beneath the SCCC, the high temperatures at the base of the model are attributed to the absence of the LCA and LCCU, and the great thickness of low thermal conductivity tuffs that fill the caldera (e.g., BN, 2002, Figures 4-31 and 4-37).

A series of maps of simulated temperatures at different elevations indicates that temperature differences between the intra- and extra-caldera areas become less with increasing elevation (Figure C.7-2). The muted differences between intra- and extra-caldera temperatures at higher elevations are a consequence of the increasing influence of the specified upper boundary temperatures (Figure C.6-1) and the lateral as well as vertical flow of heat. Evidence for the lateral flow of heat is provided by cross-sections of simulated temperature profiles taken along east-west (Figure C.7-3) and north-south transects (Figure C.7-4). Heat flows from areas of higher to lower temperature in a direction perpendicular to the temperature contours (isotherms), so the isotherms in these cross-sections indicate that some heat will move away from the caldera areas into the surrounding rock. An interesting consequence of this conclusion is that vertical heat flux will decrease with elevation within the calderas and increase with elevation in the adjacent extra-caldera areas, even in the absence of groundwater flow.

The temperatures simulated with a specified heat flux of 85 mW/m² are compared to the measured temperatures in Figure C.7-5. The scatterplot shown in Figure C.7-5 compares individual pairs of measured and calculated temperatures, coded with different symbols according to borehole. The figure indicates that although some of the simulated and measured temperatures fall on or near the “one-to-one” line (most notably temperatures for wells ER-EC-6, U-19i, and PM-1), most of the simulated temperatures are too warm relative to the measured temperatures. This suggests that, in general, a uniform specified heat flux of 85 mW/m² is too high compared with the actual heat flux.

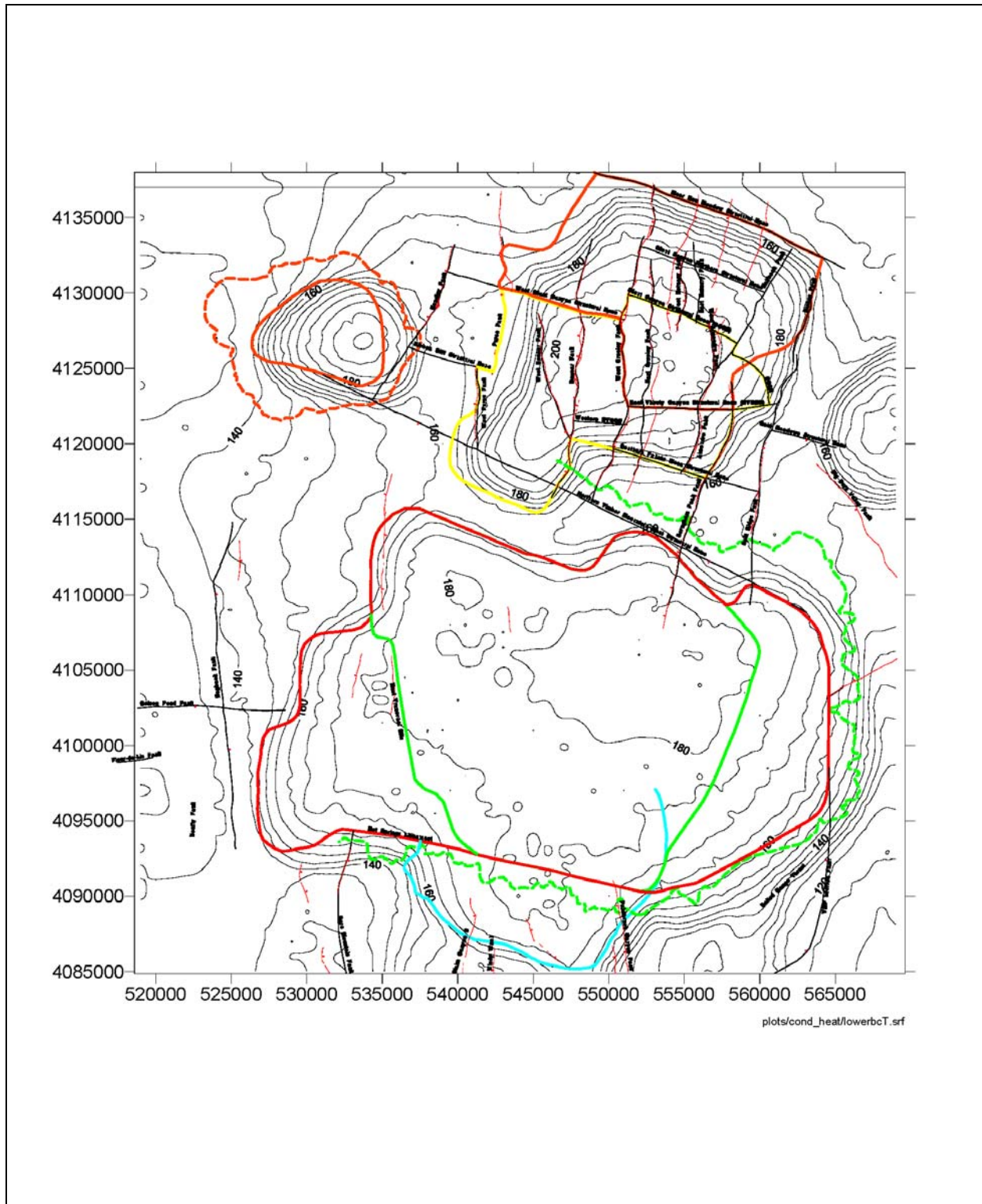


Figure C.7-1
Simulated Temperature (°C) at the Lower Boundary for a Uniform Heat Flux of 85 mW/m²

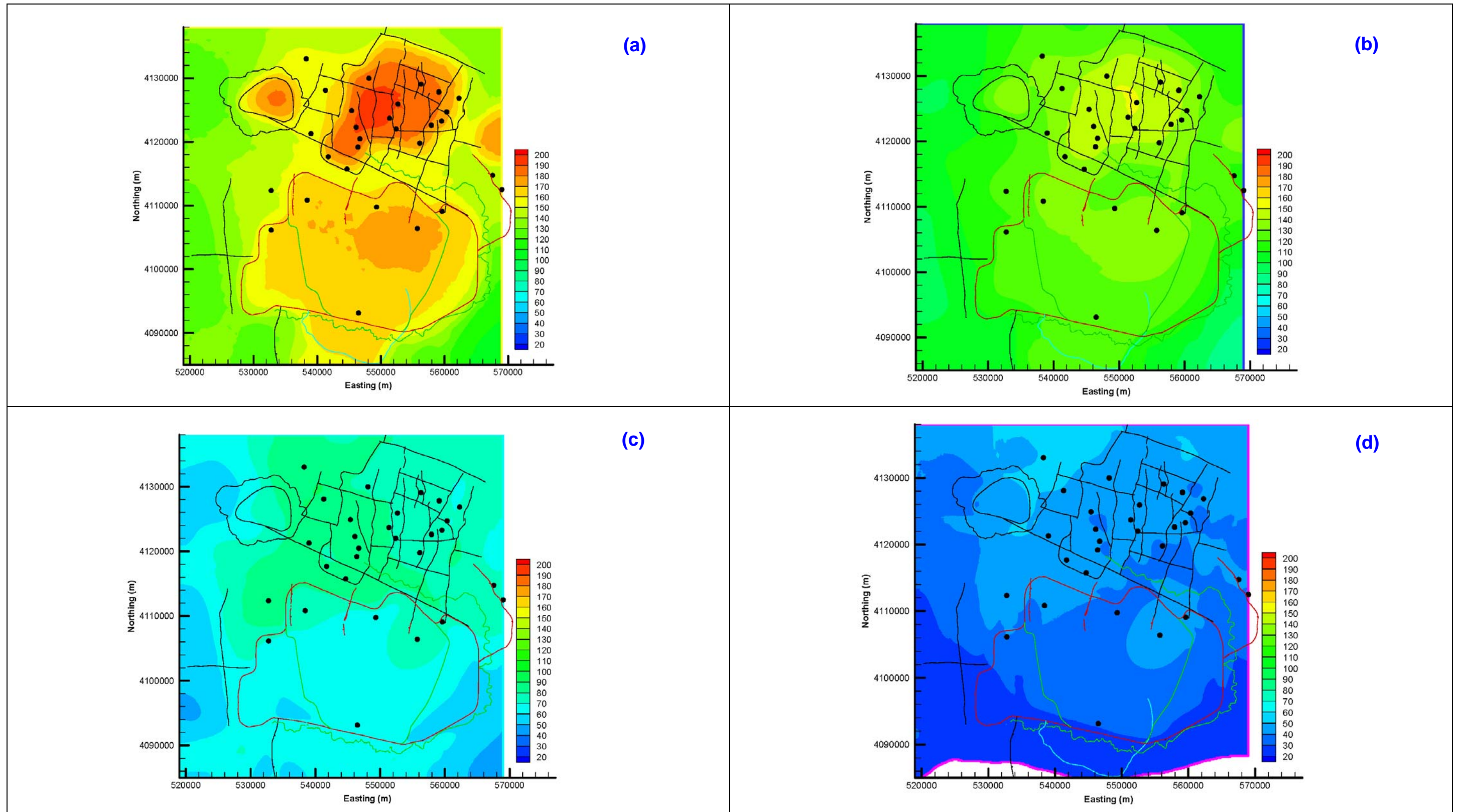


Figure C.7-2
 Simulated Temperatures ($^{\circ}\text{C}$) for a Specified Lower Heat Flux of 85 mW/m^2 at Four Elevations (a) $z = -3,200 \text{ m}$, (b) $z = -2,000$, (c) $z = 0 \text{ m}$, and (d) $z = 1,000 \text{ m}$

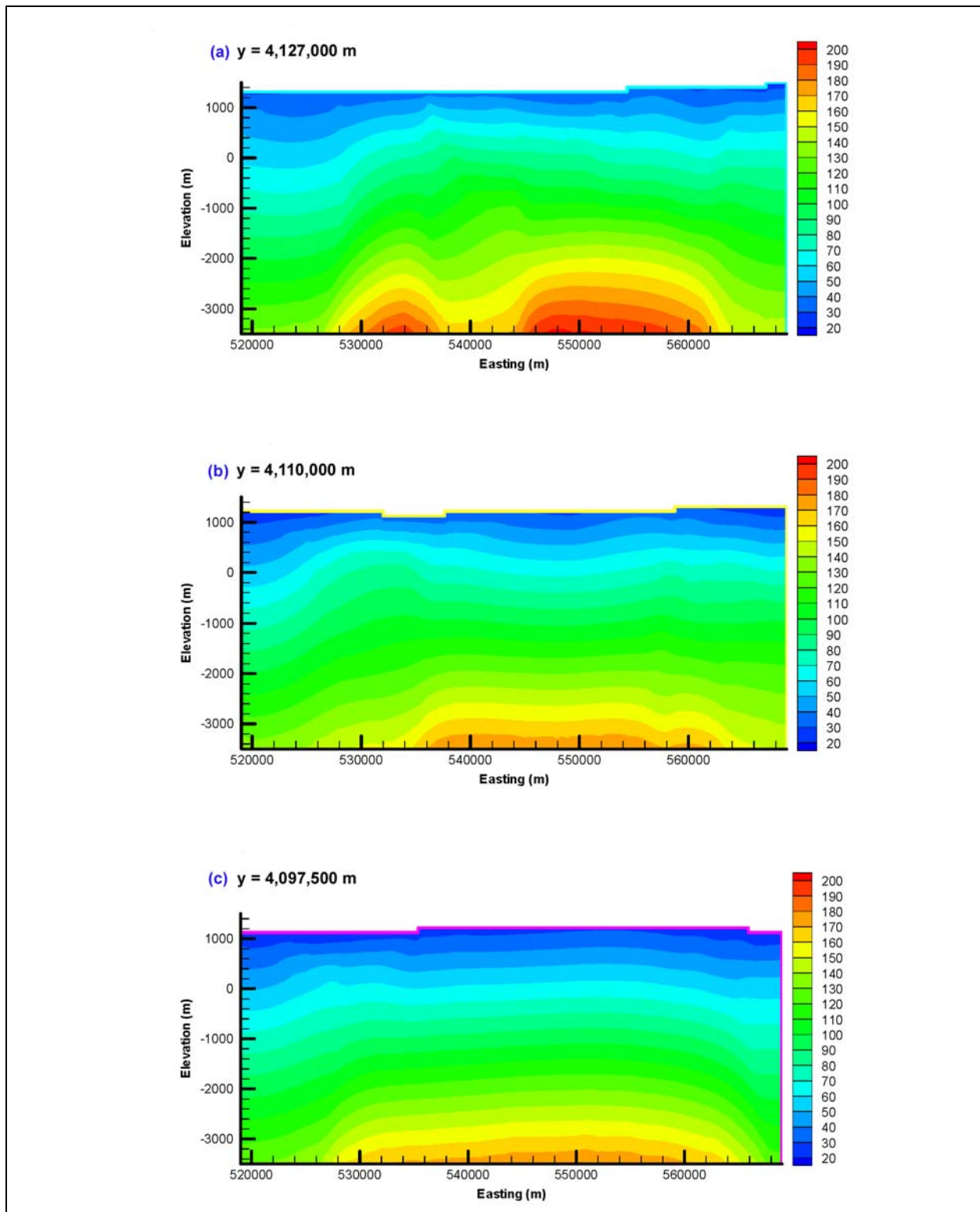


Figure C.7-3
East-West Transects for Uniform 85 mW/m^2 Lower Boundary Flux Simulation at (a) $y = 4,127,000$ m, (b) $y = 4,110,000$ m, and (c) $y = 4,097,500$ m, Corresponding Approximately to Transects C-C', E-E', and B-B' (BN, 2002)

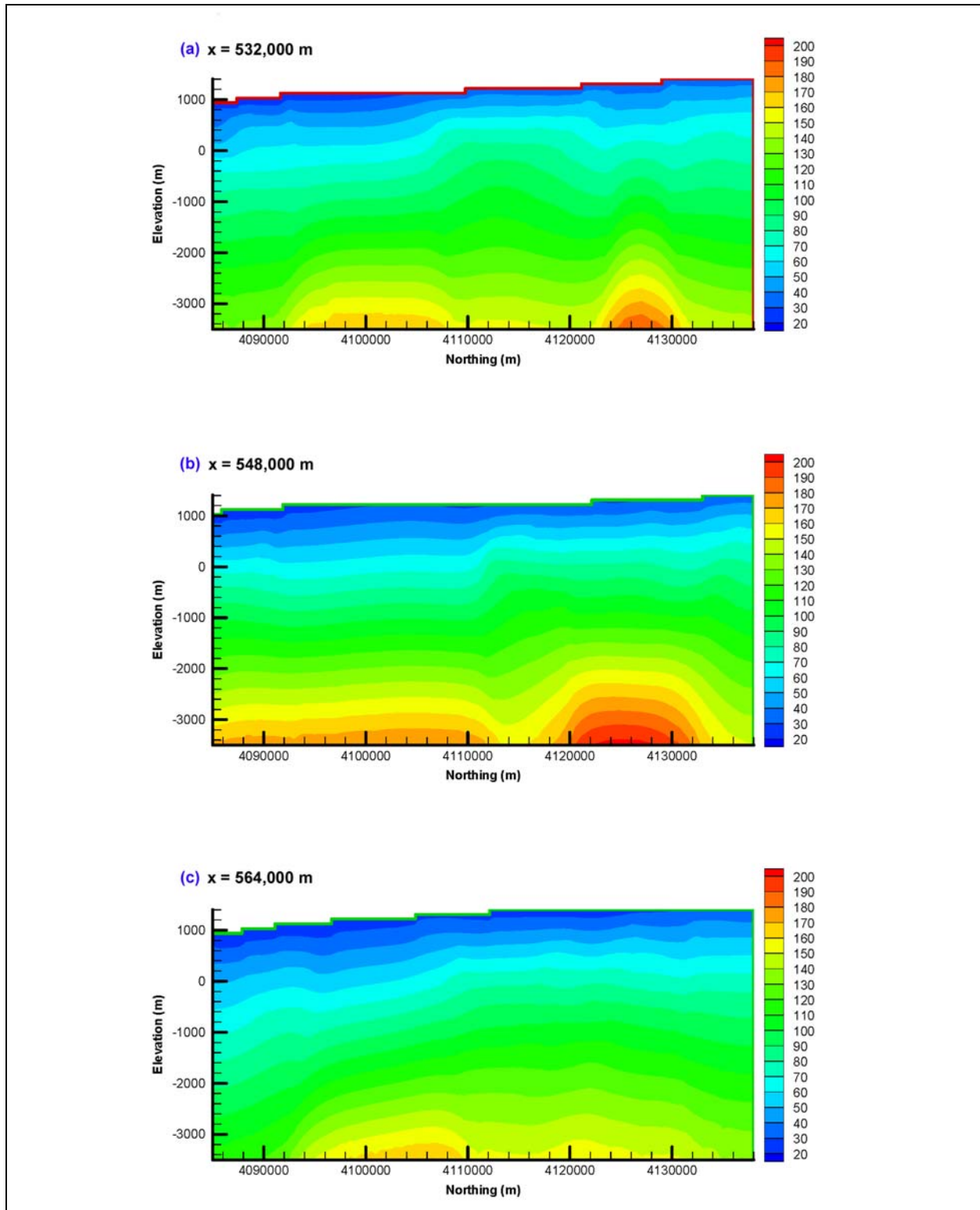


Figure C.7-4
North-South Transects for Uniform 85 mW/m² Lower Boundary Flux Simulation at
(a) x = 532,000 m, (b) x = 548,000 m, and (c) x = 564,000 m,
Corresponding Approximately to Transects G-G', H-H', and I-I' (BN, 2002)

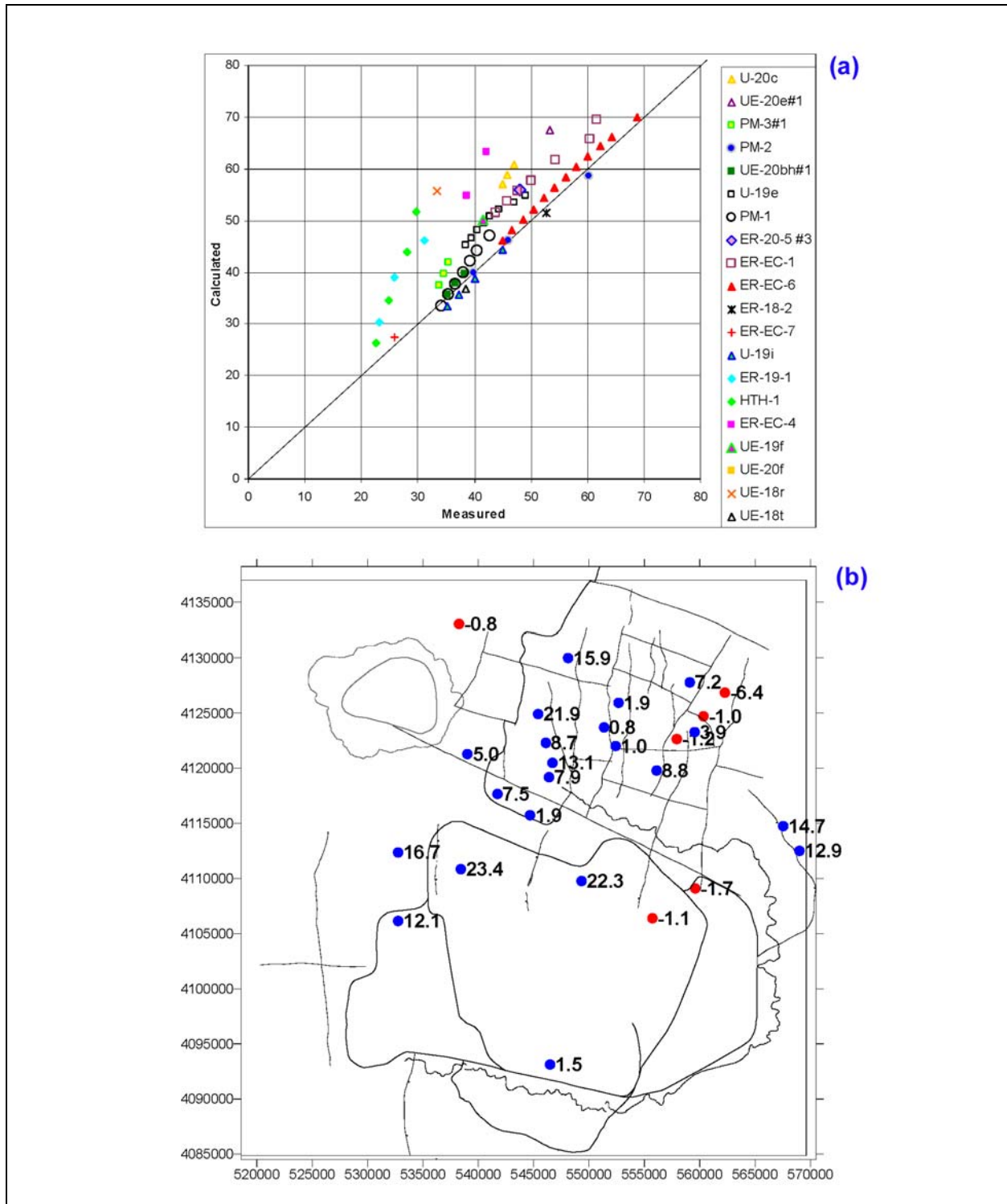


Figure C.7-5
Results from Forward Model with a Uniform Lower Heat Flux of 85 mW/m² and
Base-Case Thermal Conductivities for all 46 HSUs Listed in Table C.5-1
 (a) Simulated Versus Measured Temperatures and (b) Map of Average Residual Temperatures.
 Objective Function $\phi = 1308$

The map shown in [Figure C.7-5](#) displays the distribution of “average temperature residuals” for each borehole with reliable temperature measurements in the PM/OV flow domain. (The measurements are from depth intervals with linear temperature gradients highlighted in [Attachment A, Table A2](#), and are identified by crosses in [Attachment A, Figures C1 to C30](#)). The average temperature residual is calculated as the average difference between all pairs of simulated and measured temperatures in a borehole. The root-mean square errors (RMSE) at individual boreholes were also computed and found to be similar to the average temperature residuals. However, average temperature residuals, rather than more standard measures of fit such as RMSE values, are shown to indicate where the simulated temperatures are generally higher (positive residuals) or lower (negative residuals) than the measured temperatures. The distribution of average borehole residuals supports the interpretation that the actual heat flux is lower than the specified heat flux of 85 mW/m² value at most locations throughout the model domain ([Figure C.7-5 \(b\)](#)).

Similar plots summarize the results from simulations that consider specified lower heat fluxes of 65 and 45 mW/m² ([Figures C.7-6 and C.7-7](#)) and a specified uniform lower boundary temperature of 160°C ([Figure C.7-8](#)). The temperatures simulated with a uniform lower heat flux of 65 mW/m² provide the best overall match to the measured temperatures, as indicated by the symmetry of the simulated and measured temperatures around the one-to-one line and the relatively low value of the objective function (a measure of the degree of mismatch between the simulated and measured temperatures), which is defined in the following section. The objective function drops from 1,308 to 339 when the heat flux at the base of the model decreases from 85 to 65 mW/m², indicating much better overall agreement between the calculated and measured temperatures at the smaller heat flux. However, the simulated temperatures at some boreholes (for example, ER-19-1, HTH-1, UE-18r, and ER-EC-4) remain much warmer than the measured temperatures at a heat flux of 65 mW/m², whereas the satisfactory match obtained at other boreholes for a heat flux of 85 mW/m² begins to deteriorate. Reducing the heat flux at the base of the model further to 45 mW/m² increases the objective function to 1,186 and results in an under-estimation of measured temperatures at most boreholes in the PM/OV model domain ([Figure C.7-7](#)). However, even for a heat flux of 45 mW/m², the heat conduction model overestimates the measured temperatures at boreholes ER-19-1, HTH-1, UE-18r and ER-EC-4, suggesting that either additional modifications must be made to the model parameters or boundary conditions, or that processes other than heat conduction are affecting the measured temperatures at these boreholes.

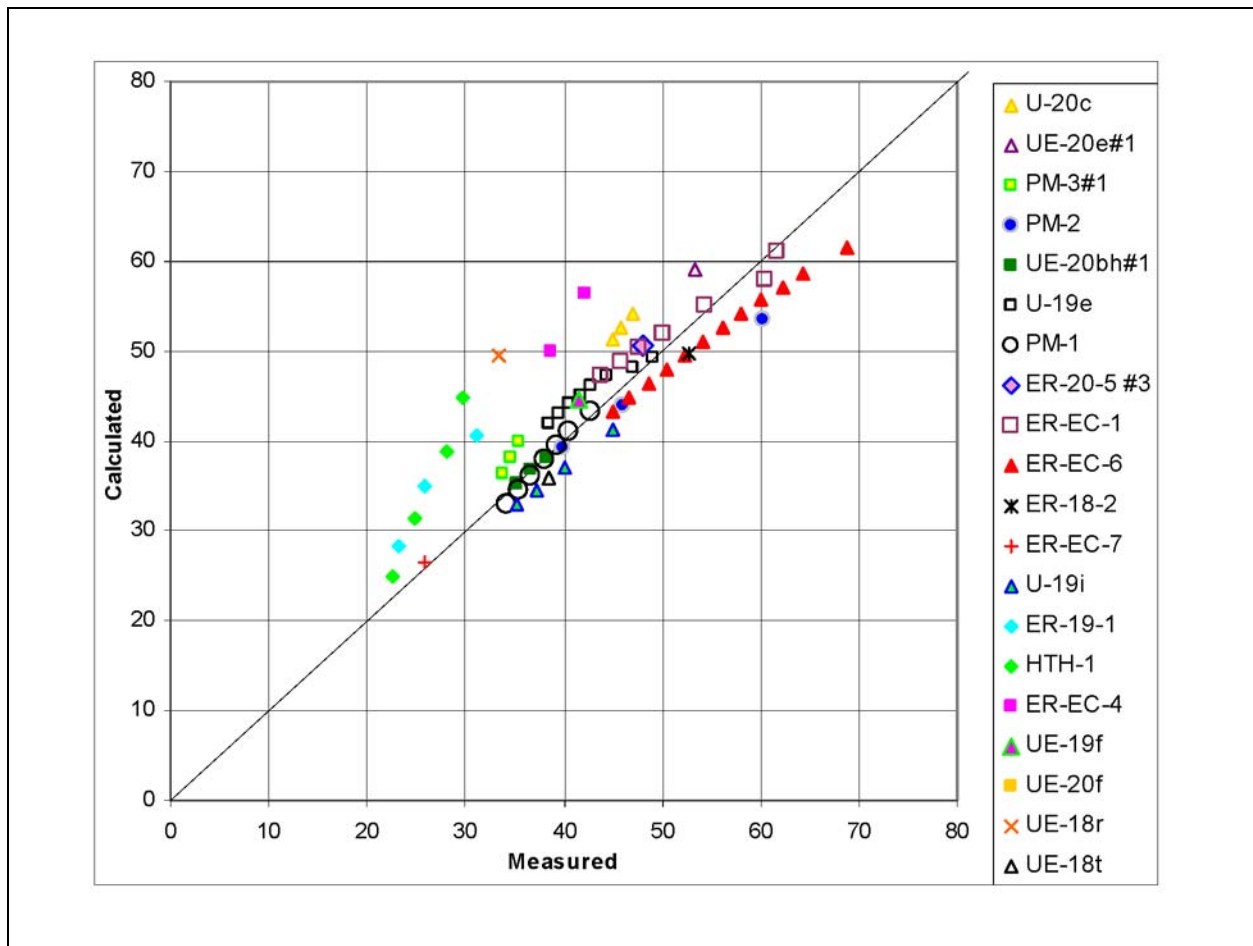


Figure C.7-6
Simulated Versus Measured Temperatures for Uniform Lower Heat Flux of 65 mW/m² and Base-Case Thermal Conductivities for all 46 HSUs Listed in Table C.5-1
 Objective Function $\phi = 339$

C.7.2 Inverse Modeling To Optimize Grouped Thermal Conductivities and Deep Heat Fluxes

C.7.2.1 Inverse Modeling Background Summary

Inverse modeling is used to estimate optimal values for uncertain model parameters that minimize the difference between simulated and observed system characteristics. In this study, the observations are temperatures measured in deep boreholes. The model parameters to be optimized are thermal conductivities for HSUs and specified heat fluxes at the base of the model. The objective function, ϕ , that the inversion seeks to minimize is the sum of the weighted square weighted residuals defined as

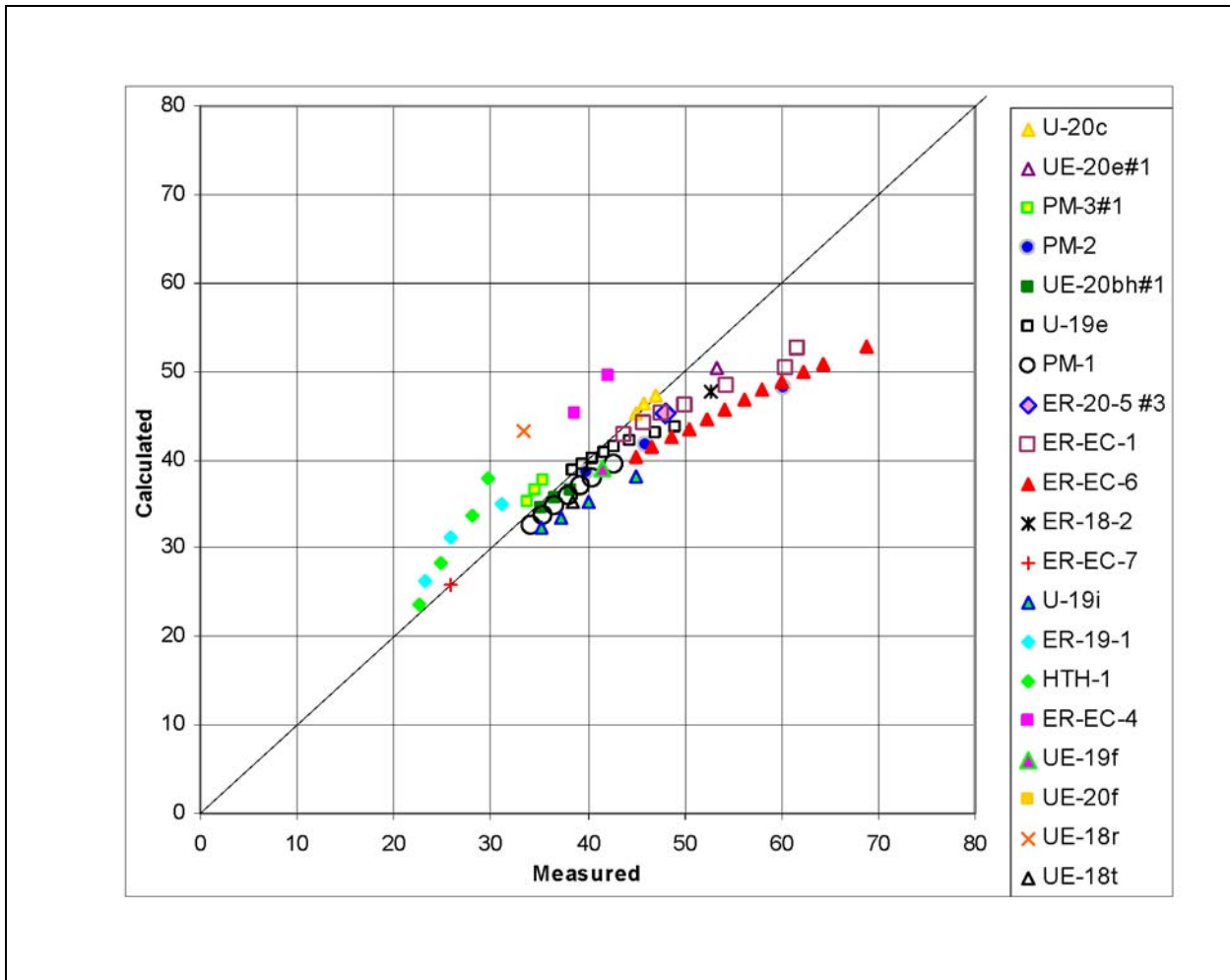


Figure C.7-7

Simulated Versus Measured Temperatures for Uniform Lower Heat Flux of 45 mW/m² and Base-Case Thermal Conductivities for all 46 HSUs Listed in Table C.5-1

Objective Function $\phi = 1,186$

$$\phi = \sum_{i=1}^m (w_i r_i)^2 \tag{C.7-1}$$

where: m is the number of observations,
 w is the weight assigned to each observation, and
 r is the residual between simulated and observed temperatures for each observation.

Temperature observations from multiple boreholes distributed throughout the domain are used in the calibration. The number of observations used per borehole varies between 1 and 12, depending on grid resolution at the location of the borehole and quality of data. In this study, the weights for each

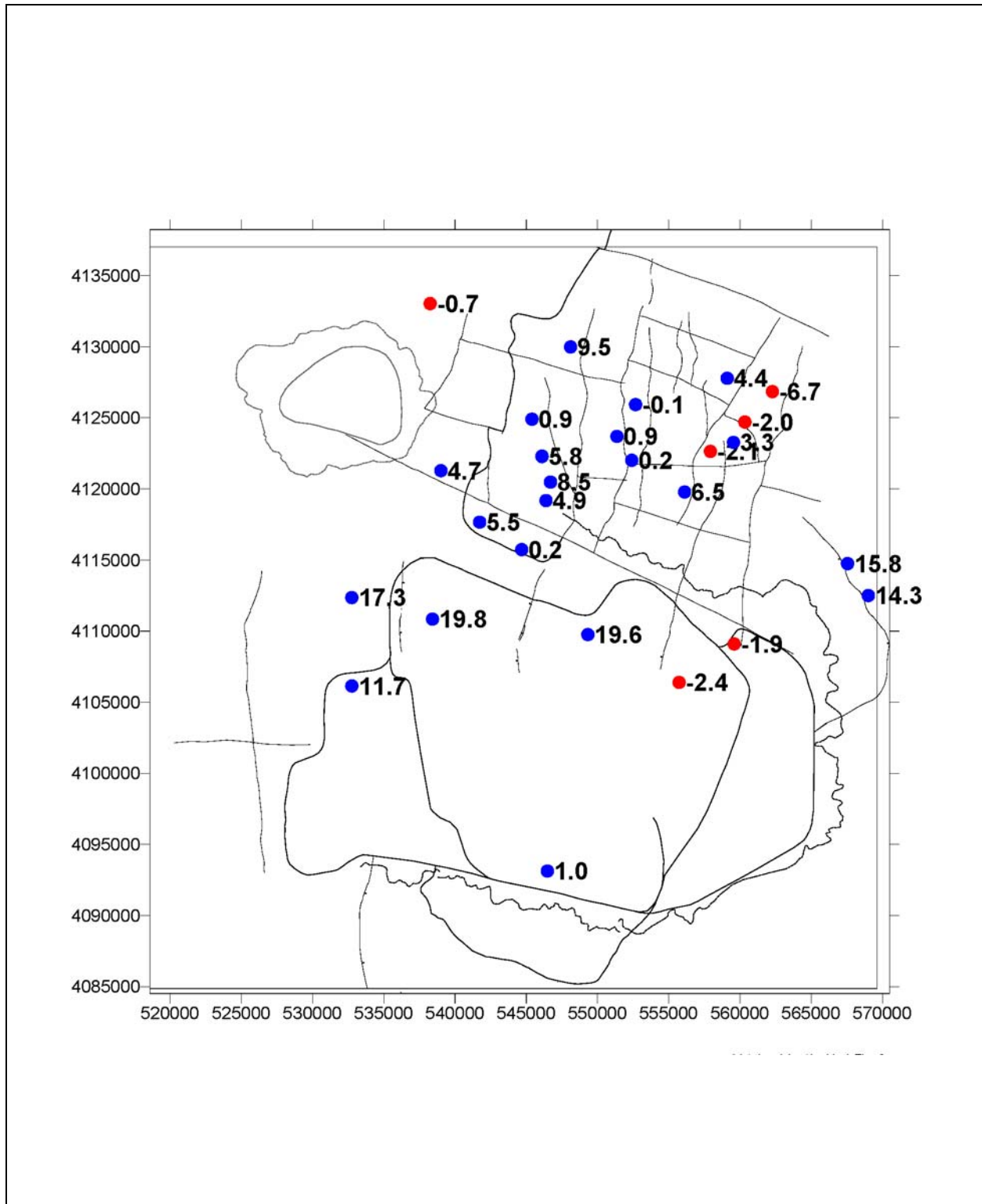


Figure C.7-8
Average Residual Temperature (°C) in Deep Saturated Boreholes
Simulations Use Specified Uniform Temperature at Lower Boundary of 160°C

observations (w_i) are assigned such that they add up to 1 for each borehole. This has the effect of weighting each borehole equivalently in the calibration, thereby emphasizing the importance of the geographic coverage in the data.

Parameter optimization is accomplished by coupling the PEST parameter estimation software (Doherty, 2000) with the FEHM heat conduction model for the PM/OV flow domain. The Gauss-Marquardt-Levenberg algorithm used by PEST is described in detail in Chapter 2 of the PEST manual. Summarizing the process, PEST takes control of FEHM and conducts the necessary simulations to estimate derivatives of model-generated observations with respect to uncertain model parameters. The matrix containing these derivatives, known as the Jacobian matrix, is then used to estimate an improved parameter set that will reduce the objective function defined above. By comparing parameter changes and the reduction in the objective function achieved in an iteration with those achieved in the previous iteration, PEST determines whether to take another optimization iteration.

C.7.2.2 Inverse Models for the PM/OV Flow Domain

The analysis of model errors associated with the forward heat conduction models indicates that no single value of specified heat flux or temperature can be found that will allow the models which use the base case estimates of thermal conductivities to match all of the temperature data. This conclusion suggests that either the actual thermal conductivities are different than their initial estimates, or that boundary conditions are more complex than initially assumed. Initial attempts to optimize both thermal conductivities and boundary conditions with PEST indicated that the estimates of thermal conductivity and heat flux are strongly correlated and cannot be estimated simultaneously with confidence. Therefore, it is necessary to specify one when the other is being estimated. The two inverse models described in the remainder of this report (1) optimize thermal conductivities for nine groups of HSUs, assuming a specified uniform heat flux of 65 mW/m² at the base of the model (a value suggested by the forward model runs as the optimal uniform heat flux), and (2) optimize specified heat fluxes along the lower boundary in six independent intra- and extra-caldera areas of the model, using the initial estimates of thermal conductivity for each of the 46 HSUs (Table C.5-1).

C.7.2.2.1 Calibrating Thermal Conductivities of Volcanic HSUs with a Specified Heat Flux of 65 mW/m²

The first inverse model was calibrated under the assumption that a heat flux of 65 mW/m² at the base of the heat-conduction model adequately characterizes the deep heat flux within the PM/OV flow domain and that model errors, as represented by the temperature residuals, are entirely the result of uncertainty in the original thermal conductivity estimates (Table C.5-1). The goal of this inverse model is to find a set of thermal conductivity values that allows the model to match the temperature data for this uniform heat flux. In this inverse model, the thermal conductivities of the 46 HSUs were first grouped into 9 classes in order to minimize the number of thermal conductivity parameters that need to be estimated through inverse modeling. The nine groups (Table C.7-1) were defined based the similarity of thermal conductivity estimates in the original 46 HSUs (Table C.5-1). However, note that because HSUs were initially defined based on their hydraulic properties, whereas thermal conductivity is affected by somewhat unrelated lithologic and mineralogic characteristics, there is not always an exact correspondence between an HSUs classification as an aquifer, confining unit or composite unit and its assignment to a specific thermal conductivity group (Table C.7-1). As an example, volcanic HSUs were first sorted according to whether they represented intra-caldera (Group 6) or extra-caldera (Groups 7 and 8) rocks. Then, based on borehole stratigraphic logs, extra-caldera HSUs with a large percentage of high thermal conductivity lava were sorted into Group 7, whereas extra-caldera HSUs that contained only a small percentage of lava were sorted into Group 8.

**Table C.7-1
Optimal Thermal Conductivity Estimates and Fixed Thermal Conductivities
Used with a Heat Flux of 65 mW/m²**

Class ^a	Type	Lambda (W/m ² ·K)
1	Fixed	3.9
2	Fixed	4.95
3	Fixed	3.1
4	Fixed	2.6
5	Fixed	2.1
6	Calibrated	2.0
7	Calibrated	2.1
8	Calibrated	4.7
9	Fixed	1.2

^aFor HSUs in class, refer to Table C.5-1.

An initial attempt to optimize the thermal conductivities of all 9 classes using a fixed value for heat flux of 65 mW/m² at the base of the model indicated that the calibration is most sensitive to the thermal conductivities of the volcanic units and that the measured temperatures provide little information about the thermal conductivities of the non-volcanic units. This result is understandable given that most of the observed temperatures used in the calibration were measured in the volcanic units. Therefore, the calibration strategy was modified so that only the thermal conductivities of Classes 6, 7, and 8 were allowed to vary during optimization. Thermal conductivities of the remaining classes were fixed at their base-case values.

The temperatures simulated with the calibrated model are compared to the measured temperatures in [Figure C.7-9](#). The calibrated model has a better overall fit to the data compared to the forward model that used the base-case thermal conductivity estimates for the 46 HSUs and the same specified heat flux (compare [Figures C.7-6](#) and [C.7-9](#)). The improved fit is indicated by the decrease in the objective function from 339 to 256 and the greater symmetry of the simulated and measured temperatures around the one-to-one line using the calibrated model. However, several other factors indicate that the calibrated model is unsatisfactory, despite its overall reduction in the objective function and the improved symmetry of its residuals. First, temperature data from some boreholes that had previously been well matched by the forward model (for example, data from boreholes PM-2, ER-EC-1 and ER-EC-6) are now farther from the one-to-one line, complicating the interpretation of data from locations that formerly were interpreted to be consistent with pure heat conduction. At the same time, only slight improvements in the match between simulated and measured temperatures were made for boreholes that lie furthest from the one-to-one line (HTH-1 and ER-19-1) which are more likely to be genuinely affected by non-conductive heat transport processes. Second, although the thermal conductivity values estimated for Classes 6 and 7 are reasonable ([Table C.7-1](#)), the thermal conductivity of 4.7 W/m•°K estimated for HSU Class 8 is approximately twice the value expected on the basis of its constituent rock types, calling into question the physical realism of the model. In conclusion, although the calibration procedure successfully reduced the objective function, it did so with non-plausible parameters, raising doubts about the overall reliability of these calibration results. Based on these results and those of the forward models that indicated different heat fluxes matched data from some areas better than others, the use of a single specified value of heat flux in model calibration was abandoned in order to pursue the approach described in the following section.

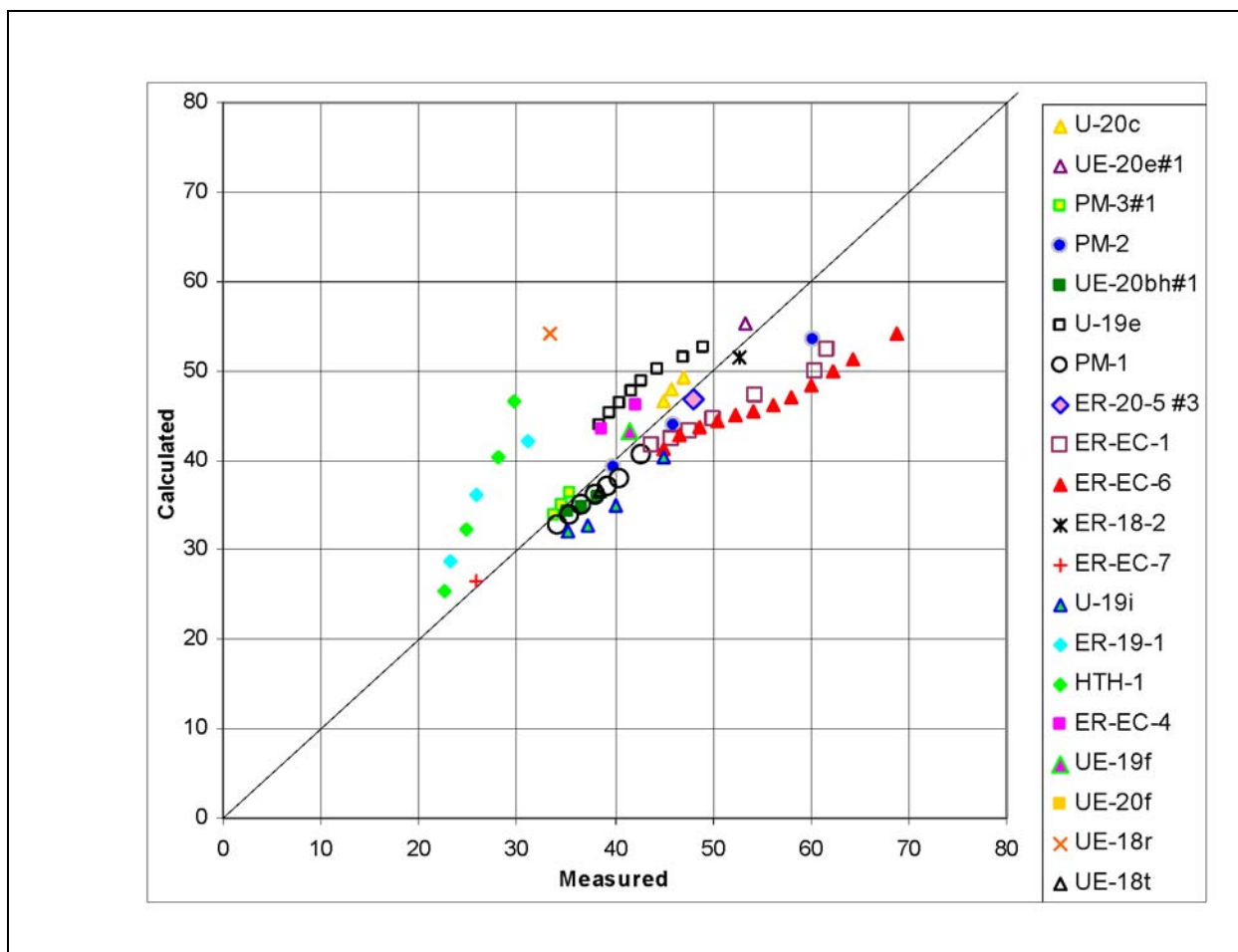


Figure C.7-9

Simulated Versus Measured Temperatures for Specified Lower Heat Flux of 65 mW/m² and Calibrated Thermal Conductivities for Volcanic HSU Groupings 6, 7, and 8 Listed in Table C.7-1

Objective Function $\phi = 256$

C.7.2.2.2 Calibrating Heat Fluxes at the Base of the Model Domain

Studies of geothermal systems in the western United States have concluded that deep heat flux can change dramatically over short distances due to anomalies in the upper crust (Barroll, 1989; Jiracek et al., 1996). In recognition that similar variability may exist in the PM/OV model domain, a second set of inverse models was created with PEST to estimate the heat-flux for different areas that were defined at the base of the model. These inverse models used the base-case thermal conductivities estimated for each of the 46 HSUs (Table C.5-1) and held these values fixed during the calibration.

The number of zones used to distribute heat flux at the base of the model was limited to seven because excessive refinement would lead to an unconstrained fit to the data (similar to the situation where too many degrees of freedom in a polynomial fit renders the physical significance of the fit meaningless). These zones were defined based on the hydrogeology of the system and a spatial analysis of temperature residuals from the forward models that indicates certain areas are regions of higher- or lower-than-average heat flux. The intra-caldera areas were divided into four zones, one each for the Black Mountain caldera and SCCC, and two for the Timber Mountain caldera complex. The definition of two separate zones for the Timber Mountain caldera complex was motivated by the sharp contrast in temperature profiles between the seven wells in the western two-thirds of the complex and the three wells in the eastern third. The distribution of HSUs in the stratigraphic framework model (BN, 2002) does not indicate any differences in the distribution of HSUs that can explain these differences, except that beds in the western and eastern parts of the Timber Mountain caldera complex dip in opposite directions. The extra-caldera area was divided into three zones: one east of the Timber Mountain caldera complex and SCCC, one north of the Black Mountain caldera, and a third containing all other extra-caldera areas.

The final calibrated heat fluxes for each of the seven zones at the base of the model are shown in [Figure C.7-10](#). The estimated heat flux of 100 mW/m² in the eastern third of the Timber Mountain caldera complex is the highest of any zone in the model. (Note that the initial model results indicated the model is insensitive to the value of heat flux at the base of the Black Mountain caldera because of the lack of temperature data from that caldera, so the heat flux in this zone was subsequently tied to the estimate for the eastern third of the Timber Mountain caldera complex.). The estimated heat flux in the western two-thirds of the Timber Mountain caldera complex is approximately half (49 mW/m²) the heat flux estimated for the eastern third. The SCCC has a relatively high estimated heat flux of 73 mW/m². Of the extra-caldera areas, the northwest zone also has a relatively high estimated heat flux (90 mW/m²) that is exceeded only by the heat flux in eastern Timber Mountain. Other extra-caldera areas have estimated heat fluxes of 45 mW/m², a value that defines the lower limit of the range of possible heat fluxes to be searched by PEST for the optimal heat flux. This lower limit was imposed on the PEST calibration based on the results of the forward models.

The temperatures simulated with this model are compared to the measured temperatures in [Figure C.7-11](#). The distribution of simulated and measured temperatures around the one-to-one line

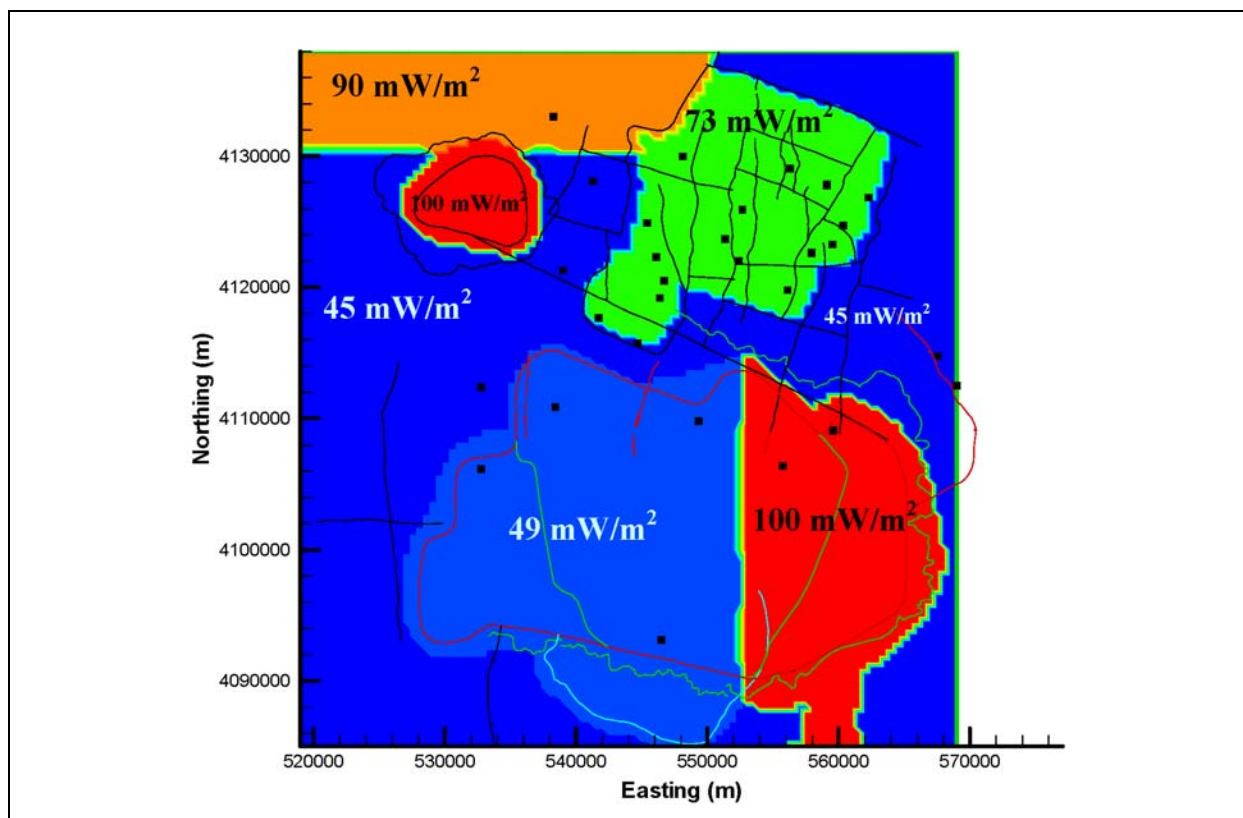


Figure C.7-10
Calibrated Heat Fluxes at Base of Model

is similar to that found for the inverse model with optimized thermal conductivities for the grouped HSU classes (Figure C.7-9). Likewise, the value of the objective function for this model ($\phi = 262$) is similar to that associated with the previous inverse model ($\phi = 256$). In spite of the general similarity between the results of the two inverse models, the model with variable heat flux at the base of the model is considered as the preferred model in this study because it does not obviously conflict with known data, whereas the previous inverse model required implausible thermal conductivity values for certain HSU groups to match the data.

The distribution of temperatures simulated with this inverse model is shown in map view in Figure C.7-12 and along east-west and north-south transects in Figures C.7-13 and C.7-14. The simulated temperature distribution displays many of the same characteristics that have been noted previously in connection with temperature distributions simulated with a uniform heat flux of 85 mW/m² (Figures C.7-2 to C.7-4). However, significant differences between results from these two simulations exist in the western part of the Timber Mountain caldera complex, where the

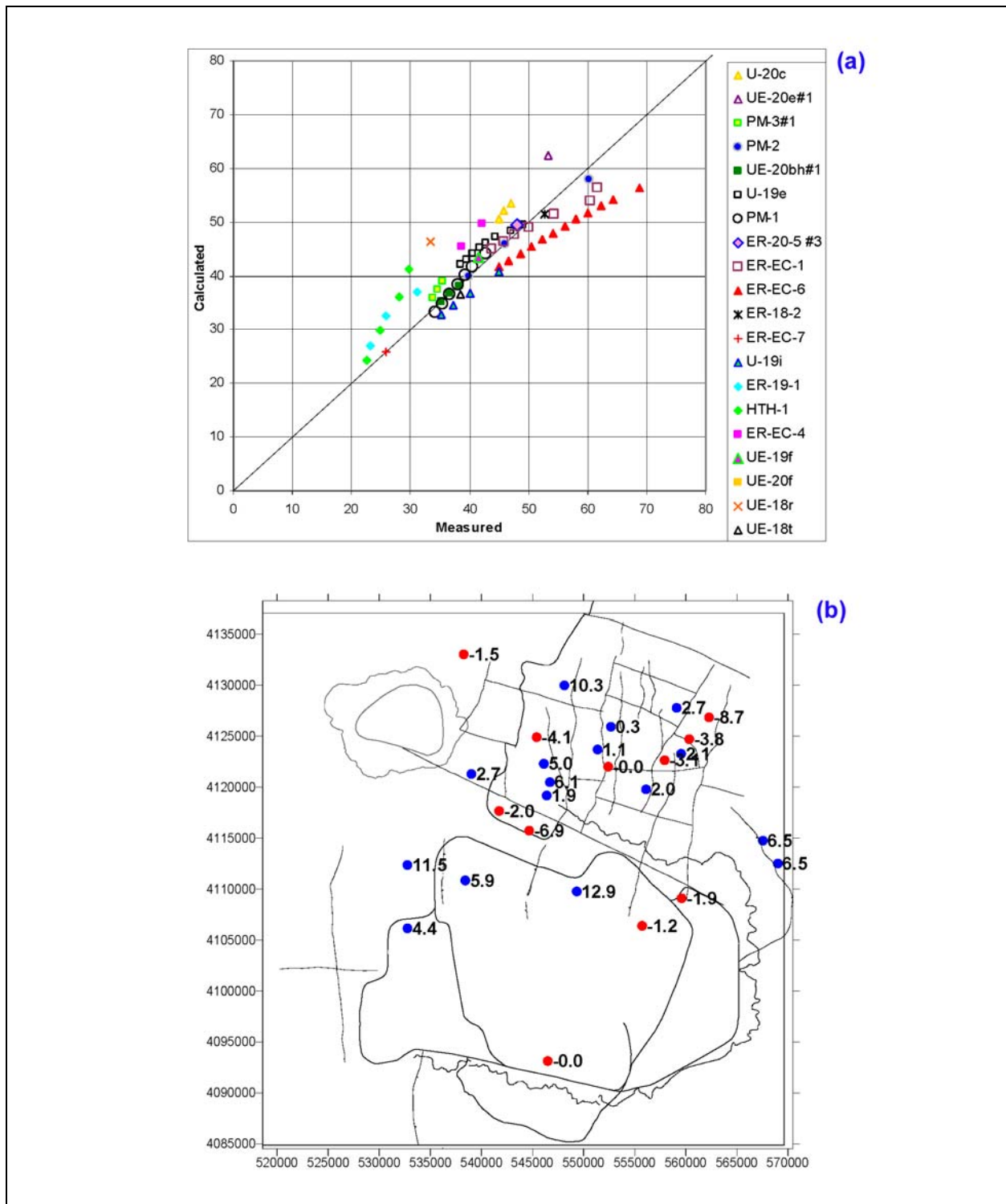


Figure C.7-11
Results from Inverse Model with Calibrated Heat Fluxes in Multiple Zones and Thermal Conductivities Assigned for all 46 HSUs Listed in Table C.5-1
 (a) Simulated Versus Measured Temperatures and (b) Map of Average Residual Temperatures.
 Objective Function $\phi = 262$

temperatures simulated with the inverse model are much lower because of the smaller heat flux value estimated with the inverse model in this area (Figures C.7-2 and C.7-12).

C.7.2.3 Evaluation of Deep Subregional Heat Flux Estimates

The deep heat fluxes of 45 to 100 mW/m² estimated with the inverse model described in Section C.7.2 were compared with heat flux estimates calculated directly from measured borehole temperature profiles and base case thermal conductivity values (Table C.5-1) to evaluate if the model estimates (Figure C.7-10) are reasonable. The heat fluxes estimated from borehole temperature profiles include data from the deep unsaturated zone, where the intra-borehole flow of groundwater is not a factor (Attachment A, Tables A1 and A2). Based on estimates of heat flux derived directly from the measured temperature profiles (Table C.7-2), the estimates of deep heat flux estimated with the inverse model generally seem reasonable. Each of the 6 distinct subregions defined at the base of the model are discussed briefly below.

C.7.2.3.1 Subregion (1), North of Black Mountain

Based on the heat fluxes of 54.8 and 57.3 mW/m² estimated directly from temperature logs at high elevations in borehole PM-2 (Table C.7-2), the model calibrated value of 90 mW/m² appears to be an overestimate of the deep heat flux in subregion (1). However, the simulated and measured temperatures at borehole PM-2 are in good agreement (Figure C.7-11 and Attachment A, Figure C11), indicating that the high heat flux of 90 mW/m² estimated for the base of the model in this area may have decreased with elevation because of the lateral spreading of heat from this subregion (Figure C.7-12).

C.7.2.3.2 Subregion (2), Silent Canyon Caldera Complex

Heat fluxes calculated directly from relatively linear parts of borehole temperature logs in subregion (2) are highly variable, ranging from about 22 to 162 mW/m² (Table C.7-2). However, within the individual structural zones of subregion (2) defined in Figure C.4-2, the variability of the heat flux estimates is generally smaller than the overall variability. For instance, heat flux estimates in structural Zones 1 and 7 are generally between 40-50 and 30-60 mW/m², respectively, whereas heat flux estimates in structural Zone 4 range between about 80 and 130 mW/m² (Table C.7-2). Given the variability of heat flux estimates within and between structural zones, and the difficulty of applying

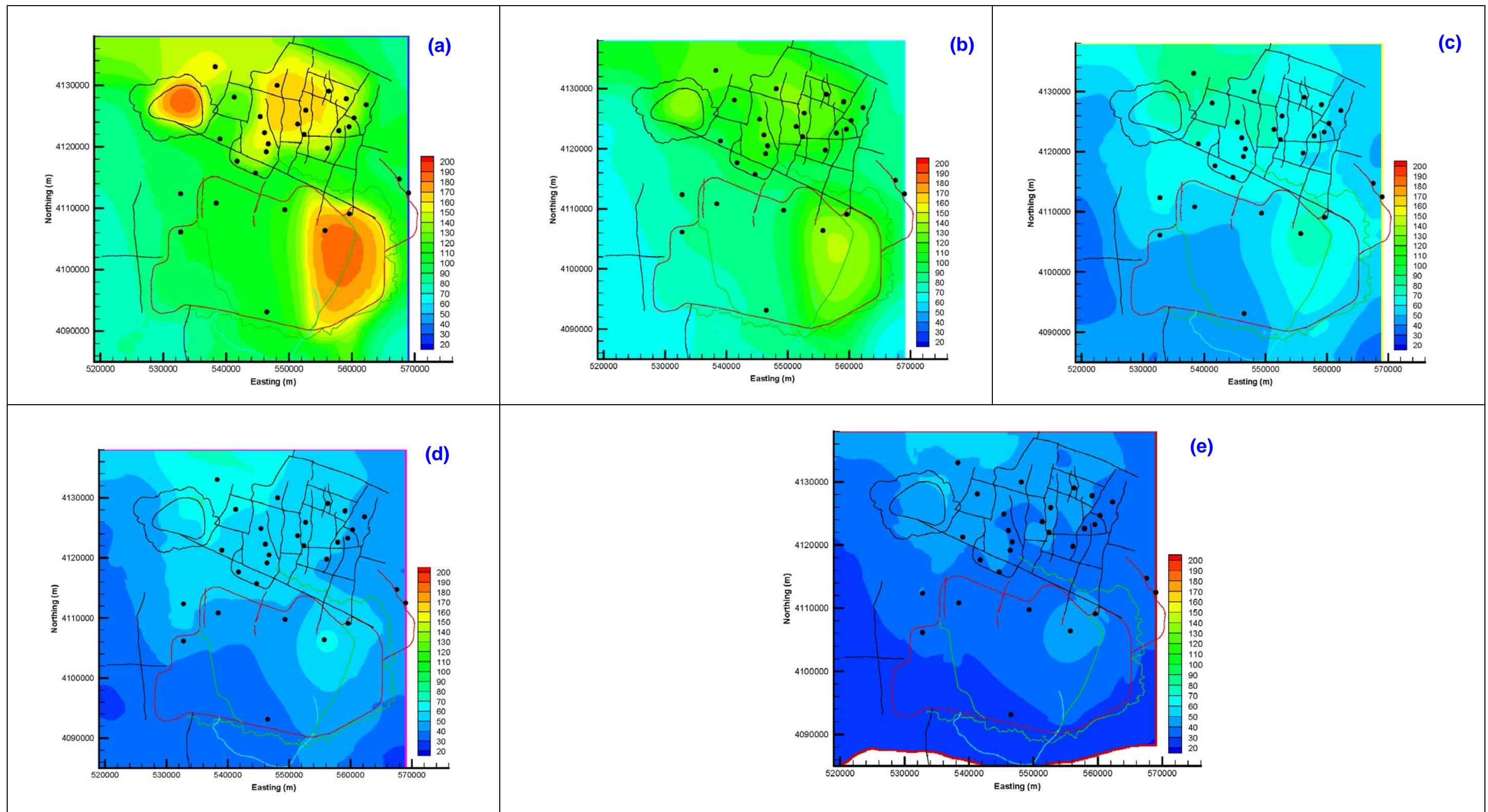


Figure C.7-12
Simulated Temperatures (°C) at 5 Elevations for Calibrated Thermal Fluxes in 6 Zones on Lower Boundary: (a) -3,200 m, (b) -2,000 m, (c) 0 m, (d) 500 m, and (e) 1,000 m

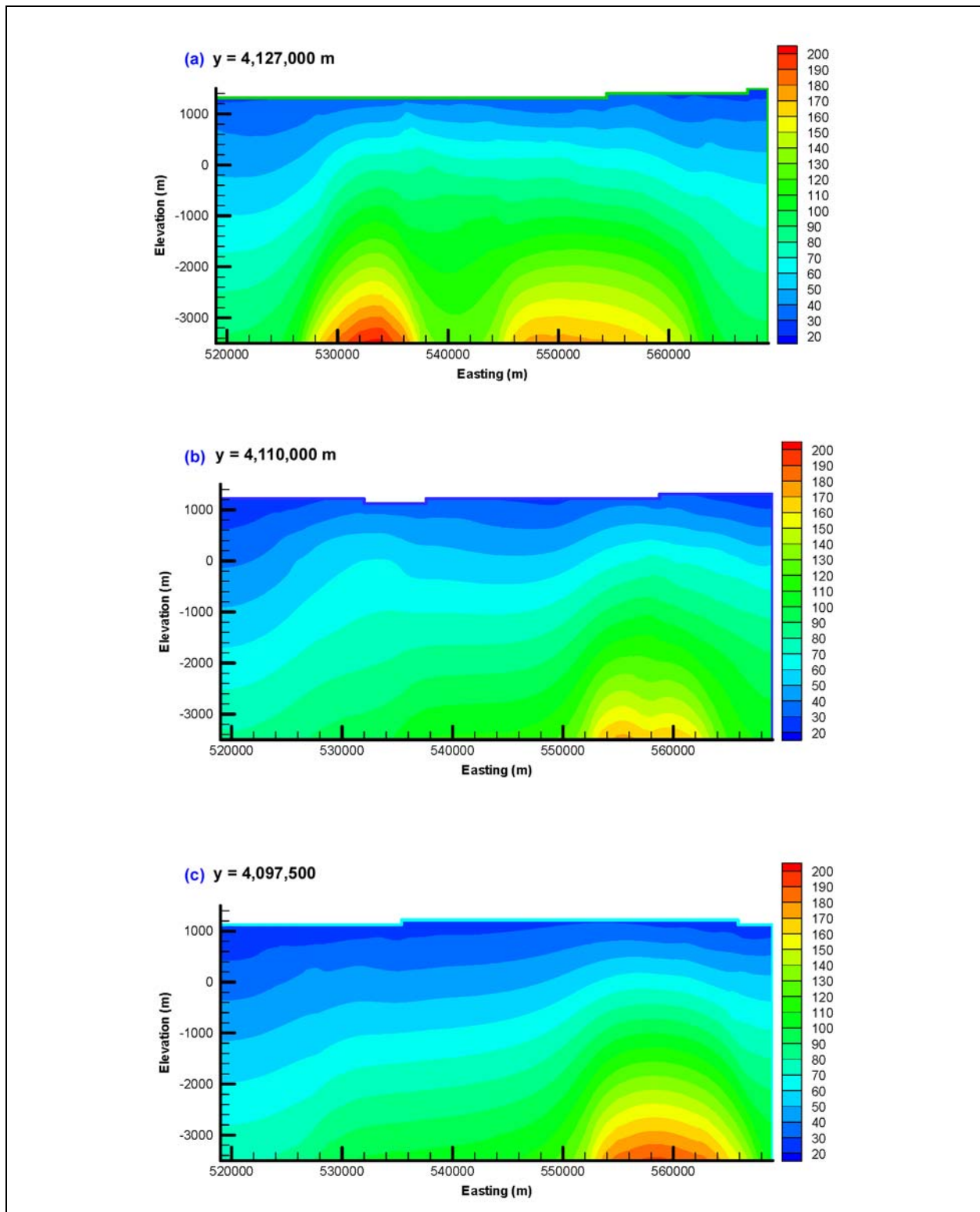


Figure C.7-13
East-West Transects for Calibrated Six-Zone Heat-Flux Model at
(a) $y = 4,127,000$ m, (b) $y = 4,110,000$ m, and (c) $y = 4,097,500$ m,
Corresponding Approximately to Transects C-C', E-E', and B-B' (BN, 2002)

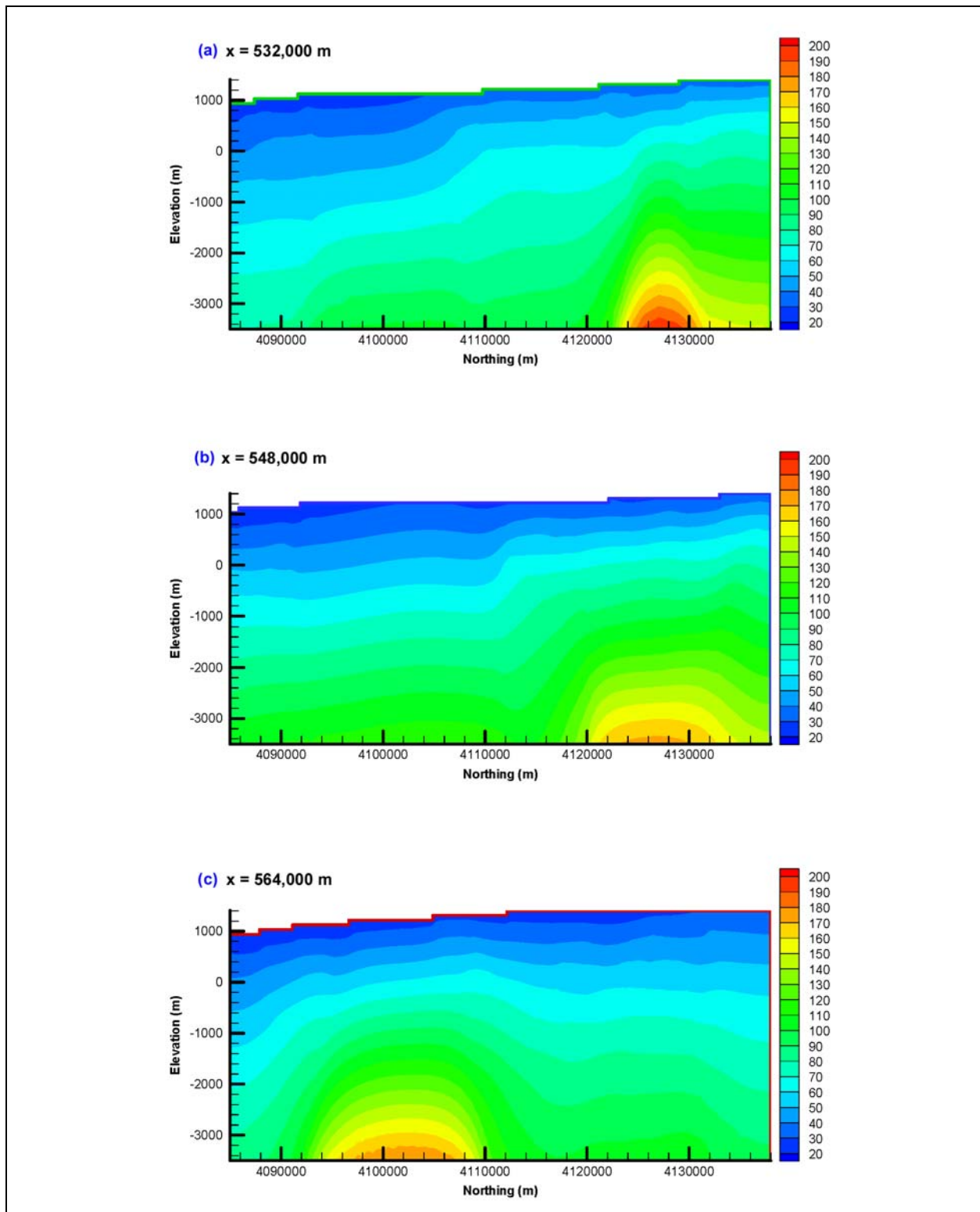


Figure C.7-14
North-South Transects for Calibrated Six-Zone Heat-Flux Model at (a) $x = 532,000$ m, (b) $x = 548,000$ m, and (c) $x = 564,500$ m, Corresponding Approximately to Transects G-G', H-H', and I-I' (BN, 2002)

Table C.7-2
Subregional Lower Boundary Heat Flux Estimates^a
 (Page 1 of 5)

Borehole	Elevation Range (m)	Structural Zone Number	HSU	Measured Type ^b	Estimated Heat Flow (mW/m ²)	Temperature Log (Date)	Calibrated Model Heat Flux (mW/m ²)
Subregion (1), North of Black Mountain							
PM-2	1,251.5 to 986.3	6	PBRCM	sz	54.8	7/11/1964	90
PM-2	983.3 to 949.8	6	PBRCM	sz	57.3	7/11/1964	90
Subregion (2), Silent Canyon Caldera Complex							
ER-20-5#3	1,275.0 to 1,242.98	1	LPCU	cwl	48.7	2/6/1996Inl	72.7
U-20c	1,301.8 to 1,277.4	1	BA	uz	49.1	4/5/1965	72.7
U-20c#1	576.4 to 481.9	1	CHZCM	sz	49.4	9/27/1968	72.7
U-20y	1,388.9 to 1,343.2	1	TCA	uz	42.1	1/2/1975	72.7
UE-20d	1,328.9 to 1,284.4	1	BA	uz	50.5	7/28/1964	72.7
UE-20e#1	370.9 to 352.7	2	BRA	sz	78.1	6/2/1964	72.7
ER-20-6#1	1,373.4 to 1,355.5	3	UPCU	uz	54.1	3/7/1996	72.7
ER-20-6#1	1,329.2 to 1,322.5	3	LPCU	sz	104.0	5/1/1996	72.7
ER-20-6#1	1,322.5 to 1,318.3	3	LPCU	sz	108.4	5/1/1996	72.7
ER-20-6#3	1,354.9 to 1,339.7	3	CHZCM	cwl	60.0	2002	72.7
U-20WW	1,345.3 to 1,328.5	3	CHZCM	cwl	53.1	2000-2002	72.7
UE-20n#1	1,347.1 to 1,331.8	3	CHZCM	cwl	70.9	2000-2002	72.7
ER-EC-1	1,270.3 to 1,212.5	4	FCCU	cwl	29.0	2/17/2000	72.7
ER-EC-1	535.1 to 503.7	4	CFCM	sz	85.3	2/17/2000	72.7
ER-EC-1	503.1 to 494.9	4	CFCM	sz	87.9	2/17/2000	72.7
ER-EC-6	1,271.6 to 1,240.5	4	FCCU	cwl	79.9	3/8/2000	72.7
ER-EC-6	754.0 to 742.2	4	TSA	sz	100.8	3/8/2000	72.7
ER-EC-6	741.7 to 663.2	4	TSA	sz	119.6	3/8/2000	72.7
ER-EC-6	546.4 to 529.3	4	CHCU	sz	116.6	3/8/2000	72.7
ER-EC-6	528.8 to 501.6	4	CHCU	sz	108.9	3/8/2000	72.7

Table C.7-2
Subregional Lower Boundary Heat Flux Estimates^a
 (Page 2 of 5)

Borehole	Elevation Range (m)	Structural Zone Number	HSU	Measured Type ^b	Estimated Heat Flow (mW/m ²)	Temperature Log (Date)	Calibrated Model Heat Flux (mW/m ²)
Subregion (2), Silent Canyon Caldera Complex, continued							
ER-EC-6	501.1 to 480.1	4	CFCM	sz	124.9	3/8/2000	72.7
ER-EC-6	479.5 to 455.9	4	CFCM	sz	126.6	3/8/2000	72.7
ER-EC-6	455.4 to 405.4	4	CFCM	sz	127.0	3/8/2000	72.7
ER-EC-6	404.9 to 367.1	4	CFCM	sz	131.5	3/8/2000	72.7
U-20bg	1,380.7 to 1,361.5	7	CHZCM	uz	28.9	6/22/1992	72.7
UE-20ab	1,487.7 to 1,426.8	7	CHVCM	uz	47.1	6/5/1978	72.7
ER-20-2#1	1,340.4 to 1,323.6	7	CHZCM	cwl	51.1	2000-2002	72.7
PM-1	1,358.5 to 1,330.4	7	CHZCM	cwl	46.1	8/3/1994	72.7
PM-1	1,042.1 to 1,029.9	7	BFCU	sz	60.2	8/3/1994	72.7
PM-1	1,029.8 to 972.6	7	BFCU	sz	56.9	8/3/1994	72.7
PM-1	972.3 to 931.4	7	BFCU	sz	55.9	8/3/1994	72.7
UE-20bh#1	1,321.7 to 1,306.4	7	CHZCM	cwl	51.1	2000-2002	72.7
UE-20bh#1	1,199.8 to 1,169.2	7	CHZCM	sz	48.7	10/1/1991	72.7
U-19aj	1,490.8 to 1,435.9	8	BFCU	uz	22.3	12/9/1980	72.7
U-19aS	1,496.9 to 1,393.2	8	CHVTA	uz	28.5	10/4/1964	72.7
U-19e	1,481.0 to 1,404.8	8	BFCU	uz	32.1	3/6/1966	72.7
U-19e	691.6 to 664.2	8	BRA	sz	162.1	3/6/1966	72.7
U-19e	661.1 to 642.8	8	BRA	sz	116.4	3/6/1966	72.7
U-19e	636.7 to 597.1	8	BRA	sz	119.0	3/6/1966	72.7
U-19g	1,464.3 to 1,427.7	8	CFCU	uz	32.6	11/19/1965	72.7
U-19f	1,302.7 to 1,296.6	9	CHCU	uz	43.3	7/5/1968	72.7
UE-19h	1,423.1 to 1,407.9	10	BRA	cwl	108.7	2000-2002	72.7

Table C.7-2
Subregional Lower Boundary Heat Flux Estimates^a
 (Page 3 of 5)

Borehole	Elevation Range (m)	Structural Zone Number	HSU	Measured Type ^b	Estimated Heat Flow (mW/m ²)	Temperature Log (Date)	Calibrated Model Heat Flux (mW/m ²)
Subregion (2), Silent Canyon Caldera Complex, continued							
U-19i	1,364.3 to 1,358.2	11	CFCU	uz	65.5	8/24/1967	72.7
U-19i	1,129.6 to 1,099.1	11	BFCU	sz	76.9	8/24/1967	72.7
U-19i	1,096.1 to 1,074.7	11	BFCU	sz	83.0	8/24/1967	72.7
U-19i	1,071.7 to 1,053.4	11	BFCU	sz	76.3	8/24/1967	72.7
U-19p	1,468.8 to 1,459.7	12	BFCU	uz	39.8	10/29/1975	72.7
U-19t	1,554.7 to 1,414.4	13	KA	uz	55.0	9/27/1993	72.7
U-19t	1,245.2 to 1,143.0	13	BRA	sz	92.8	9/27/1993	72.7
UE-19cWW	1,430.5 to 1,415.2	13	BFCU	cwl	62.1	2000-2002	72.7
Subregion (3), East Timber Mountain Caldera Complex and Black Mountain Caldera							
ER-18-2	1,287.8 to 1,272.5	17	TMCM	cwl	80.8	2000-2002	100
UE-18t	1,305.4 to 1,299.7	18	FCCM	cwl	58.7	12/12/1999	100
UE-18t	1,188.4 to 1,146.1	18	TMCM	sz	84.7	12/12/1999	100
UE-18t	1,143.9 to 1,088.1	18	TMCM	sz	58.8	12/12/1999	100
UE-18t	1,085.8 to 1,062.4	18	TMCM	sz	75.8	12/12/1999	100
UE-18t	1,059.9 to 1,008.6	18	TMCM	sz	86.2	12/12/1999	100

Table C.7-2
Subregional Lower Boundary Heat Flux Estimates^a
 (Page 4 of 5)

Borehole	Elevation Range (m)	Structural Zone Number	HSU	Measured Type ^b	Estimated Heat Flow (mW/m ²)	Temperature Log (Date)	Calibrated Model Heat Flux (mW/m ²)
Subregion (4), West Timber Mountain Caldera Complex							
ER-EC-2A	1264.2 to 1,248.9	15	FCCM	cwl	34.1	2000-2002	49
ER-EC-5	1225.5 to 1,212.7	15	TMCM	cwl	30.9	6/7/2000	49
UE-18r	1268.1 to 1,191.5	16	TMCM	cwl	31.5	3/16/1993	49
UE-18r	442.6 to 321.0	16	TMCM	sz	81.5	3/16/1993	49
UE-18r	321.0 to 267.6	16	TMCM	sz	78.0	3/16/1993	49
UE-18r	267.5 to 246.4	16	TMCM	sz	78.6	3/16/1993	49
UE-18r	246.3 to 181.6	16	TMCM	sz	74.4	3/16/1993	49
ER-EC-8	1,222.4 to 1,207.1	19	FCCM	cwl	104.0	2000-2002	49
ER-EC-7	1,333.3 to 1,237.0	21	FCCM	uz	40.3	8/8/1999	49
ER-EC-7	1,096 to 1,081.8	21	FCCM	sz	61.3	8/8/1999	49
Subregion (5), Extracaldera Area East of Timber Mountain and Silent Canyon Caldera Complexes							
ER-19-1#2	1,508.5 to 1,493.2	14	PBRCM	cwl	37.3	2000-2002	45
ER-19-1	999.2 to 929.2	14	LCCU1	sz	90.3	12/6/1993	45
ER-19-1	928.8 to 779.4	14	UCCU	sz	68.9	12/6/1993	45
HTH-1	1,427.4 to 1,331.7	14	PBRCM	cwl	33.2	8/19/1991	45
HTH-1	1,115.6 to 1,085.7	14	PBRCM	sz	28.1	8/19/1991	45
HTH-1	1,037.8 to 799.8	14	PBRCM	sz	30.9	8/19/1991	45
HTH-1	798.3 to 749.5	14	PBRCM	sz	26.8	8/19/1991	45
Subregion (6), Extracaldera Areas West of Silent Canyon Caldera Complex and West and South of Timber Mountain Caldera Complex							
PM-3#2	1,331.2 to 1,315.9	5	UPCU	cwl	55.6	2000-2002	45
UE-20j	1,369.5 to 1,271.9	5	PVTA	cwl	48.1	9/5/1964	45
ER-EC-4	1,237.4 to 1,222.9	20	TCVA	uz	88.9	6/2/1999	45
ER-EC-4	599.1 to 564.7	20	TMA	sz	28.5	8/25/2000	45

Table C.7-2
Subregional Lower Boundary Heat Flux Estimates^a
 (Page 5 of 5)

Borehole	Elevation Range (m)	Structural Zone Number	HSU	Measured Type ^b	Estimated Heat Flow (mW/m ²)	Temperature Log (Date)	Calibrated Model Heat Flux (mW/m ²)
Subregion (6), Extracaldera Areas West of Silent Canyon Caldera Complex and West and South of Timber Mountain Caldera Complex, continued							
ER-EC-4	564.2 to 539.4	20	TMA	sz	33.7	8/25/2000	45
ER-EC-4	518.2 to 505.2	20	TMA	sz	53.8	8/25/2000	45
ER-OV-3a2	1,122.9 to 1,107.6	22	DVCM	cwl	38.0	2000-2002	45
ER-OV-3b	1,184.5 to 1,169.3	22	AA	cwl	23.0	2000-2002	45
ER-OV-3c2	1,212.3 to 1,197.1	22	TMA	cwl	65.2	2000-2002	45

^aSee text for explanation of anomalous high heat fluxes (compiled from [Attachment A, Tables A1 and A2](#)).

^bTemperatures measured at composite water level are prone to error; estimated heat flux represents minimum value.

more detail to the distribution of deep heat flux at the base of the model, the value of 72.7 mW/m² estimated for the SCCC as a whole seems to be a reasonable average value.

C.7.2.3.3 Subregion (3), East Timber Mountain Caldera Complex and Black Mountain Caldera

The number of calibration points for this subregion was severely limited by the quality of the temperature log for borehole ER-18-2 ([Attachment A, Figure C26](#)) and the grid resolution at borehole UE-18t ([Attachment A, Figure C27](#)). The calibrated heat flux of 100 mW/m² for subregion (3), which was constrained by only 2 temperature measurements in this subregion, appears to be high, based on the heat fluxes of 58 to 86 mW/m² estimated directly from the temperature logs. Again, however, lateral spreading of heat between the base of the model at -3,500 m and the much higher elevations (>1,000 m) at which the temperature-log based estimates were made may explain part of the difference in these estimates ([Figure C.7-12](#)).

C.7.2.3.4 Subregion (4), West Timber Mountain Caldera Complex

Grid resolution and the generally poor quality of the temperature logs limited the number of calibration points in subregion (4) to one each at boreholes UE-18r, ER-EC-8 and ER-EC-7 (Figure C.7-11; Attachment A, Figures C24, C25, C28, and C30). Moreover, the simulated temperature at the measurement elevation in borehole ER-EC-7 was relatively insensitive to heat flux because of its proximity to the fixed water table temperature and there was considerable uncertainty in the water table temperature at borehole ER-EC-8 (Attachment A, Figure C28). Even in light of these issues, however, the calibrated heat flux of 49 mW/m² may be somewhat low, based on the values of heat flux of 74 to 82 mW/m² calculated directly from deep portions of the temperature log at borehole UE-18r (Table C.7-2).

C.7.2.3.5 Subregion (5), Extra-Caldera Area East of the Timber Mountain and Silent Canyon Caldera Complexes

The calibrated heat flux of 45 mW/m² may be a reasonable estimate of heat flux in Subregion (5), based on the range in heat flux of 27 to 90.3 mW/m² estimated directly from temperature logs at boreholes ER-19-1 and HTH-1 (Table C.7-2). However, temperature logs at these boreholes are interpreted to have been strongly affected by groundwater flow (see Section C.8.0), so unbiased estimates of deep heat flux may not exist for this subregion.

C.7.2.3.6 Subregion (6), Extra-Caldera Areas West of Silent Canyon Caldera Complex and West and South of the Timber Mountain Caldera Complex

The heat flux of 45 mW/m² estimated by the model calibration was driven by the relatively cool temperatures measured in boreholes PM-3 (Attachment A, Figure C10) and ER-EC-4 (Attachment A, Figure C24). A heat flux of 45 mW/m² was the permissible lower limit allowed in the calibration; heat fluxes below this value were believed to be unrealistic, given the base-case estimate of 85 mW/m² for deep regional heat flux. The cool temperatures measured in boreholes PM-3 and ER-EC-4 are interpreted to be the result of groundwater flow processes (Section C.8.0). Based on this interpretation, unbiased estimates of deep heat flux may not exist for this subregion.

C.8.0 HYDROLOGICAL SIGNIFICANCE OF TEMPERATURE RESIDUALS

The differences (residuals) between the temperatures simulated with heat-conduction models described in this report and measured temperatures reflect the potential influence of many factors. These residuals may simply be the result of uncertainties in boundary conditions, thermal conductivity estimates, hydrostratigraphy, grid resolution and other aspects of the model's construction. Alternatively, the residuals may reflect the omission of advective heat-transport processes in the heat-conduction model and so, may be indirect indicators of groundwater flow patterns in the PM/OV flow system

The one-dimensional simulations presented earlier in this appendix that include both conductive and advective heat-transport indicate that in areas of vertical groundwater movement, conductive heat fluxes can be both larger and smaller than for conduction alone, depending on elevation (Figure C.2-1). This observation is true for both upward and downward groundwater movement. In areas of upward groundwater movement, however, conductive heat fluxes increase with elevation; conversely, in areas of downward groundwater movement, conductive heat fluxes decrease with elevation. Therefore, conductive heat flux is not diagnostic of the direction of groundwater movement unless heat-flux estimates are available at multiple elevations in a borehole. Discrepancies between simulated and measured temperatures provide a more unique interpretation of flow directions when measurements from only a single elevation (or narrow range of elevations) are available. Regardless of the elevation at which the measurements are made, temperatures in areas of downward groundwater flow are always cooler, and temperatures in areas of upward groundwater flow are always warmer, than temperatures produced by heat conduction alone. Therefore, except in rare instances where reliable heat flux estimates from multiple elevations are available, the interpretations in the following sections focus on the differences between simulated and measured temperatures.

Normal faults, caldera boundaries and other structural features disrupt the continuity of HSUs in the PM/OV flow system and may provide preferential pathways across confining units. Therefore, if significant vertical flow across confining units exists, it is most likely that it occurs through these structural features. To investigate this possibility, structural features are included on maps showing the distribution of borehole temperature residuals (Figures C.7-5, C.7-8, and C.7-11). These maps were analyzed jointly with summary plots of simulated versus measured temperatures from multiple boreholes (Figures C.7-5, C.7-6, C.7-7, C.7-9, and C.7-11) and plots of simulated and measured temperature profiles at individual Wells (Attachment A, Figures C1 to C30). The analyses that follow focus on the residuals produced with the inverse variable heat-flux model described in Section C.7.2.2.2. Calibrating heat fluxes at the base of the model domain in which heat flux was estimated at six distinct zones along the bottom boundary. However, when interpreting residuals from this model, it was also considered if these residuals could be explained by other factors, such as a poor estimate of water table temperature at the well, or if the residuals were considerably smaller for the alternative heat-conduction models described in this report. Temperature residuals in the variable heat-flux model, which arose because of poor estimates of water table temperature, or which were significantly smaller in other heat conduction models, were not interpreted in terms of their possible hydrologic significance.

C.8.1 Subregion (2) - Silent Canyon Caldera Complex

In the southwestern part of the SCCC, it is likely that the deep heat flux is actually higher than the heat flux of 73 mW/m² estimated for the caldera complex as a whole with the variable heat-flux model, and that cool groundwater from the shallow saturated zone flows downward through the upper units. These interpretations are supported by a detailed examination of temperature residuals from this area, as follows. The heat-conduction model with a uniform heat flux of 85 mW/m² provides a good match to the measured temperatures at borehole ER-EC-6 (Figure C.7-5 and Attachment A, Figure C9), but underestimates the deepest measurement in the region - the temperature of 121°C measured at a 12,270 ft depth in borehole UE-20f (not shown). Conversely, simulated temperatures in nearby boreholes U20c, U20d and ER-20-5 #3 in the southwest part of the caldera complex are warmer than the measured temperatures for deep heat fluxes of either 85 or 73 mW/m² (see residuals on Figures C.7-5 and C.7-11). A heat flux of 85 mW/m² would improve the match between simulated and measured temperatures at boreholes UE-20f, ER-EC-6 and ER-EC-1, where measured

temperatures are underestimated by the model with a deep heat flux of 73 mW/m² for the SCCC (Figure C.7-10). However, the use of a higher heat flux in the heat-conduction model would increase the mismatch between simulated and measured temperatures at boreholes U20c, ER-20-5#3, and U-20d, which the model indicates are already slightly too warm for a heat flux of 73 mW/m² (Figure C.7-10). To offset the temperature increases that would result from higher deep heat fluxes, a mechanism to cool the subsurface temperatures in the southwestern part of the SCCC is required. The downward hydraulic gradient, dipping beds and discontinuous confining units (e.g., the CHCU and LPCU) in the upper part of southwest Area 20 (Wolfsberg et al. 2002; BN, 2002, cross-section J-J') indicate that hydrogeologic conditions are favorable for cool groundwater near the water table to flow downward along the dipping beds or faults to deeper aquifers such as the IA, thereby reducing temperatures and heat fluxes below the wells in this region.

In the northeastern part of the SCCC, the simulated temperatures are higher than the measured temperatures at borehole U-19e for the calibrated variable heat-flux model (Figure C.7-11 and Attachment A, Figure C15). Although the temperature data at borehole U-19e are reasonably well matched with a uniform heat flux of 45 mW/m² (Figure C.7-7), temperatures at borehole U19-i, located about 5 km to the south of borehole U-19e, are underestimated using this heat flux, and better matched with a heat flux of 85 mW/m² (Figure C.7-5 and Attachment A, Figure C15). It is possible that heat flux varies significantly within the SCCC complex. However, an alternative hydrologic explanation is that downward groundwater movement, possibly through the Halfbeak Fault (see BN, 2002, cross-section C-C') significantly cools the rocks and reduces heat flux near borehole U-19e.

C.8.2 Subregion (4) - Western Timber Mountain Caldera Complex

Borehole UE-18r was characterized by Gillespie (2003) as having dominantly conductive heat flow (~ 25 mW/m²) and reliable temperatures measurements above the bottom of the borehole casing at a depth of 496.5 m (elevation 1,192 m). Unfortunately, simulated temperatures at these elevations are dominated by the upper boundary conditions and are insensitive to the assumed thermal conductivity estimates and lower boundary conditions. Hence, it was necessary to use a deep temperature measurement from below the borehole casing as a calibration target in the inverse models. The simulated temperatures are significantly warmer than this deep measurement from borehole UE-18r

for all lower boundary conditions considered in this report (Figures C.7-5 through C.7-9 and C.7-11; Attachment A, Figures C24 and C25). The consistent overestimation of the measured temperature indicates that downward groundwater flow may have cooled the rocks near the bottom of the temperature profile. Borehole UE-18r penetrates a fault breccia (Tmrx) at depth, which suggests that groundwater flow along the fault associated with this breccia may have cooled nearby temperatures. This interpretation is also consistent with the relatively low heat flux of 25 mW/m² estimated by Gillespie (2003) above elevations of 1,192 m and the much larger heat flux (> 75 mW/m²) estimated below a 443 m elevation (Table C.7-2). Based on one-dimensional scoping simulations (Figure C.2-1), heat flux is expected to decrease with elevation in areas of downward groundwater flow. However, groundwater carbon-14 measured in the borehole is very low (Chapman et al., 1995), ruling out modern recharge as a likely influence on groundwater temperatures and suggesting that the downward movement of groundwater from laterally upgradient areas is a more likely explanation for the decrease in heat flux with elevation at borehole UE-18r.

C.8.3 Subregion (5) - Extra-Caldera Area East of Timber Mountain and Silent Canyon Caldera Complexes

The simulated temperatures at boreholes HTH-1 and ER-19-1 in the eastern part of the PM/OV flow domain were significantly warmer than the measured temperatures for all models with specified deep heat fluxes discussed in this report (Attachment A, Figures C21 and C22), including the variable heat-flux model (Figure C.7-11). Several related hypotheses involving the downward movement of groundwater may explain the relatively cool temperatures measured in boreholes HTH-1 and ER-19-1. The first hypothesis involves the downward movement of groundwater recharge in this part of the NTS. Isotopic data were not available from boreholes HTH-1 or ER-19-1 to evaluate whether young recharge is present in the groundwater at these boreholes. However, relatively high groundwater carbon-14 activities of 25 to 75 pmc in nearby boreholes WW-8, ER-30-1 and 29a #2 may indicate that the Fortymile Canyon and surrounding areas are locations with comparatively high recharge rates (SNJV, 2004 Figure 5). Downward groundwater flow would result from locally high recharge rates and cause temperatures to be relatively cool at these boreholes. The second related hypothesis involves the Belted Range Thrust Fault. This thrust fault, which intersects the lower part of borehole ER-19-1, could help to focus downward groundwater movement and reduce the measured temperatures and heat fluxes at elevations above the fault.

C.8.4 Subregion (6) - Extra-Caldera Areas West of Silent Canyon Caldera Complex, and West and South of the Timber Mountain Caldera Complex

Measured temperatures at borehole ER-EC-4 are consistently cooler than the temperatures calculated with the calibrated variable heat-flux model (Figure C.7-11 and Attachment A, Figure C29). These temperature differences, along with a decrease in the estimated heat flux from 54 to 28 mW/m² through the lower part of the borehole (Table C.7-2), indicates the presence of downward groundwater movement near this borehole. One hypothesis that might explain the low temperatures and heat flux at borehole ER-EC-4 is that HSUs in this area, including the very thick and transmissive LCA, have an apparent southward dip (BN, 2002 cross-section G-G'). As groundwater moves southward through this area, the downward flow component induced by the dip of the beds causes the groundwater to become warmer, thereby consuming heat and decreasing the temperature and heat flux in the overlying rocks. Despite the location of borehole ER-EC-4 along a major canyon, there is no evidence from geochemical and isotopic data, such as delta deuterium or carbon-14, that groundwater near borehole ER-EC-4 receives significant recharge (SNJV, 2004 Figures 5 and 6).

C.9.0 SUMMARY AND CONCLUSIONS

A 3-D steady-state heat-conduction model was developed for the PM/OV flow domain in order to (a) provide a 3-D temperature distribution for steady-state flow modeling and (b) to investigate if borehole temperature data from this region might provide information about vertical groundwater movement by identifying locations in the model domain where temperatures could not be explained by conduction. The temperature observations that could not be satisfactorily explained by the conduction model were used as the basis for developing possible explanations involving groundwater flow.

Development of the model utilized the existing hydrostratigraphy of the PM/OV flow model as the starting point. Thermal conductivities were assigned to 46 individual HSUs present in the model, based on the thermal conductivities measured on various rock types and the proportions of those rock types present in the individual HSUs. Temperatures measured in the deep unsaturated zone or shallow saturated zone were used to develop a map of water table temperatures that was used as the upper thermal boundary condition in the model. The lower boundary condition was treated as either a constant temperature boundary (160 °C), or as a specified heat flux boundary. Forward heat-conduction models assumed uniform specified heat fluxes of 45, 65, 85 and 105 mW/m² along the lower boundary of the model. Based on these forward heat-conduction models, inverse heat-conduction models were created that either (1) optimize the thermal conductivities of three groups of volcanic HSUs for a specified lower heat flux of 65 mW/m², or (2) estimate the heat flux for six intra- or extra-caldera domains at the base of the model, using the base-case estimates of thermal conductivity in each of the 46 HSUs. Evaluation of the forward and inverse models was done by comparing simulated temperatures with borehole temperatures measured over a four-decade period by various investigators. The development of a sub-set of reliable temperature measurements to use as calibration targets required careful screening of scores of digitized temperature profiles to eliminate portions of temperature logs where flow within the borehole may have disturbed *in situ*

temperatures. Limited grid resolution in parts of the model domain also limited the number of temperature measurements that could be used for direct comparison with the simulated temperatures.

Differences between temperatures simulated with the heat-conduction models and the measured temperatures are potentially the results of many factors, including (1) uncertainty in the spatial variations in the deep heat flux, (2) uncertainty in the hydrostratigraphy (especially below depths sampled by boreholes), (3) uncertainty in thermal conductivities estimates, and (4) groundwater movement. The hydrologic interpretations of the differences between simulated and measured temperatures are therefore only one of several possible explanations of these differences.

Possible hydrologic explanations of temperature residuals within the PM/OV flow domain include (1) the downward flow of cool groundwater along the West Boxcar Fault or dipping beds in the southwest corner of the Area 20 caldera, (2) the downward flow of cool groundwater near the Halfbeak Fault (Area 20 structural margin) in the northeast part of the SCCC, (3) downward groundwater flow through the brecciated rocks along the northern structural margin of the Timber Mountain caldera complex near borehole UE-18r, (4) downward groundwater movement along the Belted Range Thrust Fault near the eastern model boundary, perhaps associated with higher recharge rates in this area, and (5) a downward groundwater flow component in rocks west of the Silent Canyon and Timber Mountain caldera complexes that is induced by the southerly apparent dip of rocks (including the highly transmissive LCA) in this area. Although the hydrologic interpretations of the temperature residuals are only one of several possible explanations, they indicate areas where the numerical model of groundwater flow in the PM/OV flow domain should be examined for consistency with these explanations.

C.10.0 REFERENCES

- Beck, A.E., G. Garven, and Stegena, 1989, Hydrogeological regimes and their subsurface thermal effects, AGU Geophysical Monograph 47, IUGG v. 2.
- Arnold, B.W., G. Zyvoloski, K. Economy, and M. Wallace, 2003, Thermal transport in the saturated zone site-scale model at Yucca Mountain, International High-level Radioactive Waste Management Conference, Las Vegas, Nevada.
- Barroll, M.W., 1989, Analysis of the Socorro hydro-geothermal system, central New Mexico, Ph.D. Dissertation, 81 pp., Appendices.
- Bechtel Nevada, 2002, A hydrostratigraphic model and alternatives for the groundwater flow and contaminant transport model of corrective action units 101 and 102: Central and Western Pahute Mesa, Nye County, Nevada, DOE/NV/11718-706.
- Blankennagel, R.K., and J.E. Weir, Jr., 1973, Geohydrology of the Eastern Part of Pahute Mesa, Nevada Test Site, Nye County, Nevada: USGS Professional Paper 712-B, 35 pp.
- Bodvarsson, G.S., S. Vonder Haar, M.J. Wilt, and C.F. Tsang, 1982, Preliminary studies of the reservoir capacity and generating potential of the Baca geothermal field, New Mexico, Water Resources Research, v. 18, p. 1713-1723.
- Bodvarsson, G.S., E. Kwicklis, C. Shan, and Y.S. Wu, 2003, Estimates of percolation flux from borehole temperature data at Yucca Mountain, Nevada, Journal of Contaminant Hydrology, v.62-63, p. 3-22.
- Brodsky, N.S., M. Riggins, J. Connolly, and P. Ricci, 1997, Thermal expansion, thermal conductivity, and heat capacity measurements for boreholes UE-25 NRG-4, UE25 NRG-5, USW NRG-6, and USW NRG-7/7A, SAND95-1955, 77 pp., Appendices
- Byers, F.M., Jr., W.J. Carr, P.P. Orkild, W.D. Quinlivan, and K.A. Sargent, 1976, Volcanic suites and related cauldrons of Timber Mountain-Oasis Valley caldera complex, southern Nevada, U.S. Geol. Survey Prof. Paper 919, 70 pp.
- Chapman, J.B., R.L. Hershey, and B.F. Lyles, 1995, Groundwater velocities at the Nevada Test Site: ¹⁴Carbon-based estimates, technical report #45135, DOE/NV/11508-03 UC-703, Desert Research Institute, Las Vegas, NV.

- Constantz, J., S.W. Tyler, and E. Kwicklis, 2003, Temperature-profile methods for estimating percolation rates in arid environments, *Vadose-Zone Journal* v.2, p. 12-24.
- Doherty, J., 2000, PEST, Model-Independent Parameter Estimation Users Manual, Watermark Numerical Computing, <http://members.ozemail.com.au/~wcomp/>, distributed as freeware software with documentation from SS Popadopoulos & Associates, Inc., <http://www.sspa.com/pest> (URL confirmed July, 2002).
- Faulds, J.E., and R.J. Varga, 1998, The role of accommodation zones and transfer zones in the regional segmentation of extended terrains, in J.E. Faulds and J.H. Stewart, eds., *Accommodation zones and transfer zones: the regional segmentation of the Basin and Range Province*, GSA Special Paper 323, pp. 1-45.
- Fridrich, C.J, W.W. Dudley, Jr, and J.S. Stuckless, 1994, Hydrogeologic analysis of the saturated zone ground-water system under Yucca Mountain, Nevada, *Journal of Hydrology*, v. 154, p. 133-168.
- Giles, M.R., 1997, *Diagenesis: A quantitative perspective*, Kluwer Academic Publishers.
- Gillespie, D., 2003, Temperature data evaluation, DOE/NV/13609-22; Publication No. 45194, 35 pp.
- Grauch, V.J.S., D.A. Sawyer, C.J. Fridrich, and M.R. Hudson, 1999, Geophysical framework of the southwestern Nevada volcanic field and hydrogeologic implications, U.S. Geological Survey Professional Paper 1608, 39 pp.
- Jiracek, G.R., C.L. Kinn, C.L. Scott, M.G. Kuykendall, W.S. Baldrige, S. Biehler, L.W. Braile, J.F. Ferguson, and B. Gilpin, 1996, Tracing crustal isotherms under the western margin of the Jemez Mountains using SAGE and industry magnetotelluric data, in NMGS Guidebook, 47th Field Conference, pp. 129-133.
- Kwicklis, E., D. Broxton, D. Vaniman, and A. Wolfsberg, 2003, Investigation of the influence of faults on groundwater movement in the Pahute Mesa/Oasis Valley flow model domain, Letter Report to DOE.
- Lappin, A.R., and F.B. Nimick, 1982, Thermal properties of the Grouse Canyon Member of the Belted Range Tuff and of Tunnel Bed 5, G-tunnel, Nevada Test Site, SAND82-2203. 47 pp.
- Lin, G., J.A. Nunn, and D. Deming, 2000, Thermal buffering of sedimentary basins by basement rocks: implications arising from numerical simulations, *Petroleum Geoscience*, v. 6, pp. 299-307.
- McKinley, P.W., M.P. Long, and L.V. Benson, 1991, Chemical analyses of water from selected wells and springs in the Yucca Mountain area, Nevada and southeastern California: USGS Open-file Report 90-355, 47 pp.

- Morgan, P., J.H. Sass, and R.D. Jacobson, 1996, Heat flow in VC-2a and VC-2b, and constraints on the thermal regime of the Valles Caldera, New Mexico, in NMGS Guidebook, 47th Field Conference, pp. 231-236.
- Olmsted, F.H., and F.E. Rush, 1987, Hydrogeologic reconnaissance of the Beowawe geysers geothermal area, Nevada: *Geothermics*, v. 16, no. 1, pp. 27-46.
- Painter, S., J. Winterle, and A. Armstrong, 2003, Using temperature to test models of flow near Yucca Mountain, Nevada: *Groundwater*, v. 41, no. 5, pp. 657-666.
- Phillips, O.M., 1991, Flow and reactions in permeable rocks, Cambridge University Press, New York, pp. 34-35.
- Pottoroff, E.J., S.J. Erikson, and M.E. Campana, 1987, Hydrologic utility of borehole temperatures in areas 19 and 20, Pahute Mesa, Nevada Test Site, DOE/NV/10384-19, Publication No. 45060, 189 pp.
- Rehfeldt, K.R., 2002, Assessment of groundwater temperature logs, Geotrans Inc.
- Reiter, M., 1999, Hydrogeothermal studies on the southern part of Sandia National Laboratories/Kirtland Air Force Base—Data regarding ground-water flow across the boundary of an intermontane basin, in *Faults and Subsurface fluid flow in the shallow crust*, eds, L. Goodwin, P. Mosely, pp. 207-222.
- Rose, T.P., F.C. Benedict, Jr., J.M. Thomas, W.S. Sicke, R.L. Hershey, J.B. Paces, I.M. Farnham, and Z.E. Peterman, 2002, *Geochemical Data Analysis and Interpretation of the Pahute Mesa—Oasis Valley Groundwater Flow System, Nye County, Nevada*, Preliminary report to the National Nuclear Security Administration, U.S. Department of Energy.
- Rousseau, J.P., E.M. Kwicklis, and D.C. Gillies, eds., 1999, *Hydrogeology of the unsaturated zone, North Ramp Area of the Exploratory Studies Facility, Yucca Mountain, Nevada*, U.S. Geological Survey Water-Resources Investigations Report 98-4050, Denver, CO., 244 p.
- Sass, J.H., and A.H. Lachenbruch, 1982, Preliminary interpretation of thermal data from the Nevada Test Site, USGS Open-file Report 82-973, 30 pp.
- Sass, J.H., A.H. Lachenbruch, and C.W. Mase, 1980, Analysis of thermal data from drill holes UE25a-3 and UE25a-1, Calico Hills and Yucca Mountain, Nevada Test Site, USGS Open-file Report 80-826.
- Sass, J.H., A.H. Lachenbruch, S.S. Priest, R.J. Munroe, and W.W. Dudley, Jr., 1987, Temperature, thermal conductivity, and heat flow near Yucca Mountain, Nevada: some tectonic and hydrologic implications, USGS Open-file Report 87-649, 96 pp.

- Sass, J.H., W.W. Dudley, Jr., and A.H. Lachenbruch, 1995, Chapter 8: Regional thermal setting; in Major results of geophysical investigations at Yucca Mountain and vicinity, southern Nevada, eds. H.W. Oliver, D.A. Ponce, and W.C. Hunter, USGS Open-file Report 95-74, pp. 157-170.
- Sawyer, D.A., R.J. Fleck, M.A. Lamphere, R.G. Warren, D.E. Broxton, and M.R. Hudson, 1994, Episodic caldera volcanism in the Miocene southwestern Nevada volcanic field: Revised stratigraphic framework, 40Ar/39Ar geochronology, and implications for magmatism and extension, GSA Bulletin, v. 106, p. 1304-1318.
- Stoller-Navarro Joint Venture. 2004. *Hydrologic Data for the Groundwater Flow and Contaminant Transport Model of Corrective Action Units 101 and 102: Central and Western Pahute Mesa, Nye County, Nevada*, Rev. 0, S-N/99205-002; Shaw/13052-204. Las Vegas, NV.
- White, A.F., 1979, Geochemistry of ground water associated with tuffaceous rocks, Oasis Valley, Nevada: USGS Professional Paper 712-E, 25 pp.
- Wolfsberg, A., L. Glascoe, G. Lu, A. Olson, P. Lichtner, M. McGraw, T. Cherry, and G. Roemer, 2002, TYBO/BEHNAM: Model analysis of groundwater flow and radionuclide migration from underground nuclear tests in southwestern Pahute Mesa, Nevada, Los Alamos National Laboratory Report LA-13977, Los Alamos, New Mexico.
- Wollenberg, H.A., J.S.Y. Wang, and G. Korbin, 1983. An appraisal of nuclear waste isolation in the vadose zone in arid and semiarid regions (with emphasis on the Nevada Test Site), Lawrence Berkeley National Laboratory technical report 15010, Berkeley, California.
- Woodbury, A.D., L. Smith, and W.S. Dunbar, 1987, Simultaneous inversion of hydrogeologic and thermal data: 1 – Theory and application using hydraulic head data, Water Resources Research, v. 23, no. 8, p. 1586-1606.
- Woodbury, A.D., and L. Smith, 1988, Simultaneous inversion of hydrological and thermal data, 2. Incorporation of thermal data, Water Resources Research, v. 24, no. 3, pp. 356-372.
- Zyvoloski, G.A., B.A. Robinson, Z.V. Dash, and L. Trease, 1997. Summary of the Models and Methods for the FEHM Application – A Finite-Element Heat-and Mass-Transfer Code. Report LA-13307-MS, Los Alamos, New Mexico: Los Alamos National Laboratory.



Attachment A

Supporting Data, Calculations, and Figures for Appendix C

(As provided by Los Alamos National Laboratory)
Andrew Wolfsberg

Table A1. Depth and elevation range, hydrostratigraphic unit, and temperature gradients for deepest unsaturated-zone or cwl. Depth intervals with temperature gradients that may represent the ambient temperature gradient are shown in bold. Depth intervals with reasonable temperature gradients that are not consistent within an hsu or spatial location are bold italicized.

E	N	UZ or cwl temp (C)	Borehole	Elev range (m)	Strat ¹	Class/rock type ¹	HGU ¹	HSU ¹	Grad T (C/km)	Std dev (C/km)	R ²	Saturation (u,s) ²	Temp log (date)	l (W/m C)	Est. Heat Flow (mW/m ²)
Purse Fault-W. Boxcar Fault (1)															
545113.1	4119467.8	40.2	ER-20-1 ²⁴	1277.8 - 1261.0	Tpcm	MWT	WTA	TCA	14.8	10.8		s, below cwl	2000-2002		
546386	4119208	29.5	ER-20-5#1	1349.9 - 1301.1	Tpcm	MWT	WTA	TCA	28.2	1.5	0.99	u, deep uz	11/3/95		
546386	4119208	30.2	ER-20-5#1	1301.1 - 1276.5	Tp	BED	TCU	LPCU	30.3	2.3	0.97	u, deep uz	11/3/95	1.15	34.8
546386	4119208	32.7	ER-20-5#1	1274.2 - 1242.9	Tp	BED	TCU	LPCU	15.9	1.0	0.99	s, below cwl	11/3/95		
546385	4119177	37.2	ER-20-5#3 ⁵	1301.1 - 1275.8	Tp	BED	TCU	LPCU	60.0	10.5	0.81	u, deep uz	2/6/96Inl		
546385	4119177	36.6	ER-20-5#3 ⁵	1291.0 - 1285.1	Tp	BED	TCU	LPCU	98.8	4.4	0.99	u, deep uz	2/6/96Inl		
546385	4119177	37.2	ER-20-5#3 ⁵	1284.9 - 1275.8	Tp	BED	TCU	LPCU	117.7	1.9	0.97	u, deep uz	2/6/96Inl		
546385	4119177	38.1	ER-20-5#3 ⁵	1275.0 - 1242.9	Tp	BED	TCU	LPCU	28.2	0.8	0.97	s, below cwl	2/6/96Inl	1.73	48.7
546699	4120478	27.1	U-20c	1667.5 - 1624.8	unk	BED	VTA	PVTA	33.2	1.8	0.95	u, deep uz	4/5/65		
546699	4120478	29.8	U-20c	1624.8 - 1310.9	Tpb	LA	LFA	BA	10.3	0.6	0.98	u, deep uz	4/5/65		
546699	4120478	30.6	U-20c	1301.8 - 1277.4	Tpb	LA	LFA	BA	26.9	0.8	0.93	u, deep uz	4/5/65	1.95	52.6
546699	4120478	31.2	U-20c	1271.3 - 1164.6	Tpcm	TUF	unk	TCA	10.0	1.0	0.94	s, below cwl	4/5/65		
546699	4120478	31.8	U-20c ³	1310.9 - 1302.0	Tpb	LA	LFA	BA	24.1	0.8	0.93	u, deep uz	9/27/68		
546699	4120478	31.8	U-20c³	1301.8 - 1277.6	Tpb	LA	LFA	BA	23.4	0.8	0.99	u, deep uz	9/27/68	1.95	45.7
546699	4120478	32.4	U-20c ³	1273.3 - 1249.1	Tpcm	TUF	unk	TCA	13.1	0.4	0.98	s, below cwl	9/27/68		
546699	4120478	33.2	U-20c ³	1215.7 - 1164.8	Tpcm	TUF	unk	TCA	19.1	0.5	0.99	s, below cwl	9/27/68		
546103	4122301	27.6	U-20d	1506.3 - 1341.7	unk	BED	VTA	PVTA	18.7	1.3	0.96	u	1/31/67		
546103	4122301	28.0	U-20d	1341.7 - 1332.6	unk	BED	VTA	PVTA	59.2	1.4	0.83	u	1/31/67		
546103	4122301	35.8	U-20d	1332.6 - 1271.6	Tpb	LA	LFA	BA	56.0	2.8	0.93	u, deep uz	1/31/67	1.95	109.3
546103	4122301	35.8	U-20d	1271.6 - 1229.0	Tpb	LA ²⁸	LFA	BA	7.6	0.3	0.95	s, below cwl	1/31/67		
546103	4122301	37.5	U-20d	1229.0 - 1146.7	Tp	BED	TCU	UPCU	17.7	0.3	0.98	s, below cwl	1/31/67		
546103	4122301	39.1	U-20d	1146.7 - 1067.4	Tpcm	unk	unk	TCA	21.5	0.5	0.99	s	1/31/67		

Table A1. (continued)

E	N	UZ or cwl temp (C)	Borehole	Elev range (m)	Strat ¹	Class/rock type ¹	HGU ¹	HSU ¹	Grad T (C/km)	Std dev (C/km)	R ²	Saturation (u,s) ²	Temp log (date)	l (W/m C)	Est. Heat Flow (mW/m ²)
Purse Fault-W. Boxcar Fault (1), continued															
546103	4122301	37.8	U-20d	1332.6 - 1271.6	Tpb	LA	LFA	BA	55.1	2.6	0.96	u, deep uz	2/2/67	1.95	107.5
546103	4122301	37.8	U-20d	1271.6 - 1229.0	Tpb	LA ²⁸	LFA	BA	45.7	1.5		s, below cwl	2/2/67		
546103	4122301	40.9	U-20d	1229.0 - 1146.7	Tp	BED	TCU	UPCU	16.5	0.4		s, below cwl	2/2/67		
546103	4122301	42.3	U-20d	1146.7 - 1067.4	Tpcm	unk	unk	TCA	17.1	0.5		s	2/2/67		
546651	4119291	25.9	U-20y	1388.9 - 1343.2	Tpcm	MWT	WTA	TCA	24.9	2.2	0.74	u	1/2/75	1.69	42.1
546651	4119291	27.8	U-20y	1328.0 - 1276.2	Tp	BED	TCU	LPCU	17.6	2.8	0.74	u, deep uz	1/2/75		
546651	4119291	28.8	U-20y	1276.2 - 1267.0	Tp	BED	TCU	LPCU	140.3	2.5	0.94	s, below cwl	1/2/75		
546103	4122275	26.9	UE-20d	1510.0 - 1342.3	unk	BED	VTA	PVTA	17.2	1.1	0.98	u	7/28/64		
546103	4122275	27.0	UE-20d	1342.3 - 1328.9	unk	BED	VTA	PVTA	28.3	0.3	0.97	u	7/28/64		
546103	4122275	32.0	UE-20d	1328.9 - 1284.4	Tpb	LA	LFA	BA	25.9	3.6	0.82	u, deep uz	7/28/64	1.95	50.5
546103	4122275	32.0	UE-20d	1281.4 - 1229.6	Tpb	LA ²⁸	LFA	BA	33.5	3.0	0.65	s, below cwl	7/28/64		
546103	4122275	36.8	UE-20d	1229.6 - 1162.5	Tp	BED	TCU	UPCU	25.2	1.4	0.94	s, below cwl	7/28/64		
Boxcar Fault-W. Greeley Fault (3)															
551362.9	4123691.8	25.6	ER-20-6#1	1373.4 - 1355.5	Tpd	BED	TCU	UPCU	44.7	4.4	0.93	u, deep uz	3/7/96	1.15	51.5
551362.9	4123691.8	30.5	ER-20-6#1	1348.5 - 1329.2	Tpd	BED	TCU	UPCU	31.1	0.8	0.92	s, below cwl	3/7/96	1.73	53.8
551362.9	4123691.8	30.3	ER-20-6#1 ²¹	1353.2 - 1329.2	Tpd	BED	TCU	UPCU	33.0	0.7	0.99	s, below cwl	5/1/96	1.73	57.1
551362.9	4123691.8	29.9	ER-20-6#1 ²¹	1355.1 - 1339.8	Tpd	BED	TCU	UPCU	54.6			s, below cwl	2002	1.73	94.5
551328	4123661.8	29.4	ER-20-6#2 ²²	1355.0 - 1339.7	Tpd,Tp	BED	TCU	UPCU,L	47.6			s, below cwl	2002	1.73	82.3
551295.7	4123578.8	28.7	ER-20-6#3 ²³	1354.9 - 1339.7	Thp	LA ³¹	LFA	CHZCM	34.7			s, below cwl	2002	1.73	60.0
550614	4122711.7	31.9	U-20WW	1345.3 - 1328.5	Thp	LA	LFA	CHZCM	24.6	9.7		s, below cwl	2000-2002	2.16	53.1
551273.2	4121483.8	34.5	UE-20n#1	1347.1 - 1331.8	Thp	LA ³¹	LFA	CHZCM	41.0	5.4		s, below cwl	2000-2002	1.73	70.9

Table A1. (continued)

E	N	UZ or cwl temp (C)	Borehole	Elev range (m)	Strat ¹	Class/ rock type ¹	HGU ¹	HSU ¹	Grad T (C/km)	Std dev (C/km)	R ²	Saturation (u,s) ²	Temp log (date)	l (W/m C)	Est. Heat Flow (mW/m ²)
S of Silent Canyon caldera structural margin-N of Timber Mountain caldera topographic margin (4)															
541730	4117660	36.5	ER-EC-1 ¹⁶	1294.7 - 1270.3	Tmrf	NWT	TCU	FCCU	2.7	5.6	0.55	u, deep uz	4/20/99		
541730	4117660	37.0	ER-EC-1 ¹⁶	1270.2 - 1211.8	Tmrf	NWT	TCU	FCCU	9.0	6.3	0.94	s, below cwl	4/20/99		
541730	4117660	32.6	ER-EC-1 ¹⁷	1271.1 - 1255.9	Tmrf	NWT	TCU	FCCU	19.7			s, below cwl	2000-2002	1.42	28.0
541730	4117660	33.8	ER-EC-1 ¹⁷	1270.3 - 1212.5	Tmrf	NWT	TCU	FCCU	21.1	3.3	0.74	s, below cwl	2/17/00	1.42	30.0
544673	4115729	40.0	ER-EC-6 ¹⁸	1296.7 - 1273.6	Tmrf	BED	TCU	FCCU	23.0	6.6	0.86	u, deep uz	3/20/99		
544673	4115729	40.6	ER-EC-6 ¹⁸	1267.7 - 1240.4	Tmrf	BED	TCU	FCCU	39.7	13.0	0.87	s, below cwl	3/20/99		
544673	4115729	35.3	ER-EC-6 ¹⁹	1273.5 - 1258.3	Tmrf	BED	TCU	FCCU	45.9			s, below cwl	2000-2002		
544673	4115729	35.7	ER-EC-6¹⁹	1271.6 - 1240.5	Tmrf	BED	TCU	FCCU	46.2	3.7	0.92	s, below cwl	3/8/00	1.73	79.9
Handley Fault-Purse Fault (5)															
539012	4121281	28.8	PM-3#1 ⁴	1348.1 - 1330.5	Tmrf	NWT	TCU	UPCU	37.1	0.7	0.99	u, deep uz	12/15/99	1.16	43.1
539012	4121281	32.5	PM-3#1 ⁴	1330.6 - 1315.3	Tmrf	IWT,BED	TCU	UPCU	54.1	9.7		s, below cwl	2000-2002	1.53	82.8
539012	4121281	28.8	PM-3#1 ⁴	1326.8 - 1320.1	Tmrf	BED	TCU	UPCU	48.4	0.6	0.99	s, below cwl	12/15/99	1.73	83.8
539012	4121281	28.8	PM-3#1 ⁴	1320.1 - 1258.0	Tmrf	NWT	TCU	UPCU	11.6	0.5	0.96	s	12/15/99		
539012	4121281	28.8	PM-3#1 ⁴	1258.0 - 1241.5	Tmrf	NWT	TCU	UPCU	32.1	0.5	0.99	s	12/15/99		
539012	4121281	31.8	PM-3#2 ⁴	1331.2 - 1315.9	Tmrf	IWT,BED	TCU	UPCU	36.1	7.3		s, below cwl	2000-2002	1.54	55.6
541285.3	4128082	29.7	UE-20j	1521.9 - 1412.1	Tmrf	MWT	WTA	TMA	-17.4		0.92	u, deep uz	9/5/64		
541285.3	4128082	32.7	UE-20j	1406.0 - 1393.9		MWT	WTA	TMA	-0.9		0.23	s, below cwl	9/5/64		
541285.3	4128082	33.2	UE-20j	1384.7 - 1372.5	Tmrf	NWT	unk	TMA	29.7		0.98	s, below cwl	9/5/64		
541285.3	4128082	35.6	UE-20j	1369.5 - 1271.9	Tptb	BED	VTA	PVTA	27.8		0.98	s, below cwl	9/5/64	1.73	48.1
541285.3	4128082	26.1	UE-20j	1521.9 - 1409.1	Tmrf	MWT	WTA	TMA	9.5		0.82	u, deep uz	10/10/64		
541285.3	4128082	23.9	UE-20j	1406.0 - 1393.9		MWT	WTA	TMA	-38.3		0.72	s, below cwl	10/10/64		
541285.3	4128082	23.9	UE-20j	1384.7 - 1372.5	Tmrf	NWT	unk	TMA	10.2		0.50	s, below cwl	10/10/64		
541285.3	4128082	27.1	UE-20j	1369.5 - 1271.9	Tptb	BED	VTA	PVTA	32.0			s, below cwl	10/10/64		

Table A1. (continued)

E	N	UZ or cwl temp (C)	Borehole	Elev range (m)	Strat ¹	Class/rock type ¹	HGU ¹	HSU ¹	Grad T (C/km)	Std dev (C/km)	R ²	Saturation (u,s) ²	Temp log (date)	l (W/m C)	Est. Heat Flow (mW/m ²)
Handley Fault-Purse Fault (5), continued															
541285.3	4128082	31.4	UE-20j	1521.9 - 1470.1	Tmrp	MWT	WTA	TMA	3.0		0.10	u, deep uz	10/21/64		
541285.3	4128082	36.0	UE-20j	1467.0 - 1415.2		MWT	WTA	TMA	-1.9		0.01	u, deep uz	10/21/64		
541285.3	4128082	38.6	UE-20j	1384.7 - 1372.5	Tmrp	NWT	unk	TMA	-8.4		0.25	s, below cwl	10/21/64		
541285.3	4128082	36.9	UE-20j	1369.5 - 1271.9	Tptb	BED	VTA	PVTA	-15.7			s, below cwl	10/21/64		
NW of Handley Fault (6)															
538256.7	4133028.2	35.3	PM-2	1538.0 - 1407.0	Tqu	BED	unk	PBRCM	41.8	3.6	0.90	u, deep uz	6/6/64	1.15	48.1
538256.7	4133028.2	35.6	PM-2	1403.9 - 1367.3	Tbq	NWT	unk	PBRCM	26.9	1.4	0.67	u, deep uz	6/6/64		
538256.7	4133028.2	37.6	PM-2	1364.3 - 1303.3	Tbq	NWT	unk	PBRCM	20.4	0.4	0.99	s, below cwl	6/6/64		
538256.7	4133028.2	37.6	PM-2 ²⁰	1538.0 - 1407.0	Tqu	BED	unk	PBRCM	34.9	0.8	0.95	u, deep uz	7/11/64		
538256.7	4133028.2	39.8	PM-2 ²⁰	1403.9 - 1303.3	Tbq	NWT	unk	PBRCM	22.5	0.5	0.98	u, deep uz	7/11/64		
538256.7	4133028.2	40.5	PM-2 ²⁰	1300.3 - 1275.9	Tbq	BED	unk	PBRCM	27.2	0.4	0.97	u, deep uz	7/11/64		
538256.7	4133028.2	41.4	PM-2 ²⁰	1272.8 - 1254.6		BED		PBRCM	20.6	0.4	0.96	s, below cwl	7/11/64		
538256.7	4133028.2	51.8	PM-2 ²⁰	1251.5 - 986.3	Tor	NWT	unk	PBRCM	38.6	0.5	1.00	s, below cwl	7/11/64	1.42	54.8
538256.7	4133028.2	53.3	PM-2 ²⁰	983.3 - 949.8	Tqm	NWT	unk	PBRCM	40.4	0.4	0.99	s, below cwl	7/11/64	1.42	57.3
W. Greeley Fault-E. Greeley Fault (7)															
553210.6	4118447.1	30.0	ER-20-2#1	1340.4 - 1323.6	Thp	BED	TCU	CHZCM	29.5	4.0		s, below cwl	2000-2002	1.73	51.1
552668.1	4125925.1	32.4	PM-1 ²⁷	1358.5 - 1330.4	Thp	FB	LFA	CHZCM	24.4	4.0	0.99	s, below cwl	8/3/94	1.89	46.1
552668.1	4125925.1	32.3	PM-1 ²⁷	1359.6 - 1342.9	Thp	FB	LFA	CHZCM	44.3	5.4		s, below cwl	2000-2002	1.89	83.7
552512	4121139	26.4	U-20bg	1546.5 - 1477.4	Thp	LA	LFA	CHZCM	20.7	1.2	1.00	u, deep uz	6/22/92		
552512	4121139	29.7	U-20bg	1477.4 - 1380.7	Thp	LA	LFA	CHZCM	34.5	1.9	1.00	u, deep uz	6/22/92		
552512	4121139	30.2	U-20bg	1380.7 - 1361.5	Thp	BED	TCU	CHZCM	25.2	1.9	0.97	u, deep uz	6/22/92	1.15	28.9
552512	4121139	32.1	U-20bg	1350.1 - 1334.8	Thp	BED	TCU	CHZCM	3.3	3.3		s, below cwl	2000-2002		

Table A1. (continued)

E	N	UZ or cwl temp (C)	Borehole	Elev range (m)	Strat ¹	Class/ rock type ¹	HGU ¹	HSU ¹	Grad T (C/km)	Std dev (C/km)	R ²	Saturation (u,s) ²	Temp log (date)	l (W/m C)	Est. Heat Flow (mW/m ²)
W. Greeley Fault-E. Greeley Fault (7), continued															
552284.5	4125130.3	25.8	UE-20ab	1487.7 - 1426.8	Thp	LA	LFA	CHVCM	24.0	1.4	0.95	u, deep uz	6/5/78	1.95	46.7
552284.5	4125130.3	27.1	UE-20ab	1423.7 - 1396.3	Thp	LA ²⁹	LFA	CHVCM	45.9	1.2	0.96	u, deep uz	6/5/78	1.15	52.8
552284.5	4125130.3	27.9	UE-20ab	1393.2 - 1368.9	Thp	LA ³⁰	LFA	CHVCM	33.1	1.3	0.91	u, deep uz	6/5/78	1.26	41.7
552284.5	4125130.3	28.2	UE-20ab	1365.8 - 1356.7	Thp	FB	LFA	CHVCM	16.6		0.34	u, deep uz	6/5/78		
552284.5	4125130.3	32.1	UE-20ab	1350.6 - 1268.3		FB ²⁸		CHVCM	23.7		1.00	s, below cwl	6/5/78	1.89	44.9
552402	4122007	30.7	UE-20bh#1 ⁶	1410.2 - 1389.2	Thp	BED	TCU	CHZCM	28.3	2.2	0.98	u	10/1/91		
552402	4122007	32.0	UE-20bh#1 ⁶	1389.1 - 1350.1	Thp	BED	TCU	CHZCM	33.9	1.9	1.00	u, deep uz	10/1/91	1.15	39.0
552402	4122007	33.6	UE-20bh#1 ⁶	1348.5 - 1331.0	Thp	BED	TCU	CHZCM	32.8	1.2	1.00	s, below cwl	10/1/91		
552402	4122007	34.1	UE-20bh#1 ⁶	1321.7 - 1306.4	Thp	BED	TCU	CHZCM	29.5	7.3		s, below cwl	2000-2002	1.73	51.1
Silent Canyon Struc Zone-W and E Estuary Faults (8)															
559768	4128539	22.2	U-19aj	1490.8 - 1435.9	Tcbx	TB	TCU	BFCU	11.5	1.6	0.74	u, deep uz	12/9/80	1.95	22.3
555857	4125371	28.7	U-19aS	1496.9 - 1393.2	Thp	NWT	VTA	CHVTA	24.6	0.4	0.99	u, deep uz	10/4/64	1.16	28.5
554585.6	4126723	30.8	U-19bk	1428.1 - 1412.9	unk	unk	unk	unk	9.8	3.3		s, below cwl	2000-2002		
559101	4127775	28.1	U-19e	1502.4 - 1484.1	Tcbx	LA ³⁰	LFA	BFCU	29.3	2.0	0.81	u, deep uz	3/6/66	1.26	37.0
559101	4127775	30.1	U-19e	1481.0 - 1404.8	Tcbjp	NWT	TCU	BFCU	23.5	2.2	0.94	u, deep uz	3/6/66	1.16	27.3
559101	4127775	34.0	U-19e	1401.8 - 1340.8	Tcbjp	NWT	TCU	BFCU	6.3	0.5	0.86	s, below cwl	3/6/66		
556340	4129244	35.9	U-19g ⁸	1500.8 - 1491.7	Tcu	BED	TCU	CHVCM	19.9	0.4	0.91	u	11/19/65		
556340	4129244	36.3	U-19g ⁸	1488.6 - 1467.3	Tcj	BED	TCU	CFCU	15.5	0.9	0.85	u	11/19/65		
556340	4129244	37.5	U-19g ⁸	1464.3 - 1427.7	Tcps	BED	TCU	CFCU	28.3	0.9	0.97	u, deep uz	11/19/65	1.15	32.6
556340	4129244	39.0	U-19g ⁸	1415.5 - 1403.3	Tcg	ITL	LFA	CFCU	7.3	1.1	0.17	s, below cwl	11/19/65		

Table A1. (continued)

E	N	UZ or cwl temp (C)	Borehole	Elev range (m)	Strat ¹	Class/ rock type ¹	HGU ¹	HSU ¹	Grad T (C/km)	Std dev (C/km)	R ²	Saturation (u,s) ²	Temp log (date)	l (W/m C)	Est. Heat Flow (mW/m ²)
E. Greeley Fault-Almendo Fault (9)															
555683.6	4120389.3	26.3	U-19bh	1426.2 - 1411.0	Tpe,Tpr	NWT ³¹ ,L	TCU	PLFA ³³	9.8	3.3		s, below cwl	2000-2002	1.49	14.6
556107	4119811	26.4	U-19f	1394.2 - 1366.7	Tpe	VT ²⁹	WTA	PLFA	35.6	0.7	0.97	u	7/5/68	1.15	41.0
556107	4119811	28.5	U-19f	1357.6 - 1327.1	Tpe	BED	TCU	CHCU	33.3	1.0	0.96	u	7/5/68	1.15	38.3
556107	4119811	29.1	U-19f	1302.7 - 1296.6	Thp	NWT	TCU	CHCU	43.7	1.3	0.98	u, deep uz	7/5/68	1.16	50.7
556107	4119811	29.7	U-19f	1293.6 - 1281.4	Thp	NWT	TCU	CHCU	22.1	1.3	0.86	s, below cwl	7/5/68	1.42	31.3
Halfbeak Fault-Moor Hen Meadow-Silent Canyon Northern Struc Zones (10)															
555488.4	4132881.8	29.2	UE-19h	1423.1 - 1407.9	Tbdl	LA	LFA	BRA	50.3	6.2		s, below cwl	2000-2002	2.16	108.7
Almendo Fault-Scrugham Peak Fault (11)															
557922	4122638	30.9	U-19i	1379.5 - 1373.4	Tcu	NWT	VTA	CHVTA	31.0	1.2	0.90	u, deep uz	8/24/67		
557922	4122638	31.1	U-19i	1364.3 - 1358.2	Tcps	NWT	VTA	CFCU	56.5	1.4	0.88	u, deep uz	8/24/67	1.16	65.5
557922	4122638	32.6	U-19i	1352.1 - 1336.9	Tcps	NWT	VTA	CFCU	30.8	1.4	0.98	s, below cwl	8/24/67		
557922	4122638	37.5	U-19i	1333.8 - 1208.8	Tcps	NWT	TCU	CFCU	39.2	1.4	0.99	s, below cwl	8/24/67		
Scrugham Peak Fault-Split Ridge Fault (12)															
559542	4123267	28.0	U-19p ⁹	1502.4 - 1435.3		WTA, DWT,NW	TCU	BFCU	42.3	2.1	0.95	u, deep uz, hsu	10/29/75		
559542	4123267	25.9	U-19p ⁹	1502.4 - 1484.1	Tcbx	DWT ³⁰	WTA	BFCU	26.8	2.0	0.65	u, deep uz	10/29/75	1.26	33.8
559542	4123267	26.2	U-19p ⁹	1478.0 - 1471.9	Tcblr	NWT ³¹	TCU	BFCU	38.3	1.1	1.00	u, deep uz	10/29/75	1.16	44.4
559542	4123267	26.6	U-19p⁹	1468.8 - 1459.7	Tcblp	NWT³¹	TCU	BFCU	42.7	1.4	0.95	u, deep uz	10/29/75	1.16	49.5
559542	4123267	27.6	U-19p ⁹	1453.6 - 1444.4	Tcblp	NWT ³¹	TCU	BFCU	27.3	1.4	1.00	u, deep uz	10/29/75	1.16	31.7
559542	4123267	29.9	U-19p ⁹	1429.2 - 1161.0	Tcblp	NWT	TCU	BFCU	8.0	1.4	0.97	s, below cwl	10/29/75		

Table A1. (continued)

E	N	UZ or cwl temp (C)	Borehole	Elev range (m)	Strat ¹	Class/ rock type ¹	HGU ¹	HSU ¹	Grad T (C/km)	Std dev (C/km)	R ²	Saturation (u,s) ²	Temp log (date)	l (W/m C)	Est. Heat Flow (mW/m ²)
Halfbeak Fault-Rickey Fault-Moor Hen Meadow Struc Zone (13)															
560900.4	4127416.2	26.4	U-19bj	1493.4 - 1478.1	Tcpk	LA	LFA	KA	8.2	2.8		s, below cwl	2000-2002	2.16	17.7
		28.9	U-19t	1554.7 - 1414.4	Tcpk	"FB"	LFA	KA	28.2	3.4	0.99	u, deep uz	9/27/93	1.95	55.0
		29.6	U-19t	1414.3 - 1409.3	Tcpk	"FB"	LFA	KA	122.5	2.3	1.00	u, deep uz	9/27/93		
		32.1	U-19t	1408.2 - 1384.8	Tcpk	"FB"	LFA	KA	65.7	4.2	1.00	s, below cwl	9/27/93		
		33.6	U-19t	1384.8 - 1364.8	Tcpk	"FB"	LFA	KA	70.8	4.8	0.99	s	9/27/93		
560339	4124702	34.7	UE-19cWW⁷	1477.1 - 1448.9	Tcps	BED	TCU	CFCU	38.8	1.2	1.00	u,17-20 m above cwl	11/13/92	1.15	44.6
560339	4124702	34.8	UE-19cWW ⁷	1448.9 - 1442.5	Tcps	BED	TCU	CFCU	20.3	1.0	0.99	u,11-14 m above cwl	11/13/92		
560339	4124702	34.8	UE-19cWW ⁷	1435.1 - 1430.2	Tcps	BED	TCU	CFCU	5.5	0.9	0.89	u, deep uz	11/13/92		
560339	4124702	31.9	UE-19cWW ⁷	1430.5 - 1415.2	Tcps	NWT	TCU	BFCU	43.7	6.2		s, below cwl	2000-2002	1.42	62.1
560339	4124702	34.8	UE-19cWW ⁷	1426.2 - 1419.1	Tcbr	NWT	TCU	BFCU	7.2	1.1	0.96	s, below cwl	11/13/92		
Split Ridge Fault-Rainier Mesa/Ammonia Tanks Caldera Topographic Margin (14)															
567542	4114743	18.7	ER-19-1	1582.1 - 1565.5		BED	TCU	PBRCM	56.1	4.9	0.89	u, deep uz	11/17/93	1.15	64.5
567542	4114743	18.3	ER-19-1	1582.1 - 1571.1	Tn3D	BED	TCU	PBRCM	65.3	5.6	0.79	u, deep uz	11/17/93		
567542	4114743	18.7	ER-19-1	1571.0 - 1565.5	Ton2	BED	TCU	PBRCM	75.1	3.1	0.96	u, deep uz	11/17/93		
567542	4114743	21.9	ER-19-1	1561.9 - 1533.0	Ton2	BED	TCU	PBRCM	18.3	1.6	0.96	s, below cwl	11/17/93		
567542	4114743	27.1	ER-19-1#1	1326.6 - 1311.3	Tor	BED	TCU	PBRCM	26.3	10.7		s, below cwl	2000-2002	1.73	45.4
567542	4114743	22.7	ER-19-1#2	1508.5 - 1493.2	Ton2	NWT	TCU	PBRCM	26.3	5.4		s, below cwl	2000-2002	1.42	37.3
567542	4114743	22.0	ER-19-1#3	1564.8 - 1549.6	Ton2	BED	TCU	PBRCM	3.3	16.4		s, below cwl	2000-2002		
569000.3	4112499	22.6	HTH-1 ³⁴	1427.4 - 1331.7	Toy	BED	unk	PBRCM	17.1	3.4	0.94	s, below cwl	8/19/91	1.73	29.6
569000.3	4112499	23.2	HTH-1 ³⁴	1330.1 - 1298.1	Tor	PWT	WTA	PBRCM	22.2	3.3	0.78	s, below cwl	8/19/91	1.66	36.8

Table A1. (continued)

E	N	UZ or cwl temp (C)	Borehole	Elev range (m)	Strat ¹	Class/ rock type ¹	HGU ¹	HSU ¹	Grad T (C/km)	Std dev (C/km)	R ²	Saturation (u,s) ²	Temp log (date)	l (W/m C)	Est. Heat Flow (mW/m ²)
E of Thirst Canyon Lineament-S of Silent Canyon caldera Structural Margin (15)															
538421	4110841	18.6	ER-EC-2A ¹²	1300.7 - 1286.9	Tfbw	VL	LFA	FCCM	83.3	9.5	0.99	u, deep uz	2/7/00		
538421	4110841	20.1	ER-EC-2A ¹²	1286.8 - 1266.7	Tfbw	PL	LFA	FCCM	74.8	10.6	0.99	u, deep uz	2/7/00		
538421	4110841	22.8	ER-EC-2A ¹²	1266.7 - 1237.3	Tfbw	BED	TCU	FCCM	88.7	14.1	0.99	u, deep uz	2/7/00		
538421	4110841	32.6	ER-EC-2A ¹²	1262.5 - 1236.0	Tfbw	BED	TCU	FCCM	19.4	1.1	0.98	u, deep uz	2/9/00	1.15	22.3
538421	4110841	25.9	ER-EC-2A ¹²	1237.2 - 1176.4	Tfbw	BED	TCU	FCCM	53.2	10.6	0.96	s, below cwl	2/7/00		
538421	4110841	36.0	ER-EC-2A ¹²	1236.0 - 1095.0	Tfbw	BED	TCU	FCCM	25.6	1.2	0.91	s, below cwl	2/9/00		
538421	4110841	35.7	ER-EC-2A ¹²	1176.2 - 1166.7	Tfbw	BED	TCU	FCCM	605.2	51.6	0.68	s, below cwl	2/7/00		
538421	4110841	36.3	ER-EC-2A ¹²	1166.6 - 1094.9	Tfbw	BED	TCU	FCCM	6.2	14.6	0.37	s, below cwl	2/7/00		
538421	4110841	31.8	ER-EC-2A ¹³	#REF! - #REF!	Tfbw	BED	TCU	FCCM	19.7			s, below cwl	2000-2002	1.73	34.1
538701.8	4104136.9	28.2	ER-EC-5 ²⁵	1225.5 - 1212.7	Tmar	DWT-VT	WTA	TMCM	16.5		0.89	s, below cwl	6/7/00	1.86	30.6
538701.8	4104136.9	28.4	ER-EC-5 ²⁵	1212.2 - 1186.4	Tmar	MWT	WTA	TMCM	17.5		0.96	s, below cwl	6/7/00	1.78	31.2
538701.8	4104136.9	26.9	ER-EC-5 ²⁵	1237.5 - 1222.3	Tmar	DWT-VT	WTA	TMCM	26.2	14.2		s, below cwl	2000-2002		
Ammonia Tanks Caldera Struc Margin-W of Scrugham Peak Fault (16)															
549322	4109762	23.0	UE-18r ¹¹	1290.8 - 1272.2	Tma	PWT	WTA	TMCM	71.2	3.7	0.96	u, deep uz	3/16/93	1.26	89.8
549322	4109762	27.1	UE-18r ¹¹	1268.1 - 1191.5	Tma	PWT	WTA	TMCM	18.3	1.1	1.00	s, below cwl	3/16/93	1.66	30.4
549322	4109762	26.7	UE-18r ¹¹	1272.2 - 1256.9	Tma	PWT	WTA	TMCM	19.7	6.6			2000-2001	1.66	32.7
549322	4109762	26.7	UE-18r ¹¹	1272.2 - 1256.9	Tma	PWT	WTA	TMCM	10.9	13.5		s, below cwl	2000-2002		

Table A1. (continued)

E	N	UZ or cwl temp (C)	Borehole	Elev range (m)	Strat ¹	Class/ rock type ¹	HGU ¹	HSU ¹	Grad T (C/km)	Std dev (C/km)	R ²	Saturation (u,s) ²	Temp log (date)	l (W/m C)	Est. Heat Flow (mW/m ²)
Ammonia Tanks Caldera Struc Margin-E of Scrugham Peak Fault (17)															
555725	4106389	31.0	ER-18-2 ¹⁰	1398.8 - 1394.6	Tmawr	NWT	TCU	TMCM	55.9	5.4	0.95	u	7/14/99		
555725	4106389	34.4	ER-18-2 ¹⁰	1394.6 - 1329.3	Tmawr	NWT-DW	WTA	TMCM	48.0	9.8	0.98	u	7/14/99		
555725	4106389	36.7	ER-18-2 ¹⁰	1329.3 - 1293.4	Tmawp	BED	TCU	TMCM	64.7	6.7	1.00	u	7/14/99		
555725	4106389	37.9	ER-18-2 ¹⁰	1293.4 - 1271.4	Tmar	NWT	TCU	TMCM	59.4	8.2	0.99	u	7/14/99		
555725	4106389	38.3	ER-18-2 ¹⁰	1271.4 - 1266.8	Tmar	PWT	WTA	TMCM	99.2	5.2	0.97	u	7/14/99		
555725	4106389	40.3	ER-18-2 ¹⁰	1264.0 - 1229.4	Tmar	MWT	WTA	TMCM	52.1	8.5	0.96	u, deep uz	7/14/99	1.69	88.0
555725	4106389	45.9	ER-18-2 ¹⁰	1227.0 - 1197.0	Tmar	MWT ²⁸	WTA	TMCM	68.9	9.1	0.97	s, below cwl	7/14/99	1.78	122.7
555725	4106389	46.5	ER-18-2 ¹⁰	1287.8 - 1272.5	Tmar	NWT	TCU	TMCM	56.9	16.4		s, below cwl	2000-2002	1.42	80.8
E of Ammonia Tanks Caldera Struc Margin-Within Rainier Mesa Caldera Struc Margin (18)															
560804.7	4100463	25.5	ER-30-1	1276.6 - 1199.1	Tfdb	BS	LFA	FCCM	17.3	4.3	0.99	s, below cwl		2.1	36.4
560804.7	4100463	25.9	ER-30-1	1198.9 - 1175.7	Tg	NWT	TCU	FCCM	18.4	5.4	0.94	s, below cwl		1.42	26.2
559591	4109095	33.6	UE-18t ²⁴	1305.4 - 1299.7	Tfbw	BED	TCU	FCCM	34.6	2.7	0.44	s, 20ftbelow	12/12/99	1.73	59.8
559591	4109095	34.0	UE-18t ²⁴	1293.6 - 1273.1	Tmar	MWT	WTA	TMCM	32.4	1.6	0.96	s, below cwl	12/12/99	1.78	57.7
E of Thirst Canyon Lineamint-Hogback Fault-Ammonia Tanks Caldera Struct Margin (19)															
532763.8	4106141.8	22.8	ER-EC-8	1266.0 - 1247.8	Tfb	NWT	TCU	FCCM	53.9		0.98	u, deep uz	7/22/99	1.16	62.6
532763.8	4106141.8	25.2	ER-EC-8	1247.7 - 1222.2	Tfb	BED	TCU	FCCM	88.5		0.99	u, deep uz	7/22/99	1.15	101.8
532763.8	4106141.8	36.1	ER-EC-8	1222.4 - 1207.1	Tfb	BED	TCU	FCCM	85.3	14.2		s, below cwl	2000-2002	1.73	147.6
W of Thirst Canyon Lineamint-SW of Silent Canyon Caldera Struct Margin (20)															
532760	4112356	21.2	ER-EC-4	1297.7 - 1263.4	Ttr	NWT	VTA	TCVA	51.6	8.0	1.00	u, deep uz	6/2/99		
532760	4112356	22.1	ER-EC-4	1263.3 - 1250.2	Ttr	PWT	WTA	TCVA	60.1	6.6	0.97	u, deep uz	6/2/99	1.26	75.7
532760	4112356	22.5	ER-EC-4	1250.2 - 1243.5	Ttr	MWT	WTA	TCVA	75.6	7.0	0.96	u, deep uz	6/2/99	1.69	127.7
532760	4112356	23.0	ER-EC-4	1243.5 - 1237.4	Ttr	PWT-MV	WTA	TCVA	78.8	7.9	0.93	u, deep uz	6/2/99	1.69	133.2
532760	4112356	23.8	ER-EC-4	1237.4 - 1222.9	Ttr	BED	VTA	TCVA	55.0	7.6	0.98	u, deep uz	6/2/99	1.15	63.3
532760	4112356	35.8	ER-EC-4	1216.0 - 1180.2	Ttr	MWT,NWT,PW		TCVA	29.8	6.7	0.66	s, below cwl	6/2/99		

Table A1. (continued)

E	N	UZ or cwl temp (C)	Borehole	Elev range (m)	Strat ¹	Class/ rock type ¹	HGU ¹	HSU ¹	Grad T (C/km)	Std dev (C/km)	R ²	Saturation (u,s) ²	Temp log (date)	l (W/m C)	Est. Heat Flow (mW/m ²)
W of Thirst Canyon Lineamint-SW of Silent Canyon Caldera Struc Margin (20), continued															
532760	4112356	36.7	ER-EC-4 ¹⁴	1222.5 - 1207.4	Ttr	BED,NW	VTA, V	TCVA ³³	70.0	17.2		s, below cwl	2000-2002	1.66	115.9
532760	4112356	36.6	ER-EC-4 ¹⁴	1215.7 - 1210.2	Ttr	MWT	WTA	TCVA	22.6		0.89	s, below cwl	8/25/00		
532760	4112356	36.8	ER-EC-4 ¹⁴	1209.6 - 1188.8	Ttr	NWT	VTA	TCVA	7.1		0.62	s, below cwl	8/25/00		
532760	4112356	36.2	ER-EC-4 ¹⁵	1297.7 - 1263.4	Ttr	NWT	VTA	TCVA	62.2	8.7	0.98	u, deep uz	6/14/99		
532760	4112356	36.7	ER-EC-4 ¹⁵	1263.3 - 1250.2	Ttr	PWT	WTA	TCVA	50.1	13.7	0.89	u, deep uz	6/14/99		
532760	4112356	37.3	ER-EC-4 ¹⁵	1250.2 - 1243.5	Ttr	MWT	WTA	TCVA	74.4	9.4	0.90	u, deep uz	6/14/99		
532760	4112356	37.6	ER-EC-4 ¹⁵	1243.5 - 1237.4	Ttr	PWT-MV	WTA	TCVA	35.7	10.2	0.74	u, deep uz	6/14/99		
532760	4112356	37.4	ER-EC-4 ¹⁵	1237.4 - 1222.5	Ttr	BED	VTA	TCVA	-15.5	56.3	0.47	u, deep uz	6/14/99		
532760	4112356	43.5	ER-EC-4 ¹⁵	1216.0 - 1210.0	Ttr	MWT	WTA	TCVA	14.4	8.2	0.40	s, below cwl	6/14/99		
532760	4112356	43.4	ER-EC-4 ¹⁵	1209.9 - 1188.7	Ttr	NWT	VTA	TCVA	-7.9	8.1	0.72	s, below cwl	6/14/99		
Claim Canyon Caldera Struc Margin (21)															
546483.5	4093127.3	19.1	ER-EC-7	1333.3 - 1237.0	Tfbw	LA	LFA	FCCM	20.7		0.97	u, deep uz	8/8/99	1.95	40.3
546483.5	4093127.3	23.9	ER-EC-7	1236.6 - 1221.3	Tfbw	LA	LFA	FCCM	6.6	6.6		s, below cwl	2000-2002		
Oasis Valley (22)															
526298.8	4094586.9	21.6	ER-OV-3a2	1122.9 - 1107.6	Tf	MWT	WTA	DVCM	21.3	12.6		s, below cwl	2000-2002	1.78	38.0
526298.8	4094586.9	19.9	ER-OV-3a3 ³⁴	1154.2 - 1138.9	Tf	'WT-MW'	WTA	DVCM	27.9	5.4		s, below cwl	2000-2002	1.66	46.3
526298.8	4094586.9	20.5	ER-OV-3a ³²	1154.3 - 1139.0	Tf	'WT-MW'	WTA	DVCM	41.0	12.6		s, below cwl	2000-2002	1.66	68.1
531007.6	4097776.6	23.7	ER-OV-3b	1184.5 - 1169.3	Tgs	AL	AA	AA	16.4	7.3		s, below cwl	2000-2002	1.4	23.0
520280.1	4099808.5	19.6	ER-OV-5 ³²	1190.5 - 1176.0	Tgs	AL	AA	AA	22.6	9.7		s, below cwl	2000-2002	1.4	31.6

Table A1. (continued)

E	N	UZ or cwl temp (C)	Borehole	Elev range (m)	Strat ¹	Class/ rock type ¹	HGU ¹	HSU ¹	Grad T (C/km)	Std dev (C/km)	R ²	Saturation (u,s) ²	Temp log (date)	l (W/m C)	Est. Heat Flow (mW/m ²)
Oasis Valley (22), continued															
528416.7	4104084.1	24.3	ER-OV-1 ³²	1235.9 - 1220.6	Tf	LA ^{29,30}	LFA	FCCM	218.7	29.5		s, below cwl	2000-2002	1.66	363.1
526310	4098715.8	19.5	ER-OV-2 ³²	1174.1 - 1158.8	Tgs	AL	AA	AA	15.3	11.2		s, below cwl	2000-2002	1.4	21.4
525671.4	4089315.7	22.8	ER-OV-4a ³²	1057.0 - 1042.4	Tgs	AL	AA	AA	36.1	7.3		s, below cwl	2000-2002	1.4	50.5
528416.9	4104084.5	23.6	ER-OV-6a ³²	1236.8 - 1222.1	Tf	LA ²⁹	LFA	FCCM	219.4	27.5		s, below cwl	2000-2002	1.73	379.6
528416.9	4104084.5	23.4	ER-OV-6a2 ³⁴	1235.6 - 1223.4	Tf	LA ^{29,30}	LFA	FCCM	172.0	28.0		s, below cwl	2000-2002	1.66	285.6
535494.2	4094374.1	24.0	ER-OV-3c	1212.3 - 1197.1	Tma	JWT-PW	VTA	TMA	47.6	7.2		s, below cwl	2000-2002	1.42	67.6
535494.2	4094374.1	24.0	ER-OV-3c2	1212.3 - 1197.1	Tma	JWT-PW	VTA	TMA	44.3	9.7		s, below cwl	2000-2002	1.42	62.9

¹Explanation of abbreviations can be found at the end of this attachment.

²u - unsaturated zone, s - saturated zone, uz - unsaturated zone, cwl - composite water level in well

³Cased to 1449 m depth.

⁴Cased to 653.8 m depth.

⁵Cased to 950 m depth on 1/22/96.

⁶Cased to 590.1 m depth on 8/27/91.

⁷Cased to 737.9 m depth.

⁸Cased to 978.5 m depth in 1/65.

⁹Cased to 921.1 m depth.

¹⁰Cased to 653.2 m depth in 4/99.

¹¹Cased to 496.5 m depth.

¹²Cased to 415.7 m depth.

Table A1. (continued)

¹³Borehole gravel packed and casing perforated over three intervals between depths of 498.3-681.5 m, 922-1081.6 m, and 1344.1-1511.9 m

¹⁴Casing perforated over three intervals between depths of 301.5-372.1 m, 582.2-686.7 m, and 945.9-1037.8 m

¹⁵Cased to 263.7 m depth.

¹⁷Casing perforated over three intervals between depths of 700.4-860 m, 1020.3-1146.2 m, and 1355.9-1447.6 m

¹⁶Cased to 667.4 m depth.

¹⁸Cased to 485.1 m depth.

¹⁹Casing perforated over four intervals between depths of 496.3-570 m, 668.9-764 m, 1047.8-1161.5 m, and 1347.4-1494.6 m

²⁰Casing set to 762 m depth on 6/7/64

²¹Borehole gravel packed and casing perforated over two intervals between depths of 742.8-843.4 m and 858-898.2 m

²²Borehole gravel packed and casing perforated over two intervals between depths of 735.8-840.3 m and 851.3-897.6 m

²³Borehole gravel packed and casing perforated between 755.9-855.6 m depth

²⁴Cased to 577.9 m depth.

²⁵Borehole gravel packed and casing perforated over three intervals between depths of 361.8-439.8, 565.2-654.1, and 677.5-755.9 m.

²⁶Cased to 590.4 m depth.

²⁷Cased to 2299.1 m depth.

²⁸Large rise in temperature at cwl suggests warm water convecting in along FB or LFA

²⁹Alteration is vitric, bedded.

³⁰Alteration is devitrified.

³¹Alteration is zeolitic.

³²Shallow temperature measurement. Depth of measurement interval less than 35 m deep.

³³Harmonic mean used to calculate λ .

³⁴Casing set to 1131.1 m depth; casing perforated over five intervals between depths of 582.2-598 m, 622-625 m, 645-655 m,

Table A2. Depth and elevation range, hydrostratigraphic unit, and temperature gradients for deepest borehole temperatures. Depth intervals with deepest borehole temperature are shown in bold.

E	N	Deep bh temp (C)	Borehole	Diff from TD (m)	Elev range (m)	Strat ¹	Class/ rock type ¹	HGU ¹	HSU ¹	Grad T (C/km)	Std dev (C/km)	R ²	Total depth (m)	Temp log (date)	Sat I (W/m C)	Est. Heat Flow (mW/m ²)
Purse Fault-W. Boxcar Fault (1)																
546386	4119208	36.7	ER-20-5#1	31.5	1112.8 - 1073.6	unk	unk (NWT)	TCU	CHZCM (TSA)	7.4	1.0	0.97	860.5	11/3/95		
546386	4119208	36.5	ER-20-5#1	35.1	1112.8 - 1077.2	unk	unk (NWT)	TCU	CHZCM (TSA)	7.3	0.9	0.98	860.5	11/3/95		
546386	4119208	36.7	ER-20-5#1	31.5	1075.7 - 1073.6	unk	unk (NWT)	TCU	CHZCM (TSA)	60.6	1.1	0.99	860.5	11/3/95	1.42	86.1
546385	4119177	43.0	ER-20-5#3 ²	204.8	829.0 - 798.5	Thp	LA	LFA	CHZCM	15.6	5.0	0.93	1308.8	2/6/96		
546385	4119177	44.6	ER-20-5#3 ²	130.7	798.5 - 724.5	Thp	PL	TCU	CHZCM	20.1	3.8	0.99	1308.8	2/6/96		
546385	4119177	47.9	ER-20-5#3 ²	70.7	724.5 - 664.4	Thp	NWT	TCU	CHZCM	59.4	4.4	0.97	1308.8	2/6/96	1.42	84.3
546385	4119177	49.9	ER-20-5#3 ²	14.6	664.4 - 608.4	Thr ²⁴	NWT	TCU	CHZCM	40.9	4.5	0.96	1308.8	2/6/96	1.42-2.1	58-85.8
546385	4119177	49.8	ER-20-5#3 ²	14.5	608.4 - 608.3	unk	unk	TCU	CHZCM				1308.8	2/6/96		
546699	4120478	45.0	U-20c#1	137.1	660.2 - 588.6	Thp	LA	LFA	CHZCM	6.2	0.7	0.98	1463.0	9/27/68		
546699	4120478	45.4	U-20c#1	125.1	588.7 - 576.5	Thp	LA	LFA	CHZCM	39.1	0.7	0.98	1463.0	9/27/68		
546699	4120478	48.2	U-20c#1	30.4	576.4 - 481.9	Th	BED	TCU	CHZCM	28.5	1.1	0.99	1463.0	9/27/68	1.73	49.4
546699	4120478	38.5	U-20c	124.9	660.1 - 576.3	Thp	LA	LFA	CHZCM	19.8	0.8	0.98	1463.0	4/5/65		
546699	4120478	39.9	U-20c	0.0	576.3 - 451.4	Th	BED	TCU	CHZCM	13.4	0.6	0.97	1463.0	4/5/65		
546103	4122301	40.5	U-20d	107.3	933.3 - 735.2	Thp	BED	TCU	CHZCM	16.5	0.3	1.00	1277.7	1/31/67	1.73	28.6
546103	4122301	41.3	U-20d	32.9	735.2 - 660.8	Thr ²⁴	NWT	TCU	CHZCM	9.9	0.2	0.99	1277.7	1/31/67	2.10	20.8
546103	4122301	41.4	U-20d	9.7	660.8 - 637.6	Thp	LA	LFA	CHZCM	7.0	0.2	0.94	1277.7	1/31/67		
546103	4122301	41.4	U-20d	9.7	637.6 - 637.6	Thp	LA	LFA	CHZCM				1277.7	1/31/67		
546651	4119291	32.9	U-20y	12.8	1160.3 - 1126.8	Tptm	NWT	unk	TSA	59.5	0.6	0.99	793.1	1/2/75	1.42	84.4
546651	4119291	33.5	U-20y	0.6	1126.8 - 1114.6	Tptm	NWT	unk	TSA	25.7	0.3	0.98	793.1	1/2/75	1.42	36.5

Table A2. (continued)

E	N	Deep bh temp (C)	Borehole	Diff from TD (m)	Elev range (m)	Strat ¹	Class/ rock type ¹	HGU ¹	HSU ¹	Grad T (C/km)	Std dev (C/km)	R ²	Total depth (m)	Temp log (date)	Sat l (W/m C)	Est. Heat Flow (mW/m ²)
Purse Fault-W. Boxcar Fault (1), continued																
546103	4122275	39.5	UE-20d	198.8	748.0 - 735.8	Thp	BED	TCU	CHZCM	13.9	0.2	0.94	1369.2	7/28/64	1.73	24.0
546103	4122275	40.4	UE-20d	124.4	735.8 - 661.4	Thr ²⁴	NWT	TCU	CHZCM	12.1	0.3	0.99	1369.2	7/28/64	2.10	25.3
546103	4122275	40.6	UE-20d	101.2	661.4 - 638.3	Thr ²⁴	LA	LFA	CHZCM	11.5	0.3	0.94	1369.2	7/28/64	2.10	24.2
546103	4122275	43.4	UE-20d	37.2	638.3 - 574.2	Thr ²⁴	LA	LFA	CHZCM	15.4	0.4	0.99	1369.2	7/28/64	2.10	32.3
546103	4122275	44.1	UE-20d	3.7	552.9 - 540.7	Thr ²⁴	LA	LFA	CHZCM	119.8	1.0	0.99	1369.2	7/28/64	2.10	251.5
546102.7	4122275.252	46.1	UE-20d	0.9	537.7	⁵ Total borehole grad T				24.3			1369.5	8/14/64		
545400.83	4124900.362	121.0	UE-20f	431.6	-1876	⁵ Total borehole grad T				28.9			4171.5	6/25/64		
W. Boxcar Fault-Boxcar Fault (2)																
548110.45	4129980.729	53.9	UE-20e#1	382.5	370.9 - 352.7	Tct,TbdNWT,L,LCU,LF BRA ^{17,18}				29.4	1.7	0.68	1949.2	6/2/64	2.66	78.1
548110.45	4129980.729	57.2	UE-20e#1	59.4	29.6	⁵ Total borehole grad T				23.6			1949.2	5/27/64		
Boxcar Fault-W. Greeley Fault (3)																
551362.94	4123691.827	30.8	ER-20-6#1 ¹³	324.4	1329.2 - 1322.5	Tpe	BED	TCU	LPCU	60.1	1.4	0.98	975.4	5/1/96	1.73	104.0
551362.94	4123691.827	31.0	ER-20-6#1 ¹³	320.2	1322.5 - 1318.3	Tpr	BED	TCU	LPCU	62.6	2.0	0.96	975.4	5/1/96	1.73	108.4
551362.94	4123691.827	32.6	ER-20-6#1 ¹³	301.3	1318.2 - 1299.4	Thp	BED	TCU	CHZCM	91.3	2.6	0.99	975.4	5/1/96	1.73	158.0
551362.94	4123691.827	32.0	ER-20-6#1 ¹³	233.4	1235.9 - 1231.5	Thp	LA	LFA	CHZCM	11.9	0.5	0.95	975.4	5/1/96	1.66	19.7
551362.94	4123691.827	34.2	ER-20-6#1	65.1	1075.6 - 1063.2	Thp	BED	TCU	CHZCM	2.0		0.20	975.4	3/8/96		
551333.24	4121743.043	41.1	U-20a2	0.0	601.7	⁵ Total borehole grad T				20.7			1371.6	2/17/64		
550191.74	4124986.54	50.0	UE-20h	3.7	-194.5	⁵ Total borehole grad T				17.1			2196.7	8/16/64		

Table A2. (continued)

E	N	Deep bh temp (C)	Borehole	Diff from TD (m)	Elev range (m)	Strat ¹	Class/ rock type ¹	HGU ¹	HSU ¹	Grad T (C/km)	Std dev (C/km)	R ²	Total depth (m)	Temp log (date)	Sat l (W/m C)	Est. Heat Flow (mW/m ²)
S of Silent Canyon caldera structural margin-N of Timber Mountain caldera topographic margin (4)																
541730	4117660	59.2	ER-EC-1	190.6	535.1 - 503.2	Tcpe	PL	TCU	CFCM	39.2	11.5	0.99	1524.0	4/20/99		
541730	4117660	61.8	ER-EC-1	118.3	503.1 - 430.9	Tcpe	LA/FB	LFA	CFCM	37.0	9.2	1.00	1524.0	4/20/99		
541730	4117660	62.1	ER-EC-1	103.6	430.9 - 416.2	Tcpe	VL	LFA	CFCM	26.6	9.5	0.94	1524.0	4/20/99		
541730	4117660	61.8	ER-EC-1	67.4	416.2 - 380.0	Tcpe	PL	TCU	CFCM	-7.2	11.3	0.25	1524.0	4/20/99		
541730	4117660	61.7	ER-EC-1	54.6	380.0 - 367.2	Tcpe	BED	TCU	CFCM	-12.8	8.9	0.71	1524.0	4/20/99		
541730	4117660	62.4	ER-EC-1	18.6	367.2 - 331.2	Tcpk	FB	LFA	CFCM	21.7	9.2	0.90	1524.0	4/20/99		
541730	4117660	57.3	ER-EC-1 ⁸	191.1	535.1 - 503.7	Tcpe	PL	TCU	CFCM	51.4	5.7	0.97	1524.0	2/17/00	1.66	85.3
541730	4117660	57.8	ER-EC-1 ⁸	182.3	503.1 - 494.9	Tcpe	LA/FB	LFA	CFCM	40.7	5.9	0.64	1524.0	2/17/00	2.16	87.9
544673	4115729	61.7	ER-EC-6 ⁹		576.5 - 529.3	Thr ²⁴	NWT	TCU	CHCU	43.2	8.7	0.99	1524.0	3/20/99	1.42-2.41	61.4-104.2
544673	4115729	62.9	ER-EC-6 ⁹		529.2 - 501.3	Thr ²⁴	NWT	TCU	CHCU	43.4	7.1	0.97	1524.0	3/20/99	1.42-2.41	61.7-104.7
544673	4115729	59.2	ER-EC-6 ⁹	295.7	501.2 - 480.0	Tcpe	PL	TCU	CFCM	44.4	10.1	0.96	1524.0	3/20/99	1.66-2.82	73.6-125.1
544673	4115729	60.0	ER-EC-6 ⁹	271.3	479.9 - 455.6	Tcpe	LA	LFA	CFCM	39.9	11.7	0.95	1524.0	3/20/99	2.16-2.81	86.1-112.0
544673	4115729	62.4	ER-EC-6 ⁹	221.1	455.5 - 405.3	Tcpe	PL	TCU	CFCM	44.1	8.2	0.99	1524.0	3/20/99	1.66-2.82	73.2-124.4
544673	4115729	65.4	ER-EC-6 ⁹	163.1	405.2 - 347.4	Tcpe	LA	LFA	CFCM	51.6	7.9	0.99	1524.0	3/20/99	2.16-2.81	111.5-145
544673	4115729	67.6	ER-EC-6 ⁹	120.8	347.3 - 305.0	Tcpe	NWT	TCU	CFCM	57.8	9.5	0.97	1524.0	3/20/99	1.42-2.41	82.1-139.3
544673	4115729	70.8	ER-EC-6 ⁹	64.7	304.9 - 248.9	Tcpk	LA	LFA	CFCM	53.7	9.9	0.99	1524.0	3/20/99	2.16-2.81	116-150.9
544673	4115729	71.6	ER-EC-6 ⁹	43.4	248.8 - 227.6	Tcpk	PL	TCU	CFCM	43.6	9.5	0.94	1524.0	3/20/99		
544673	4115729	72.2	ER-EC-6 ⁹	11.1	227.5 - 195.3	Tcpk	LA	LFA	CFCM	14.0	9.9	0.81	1524.0	3/20/99		
544673	4115729	52.6	ER-EC-6 ^{10,9}	557.9	754.0 - 742.2	Tptm	PWT	WTA	TSA	35.8	6.5	0.77	1524.0	3/8/00	1.66-2.82	59.4-100.8
544673	4115729	55.7	ER-EC-6 ^{10,9}	478.9	741.7 - 663.2	Tptm	MWT	WTA	TSA	39.5	4.7	1.00	1524.0	3/8/00	1.78-3.03	70.3-119.6
544673	4115729	61.7	ER-EC-6 ^{10,9}	345.1	546.4 - 529.3	Thr ²⁴	NWT	TCU	CHCU	48.4	4.7	0.95	1524.0	3/8/00	1.42-2.41	68.7-116.6
544673	4115729	62.9	ER-EC-6 ^{10,9}	317.4	528.8 - 501.6	Thr ²⁴	NWT	TCU	CHCU	45.2	4.4	0.99	1524.0	3/8/00	1.42-2.41	64.1-108.9
544673	4115729	63.9	ER-EC-6 ^{10,9}	295.8	501.1 - 480.1	Tcpe	PL	TCU	CFCM	44.3	4.2	0.97	1524.0	3/8/00	1.66-2.82	73.5-124.9
544673	4115729	64.9	ER-EC-6 ^{10,9}	271.7	479.5 - 455.9	Tcpe	LA	LFA	CFCM	45.1	5.5	0.97	1524.0	3/8/00	2.16-2.81	97.3-126.6
544673	4115729	67.2	ER-EC-6 ^{10,9}	221.2	455.4 - 405.4	Tcpe	PL	TCU	CFCM	45.0	6.6	0.99	1524.0	3/8/00	1.66-2.82	74.7-127.0
544673	4115729	69.0	ER-EC-6 ^{10,9}	182.8	404.9 - 367.1	Tcpe	LA	LFA	CFCM	46.8	14.1	0.95	1524.0	3/8/00	2.16-2.81	101-131.5

Table A2. (continued)

E	N	Deep bh temp (C)	Borehole	Diff from TD (m)	Elev range (m)	Strat ¹	Class/ rock type ¹	HGU ¹	HSU ¹	Grad T (C/km)	Std dev (C/km)	R ²	Total depth (m)	Temp log (date)	Sat l (W/m C)	Est. Heat Flow (mW/m ²)
Handley Fault-Purse Fault (5)																
539012	4121281	34.4	PM-3#1	335.0	1200.4 - 1189.7	Tpcm	PWT	WTA	TCA	18.1	0.5	1.00	920.2	12/15/99 ³	1.66	30.0
539012	4121281	35.3	PM-3#1	280.2	1189.6 - 1134.8	Tpcm	MWT	WTA	TCA	16.4	0.5	0.99	920.2	12/15/99 ³	1.78	29.1
539012	4121281	35.6	PM-3#1	268.0	1134.8 - 1122.6	Tpcm	PWT	WTA	TCA	24.1	0.5	0.97	920.2	12/15/99 ³	1.66	39.9
539012	4121281	35.6	PM-3#1	265.7	1122.6 - 1120.4	Tpd	BED	TCU	LPCU	9.2	0.0	0.66	920.2	12/15/99 ³		
541285.3	4128082.007	34.3	UE-20j	746.8	1006.8 - 811.7	Tbq	TB	TCU	PBRCM	-0.6		0.13	1734.3	10/10/64		
541285.3	4128082.007	35.0	UE-20j	652.3	808.6 - 717.2	Tqj	FB	LFA	PBRCM	6.8		0.92	1734.3	10/10/64		
541285.3	4128082.007	41.6	UE-20j	566.9	714.1 - 631.9	Tqj	FB	LFA	PBRCM	93.1		0.97	1734.3	10/10/64		
541285.3	4128082.007	44.4	UE-20j	490.7	628.8 - 555.7	Tqj	NWT	unk	PBRCM	37.2		0.88	1734.3	10/10/64	1.42	52.8
541285.3	4128082.007	46.3	UE-20j	387.1	552.6 - 452.0	Tqc	LA	LFA	PBRCM	16.3		0.97	1734.3	10/10/64		
541285.3	4128082.007	46.3	UE-20j	359.7	442.9 - 424.6	Tqc	NWT	TCU	PBRCM	3.6		0.26	1734.3	10/10/64		
541285.3	4128082.007	45.5	UE-20j	338.3	421.5 - 403.3	Tor	NWT	TCU	PBRCM	-48.7		0.91	1734.3	10/10/64		
541285.3	4128082.007	46.1	UE-20j	347.5	412.4	⁵ Total borehole grad T				24.0			1734.3	10/10/64		
541285.3	4128082.007	38.0	UE-20j	746.8	1006.8 - 811.7	Tbq	TB	TCU	PBRCM	2.8	0.5	0.95	1734.3	10/21/64		
541285.3	4128082.007	38.4	UE-20j	652.3	808.6 - 717.2	Tqj	FB	LFA	PBRCM	4.2	0.3	0.95	1734.3	10/21/64		
541285.3	4128082.007	47.3	UE-20j	566.9	714.1 - 631.9	Tqj	FB	LFA	PBRCM	132.4	3.1	0.93	1734.3	10/21/64		
541285.3	4128082.007	38.3	UE-20j	652.3	732.4 - 717.2	Tqj	FB	LFA	PBRCM	28.6		0.97	1734.3	11/8/64		
541285.3	4128082.007	41.0	UE-20j	566.9	714.1 - 631.9	Tqj	FB	LFA	PBRCM	29.9		0.99	1734.3	11/8/64		
541285.3	4128082.007	43.7	UE-20j	490.7	628.8 - 555.7	Tqj	NWT	unk	PBRCM	36.3		0.99	1734.3	11/8/64	1.42	51.6
541285.3	4128082.007	45.4	UE-20j	387.1	552.6 - 452.0	Tqc	LA	LFA	PBRCM	15.6		0.91	1734.3	11/8/64		
541285.3	4128082.007	45.2	UE-20j	359.7	442.9 - 424.6	Tqc	NWT	TCU	PBRCM	-4.6		0.62	1734.3	11/8/64		
541285.3	4128082.007	43.1	UE-20j	286.5	421.5 - 351.4	Tor	NWT	TCU	PBRCM	-35.1		0.97	1734.3	11/8/64		
541285.3	4128082.007	44.0	UE-20j	265.2	348.4 - 330.1	Tot	NWT	TCU	PBRCM	47.1		0.96	1734.3	11/8/64		

Table A2. (continued)

E	N	Deep bh temp (C)	Borehole	Diff from TD (m)	Elev range (m)	Strat ¹	Class/ rock type ¹	HGU ¹	HSU ¹	Grad T (C/km)	Std dev (C/km)	R ²	Total depth (m)	Temp log (date)	Sat l (W/m C)	Est. Heat Flow (mW/m ²)
NW of Handley Fault (6)																
538256.72	4133028.18	53.7	PM-2	45.7	1251.5 - 986.3	Tor	NWT	unk	PBRCM	58.2	2.0	0.89	762	6/6/64		
538256.72	4133028.18	54.2	PM-2	9.1	983.3 - 949.8	Tqm	NWT	unk	PBRCM	15.0	0.3	0.94	762	6/6/64		
538256.72	4133028.18	51.8	PM-2 ⁷	807.7	1251.5 - 986.3	Tor	NWT	unk	PBRCM	38.6	0.5	1.00	1524	7/11/64	1.42	54.8
538256.72	4133028.18	53.3	PM-2 ⁷	771.1	983.3 - 949.8	Tqm	NWT	unk	PBRCM	40.4	0.4	0.99	1524	7/11/64	1.42	57.3
538256.72	4133028.18	56.9	PM-2	652.3	946.7 - 830.9	Tot	NWT	unk	PBRCM	27.8	0.7	0.97	1524	7/11/64		
538256.72	4133028.18	62.3	PM-2	493.8	827.8 - 672.4	Tqm	FB,LA,I	LFA	PBRCM	33.5	0.6	0.99	1524	7/11/64		
538256.72	4133028.18	63.4	PM-2	454.2	669.3 - 632.8	Toh	NWT	unk	PBRCM	29.4	0.2	0.99	1524	7/11/64		
538256.72	4133028.18	64.0	PM-2	426.7	629.7 - 605.3	Toh	FB	LFA	PBRCM	21.8	0.3	0.99	1524	7/11/64		
538256.72	4133028.18	65.5	PM-2	329.2	602.3 - 507.8	Toh	NWT	unk	PBRCM	15.7	0.4	0.97	1524	7/11/64		
538256.72	4133028.18	65.5	PM-2	307.8	504.7 - 486.5	Toh	BED	unk	PBRCM	-2.8	0.1	0.68	1524	7/11/64		
538256.72	4133028.18	83.8	PM-2	1019.3	45.1	⁵ Total borehole grad T				43.0			2676.8	8/10/64		
W. Greeley Fault-E. Greeley Fault (7)																
552668.11	4125925.142	65.5	PM-1	15.2	-381.0	⁵ Total borehole grad T				22.3			2395.1	5/1/64		
552668	4125925	40.5	PM-1	1426.2	1042.1 - 1029.9	Tcblr	NWT	TCU	BFCU	25.0	1.1	0.99	2395.1	8/3/94 ³	1.42-2.41	35.5-60.2
552668	4125925	41.9	PM-1	1368.8	1029.8 - 972.6	Tcblp	NWT	TCU	BFCU	23.6	1.4	1.00	2395.1	8/3/94 ³	1.42-2.41	33.5-56.9
552668	4125925	42.8	PM-1	1327.7	972.3 - 931.4	Tcblp	NWT	TCU	BFCU	23.2	2.8	1.00	2395.1	8/3/94 ³	1.42-2.41	32.9-55.9
552284.53	4125130.301	32.1	UE-20ab	30.2	1265.2 - 1259.1	Thp	LA	LFA	CHVCM	8.2		1.00	777	6/5/78		
552402	4122007	36.4	UE-20bh#1	61.0	1239.5 - 1227.4	Thp	LA,DV	LFA	CHZCM	26.9	1.2	1.00	856.5	10/1/91 ³	1.66	44.6
552402	4122007	37.2	UE-20bh#1	42.8	1227.3 - 1209.1	Thp	LA,GL	LFA	CHZCM	43.5	1.2	1.00	856.5	10/1/91 ³	1.73	75.3
552402	4122007	37.5	UE-20bh#1	33.5	1209.0 - 1199.9	Thp	LA,DV	LFA	CHZCM	36.3	1.3	0.99	856.5	10/1/91 ³	1.66	60.3
552402	4122007	38.2	UE-20bh#1	2.8	1199.8 - 1169.2	Thp	LA,ZE,I	LFA	CHZCM	22.6	1.1	0.98	856.5	10/1/91 ³	2.16	48.7

Table A2. (continued)

E	N	Deep bh temp (C)	Borehole	Diff from TD (m)	Elev range (m)	Strat ¹	Class/ rock type ¹	HGU ¹	HSU ¹	Grad T (C/km)	Std dev (C/km)	R ²	Total depth (m)	Temp log (date)	Sat l (W/m C)	Est. Heat Flow (mW/m ²)
Silent Canyon Struc Zone-W and E Estuary Faults (8)																
559768	4128539	23.8	U-19aj	0.0	1432.9 - 1429.8	Tcblp	TB	TCU	BFCU				670.6	12/9/80		
555857	4125371	30.9	U-19aS	104.8	1079.3 - 1073.2	Tcblr	BED	TCU	BFCU	29.2	0.1	1.00	1092.4	10/4/64	1.73-2.94	50.5-85.7
555857	4125371	31.3	U-19aS	71.3	1070.2 - 1039.7	Tcblr	NWT	TCU	BFCU	5.5	0.9	0.50	1092.4	10/4/64		
555857	4125371	31.3	U-19aS	65.2	1036.6 - 1033.6	Tcblp	NWT	TCU	BFCU				1092.4	10/4/64		
559101	4127775	41.9	U-19e ²⁰	222.5	834.8 - 792.2	Tbdl	MWT	WTA	BRA	25.0	0.5	0.99	1539.2	3/6/66		
559101	4127775	42.7	U-19e ²⁰	188.9	789.1 - 758.6	Tbdl	BED	unk	BRA	23.1	0.6	0.98	1539.2	3/6/66		
559101	4127775	44.3	U-19e ²⁰	138.1	731.2 - 706.8	Tbdl	DWT	WTA	BRA	47.7	1.7	0.93	1540.2	3/6/66		
559101	4127775	46.6	U-19e ²⁰	96.4	691.6 - 664.2	Tbdl	PWT	WTA	BRA	57.5	1.1	0.98	1541.2	3/6/66	1.66-2.82	95.4-162.1
559101	4127775	47.5	U-19e ²⁰	76.1	661.1 - 642.8	Tbdk	PWT	WTA	BRA	41.3	0.8	0.97	1542.2	3/6/66	1.66-2.82	68.5-116.4
559101	4127775	49.4	U-19e ²⁰	32.4	636.7 - 597.1	Tbds	LA	LFA	BRA	42.3	1.2	0.97	1544.2	3/6/66	2.16-2.81	91.5-119.0
559101	4127775	49.2	U-19e ²⁰	4.0	636.7 - 569.7	Tbds	LA	LFA	BRA				1543.2	3/6/66		
556340	4129244	42.2	U-19g	21.9	1089.4 - 1071.1	Tbdl	LA	LFA	BRA	9.6	0.4	0.85	1003.4	11/19/65		
559111.73	4127849.312	46.6	UE-19e	342.9	621.5	⁵ Total borehole grad T				22.6			1830.3	8/23/64		
556306.09	4129056.774	61.6	UE-19gS	1.8	-238.0	⁵ Total borehole grad T				21.3			2287.8	5/4/65		
E. Greeley Fault-Almendro Fault (9)																
556107	4119811	30.3	U-19f	4.3	1226.5	Tci	LA	LFA	IA				830.3	7/5/68		
556107.49	4119780.695	41.1	UE-19fs	777.2	711.7	⁵ Total borehole grad T				21.0			2118.4	8/20/65		

Table A2. (continued)

E	N	Deep bh temp (C)	Borehole	Diff from TD (m)	Elev range (m)	Strat ¹	Class/ rock type ¹	HGU ¹	HSU ¹	Grad T (C/km)	Std dev (C/km)	R ²	Total depth (m)	Temp log (date)	Sat l (W/m C)	Est. Heat Flow (mW/m ²)
Halfbeak Fault-Moor Hen Meadow-Silent Canyon Northern Struc Zones (10)																
		61.1	UE-19d	344.1		⁵ Total borehole grad T				24.3			2343.6	6/25/64		
555488	4132882	28.2	UE-19h ¹⁹	460.9	1421.0 - 1398.1	Tbdl	LA	LFA	BRA	47.9	0.6	1.00	1129.3	12/15/99 ³	2.16-2.81	103.5-134.6
555488	4132882	28.3	UE-19h ¹⁹	457.7	1398.1 - 1394.9	Tbdl	LA	LFA	BRA	22.6	0.6	0.99	1129.3	12/15/99 ³		
555488	4132882	28.4	UE-19h ¹⁹	449.9	1394.9 - 1387.1	Tbdl	LA	LFA	BRA	13.6	0.6	1.00	1129.3	12/15/99 ³		
555488	4132882	28.4	UE-19h ¹⁹	444.7	1387.1 - 1382.0	Tbdl	LA	LFA	BRA	4.6	0.4	0.95	1129.3	12/15/99 ³		
555488.44	4132881.785	31.1	UE-19h ¹⁹	75.9	1013.2	⁵ Total borehole grad T				17.4			1129.3	7/31/65		
Almendo Fault-Scrugham Peak Fault (11)																
557922	4122638	40.8	U-19i ²²	238.6	1129.6 - 1099.1	Tcblp	NWT	TCU	BFCU	31.9	0.5	0.99	1223.1	8/24/67	1.42-2.41	45.3-76.9
557922	4122638	41.6	U-19i ²²	214.2	1096.1 - 1074.7	Tcbx	NWT	TCU	BFCU	34.4	0.8	0.95	1223.1	8/24/67	1.42-2.41	48.9-83.0
557922	4122638	42.2	U-19i ²²	192.9	1071.7 - 1053.4	Tcbx	MWT	WTA	BFCU	25.2	0.2	0.99	1223.1	8/24/67	1.78-3.03	35.8-76.3
557922	4122638	45.1	U-19i ²²	64.9	1041.2 - 925.4	Tcbx	LA	LFA	BFCU	24.5	1.0	0.96	1223.1	8/24/67		
557922	4122638	45.6	U-19i ²²	0.9	916.2 - 861.4	Tcbr	NWT	TCU	BFCU	6.8	0.4	0.95	1223.1	8/24/67		
557922.26	4122592.036	73.8	UE-19i	9.8	-344.1	⁵ Total borehole grad T				25.3			2438.4	9/3/65		
Scrugham Peak Fault-Split Ridge Fault (12)																
559542	4123267	32.6	U-19p	84.2	1429.2 - 1161.0	Tcblp	NWT	TCU	BFCU	8.0	1.4	0.97	1026.0	10/29/75		
Halfbeak Fault-Rickey Fault-Moor Hen Meadow Struc Zone (13)																
560769	4124277	36.0	U-19c	267.3	1454.5 - 1442.3	Tcps	BED	TCU	CFCU				968.3	3/11/65		
560769	4124277	35.4	U-19c	270.3	1454.5 - 1445.4	Tcps	BED	TCU	CFCU	21.7	0.2	0.98	968.3	3/11/65	1.73	37.5
		42.9	U-19t		1245.2 - 1143.0	Tcpk	"FB"	LFA	KA	49.1	1.9	1.00	588.9	9/27/93 ³	1.89	92.8
		45.1	U-19t		1143.0 - 1125.1	Tcpk	"FB"	LFA	KA	129.0	2.6	0.99	588.9	9/27/93 ³		

Table A2. (continued)

E	N	Deep bh temp (C)	Borehole	Diff from TD (m)	Elev range (m)	Class/ Strat ¹ rock type ¹	HGU ¹	HSU ¹	Grad T (C/km)	Std dev (C/km)	R ²	Total depth (m)	Temp log (date)	Sat l (W/m C)	Est. Heat Flow (mW/m ²)
Halfbeak Fault-Rickey Fault-Moor Hen Meadow Struc Zone (13), continued															
562090.74	4129796.621	34.4	UE-19b1	134.1	835.8	⁵ Total borehole grad T		17.4			1371.6	6/15/64			
		35.6	JE-19cWW ²	1828.1	1419.1 - 1384.3	Tbdl	LA LFA BRA	28.5	1.2	0.98	2587.4	11/13/92 ³	2.16-2.81	61.5-80.0	
		36.6	JE-19cWW ²	1665.7	1238.8 - 1221.9	Tbdl	LA LFA BRA	34.8	1.3	0.98	2587.4	11/13/92 ³	2.16-2.81	75.1-97.7	
560338.88	4124701.599	46.6	UE-19c	1212.8	769.0	⁵ Total borehole grad T		24.6			2587.4	5/7/64			
Split Ridge Fault-Rainier Mesa/Ammonia Tanks Caldera Topographic Margin (14)															
567542	4114743	28.6	ER-19-1	223.6	1283.4 - 999.3	MWT,DWT,NWT,PW	PBRCM	16.5		0.99	1095.8	12/6/93 ⁴			
567542	4114743	31.5	ER-19-1	153.5	999.2 - 929.2	CZw	SLT/QI SCU LCCU1	40.5		0.99	1095.8	12/6/93 ⁴	2.23-3.9	90.3-158.0	
567542	4114743	34.8	ER-19-1	3.7	928.8 - 779.4	MDc	SLT SCU UCCU	18.8	1.4	0.99	1095.8	12/6/93 ⁴	3.1-3.66	58.3-68.9	
569000	4112499	24.4	HTH-1 ⁶	583.4	1201.8 - 1177.7	Tor	MWT WTA PBRCM	45.7	4.0	0.84	1282.0	8/19/91 ³	1.78	81.3	
569000	4112499	25.1	HTH-1 ⁶	522.7	1147.0 - 1117.1	Tor	MWT WTA PBRCM	27.0	3.8	0.80	1282.0	8/19/91 ³	1.78	48.1	
569000	4112499	25.7	HTH-1 ⁶	491.3	1115.6 - 1085.7	Tor	PWT WTA PBRCM	17.0	2.3	0.75	1282.0	8/19/91 ³	1.66	28.1	
569000	4112499	29.3	HTH-1 ⁶	205.4	1037.8 - 799.8	Tot	NWT ²³ TCU PBRCM	12.8	3.1	0.99	1282.0	8/19/91 ³	1.42-2.41	18.2-30.9	
569000	4112499	29.8	HTH-1 ⁶	155.1	798.3 - 749.5	Tot	BED ²³ TCU PBRCM	9.1	3.5	0.66	1282.0	8/19/91 ³	1.73-2.94	15.8-26.8	
E of Thirst Canyon Lineament-S of Silent Canyon caldera Structural Margin (15)															
538421	4110841	46.7	ER-EC-2A	115.9	282.2 - 94.0	Tmaw ¹	NWT/B TCU TMCM	15.2	9.4	0.99	1516.1	2/7/00	1.73-2.94	26.7-44.6	
538421	4110841	46.9	ER-EC-2A	106.1	93.9 - 84.2	Tmaw	MWT WTA TMCM	13.7	13.2	0.46	1516.1	2/7/00	1.78-3.03	24.4-41.5	
538421	4110841	47.3	ER-EC-2A	64.1	84.1 - 42.1	Tmaw	NWT/R TCU TMCM	10.0	11.7	0.79	1516.1	2/7/00	1.42-2.41	14.2-24.1	
538421	4110841	48.6	ER-EC-2A	-2.6	42.1 - -24.5	Tmar	MWT WTA TMCM	23.9	12.1	0.97	1516.1	2/7/00	1.78-3.03	42.5-72.3	
538421	4110841	48.6	ER-EC-2A	-2.6	-24.5	Tmar	MWT WTA TMCM				1516.1	2/7/00			
538421	4110841	48.3	ER-EC-2A	116.1	281.8 - 94.2	Tmaw ¹	NWT/B TCU TMCM	16.2	2.8	0.99	1516.1	2/9/00	1.73-2.94	28-47.7	
538421	4110841	48.4	ER-EC-2A	106.4	93.6 - 84.5	Tmaw	MWT WTA TMCM	24.6	2.8	0.76	1516.1	2/9/00	1.78-3.03	43.7-74.4	
538421	4110841	49.4	ER-EC-2A	64.1	83.9 - 42.1	Tmaw	NWT/R TCU TMCM	21.3	2.5	0.99	1516.1	2/9/00	1.42-2.41	30.2-51.2	
538421	4110841	50.5	ER-EC-2A	11.3	41.5 - -10.7	Tmar	MWT WTA TMCM	21.1	2.1	0.99	1516.1	2/9/00	1.78-3.03	37.5-63.9	

Table A2. (continued)

E	N	Deep bh temp (C)	Borehole	Diff from TD (m)	Elev range (m)	Class/ Strat ¹ rock type ¹	HGU ¹	HSU ¹	Grad T (C/km)	Std dev (C/km)	R ²	Total depth (m)	Temp log (date)	Sat l (W/m C)	Est. Heat Flow (mW/m ²)
E of Thirst Canyon Lineament-S of Silent Canyon caldera Structural Margin (15), continued															
538702	4104334	28.6	ER-EC-5	-0.6	1117.7 - 784.9	Tmar,	MWT	WTA	TMCM	0.9	0.68	762.0	7/5/99		
538702	4104334	30.1	ER-EC-5	6.0	791.4	Tmap	VT	WTA	TMCM			762.0	7/7/99		
538702	4104334	29.9	ER-EC-5 ¹⁴	22.6	864.5 - 808.1	Tmap	MWT-E	WTA	TMCM	0.4	0.10	762.0	6/7/00		
Ammonia Tanks Caldera Struct Margin-W of Scrugham Peak Fault (16)															
549322	4109762	35.0	UE-18r	158.2	442.6 - 321.0	Tmrx	NWT	VTA	TMCM	33.8	1.2	1525.2	3/16/93 ³	1.42-2.41	48-81.5
549322	4109762	36.5	UE-18r	104.8	321.0 - 267.6	Tmr	MWT	WTA	TMCM	27.7	1.2	1525.2	3/16/93 ³	1.78-2.82	49.2-78
549322	4109762	37.0	UE-18r	83.6	267.5 - 246.4	Tmr	VT	WTA	TMCM	23.0	1.1	1525.2	3/16/93 ³	2.01-3.42	46.2-78.6
549322	4109762	38.5	UE-18r	18.8	246.3 - 181.6	Tmrx	TB	WTA	TMCM	23.2	1.1	1525.2	3/16/93 ³	1.89-3.21	43.8-74.4
Ammonia Tanks Caldera Struct Margin-E of Scrugham Peak Fault (17)															
555725	4106389	50.9	ER-18-2	201.9	1188.1 - 1097.2	Tmar	WT-DW	WTA	TMCM	62.1	10.4	762.0	7/14/99	2.82	175.0
555725	4106389	52.9	ER-18-2	35.0	963.3 - 930.2	Tmar	WT-DW	WTA	TMCM	53.2	10.8	762.0	7/14/99	2.82	150.0
E of Ammonia Tanks Caldera Struct Margin-Within Rainier Mesa Caldera Struct Margin (18)															
560804.66	4100462.968	28.0	ER-30-1	145.5	1165.8 - 1126.9	Tfbw	BED	TCU	FCCM	42.5	4.1	435	3/22/94	1.73	73.4
559591	4109095	37.8	UE-18t	353.3	1188.4 - 1146.1	Tmab	BED	TA,TC	TMCM	28.8	1.3	792.5	12/12/99 ³	1.73-2.94	49.8-84.7
559591	4109095	39.3	UE-18t	295.3	1143.9 - 1088.1	Tmrb	NWT	TCU	TMCM	24.4	0.9	792.5	12/12/99 ³	1.42-2.41	42.2-58.8
559591	4109095	40.0	UE-18t	269.6	1085.8 - 1062.4	Tmrr ²⁴	MWT, V ¹	WTA	TMCM	31.4	0.8	792.5	12/12/99 ³	1.78-2.41	54.4-75.8
559591	4109095	42.0	UE-18t	215.8	1059.9 - 1008.6	Tmrr ²⁴	MWT	WTA	TMCM	35.8	6.46*	792.5	12/12/99 ³	1.78-2.41	61.9-86.2
E of Thirst Canyon Lineament-Hogback Fault-Ammonia Tanks Caldera Struct Margin (19)															
532764	4106142	36.9	ER-EC-8	-10.8	700.4	Tmap	MWT	WTA	TMCM			609.6	7/22/99		

Table A2. (continued)

E	N	Deep bh temp (C)	Borehole	Diff from TD (m)	Elev range (m)	Class/ Strat ¹ rock type ¹	HGU ¹	HSU ¹	Grad T (C/km)	Std dev (C/km)	R ²	Total depth (m)	Temp log (date)	Sat I (W/m C)	Est. Heat Flow (mW/m ²)	
W of Thirst Canyon Lineament-SW of Silent Canyon Caldera Struc Margin (20)																
532760	4112356	51.6	ER-EC-4	176.8	599.1 - 564.7	Tmap	NWT	VTA	TMA	45.3	7.5	1.00	1062.8	6/14/99	1.42	64.4
532760	4112356	52.9	ER-EC-4	151.2	564.7 - 539.1	Tmab	BED	TCU	TMA	52.2	8.5	1.00	1062.8	6/14/99	1.73	90.3
532760	4112356	53.4	ER-EC-4	142.4	539.1 - 530.3	Tmrbr	RWT	TCU	TMA	59.9	8.6	0.96	1062.8	6/14/99	1.73	103.7
532760	4112356	54.0	ER-EC-4	130.8	530.2 - 518.7	Tmrbr	BED	TCU	TMA	54.4	15.6	0.93	1062.8	6/14/99	1.73	94.0
532760	4112356	54.9	ER-EC-4	116.2	518.6 - 504.1	Tmrp	NWT	TCU	TMA	54.6	9.6	0.98	1062.8	6/14/99	1.42	77.5
532760	4112356	56.6	ER-EC-4	74.1	504.0 - 462.0	Tmrp	PWT	WTA	TMA	42.7	8.1	1.00	1062.8	6/14/99	1.66	70.9
532760	4112356	58.1	ER-EC-4	50.9	462.0 - 438.9	Tmrp	MWT	WTA	TMA	63.7	8.4	0.98	1062.8	6/14/99	1.78	113.5
532760	4112356	58.7	ER-EC-4	44.8	438.8 - 432.8	Tmrp	VT	WTA	TMA	100.8	8.5	0.95	1062.8	6/14/99		
532760	4112356	62.0	ER-EC-4	24.7	432.7 - 412.7	Tmrp	DWT	WTA	TMA	163.8	11.8	0.98	1062.8	6/14/99	1.66	271.9
532760	4112356	62.9	ER-EC-4	20.5	412.6 - 408.4	Tmrp	VT	WTA	TMA	244.1	10.9	0.97	1062.8	6/14/99		
532760	4112356	64.2	ER-EC-4	7.2	408.3 - 395.1	Tmrp	NWT	TCU	TMA	112.7	11.9	0.92	1062.8	6/14/99	1.42	160.0
532760	4112356	64.2	ER-EC-4	-3.5	384.4	Tmrp	NWT	TCU	TMA				1062.8	6/14/99		
532760	4112356	42.1	ER-EC-4 ¹²	176.8	599.1 - 564.7	Tmap	NWT	VTA	TMA	20.0	2.1	0.99	1062.8	8/25/00 ³	1.42	28.5
532760	4112356	42.6	ER-EC-4 ¹²	151.4	564.2 - 539.4	Tmab	BED	TCU	TMA	19.5	2.4	0.97	1062.8	8/25/00 ³	1.73	33.7
532760	4112356	42.7	ER-EC-4 ¹²	142.4	538.9 - 530.3	Tmrbr	RWT	TCU	TMA	19.5	2.7	0.82	1062.8	8/25/00 ³		
532760	4112356	43.0	ER-EC-4 ¹²	130.8	529.8 - 518.7	Tmrbr	BED	TCU	TMA	24.7	3.0	0.88	1062.8	8/25/00 ³		
532760	4112356	43.5	ER-EC-4 ¹²	117.3	518.2 - 505.2	Tmrp	NWT	TCU	TMA	37.9	2.2	0.95	1062.8	8/25/00 ³	1.42	53.8
532760	4112356	44.6	ER-EC-4 ¹²	74.2	503.7 - 462.1	Tmrp	PWT	WTA	TMA	22.4	3.2	0.93	1062.8	8/25/00 ³		
532760	4112356	44.8	ER-EC-4 ¹²	51.3	461.6 - 439.2	Tmrp	MWT	WTA	TMA	8.0	2.9	0.70	1062.8	8/25/00 ³		
532760	4112356	44.9	ER-EC-4 ¹²	45.3	438.8 - 433.2	Tmrp	VT	WTA	TMA	23.2	2.5	0.71	1062.8	8/25/00 ³		
532760	4112356	45.8	ER-EC-4 ¹²	25.0	432.7 - 412.9	Tmrp	DWT	WTA	TMA	40.1	2.1	0.96	1062.8	8/25/00 ³		
532760	4112356	46.6	ER-EC-4 ¹²	20.9	412.4 - 408.8	Tmrp	VT	WTA	TMA	242.1	1.9	0.99	1062.8	8/25/00 ³		
532760	4112356	46.7	ER-EC-4 ¹²	19.9	408.3 - 407.8	Tmrp	NWT	TCU	TMA	<3			1062.8	8/25/00 ³		
Claim Canyon Caldera Struc Margin (21)																
546484	4093127	26.9	ER-EC-7 ¹⁵	53.5	1112.6 - 1095.6	Tfbr	LA	LFA	FCCM	21.8		0.97	422.5	8/8/99		
546484	4093127	27.3	ER-EC-7 ¹⁵	39.6	1096 - 1081.8	Tfb	LA	LFA	FCCM	28.4		0.94	422.5	8/8/99	2.16	61.3
546484	4093127	26.6	ER-EC-7 ¹⁶	41.5	1095.5 - 1083.7	Tfb	LA	LFA	FCCM	33.0		0.98	422.5	6/1/00		

Table A2. (continued)

¹Explanation of abbreviations can be found at the end of this attachment

²Depth corrected for borehole deviation from vertical by 13.18° at bottom of well

³Temperature logged more than one year after drilling

⁴Temperature logged about 5 months after drilling

⁵Blankennagel and Weir (1973): total borehole temperature gradient for all hydrostratigraphic units from surface elevation to temperature measurement depth

⁶Casing perforated over five intervals from 582.2 to 740.7 m depth; cased to 1131.1 m depth.

⁷Cased to 762 m

⁸Casing perforated over three intervals between depths of 700.4-860 m, 1020.3-1146.2 m, and 1355.9-1447.6 m. Analcime found at depth.

⁹Intense low-temperature hydrothermal alteration below the Rhyolite of Benham of the Paintbrush Group (analcime is the zeolite in minor amounts)

¹⁰Casing perforated over four intervals between depths of 496.3-570 m, 668.9-764 m, 1047.8-1161.5 m, and 1347.4-1494.6 m

¹¹Original description: Tmx, 948-1256 m depth, landslide breccia (argillite, interbedded sediments, limestone block, intracaldera tuff breccia in zeolitized tuff matrix)

¹²Casing perforated over three intervals between depths of 301.5-372.1 m, 582.2-686.7 m, and 945.9-1037.8 m. Temperature gradients low throughout borehole, approximately one week after hydraulic tests. Is this borehole significantly affected by pumping? Is there not-yet-equilibrated borehole mixing between intervals?

¹³Casing perforated and gravel packed over two intervals between depths of 742.8.4-843.4 m and 858-898.2 m

¹⁴Borehole gravel packed and casing perforated over three intervals between depths of 361.8-439.8, 565.2-654.1, and 677.5-755.9 m

¹⁵Cased to 265.8 m

¹⁶Borehole gravel packed and casing perforated over two intervals between depths of 278-312.1 and 360.9-399.3 m

¹⁷Harmonic mean used to calculate λ

¹⁸Deep intracaldera thermal conductivity used to estimate heat flux

¹⁹Cased to 707.4 m

²⁰May not have been cased to 1529 m depth at time of temperature log

²¹Cased to 737.9 m

²²May not have been cased to 1220.4 m depth at time of temperature log

²³Low-temperature hydrothermal alteration (analcime is the zeolite in minor amounts; chalcedony present).

²⁴Basalt/mafic-rich composition

Table B1. Range of SZ thermal conductivity estimates for rock types in HSU

HSU #	Group # ¹	HSU ²	HGU	Alteration ³	Rock type ³	Representative Wells Penetrating HSU ⁴	Stratigraphy ³	Dominant lithology ³	low (W/m C) ⁵	base (W/m C) ⁵	high (W/m C) ⁵
1	1	LCCU	CCU		SLT/QTZ/SS		CZ (Wood Canyon Fm, Stirling Qtzite, Johnnie Fm)	Qtzite, silica-cemented siltst	2.23	3.9	5.8
2	2	LCA	CA		DM		DSsl	Ds,ls	4.67	4.95	5.23
3	3	UCCU	CCU/SCU		SLT	ER-19-1	MDC (Eleana Fm, Chainman Shale)	Argillite, shale, limestone	2.47	3.1	3.66
4	1	LCCU1	CCU/SCU		SLT/QTZ/SS	ER-19-1	CZ (Wood Canyon Fm, Stirling Qtzite, Johnnie Fm)	Qtzite, silica-cemented siltst	2.23	3.9	5.8
5	2	LCA3	CA		DM	HTH-1	DSsl	Ds,ls	4.67	4.95	5.23
6	4	MGCU	GCU		IN			Qtz monzonite, granodiorite	2.26	2.26	2.6
7	4	SCICU	IICU		IN			Granite	2.6	2.6	2.9
8	4	CHICU	IICU		IN			Granite, marble, argillite	2.6	2.6	2.9
9	4	CCICU	IICU		IN			Granite	2.6	2.6	2.9
10	4	RMICU	IICU		IN			Granite	2.6	2.6	2.9
11	4	ATICU	IICU		IN			Granite	2.6	2.6	2.9
12	5	BMICU	IICU		IN			Diorite	2.1	2.1	2.41

Table B1. Range of SZ thermal conductivity estimates for rock types in HSU (continued).

HSU #	Group # ¹	HSU ²	HGU	Alteration ³	Rock type ³	Representative Wells Penetrating HSU ⁴	Stratigraphy ³	Dominant lithology ³	l low (W/m C) ⁵	l base (W/m C) ⁵	l high (W/m C) ⁵
13	6	PBRCM	TCU, WTA, LFA	ZE, DV, QC, AR, AB	NWT, BED, PWT, MWT, DWT, TB, FB, LA, IN	PM-2, PM-3 , U-19d #2, UE-19c, UE-19gS, U-20m, UE-20f, UE-20j , UE-20p, ER-19-1 #1, #2, #3, HTH-1, WW 8	Tbgb, Tbg, Tln, Tn, Tn3D, Tn4AF, Tn4J, Tn4K, To, Toa, Toh, Ton2, Tor, Tot, Toy, Tqc, Tqh, Tqj, Tqm, Tqu, Trg, Trl, Trpd, Trr, Tub, unk	Zeolitic tuff, devitrified tuff, lava	1.71	2.13	2.71
14	6	BRA	LFA, WTA, TCU, VTA,	DV, ZC, ZE, AB, PY, QC, KF	LA, FB, BED, NWT, MWT, PWT, DWT, PL	PM-1, PM-3 , U-19c, U-19d #2, U-19g, U-19e, U-19u, UE-19b, UE-19b#1, UE-19c, UE-19e, UE-19h, UE-19fS, UE-19gS, UE-19i, U-20m, UE-20f, UE-20j , UE-20p, UE-20e #1, WW-8	Tbd, Tbdb, TbdC, Tbdk, Tbdl, Tbds, Tbg, Tbgb, Tbgm, Tbgp, Tbgr, Tbgs, Tbg, Tcl, Tn4JK, Trl, Trr, unk	Lava, devitrified tuff, zeolitic tuff	1.84	2.63	3.06
15	6	BFCU	TCU	ZE, ZC, DV	BED, NWT, LA	PM-3 , PM-1, U-19ab, U-19ab#2,#3, U-19ai, U-19aj , U-19aS, U-19ba #1,#2,#3 , U-19e, U-19g , U-19i, U-19p, U-19v, UE-19c, UE-19e , UE-19fS, UE-19gS , UE-19i, UE-19z , U-20g, U-20m, UE-20f, UE-20h	Tbdl, Tcblp, Tcblr, Tcbp, Tcbr, Tcbs, Tcbx, Tct	Zeolitic tuff, lava	1.57	2.61	2.95
16	7	KA	LFA, TCU	DV, GL, ZE, ZC	LA, FB, PL	U-19ba, U-19ba #1, #2, U-19ba #3, U-19bj, U-19t	Tcg, Tcpk	Lava, Zeolitic tuff	1.77	1.85	1.89

Table B1. Range of SZ thermal conductivity estimates for rock types in HSU (continued).

HSU #	Group # ¹	HSU ²	HGU	Alteration ³	Rock type ³	Representative Wells Penetrating HSU ⁴	Stratigraphy ³	Dominant lithology ³	l low (W/m C) ⁵	l base (W/m C) ⁵	l high (W/m C) ⁵
17	8	CFCU	TCU, LFA, VTA	ZC, ZE, DV, GL	LA, NWT, BED	PM-1, U-19ab, U-19ab#2,#3, U-19ae, U-19aS, U-19aS#1, U-19c, U-19g, U-19i, U-19v, UE-19c, UE-19fS, UE-19gS, UE-19i	Tcg, Tci, Tcj, Tcpg, Tcps, Tcu, unk	Zeolitic tuff, lava, vitric tuff	1.43	1.61	1.79
18	7	CFCM	Mostly LFA, some TCU	DV, QF, AR, PY, CH, ZA, ZC	LA, FB, BED, NWT	ER-EC-1, ER-EC-6, U-20aa, U-20g, U-20i, UE-20e #1, UE-20f, UE-20h, UE-20j	Tcbs, Tcf, Tci, Tcj, Tcpe, Tcpg, Tcps, Tcu, unk	Lava, Zeolitic tuff	1.78	1.87	1.96
19	7	IA	LA	DV, GL, ZC	LA, MWT, FB	U-19f, UE-19fS, UE-20f	Tci	Lava	1.65	1.86	2.06
20	7	CHCU	TCU, LFA	ZC	NWT, BED, PL	PM-3, ER-EC-1, ER-EC-6, U-19f, U-19ae, UE-19fS	Tcg, Tci, Thp, Thr, Tpe, Tpr, Tptb	Zeolitic tuff, Lava	1.56	1.84	2.12
21	7	CHZCM	LFA, TCU, VTA	ZC, ZE, ZA, DV, GL	LA, FB, PL, BED	ER-20-5#1,#3, ER-20-2#1, U-20a, U-20a#2WW, U-20aa, U-20ah, U-20ai, U-20an, U-20ar#1, U-20aw, U-20ax, U-20ay, U-20az, U-20bd, U-20bd#1, #2, U-20be, U-20bf, U-20bg, U-20c, U-20d, U-20e, U-20e#1, U-20g, U-20i, U-20n, U-20WW, UE-20ad, UE20av, UE-20c, UE-20d, UE-20e, UE-20e#1, UE-20f, UE-20h, UE-20n#1, UE-20bh#1	Tcj, Tcu, Th, Thp, Thr, Tmw, Tpr, Tpt, Tptm, unk	Zeolitic tuff, Lava	1.67	1.81	1.95
22	7	CHVCM	VTA, LFA, TCU	GL, DV, ZC, ZA	LA, FB, NWT, BED	U-19au, U-19au#1, U-20am, UE-20ab	Tcj, Tcps, Tcu, Thp, Tpt, unk	Vitric tuff, Lava	1.48	1.7	1.93

Table B1. Range of SZ thermal conductivity estimates for rock types in HSU (continued).

HSU #	Group # ¹	HSU ²	HGU	Alteration ³	Rock type ³	Representative Wells Penetrating HSU ⁴	Stratigraphy ³	Dominant lithology ³	l low (W/m C) ⁵	l base (W/m C) ⁵	l high (W/m C) ⁵
23	8	CHVTA	VTA, TCU	GL, ZC	NWT, BED, PL	U-19aS, U-19aS#1, U-19bg#1, U-19bj, U-19c, U-19v, U-19yS, UE-19i	Tcj, Tcpk, Tcps, Tcu, Th, Thp, Tmt, Tpe, Tpr, Tptb, unk	Vitric, zeolitic tuff	1.42	1.5	1.61
24	7	YMCFCM	TCU, LFA, WTA, unk	ZE, ZM, ZC, ZA, AR, QC, AB, CC, KF, DV	NWT, BED, MWT, PWT, LA	UE-29a #2	Tcby, Tcp, Tct, Thp, Thr	Zeolitic tuff, Lava	1.66	1.86	2.16
25	8	TSA	WTA, TCU, unk	DV, QF, GL, ZE, unk	NWT, PWT, TUF, MWT, VT	ER-EC-1, ER-EC-6, ER-20-5 #1, ER-20-5 #3, U-20c, U-20d, U-20y, UE-20c, UE-20d	Tptm	Devitrified tuff	1.57	1.69	1.81
26	8	LPCU	TCU, unk	ZE, ZC, ZA, QZ, QF, PY, CH, unk	NWT, BED, TB, WBE	PM-3, ER-EC-1, ER-EC-6, ER-20-5 #1, ER-20-6 #1, #2, #3, U-20av, U-20bd, U-20bd #1, #2, U-20c, U-20d, U-20m, U-20y, UE-20av, UE-20c, UE-20f, UE-20d	Thr, Tp, Tpcm, Tpd, Tpe, Tpr, Tptb, Tptm, Tptx	Zeolitic tuff	1.52	1.69	1.86
27	7	PLFA	LFA, WTA, TCU, VTA, unk	DV, GL, ZC, ZE, VP, AR, unk	LA, FB, PL, NWT, BED, MWT, DWT, VT, PWT, unk	U-19ad, U-19aq, U-19ar, U-19ay, U-19az, U-19bg#1, U-19bg, U-19bh, U-19yS, U-19x	Tpe, Tpr, Tptb, unk	Lava, Devitrified tuff, Zeolitic tuff, Vitric tuff	1.58	1.75	1.92
28	7	TCA	WTA, unk	DV, QF, VP, QC, QZ, ZE, unk	MWT, PWT, DWT, VT, unk, TUF	PM-3, ER-EC-1, ER-EC-6, ER-20-1, U-20d, U-20c, UE-20d, UE-20c, UE-20f	Tpcm, Tpcr	Devitrified tuff	1.7	1.75	1.8

Table B1. Range of SZ thermal conductivity estimates for rock types in HSU (continued).

HSU #	Group # ¹	HSU ²	HGU	Alteration ³	Rock type ³	Representative Wells Penetrating HSU ⁴	Stratigraphy ³	Dominant lithology ³	l low (W/m C) ⁵	l base (W/m C) ⁵	l high (W/m C) ⁵
29	8	UPCU	TCU, VTA, LFA, unk	ZC, ZE, GL , QF, KF , unk, OP	NWT, BED, unk, TUF, RWT, FB, BS, TB	PM-3, ER-EC-1, ER-EC-6 , ER-20-6#2, ER-20-6#1, U-20as, U-20bb, U-20bb#1, U-20bc, U-20bd, U-20bd#2, U-20d, UE-20d, UE-20f, UE-20n #1	Tm, Tmrf, Tmrh, Tmt, Tmw, Tp, Tpb, Tpc, Tpcm, Tpcr, Tpcx, Tpcy, Tpcyp, Tpd, Tpe, unk	Zeolitic tuff , Vitric tuff, Basalt, Lava	1.59	1.69	1.8
30	7	BA	LFA, TCU, unk	GL , DV, ZE, QZ, unk , QF, OP	LA, PL, FB, VL	ER-EC-6, ER-EC-1, U-20ak, U-20ao, U-20bb, U-20bb #1, UE-20d, U-20d	Tpb	Lava , Devitrified tuff, Zeolitic tuff	1.7	1.9	2.11
31	8	PVTA	VTA, WTA, LFA, TCU, unk	GL , DV, ZE, ZC, unk, VP, AR	MWT, PWT, DWT, VT, NWT, BED, TUF, unk, RWT, BS, PL	U-19c, U-20bb, U-20bb#1, U-20m, UE-20f, UE-20j	Tm, Tmra, Tmrd, Tmrf, Tmrh, Tmt, Tp, Tpb, Tpcm, Tpd, Tpe, Tpr, Tptb, unk	Vitric tuff , Devitrified tuff , Zeolitic tuff , Lava, Basalt	1.54	1.68	1.82
32	7	PCM	WTA, VTA, TCU, LFA, unk, AA	DV, VP, GL , ZC, ZE, unk, AR, CC , QC , OP	DWT, MWT, VT, PWT, NWT, BED, LA, AL	UE-29a #2	QTa, Tpcp, Tpg, Tpp, Tptbr, Tptp, Tptr, Tpv, Tpy	Devitrified tuff , Vitric tuff , Zeolitic tuff, Lava, Alluvium	1.42	1.95	2.16
33	2	LCA3a									
34	8	FCCU	TCU	ZE	NWT, BED	ER-EC-1, ER-EC-6	Tmrf	Zeolitic tuff	1.42	1.58	1.73

Table B1. Range of SZ thermal conductivity estimates for rock types in HSU (continued).

HSU #	Group # ¹	HSU ²	HGU	Alteration ³	Rock type ³	Representative Wells Penetrating HSU ⁴	Stratigraphy ³	Dominant lithology ³	l low (W/m C) ⁵	l base (W/m C) ⁵	l high (W/m C) ⁵
35	6	SCVCU	NA	NA	NA	NA	NA	NA	2.16	2.61	2.79
36	8	TMA	WTA, VTA, unk, TCU, LFA, ICU, AA	unk, GL, DV, VP, ZE, ZC, QF, QZ, CC, OP, AR, KF	MWT, PWT, DWT, VT, unk, TUF, WT, NWT, BED, RWT, AL, BD, LA	ER-EC-4, ER-OV-3c, ER-OV-3c2, U-20m, UE-20j, UE-20p	Tfbr, Tfbw, Tg, Tm, Tma, Tmab, Tmap, Tmar, Tmay, Tmr, Tmra, Tmrb, Tmrr, Tt, Ttl, Ttp, Ttt, Tyb, unk	Devitrified tuff, Vitric tuff, Zeolitic tuff, Lava, Alluvium	1.46	1.59	1.73
37	7	THCM	TCU, WTA, VTA	ZE, GL, DV, QZ	BED, MWT	ER-EC-1, ER-EC-6	Tmat	Zeolitic tuff, Vitric tuff, Devitrified tuff	1.67	1.81	1.95
38	7	THLFA	LFA, AA	DV, QZ, GL, ZE, unk	LA, VL, PL, AL	ER-EC-1, ER-EC-6	Tmat, Qay	Lava, Alluvium	1.66	1.86	2.16
39	6	TMCM	TCU, WTA, VTA, LFA, AA	QF, DV, ZE, QZ, VP, GL, ZA, QZ, QC, AB, AR, KF, KA, CC, CH, PY	MWT, PWT, DWT, LB, VT, NWT, BED, LA, RWT, TB, TG, TS, TSS, FB	ER-EC-2a, ER-EC-5, ER-EC-8, ER-30-1, ER-18-2, UE-18r, UE-18t	Tma, Tmab, Tmac, Tmap, Tmar, Tmat, Tmaw, Tmawp, Tmawr, Tmay, Tmr, Tmrb, Tmrr, Tmrx, Tmx	Zeolitic tuff, Devitrified tuff, Lava, Vitric tuff, Alluvium	1.7	2.79	2.98
40	7	FCA	NA	NA	NA	NA	NA	NA	1.66	1.86	2.16
41	7	FCCM	LFA, TCU, WTA, unk, VTA, AA	ZE, DV, GL, QZ, QF, QC, CC, AB, PI, MP, CH, PY, unk, AR	MWT, PWT, NWT, TB, unk, RWT, BED, TSS, PL, LA, FB, VL, BS, TSLT, WT, AL	ER-EC-2a, ER-EC-4, ER-EC-7, ER-EC-8, ER-OV-1, ER-OV-6a, ER-OV-6a2, UE-18t	Qay, Tf, Tfb, Tfbb, Tfbc, Tfbr, Tfbw, Tfdb, Tff, Tfl, Tfu, Tg, Tgc, unk	Zeolitic tuff, Lava, Devitrified tuff, Vitric tuff, Basalt, Alluvium	1.58	1.74	1.89

Table B1. Range of SZ thermal conductivity estimates for rock types in HSU (continued).

HSU #	Group # ¹	HSU ²	HGU	Alteration ³	Rock type ³	Representative Wells Penetrating HSU ⁴	Stratigraphy ³	Dominant lithology ³	l low (W/m C) ⁵	l base (W/m C) ⁵	l high (W/m C) ⁵
42	7	DVA	NA	NA	NA	NA	NA	NA	1.66	1.86	2.16
43	8	DVCM	TCU, WTA	DV, AR, QF	NWT, MWT, PWT	ER-OV-03a2, ER-OV-03a3, ER-OV-03a	Tf, Tma	Devitrified tuff	1.43	1.56	1.68
44	8	TCVA	WTA, VTA, LFA, unk, TCU, AA	unk, DV, GL, VP, ZE, CC, QF	MWT, PWT, DWT, NWT, BED, RWT, WT, TUF, ITL, LA, AL, CL	ER-EC-4	Tfb, Tfbr, Tfbw, Tftr, Tmap, Tt, Ttc, Ttcl, Ttcm, Ttg, Ttp, Ttr, Ttt, unk	Devitrified tuff, Vitric tuff, Lava, Zeolitic tuff, Alluvium	1.42	1.64	1.78
45	7	YVCM	LFA, WTA, AA	unk, DV, VP	AL, BS, PWT	TP/AFB1, ER-18-2, ER-EC-4	Ta, Tg, Ts, Tsc, Ty	Devitrified tuff, Basalt, Alluvium	1.67	1.81	1.95
46	9	AA	AA, VTA, WTA, LFA, TCU	unk, GL, VP, AR, CC, ZE, ZC	AL, TS, RWT, BS, NWT, BED, PWT, MWT, PWT	ER-OV-02, ER-OV-03b, ER-OV-04a, ER-OV-05	Qa, QTa, Tg, Tgc, Tgs, Tt, Tte, Ttp, Ttt, Tyo	Alluvium, Devitrified tuff, Vitric tuff, Zeolitic tuff, Basalt	1.33	1.44	1.44

¹Group number used to assign lumped thermal conductivities for calibration purposes

²HSU in bold is more indurated, intracaldera tuff

³Dominant lithology, alteration, rock type, or stratigraphy in bold

⁴Borehole in bold is located outside the caldera for intracaldera HSU or inside a caldera for extracaldera HSU

⁵Tuff HSU thermal conductivity estimated from harmonic mean of tuff rock types in boreholes (Table B3)

Table B2. Estimates of SZ HSU thermal conductivity. Estimates computed from harmonic mean of SZ thermal conductivity estimates (compiled in Table B3) for rock types in boreholes penetrating HSU.

HSU	Borehole	Depth range (m)	Elevation range (m)	Thickness (m)	Harmonic mean over rock types l (W/mC)	HSU l (W/mC)	Std dev l (W/mC)	Min l (W/mC)	Max l (W/mC)	Low l (W/mC)	High l (W/mC)
LCCU											
LCA											
UCCU	ER-19-1#1	942.8 - 1095.8	928.7 - 775.7	153.0	3.10 N=3	3.10		3.10	5.45	2.47	3.66
	ER-19-1#2	942.8 - 1095.8	928.7 - 775.7	153.0	3.10						
	ER-19-1#3	942.8 - 1095.8	928.7 - 775.7	153.0	3.10						
LCCU1	ER-19-1#1	872.3 - 942.7	999.1 - 928.7	70.4	3.90 N=3	3.90		2.23	5.80		
	ER-19-1#2	872.3 - 942.7	999.1 - 928.7	70.4	3.90						
	ER-19-1#3	872.3 - 942.7	999.1 - 928.7	70.4	3.90						
LCA3	HTH-1	1127.7 - 1282.0	748.6 - 594.4	154.2	4.95 N=1	4.95		4.95	4.95	4.45	5.47
MGCU								2.26	2.60		
SCICU								2.60	4.00		2.90
CHICU								2.60	5.00		2.90
CCICU								2.60	4.00		2.90
RMICU								2.60	4.00		2.90
ATICU								2.60	4.00		2.90
BMICU								2.10	2.41		
PBRCM	ER-19-1#1	544.0 - 872.3	1327.4 - 999.1	328.3	1.66 N=13	1.71-2.13	0.14,0.58	1.42	2.94	1.58	1.85-2.71
	ER-19-1#2	359.6 - 872.3	1511.8 - 999.1	512.7	1.64						
	ER-19-1#3	306.6 - 872.3	1564.8 - 999.1	565.7	1.63						
	HTH-1	165.2 - 1127.8	1711.2 - 748.6	962.6	1.91						
	PM-2	261.7 - 2676.8	1440.9 - -974.1	2415.0	1.83						
	PM-3	914.4 - 920.2	860.5 - 854.7	5.8	1.42						
	U-19d #2	2279.9 - 2343.6	-188.7 - -252.4	63.7	1.73 - 2.94						
	UE-19c	2401.9 - 2587.4	-258.2 - -443.8	185.6	1.95 - 2.86						
	UE-19gS	2002.6 - 2286.0	45.4 - -238.0	283.4	1.63 - 2.77						
	UE-20f	2974.3 - 4171.5	-1110.1 - -2307.3	1197.2	1.76 - 2.82						
	UE-20j	761.1 - 1734.3	1038.1 - 64.9	973.2	1.60						
	UE-20p	554.8 - 1524.0	1137.8 - 168.6	969.2	1.77 - 2.84						
	WW 8	612.6 - 1676.1	1123.2 - 59.7	1063.5	1.72						

Table B2. Estimates of SZ HSU thermal conductivity (continued).

HSU	Borehole	Depth range (m)	Elevation range (m)	Thickness (m)	Harmonic mean over rock types l (W/mC)	HSU l (W/mC)	Std dev l (W/mC)	Min l (W/mC)	Max l (W/mC)	Low l (W/mC)	High l (W/mC)
BRA	PM-1	1603.3 - 2395.1	395.6 - -396.2	791.8	1.86 - 2.81 N=21	1.84-2.63	0.19,0.43	1.62	3.09	1.65-2.20	2.03-3.06
	PM-3	899.2 - 914.4	875.7 - 860.5	15.2	1.67						
	U-19c	730.0 - 968.3	1413.4 - 1175.0	238.4	2.15						
	U-19d #2	664.4 - 2279.9	1426.8 - -188.7	1615.5	1.86 - 2.73						
	U-19e	894.0 - 1539.2	1214.9 - 569.7	645.2	1.76 - 2.91						
	U-19g	858.0 - 1003.4	1194.5 - 1049.1	145.4	1.58 - 2.68						
	U-19u	661.4 - 929.6	1433.5 - 1165.3	268.2	2.14 - 2.81						
	U-20m	565.4 - 704.1	1233.8 - 1095.1	138.7	1.67 - 2.84						
	UE-19b	646.2 - 710.2	1427.1 - 1363.1	64.0	2.16 - 2.81						
	UE-19b #1	645.3 - 1371.6	1427.9 - 701.6	726.3	2.08 - 2.84						
	UE-19c	724.5 - 2401.8	1419.1 - -258.2	1677.3	1.98 - 2.84						
	UE-19e	894.0 - 1830.6	1214.9 - 278.3	936.6	1.81 - 2.89						
	UE-19fS	1552.9 - 2118.4	499.9 - -65.5	565.4	1.76 - 2.87						
	UE-19gS	807.7 - 2002.5	1240.2 - 45.4	1194.8	1.71 - 2.82						
	UE-19h	643.4 - 1129.3	1423.1 - 937.3	485.8	2.07 - 2.80						
	UE-19i	1484.3 - 2438.4	600.2 - -353.9	954.1	1.99 - 2.81						
	UE-20e #1	1548.4 - 1949.2	370.9 - -29.9	400.8	1.62 - 2.76						
	UE-20f	2521.6 - 2974.2	-657.5 - -1110.1	452.6	1.82 - 3.09						
	UE-20j	573.3 - 761.1	1225.9 - 1038.1	187.8	1.67						
	UE-20p	451.0 - 554.7	1241.5 - 1137.8	103.7	1.66 - 2.82						
WW 8	325.3 - 612.6	1410.5 - 1123.2	287.3	1.62							

Table B2. Estimates of SZ HSU thermal conductivity (continued).

HSU	Borehole	Depth range (m)	Elevation range (m)	Thickness (m)	Harmonic mean over rock types l (W/mC)	HSU l (W/mC)	Std dev l (W/mC)	Min l (W/mC)	Max l (W/mC)	Low l (W/mC)	High l (W/mC)
BFCU	PM-1	956.7 - 1603.2	1042.1 - 395.6	646.5	1.42 - 2.41 N=26	1.57-2.61	0.19,0.35	1.42	3.21	1.39-2.26	1.76-2.95
	PM-3	874.8 - 899.2	900.1 - 875.7	24.4	1.56						
	U-19ab	637.4 - 685.8	1474.3 - 1425.9	48.4	1.44 - 2.44						
	U-19ab #2	643.2 - 731.5	1468.8 - 1380.4	88.4	1.42 - 2.41						
	U-19ab #3	641.3 - 731.5	1470.7 - 1380.4	90.3	1.48 - 2.51						
	U-19ai	626.1 - 632.5	1428.9 - 1422.5	6.4	1.73 - 2.94						
	U-19aj	668.0 - 670.6	1432.4 - 1429.8	2.6	1.89 - 3.21						
	U-19aS	978.6 - 1092.4	1082.2 - 968.3	113.9	1.44 - 2.45						
	U-19ba #1	657.1 - 713.2	1487.8 - 1431.6	56.2	1.86 - 3.17						
	U-19ba #2	657.1 - 713.2	1487.8 - 1431.6	56.2	1.86 - 3.17						
	U-19ba #3	655.9 - 713.2	1489.0 - 1431.6	57.4	1.87 - 3.17						
	U-19e	678.2 - 894	1430.7 - 1214.9	215.8	1.54 - 2.61						
	U-19g	651.3 - 858	1401.2 - 1194.5	206.7	1.42 - 2.41						
	U-19i	877.8 - 1223.2	1205.8 - 860.5	345.3	1.52 - 2.59						
	U-19p	670.6 - 1026.0	1432.3 - 1076.9	355.4	1.42 - 2.41						
	U-19v	832.1 - 1082.0	1263.7 - 1013.8	249.9	1.44 - 2.44						
	U-20g	887.0 - 1280.2	1085.1 - 691.9	393.2	1.42 - 2.41						
	U-20m	537.9 - 565.4	1261.3 - 1233.8	27.5	1.73 - 2.94						
	UE-19c	714.1 - 724.5	1429.5 - 1419.1	10.4	1.42 - 2.41						
	UE-19e	698.0 - 894	1410.9 - 1214.9	196.0	1.51 - 2.56						
	UE-19fS	1460.1 - 1553	592.8 - 499.9	92.9	2.04 - 2.84						
	UE-19gS	658.6 - 807.7	1389.3 - 1240.2	112.7	1.42 - 2.41						
	UE-19i	884.0 - 1484.4	1200.6 - 600.2	600.4	1.63 - 2.77						
UE-19z	669.8 - 853.4	1429.7 - 1246.0	183.6	1.45 - 2.46							
UE-20f	1859.2 - 2521.6	4.9 - -657.5	662.4	1.42 - 2.41							
UE-20h	1653.9 - 2196.4	344.7 - -197.8	542.5	1.53 - 2.60							
KA	U-19ba	655.9 - 663.5	1489.0 - 1481.3	7.7	1.89 N=5	1.85	0.08	1.70	1.89	1.77	1.93
	U-19ba #1	655.9 - 657.1	1489.0 - 1487.8	1.2	1.89						
	U-19ba #2	655.9 - 657.1	1489.0 - 1487.8	1.2	1.89						
	U-19bj	641.0 - 656.2	1493.4 - 1478.1	15.3	1.70						
	U-19t	588.3 - 588.9	1542.6 - 1542.0	0.6	1.89						

Table B2. Estimates of SZ HSU thermal conductivity (continued).

HSU	Borehole	Depth range (m)	Elevation range (m)	Thickness (m)	Harmonic mean over rock types l (W/mC)	HSU l (W/mC)	Std dev l (W/mC)	Min l (W/mC)	Max l (W/mC)	Low l (W/mC)	High l (W/mC)
CFCU	PM-1	886.7 - 956.8	1112.2 - 1042.1	70.1	1.93 N=14	1.61	0.18	1.42	1.96	1.43	1.79
	U-19ab	616.8 - 637.3	1494.8 - 1474.3	20.5	1.42						
	U-19ab #2	614.0 - 643.1	1497.9 - 1468.8	29.1	1.75						
	U-19ab #3	614.1 - 641.3	1497.9 - 1470.7	27.2	1.59						
	U-19ae	786.4 - 832.1	1278.6 - 1232.9	45.7	1.49						
	U-19aS	725.5 - 978.6	1335.3 - 1082.2	253.1	1.54						
	U-19aS #1	685.8 - 1005.8	1375.3 - 1055.2	320.1	1.56						
	U-19c	688.9 - 730	1454.5 - 1413.4	41.1	1.73						
	U-19g	628.0 - 651.4	1424.6 - 1401.2	23.4	1.96						
	U-19i	728.5 - 877.8	1355.1 - 1205.8	149.3	1.42						
	U-19v	719.3 - 832.1	1376.5 - 1263.7	112.8	1.44						
	UE-19c	713.1 - 714.1	1430.5 - 1429.5	1.0	1.73						
	UE-19fS	1336.5 - 1460	716.3 - 592.8	123.5	1.55						
UE-19i	730.9 - 883.9	1353.6 - 1200.6	123.1	1.43							
CFCM	ER-EC-1	1301.5 - 1524.0	535.1 - 312.6	222.5	1.79 N=9	1.87-1.97	0.09,0.29	1.73	2.75	1.78	1.96-2.26
	ER-EC-6	1207.0 - 1524.0	501.2 - 184.2	317.0	1.87 - 2.75						
	U-20aa	1063.7 - 1294.5	867.8 - 637.0	230.8	1.86						
	U-20g	874.8 - 887	1097.3 - 1085.1	12.2	1.90						
	U-20i	1149.1 - 1434.1	792.5 - 507.5	285.0	2.08						
	UE-20e #1	1269.8 - 1548.4	649.5 - 370.9	278.6	1.88						
	UE-20f	1644.4 - 1859.3	219.8 - 4.9	214.9	1.85						
	UE-20h	2196.4 - 2196.7	-197.8 - -198.1	0.3	1.89						
	UE-20j	530.3 - 573.3	1268.9 - 1225.9	43.0	1.73						
IA	U-19f	826.0 - 830.3	1226.5 - 1222.2	4.3	1.66 N=3	1.86	0.21	1.66	2.15	1.65	2.06
	UE-19fS	850.4 - 1336.5	1202.4 - 716.3	486.1	2.15						
	UE-20f	1323.8 - 1644.4	540.4 - 219.8	320.6	1.76						
CHCU	ER-EC-1	1097.3 - 1301.5	739.3 - 535.1	204.2	2.10 N=6	1.84-1.89	0.28,0.34	1.42	2.41	1.56	2.12-2.24
	ER-EC-6	1084.5 - 1207	623.7 - 501.2	122.5	2.10 - 2.41						
	PM-3	823.0 - 874.8	951.9 - 900.1	51.8	2.12						
	U-19ae	694.9 - 786.4	1370.1 - 1278.6	91.5	1.42						
	U-19f	759.2 - 826	1293.3 - 1226.5	66.8	1.63						
	UE-19fS	731.5 - 850.4	1321.3 - 1202.4	118.9	1.68						

Table B2. Estimates of SZ HSU thermal conductivity (continued).

HSU	Borehole	Depth range (m)	Elevation range (m)	Thickness (m)	Harmonic mean over rock types l (W/mC)	HSU l (W/mC)	Std dev l (W/mC)	Min l (W/mC)	Max l (W/mC)	Low l (W/mC)	High l (W/mC)
CHZCM	ER-20-2 #1	609.4 - 768.1	1340.4 - 1181.7	158.7	1.47 - 2.24 N=42	1.81	0.14	1.60	2.24	1.67	1.95
	ER-20-5 #1	789.7 - 860.5	1112.8 - 1042.1	70.7							
	ER-20-5 #3	902.2 - 1308.8	1000.3 - 593.7	406.6							
	ER-20-6 #1	655.3 - 975.4	1318.2 - 998.2	320.0							
	ER-20-6 #2	636.1 - 975.4	1337.5 - 998.3	339.2							
	ER-20-6 #3	615.9 - 975.4	1354.9 - 995.5	359.5							
	PM-1	639.3 - 886.7	1359.6 - 1112.2	247.4							
	U-20 WW	626.2 - 996.1	1345.3 - 975.4	369.9							
	U-20a	563.9 - 774.2	1423.4 - 1213.1	210.3							
	U-20a #2 WW	629.7 - 1371.6	1343.6 - 601.7	741.9							
	U-20aa	570.1 - 1063.8	1361.5 - 867.8	493.7							
	U-20ah	609.9 - 701.0	1354.5 - 1263.4	91.1							
	U-20ai	625.4 - 656.5	1356.7 - 1325.6	31.1							
	U-20an	606.7 - 617.5	1362.9 - 1352.1	10.8							
	U-20ar #1	601.9 - 696.5	1324.1 - 1229.6	94.5							
	U-20aw	635.8 - 640.1	1371.3 - 1367.0	4.3							
	U-20ax	662.3 - 670.6	1329.9 - 1321.6	8.3							
	U-20ay	626.6 - 640.1	1361.0 - 1347.5	13.5							
	U-20az	658.3 - 685.8	1345.1 - 1317.7	27.5							
	U-20bd	646.1 - 687.3	1330.8 - 1289.6	41.2							
	U-20bd #1	630.9 - 732.1	1346 - 1244.8	101.2							
	U-20bd #2	642.2 - 746.8	1335 - 1230.5	104.5							
	U-20be	675.1 - 676.7	1304.0 - 1302.4	1.6							
	U-20bf	650.6 - 685.8	1337.3 - 1302.1	35.2							
	U-20bg	650.4 - 670.6	1351.2 - 1331.1	20.1							
	U-20c	929.6 - 1463.0	984.8 - 451.4	533.4							
U-20d	972.3 - 1277.7	933.3 - 627.9	305.4								
U-20e	566.9 - 1174.4	1358.2 - 750.7	607.5								
U-20e #1	566.9 - 1064.1	1358.2 - 861.1	497.1								
U-20g	614.8 - 874.8	1357.3 - 1097.3	260.0								

Table B2. Estimates of SZ HSU thermal conductivity (continued).

HSU	Borehole	Depth range (m)	Elevation range (m)	Thickness (m)	Harmonic mean over rock types l (W/mC)	HSU l (W/mC)	Std dev l (W/mC)	Min l (W/mC)	Max l (W/mC)	Low l (W/mC)	High l (W/mC)
CHZCM (cont)	U-20i	580.4 - 1149.1	1361.2 - 792.5	568.7	1.94						
	U-20n	634.0 - 1301.2	1340.2 - 673.0	667.2	2.02						
	UE-20ad	582.2 - 777.2	1358.2 - 1163.1	195.1	1.60						
	UE-20av	688.8 - 796.7	1279.6 - 1171.7	107.9	1.87						
	UE-20bh #1	701.0 - 856.5	1321.8 - 1166.3	155.5	1.80						
	UE-20c	892.2 - 1630.1	1022.9 - 285.0	737.9	1.79						
	UE-20d	968.6 - 1369.2	937.6 - 537.1	400.5	1.90						
	UE-20e	556.6 - 743.7	1362.1 - 1175.0	187.1	2.03						
	UE-20e #1	556.6 - 1269.8	1362.7 - 649.5	713.2	1.85						
	UE-20f	899.1 - 1323.7	965 - 540.4	424.6	1.94						
UE-20h	641.5 - 1653.8	1357.0 - 344.7	1012.3	1.85							
UE-20n #1	634.0 - 1005.8	1335.3 - 963.5	371.8	1.69							
CHVCM	U-19au	633.1 - 670.6	1358.5 - 1321.0	37.5	1.46 N=4	1.70	0.22	1.46	1.96	1.48	1.93
	U-19au #1	633.1 - 660.5	1358.5 - 1331.1	27.4	1.50						
	U-20am	653.0 - 670.6	1356.6 - 1339.0	17.6	1.89						
	UE-20ab	652.3 - 777.2	1353.6 - 1228.6	125.0	1.96						
CHVTA	U-19aS	673.6 - 725.4	1387.1 - 1335.3	51.8	1.42 N=7	1.50	0.11	1.42	1.73	1.39	1.61
	U-19aS #1	668.1 - 685.8	1393.0 - 1375.3	17.7	1.42						
	U-19bg #1	667.5 - 685.8	1372.8 - 1354.5	18.3	1.42						
	U-19c	533.3 - 688.8	1610 - 1454.5	155.5	1.51						
	U-19v	661.4 - 719.3	1434.4 - 1376.5	57.9	1.42						
	U-19yS	682.7 - 716.3	1357.6 - 1324.1	33.5	1.73						
	UE-19i	688.2 - 730.9	1396.3 - 1353.6	42.7	1.58						
YMCFCM	UE-29a #2	65.0 - 421.5	1150.2 - 793.7	356.5	2.16 N=1	2.16		2.16	2.16		
TSA	ER-20-5 #1	659.6 - 789.7	1242.9 - 1112.8	130.1	1.78 N=9	1.69-1.82	0.12,0.41	1.42	2.94	1.57	1.81-2.24
	ER-20-5 #3	789.7 - 902.2	1112.8 - 1000.3	112.5	1.42						
	ER-EC-1	1030.5 - 1097.3	806.1 - 739.3	66.8	1.61						
	ER-EC-6	954.0 - 1084.5	754.2 - 623.7	130.5	1.73 - 2.94						
	U-20c	792.4 - 929.6	1122 - 984.8	137.2	1.86						
	U-20d	905.2 - 972.3	1000.4 - 933.3	67.1	1.65						
	U-20y	640.0 - 793.1	1267.1 - 1114.0	153.1	1.65						
	UE-20c	792.4 - 892.1	1122.6 - 1022.9	99.7	1.76						
UE-20d	902.3 - 968.7	1004 - 937.6	66.4	1.74							

Table B2. Estimates of SZ HSU thermal conductivity (continued).

HSU	Borehole	Depth range (m)	Elevation range (m)	Thickness (m)	Harmonic mean over rock types l (W/mC)	HSU l (W/mC)	Std dev l (W/mC)	Min l (W/mC)	Max l (W/mC)	Low l (W/mC)	High l (W/mC)
LPCU	ER-20-5 #1	626.4 - 659.6	1276.1 - 1242.9	33.2	1.73 N=19	1.69-1.71	0.17,0.23	1.42	2.41	1.52	1.86-1.94
	ER-20-5 #3	626.4 - 789.7	1276.1 - 1112.8	163.3	1.42						
	ER-20-6 #1	644.3 - 655.3	1329.2 - 1318.2	11.0	1.73						
	ER-20-6 #2	623.9 - 636.1	1349.7 - 1337.5	12.2	1.73						
	ER-EC-1	894.9 - 1030.5	941.7 - 806.1	135.6	2.10						
	ER-EC-6	827.5 - 954	880.7 - 754.2	126.5	1.99 - 2.41						
	PM-3	652.3 - 823	1122.6 - 951.9	170.7	1.50						
	U-20av	632.6 - 640.1	1337.6 - 1330.1	7.4	1.73						
	U-20bd	637.1 - 646.2	1339.9 - 1330.8	9.1	1.73						
	U-20bd #1	621.4 - 630.9	1355.5 - 1346	9.5	1.42						
	U-20bd #2	627.2 - 642.2	1350.0 - 1335	15.0	1.73						
	U-20c	749.9 - 792.5	1164.6 - 1122	42.6	1.73						
	U-20d	838.3 - 905.3	1067.4 - 1000.4	67.0	1.62						
	U-20m	515.2 - 538	1284.1 - 1261.3	22.8	1.42						
	U-20y	631.0 - 640.1	1276.2 - 1267.1	9.1	1.73						
	UE-20av	648.6 - 688.8	1319.8 - 1279.6	40.2	1.73						
	UE-20c	749.8 - 792.5	1165.3 - 1122.6	42.7	1.73						
	UE-20d	836.7 - 902.2	1069.5 - 1004	65.5	1.73						
	UE-20f	830.0 - 899.2	1034.2 - 965	69.2	1.56						
	PLFA	U-19ad	667.5 - 685.8	1372.2 - 1353.9	18.3						
U-19aq		642.8 - 662.9	1429.5 - 1409.4	20.1	1.69						
U-19ar		645.9 - 670.6	1398.4 - 1373.7	24.7	1.85						
U-19ay		648.9 - 657.1	1396.9 - 1388.7	8.2	1.73						
U-19az		633.7 - 649.2	1424.6 - 1409.1	15.5	1.72						
U-19bg		645.8 - 657.5	1394.5 - 1382.9	11.6	1.89						
U-19bg #1		645.8 - 667.5	1394.5 - 1372.8	21.7	1.55						
U-19bh		636.7 - 654.7	1426.2 - 1408.2	18.0	1.59						
U-19x		674.8 - 679.7	1392.0 - 1387.1	4.9	1.66						
U-19yS		628.3 - 682.8	1412.1 - 1357.6	54.5	1.66						

Table B2. Estimates of SZ HSU thermal conductivity (continued).

HSU	Borehole	Depth range (m)	Elevation range (m)	Thickness (m)	Harmonic mean over rock types l (W/mC)	HSU l (W/mC)	Std dev l (W/mC)	Min l (W/mC)	Max l (W/mC)	Low l (W/mC)	High l (W/mC)
TCA	ER-20-1	606.2 - 629.4	1277.8 - 1254.6	23.2	1.78 N=9	1.75-1.88	0.05,0.35	1.68	2.85	1.70	1.80-2.23
	ER-EC-1	821.7 - 894.9	1014.9 - 941.7	73.2	1.73						
	ER-EC-6	734.5 - 827.5	973.7 - 880.7	93.0	1.68 - 2.85						
	PM-3	574.6 - 652.3	1200.3 - 1122.6	77.7	1.74						
	U-20c	643.1 - 749.8	1271.3 - 1164.6	106.7	1.86						
	U-20d	758.9 - 838.2	1146.7 - 1067.4	79.3	1.73						
	UE-20c	648.0 - 749.8	1267.1 - 1165.3	101.8	1.76						
	UE-20d	759.5 - 836.7	1146.7 - 1069.5	77.2	1.68						
UE-20f	793.7 - 830	1070.5 - 1034.2	36.3	1.78							
UPCU	ER-20-6 #1	618.4 - 644.3	1355.1 - 1329.2	25.9	1.73 N=15	1.69-1.76	0.11,0.21	1.47	2.46	1.59	1.80-1.97
	ER-20-6 #2	618.6 - 623.9	1355.0 - 1349.7	5.3	1.73						
	ER-EC-1	788.5 - 821.7	1048.1 - 1014.9	33.2	1.73						
	ER-EC-6	647.5 - 734.6	1060.8 - 973.7	87.1	1.45 - 2.46						
	PM-3	789.9 - 920.2	1330.6 - 1200.3	130.3	1.56						
	U-20as	613.6 - 640.1	1284.4 - 1257.9	26.5	1.73						
	U-20bb	658.4 - 676.7	1239.3 - 1221.0	18.3	1.73						
	U-20bb #1	657.8 - 714.8	1239.9 - 1182.9	57.0	1.86						
	U-20bc	570.4 - 609.6	1302.9 - 1263.7	39.2	1.73						
	U-20bd	621.1 - 637	1355.8 - 1339.9	15.9	1.47						
	U-20bd #2	621.3 - 627.2	1355.9 - 1350.0	5.9	1.73						
	U-20d	676.7 - 759	1229 - 1146.7	82.3	1.73						
	UE-20d	676.7 - 759.6	1229.6 - 1146.7	82.9	1.73						
	UE-20f	545.3 - 793.7	1318.9 - 1070.5	248.4	1.73						
UE-20n #1	622.2 - 634	1347.1 - 1335.3	11.8	1.73							
BA	ER-EC-1	624.8 - 788.5	1211.8 - 1048.1	163.7	1.86 N=8	1.90	0.21	1.67	2.16	1.70	2.11
	ER-EC-6	467.8 - 647.4	1240.4 - 1060.8	179.6	1.75						
	U-20ak	622.4 - 640.1	1278.0 - 1260.3	17.7	1.67						
	U-20ao	596.5 - 655.3	1317.3 - 1258.5	58.8	1.73						
	U-20bb	644.1 - 658.4	1253.6 - 1239.3	14.3	1.73						
	U-20bb #1	637.7 - 657.8	1260 - 1239.9	20.1	2.16						
	U-20d	634.1 - 676.7	1271.6 - 1229	42.6	2.16						
	UE-20d	624.9 - 676.7	1281.4 - 1229.6	51.8	2.16						

Table B2. Estimates of SZ HSU thermal conductivity (continued).

HSU	Borehole	Depth range (m)	Elevation range (m)	Thickness (m)	Harmonic mean over rock types l (W/mC)	HSU l (W/mC)	Std dev l (W/mC)	Min l (W/mC)	Max l (W/mC)	Low l (W/mC)	High l (W/mC)
PVTA	U-19c	454.2 - 533.4	1689.2 - 1610	79.2	1.61 N=6	1.68	0.14	1.42	1.86	1.54	1.82
	U-20bb	619.9 - 644	1277.7 - 1253.6	24.1	1.73						
	U-20bb #1	617.6 - 637.6	1280.0 - 1260	20.0	1.86						
	U-20m	426.7 - 515.1	1372.5 - 1284.1	88.4	1.73						
	UE-20f	537.4 - 545.3	1326.8 - 1318.9	7.9	1.42						
	UE-20j	429.8 - 530.4	1369.5 - 1268.9	100.6	1.73						
PCM	UE-29a #2	27.6 - 65	1187.6 - 1150.2	37.4	1.95 N=1	1.95		1.42	2.16		
WWA											
FCCU	ER-EC-1	482.6 - 541.9	1271.1 - 1211.8	59.3	1.42 N=2	1.58	0.16	1.42	1.73	1.42	1.73
	ER-EC-6	434.8 - 467.9	1273.5 - 1240.4	33.1	1.73						
SCVCU											
TMA	ER-EC-4	585.8 - 1062.8	864.9 - 387.9	477.0	1.68 N=6	1.59	0.13	1.42	1.77	1.46	1.73
	ER-OV-03c	65.3 - 165.2	1212.3 - 1112.4	99.9	1.42						
	ER-OV-03c2	65.4 - 97.8	1212.3 - 1179.9	32.5	1.42						
	U-20m	381.0 - 426.7	1418.2 - 1372.5	45.7	1.69						
	UE-20j	390.2 - 429.8	1409.1 - 1369.5	39.6	1.59						
	UE-20p	277.4 - 451.1	1415.2 - 1241.5	173.7	1.77						
THCM											
THLFA											
TMCM	ER-18-2	369.4 - 762.0	1287.9 - 895.2	392.6	1.76 - 2.99 N=7	1.70-2.79	0.12,0.20	1.49	3.03	1.57-2.59	1.82-2.98
	ER-30-1	365.1 - 434.6	1051.3 - 981.8	69.5	1.78 - 3.03						
	ER-EC-2A	961.6 - 1516.1	532.5 - -21.9	554.4	1.49 - 2.54						
	ER-EC-5	309.9 - 762.0	1237.5 - 785.5	452.1	1.78 - 2.96						
	ER-EC-8	421.3 - 609.6	899.6 - 711.3	188.3	1.56 - 2.65						
	UE-18r	415.8 - 1525.2	1272.2 - 162.8	1109.4	1.64 - 2.79						
	UE-18t	286.1 - 792.5	1299.2 - 792.8	506.4	1.86 - 2.54						
FCA											

Table B2. Estimates of SZ HSU thermal conductivity (continued).

HSU	Borehole	Depth range (m)	Elevation range (m)	Thickness (m)	Harmonic mean over rock types l (W/mC)	HSU l (W/mC)	Std dev l (W/mC)	Min l (W/mC)	Max l (W/mC)	Low l (W/mC)	High l (W/mC)
FCCM	ER-30-1	137.5 - 365.2	1279.0 - 1051.3	227.7	1.90 N=9	1.74	0.15	1.45	2.02	1.58	1.89
	ER-EC-2A	229.9 - 961.6	1264.2 - 532.5	731.7	1.60						
	ER-EC-4	499.8 - 585.8	950.9 - 864.9	86.0	1.73						
	ER-EC-7	228.1 - 422.5	1236.6 - 1042.2	194.4	2.02						
	ER-EC-8	98.4 - 421.2	1222.4 - 899.6	322.8	1.45						
	ER-OV-01	5.5 - 54.9	1235.9 - 1186.5	49.3	1.74						
	ER-OV-06a	4.9 - 163.4	1236.6 - 1078.1	158.5	1.78						
	ER-OV-06a2	5.7 - 21.6	1235.6 - 1219.7	15.9	1.70						
	UE-18t	278.7 - 286.1	1306.6 - 1299.2	7.4	1.73						
DVA											
DVCM	ER-OV-03a	17.5 - 76.5	1154.3 - 1095.3	59.0	1.73 N=3	1.56	0.12	1.46	1.73	1.43	1.68
	ER-OV-03a2	48.7 - 250.2	1122.9 - 921.3	201.5	1.46						
	ER-OV-03a3	17.4 - 250.2	1154.1 - 921.3	232.8	1.48						
TCVA	ER-EC-4	228.2 - 499.9	1222.6 - 950.9	271.7	1.64 N=1	1.64		1.42	1.78		
YVCM											
AA	ER-OV-02	8.6 - 61.0	1174.1 - 1121.8	52.3	1.44 N=4	1.44		1.44	1.44		
	ER-OV-03b	105.6 - 121.9	1184.5 - 1168.2	16.3	1.44						
	ER-OV-04a	7.3 - 46.0	1056.9 - 1018.2	38.7	1.44						
	ER-OV-05	9.7 - 61.0	1190.5 - 1139.3	51.2	1.44						

Table B3. Thermal properties by lithology as reported for NTS and other rock types

Rock type	Extra Caldera				Intracaldera ³			
	λ (W/m C)	Std dev	N	Source	λ (W/m C) ⁴	Std dev	N	Source
Unsaturated zone								
Tuffaceous ss ¹	1.2			Sass et al. (1987), Bodvarsson et al. (2003)				
NWT	1.16	0.5	9	Sass et al. (1987, tables 3-1 to 3-4)				
PWT	1.26	0.37	6	Sass et al. (1987, tables 3-1 to 3-4)				
BT	1.15	0.12	4	Sass et al. (1987, tables 3-1 to 3-4)				
MWT	1.69	0.17	4	Sass et al. (1987, tables 3-1 to 3-4)				
V/WT	1.95	0.27	33	Sass et al. (1987, tables 3-1 to 3-4)				
WT, DV ²	1.1		1	Moss et al. (1982)				
NWT, ZE ²	0.68		1	Moss et al. (1982)				
Saturated zone								
Granite	1.7-4.0			Gillespie (2003)				
Granitic pluton	2.9			Lin et al. (2000)				
Diabase	2.1			Gillespie (2003)	2.41 ⁶			
Granodiorite	2.6			Gillespie (2003)				
LCA	4.95	0.28	13	Gillespie (2003)				
UCCU	2.47,3.1	0.56	18	Sass et al. (1980)				
Quartzite	5.8,4.5-7.1			Gillespie (2003)				
Qtz Monzonite	2.26	0.02	6	Morgan et al. (1996)				
Muddy ss	2.23			Gillespie (2003)				
Argillite	3.3			Gillespie (2003)				
Tuffaceous ss ³	1.44				2.38			
Clay,ss,gravel (unconsolidated volcanic alluvium)	1.33-1.83			Olmsted and Rush (1987)				
Siltstone	1.91-2.15			Gillespie (2003)				
NWT	1.42	0.31	15	Gillespie (2003)	2.41			
PWT	1.66	0.29	37	Gillespie (2003)	2.82			
BT	1.73	0.45	8	Gillespie (2003)	2.94			
MWT	1.78	0.2	19	Gillespie (2003)	3.03			
WT	1.86	0.08	2	Gillespie (2003)	3.16			
FB	1.89	0.35	7	Gillespie (2003)	3.21			
V/WT	2.01	0.09	4	Gillespie (2003)	3.42			
WT, DV ²	1.6		1	Moss et al. (1982)				
NWT, ZE ²	1.1		1	Moss et al. (1982)				
MWT-WT ⁵	1.75		16	Lappin & Nimick (1982)				
Rhyolitic Lava	2.16	0.24	7	Gillespie (2003)	3.67			
Qtz-rich WT**	1-1.2			Morgan et al. (1996)	2.52	0.11	4	Morgan et al. (1996)

¹Calico Hills Formation

²Grouse Canyon Tuff, BRA

³Alluvium (sandy gravel); gravel consists of welded tuff and rhyolite lava clasts. Sandy matrix is tuffaceous, partly zeolitized with quartz; λ assumed ~1.2 times UZ Calico Hills tuffaceous sandstone of Bodvarsson et al. (2003)

⁴Intracaldera thermal conductivities increase by 1.7 to 2.9 times flanking tuff units (Morgan et al., 1996), due to high degree of hydrothermal induration

⁵Average thermal conductivity of Grouse Canyon Tuff, BRA (porosity < 0.2)

⁶Estimate of indurated mafic-rich tuff/lava (with alteration minerals pyrite and chalcopyrite) assumed less than NWT

Table B4. Other thermal properties as reported for NTS and other areas

Rock type	Est. Heat flow (mW/m ²)	Matrix porosity	Heat capacity (J/kg C)	Density (g/cm ³)	SZ λ (W/m K)	Std dev	N	Source
Background NTS (Basin and Range)	85							Sass et al. (1995)
Granite	91			2.65				Turcotte and Schubert (1982, p.145)
Diorite				2.8				
BMICU				2.8				Bechtel Nevada (2002)
Basalt				2.9				
Granitic pluton		0.01	837		2.9			Olmsted and Rush (1987)
(MWT-WT) Grouse Canyon Tuff		0.1-0.2		2.58-2.65	1.75		16	Lappin and Nimick (1982)
TSA (Tsw1)			718-972-922 ¹					Brodsky et al. (1997)
TSA (Tsw2)			814-1114-1086 ¹					Brodsky et al. (1997)
Valles Caldera			950					Bodvarsson et al. (1982)

¹Varies with temperature

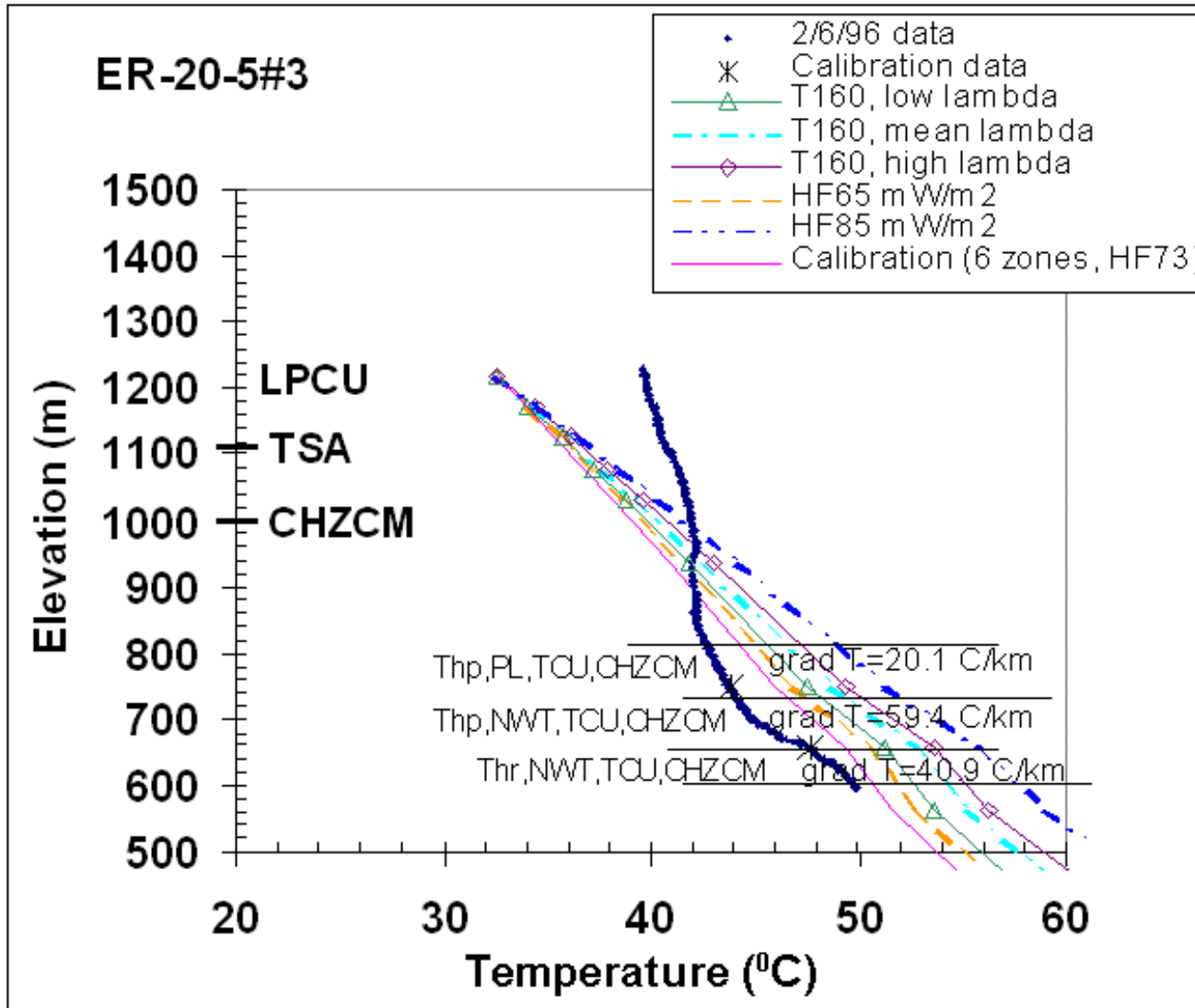


Figure C1

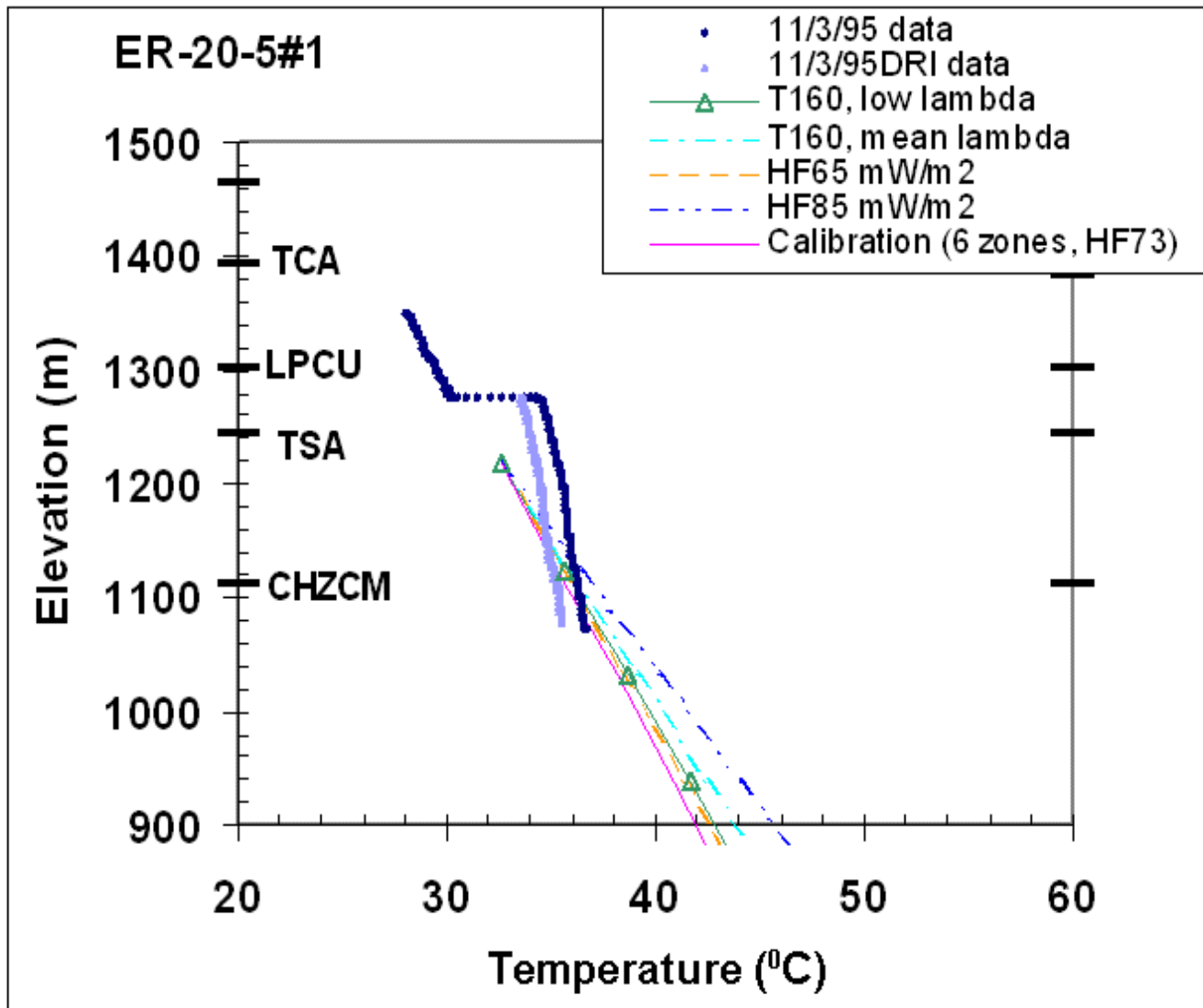


Figure C2

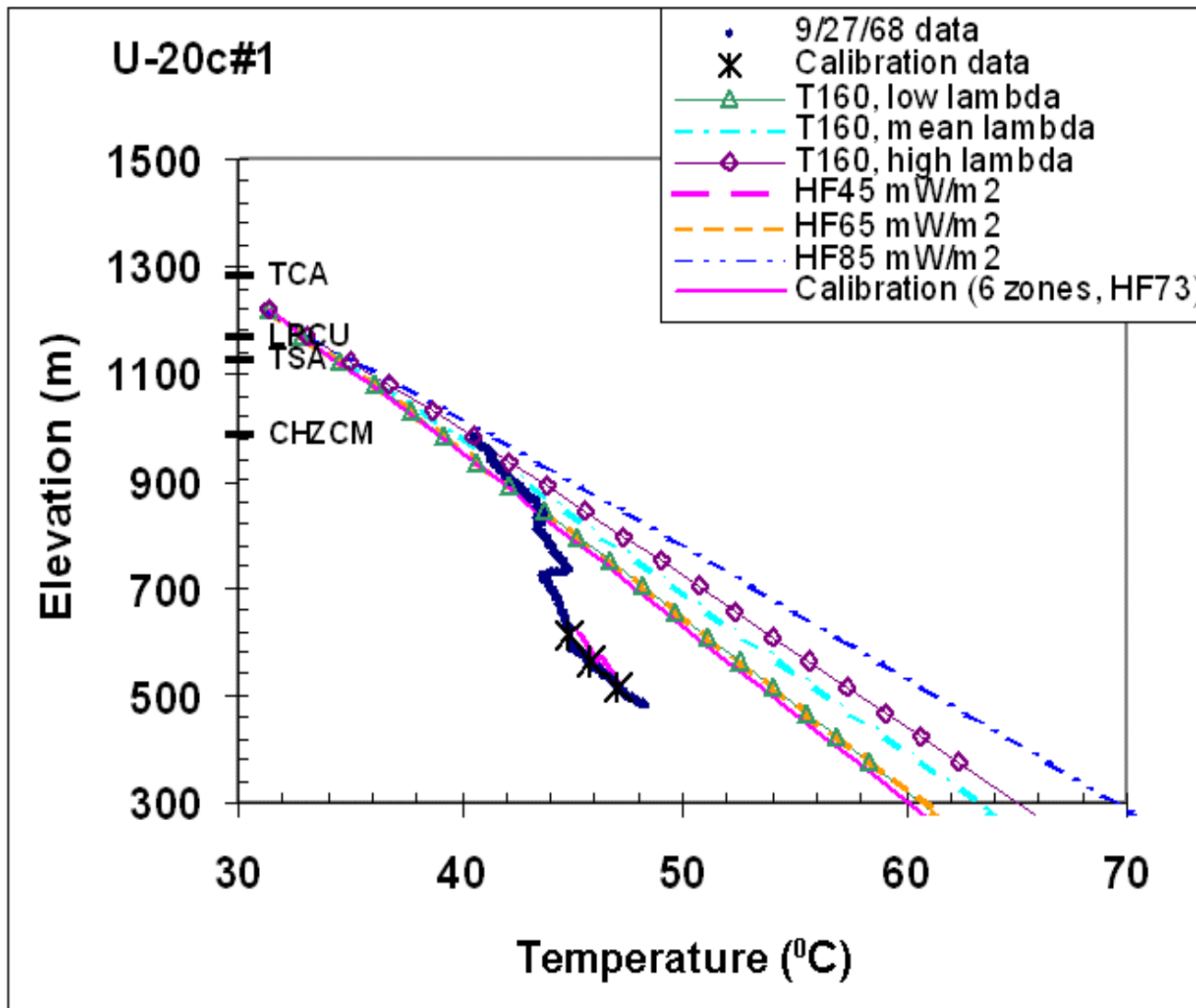


Figure C3

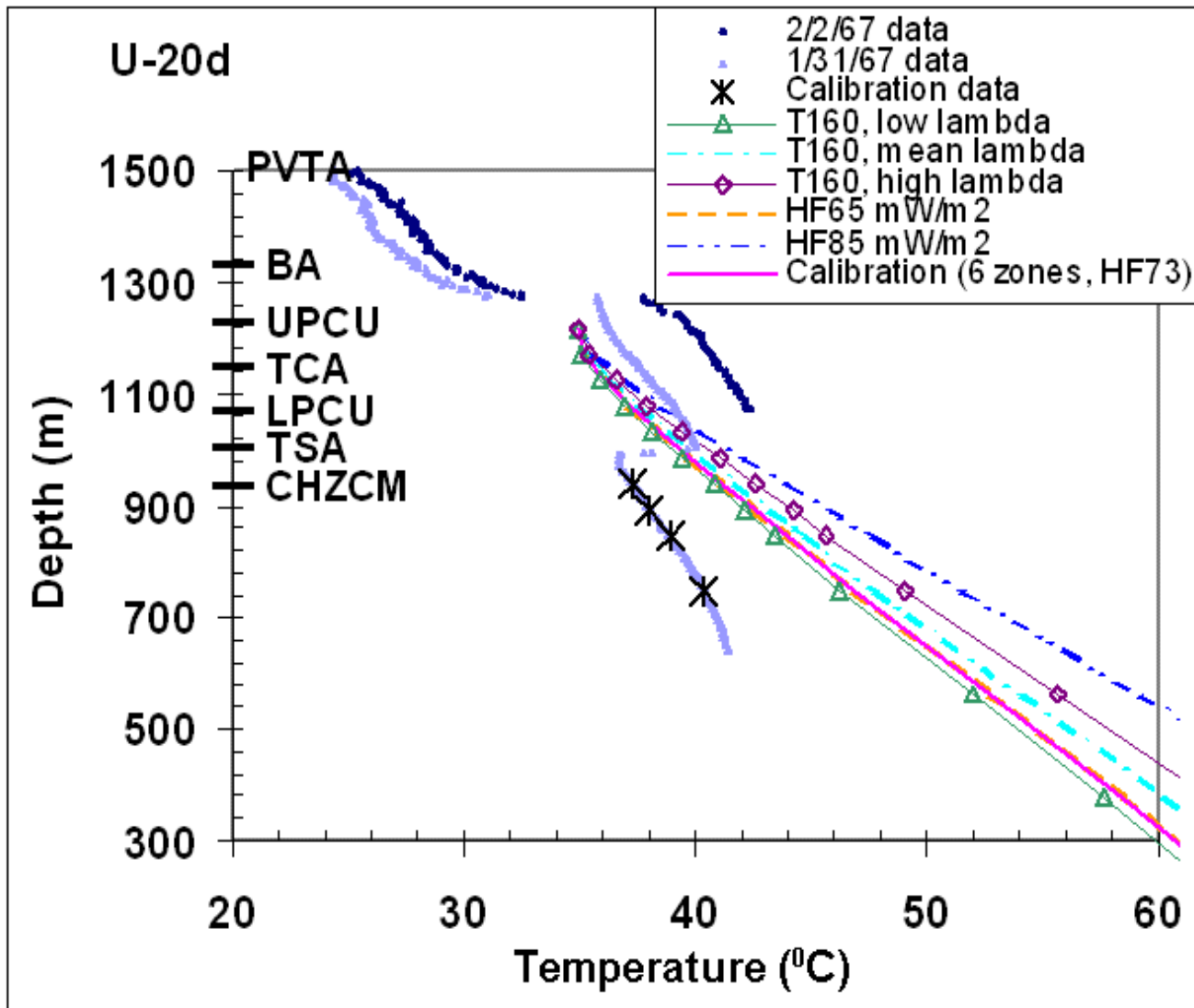


Figure C4

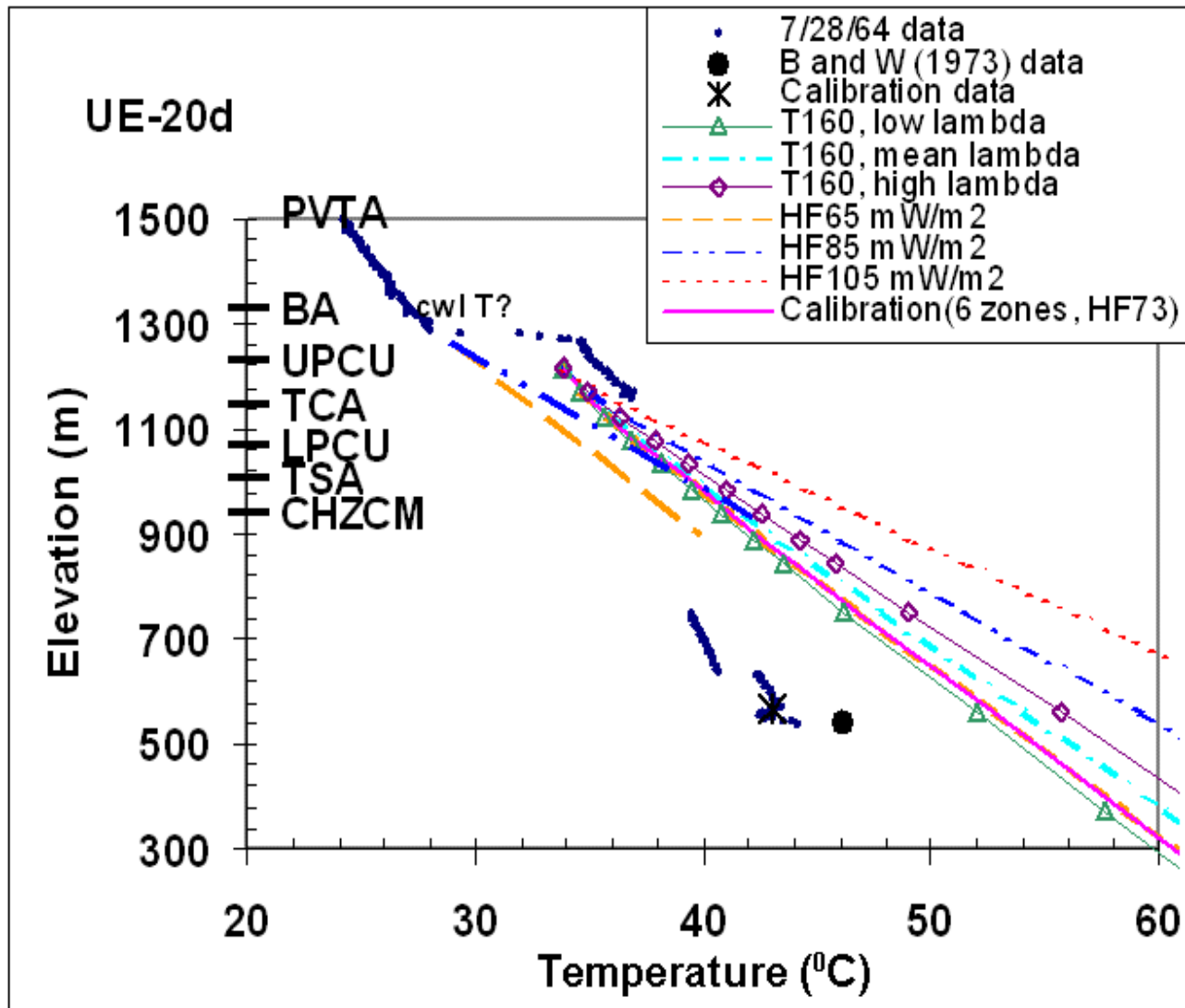


Figure C5

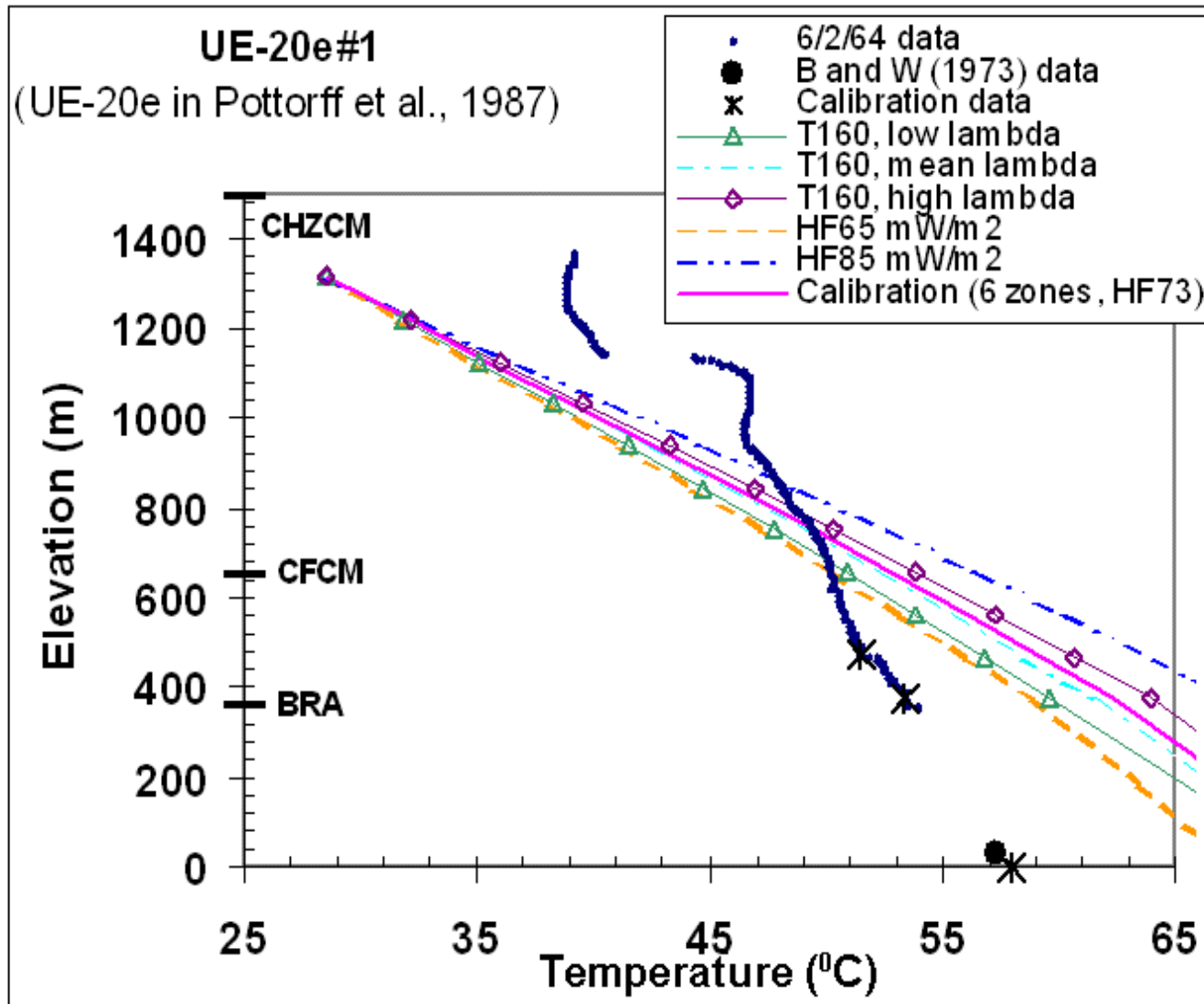


Figure C6

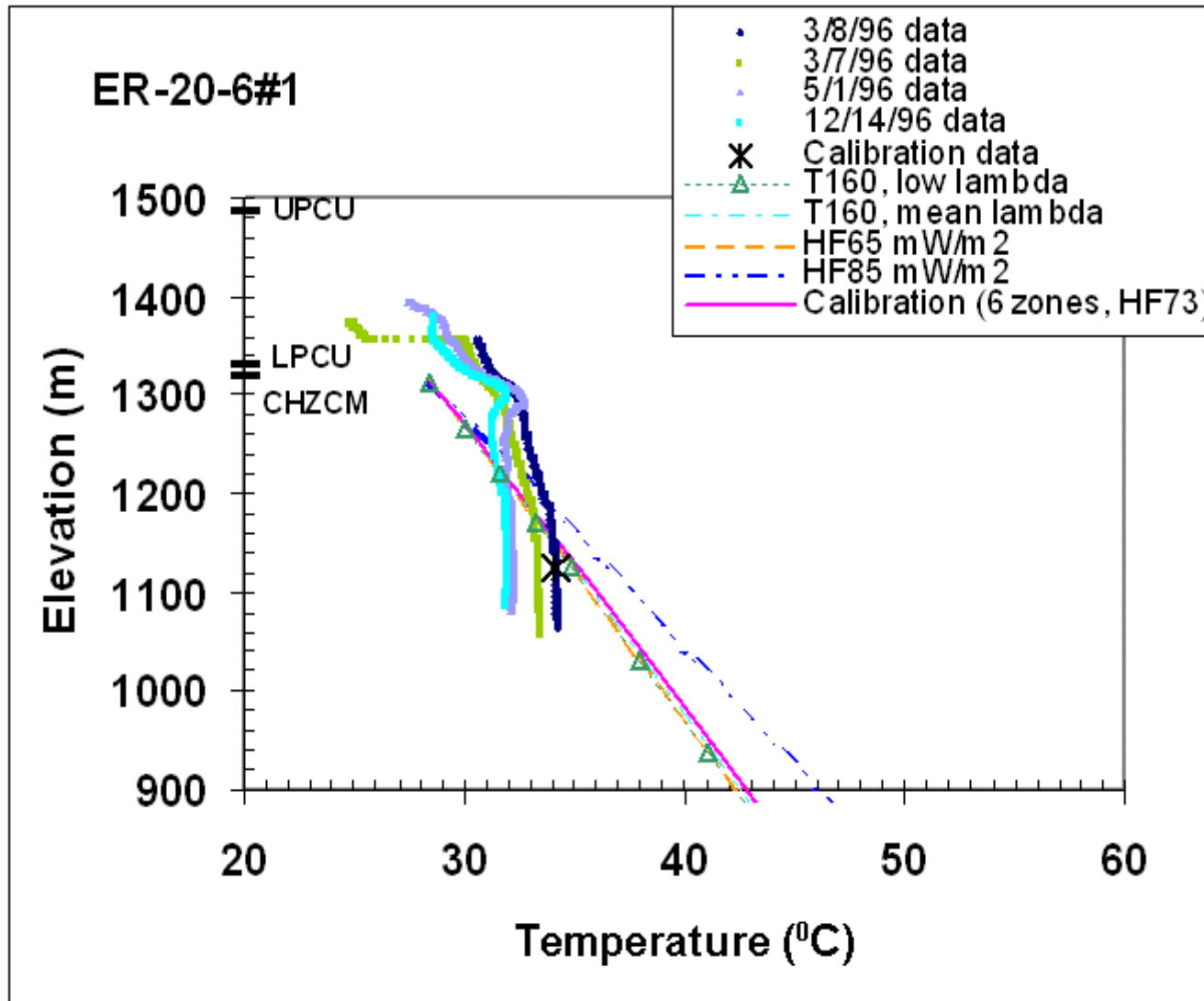


Figure C7

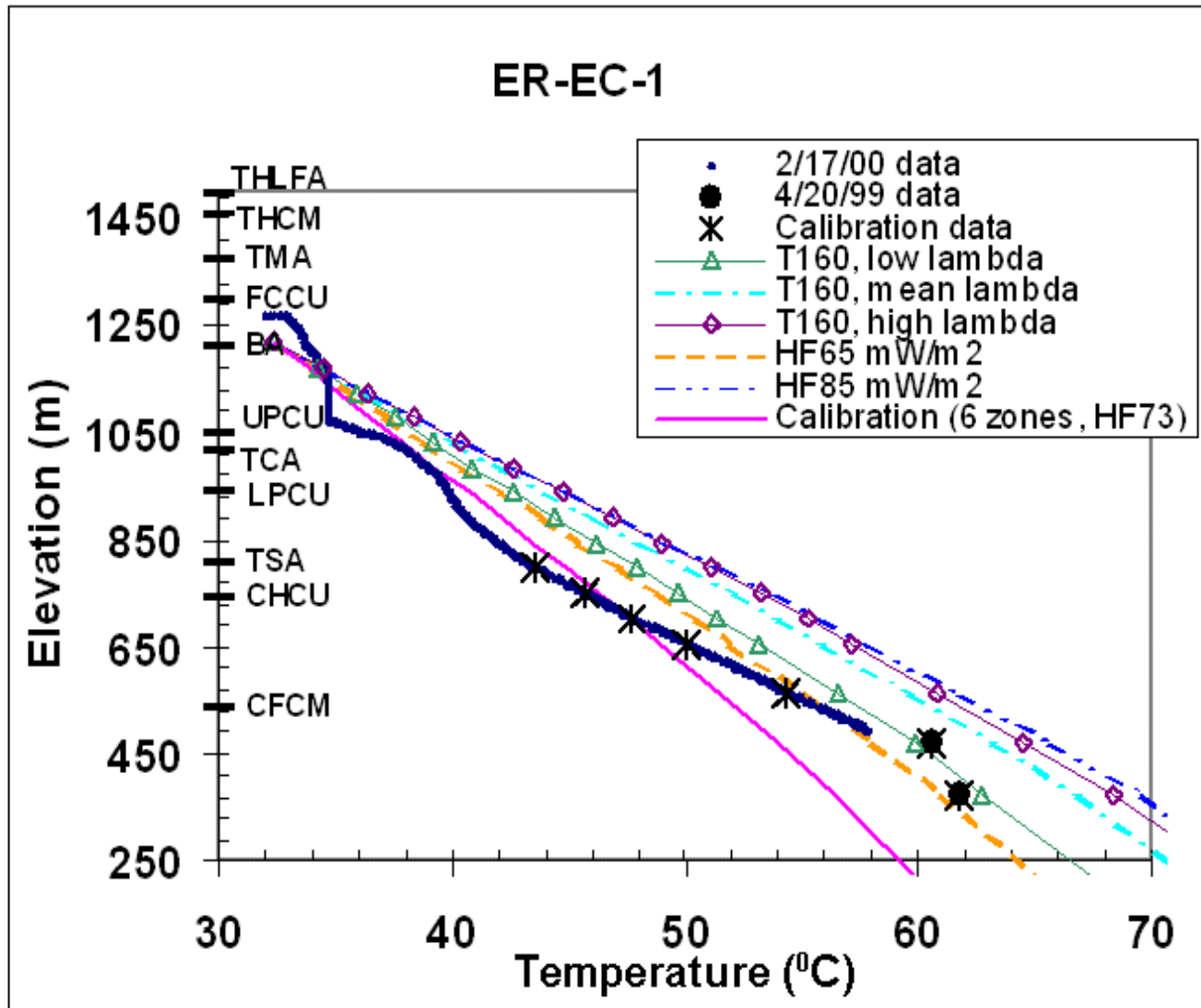


Figure C8

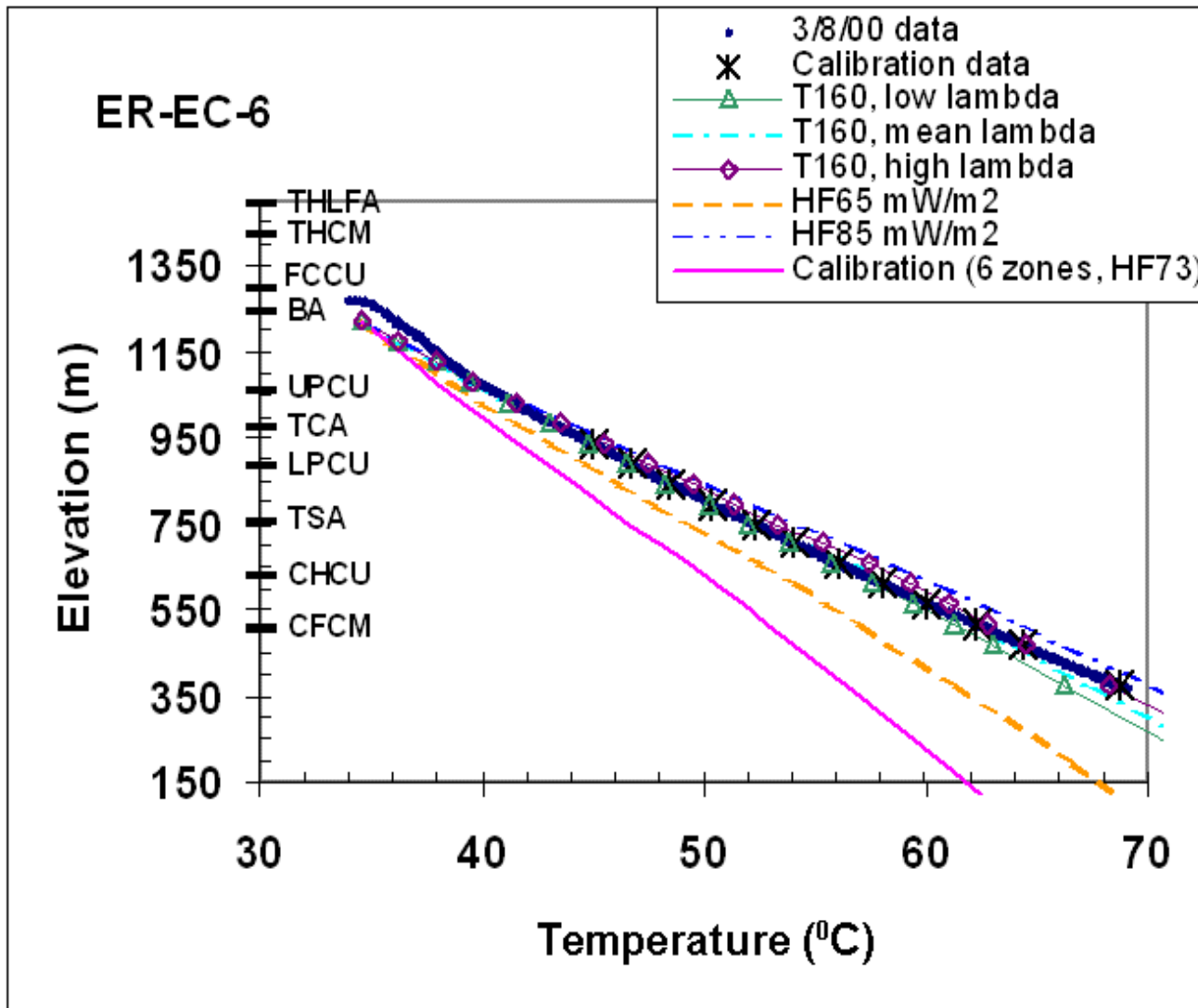


Figure C9

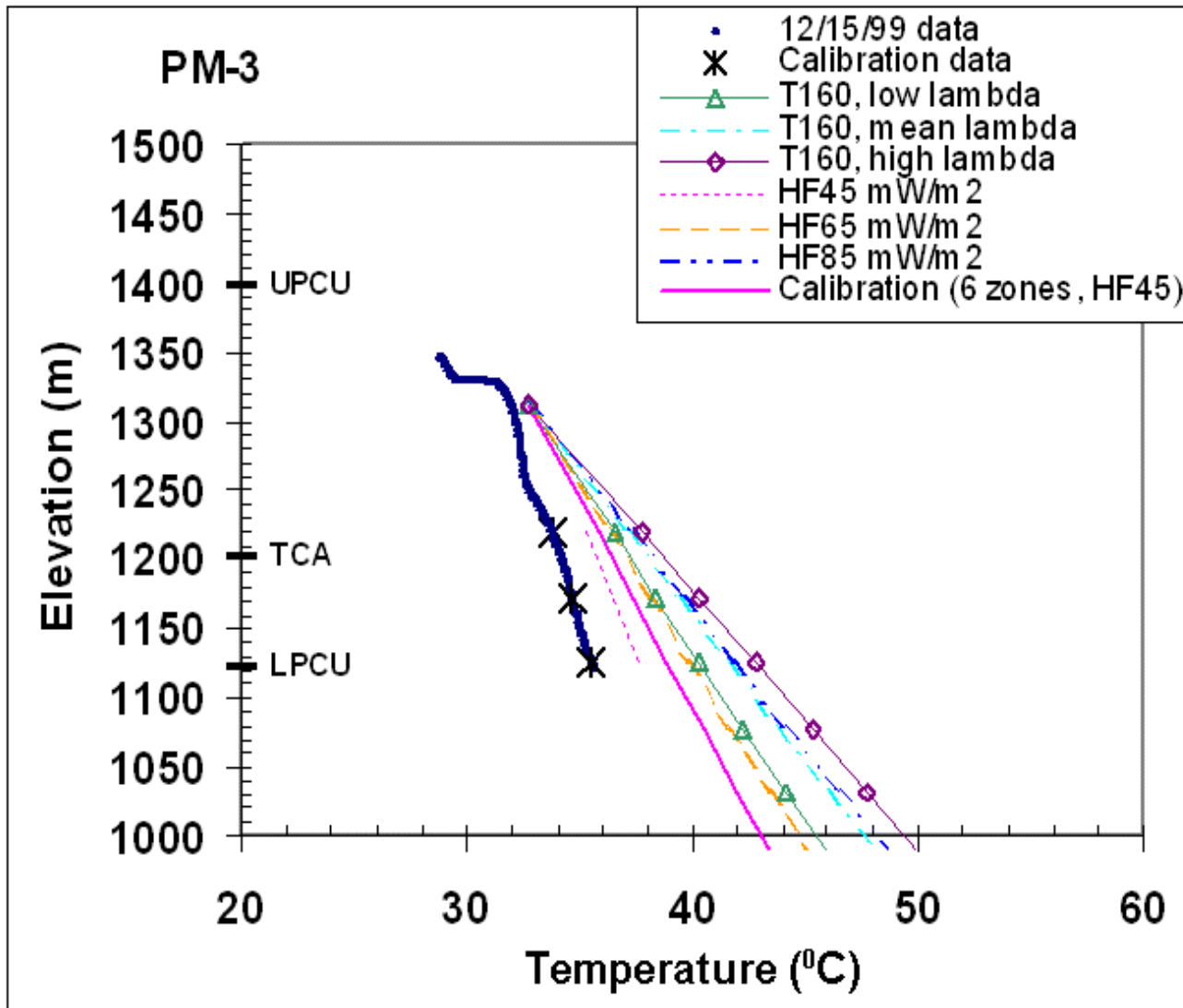


Figure C10

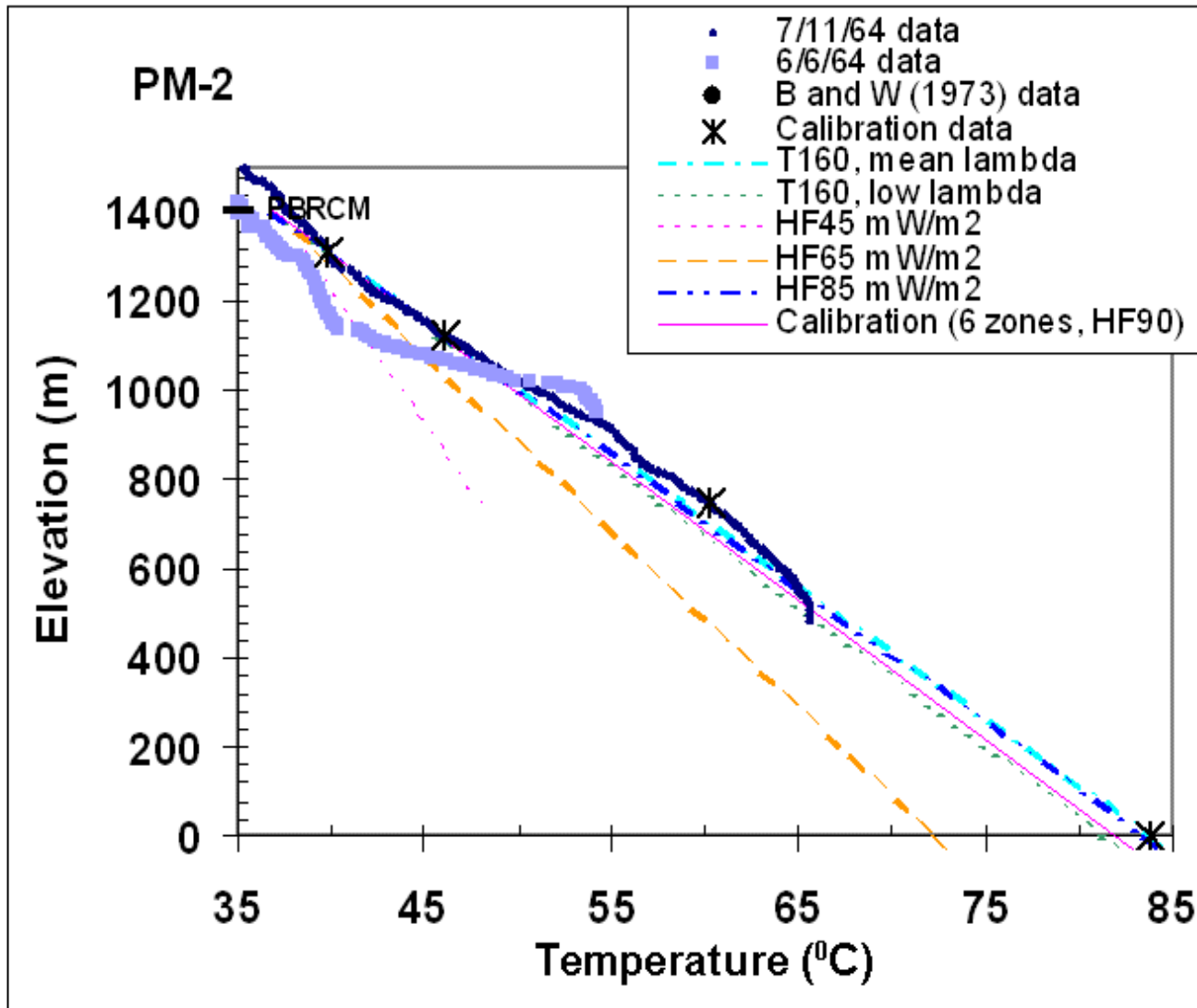


Figure C11

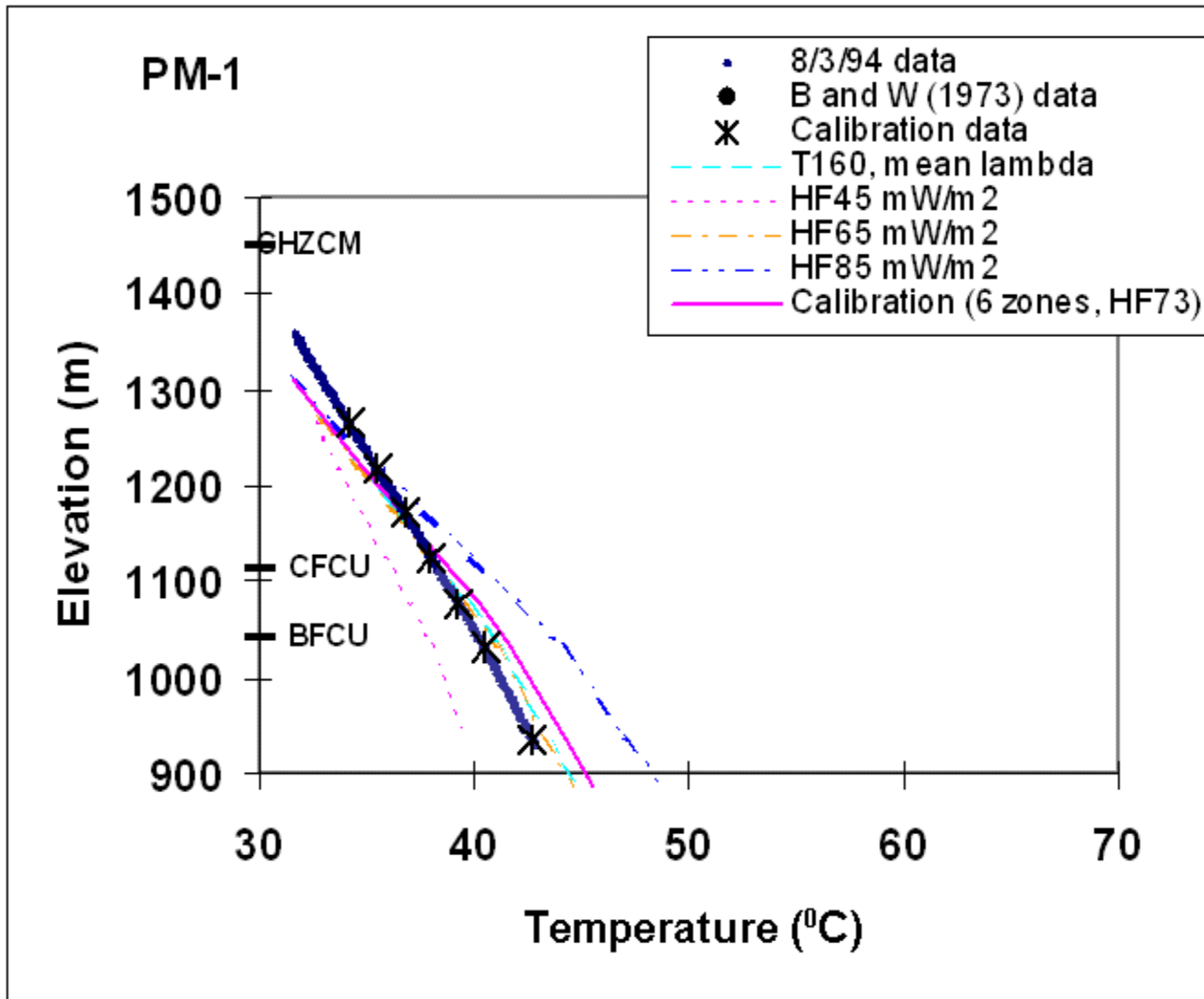


Figure C12

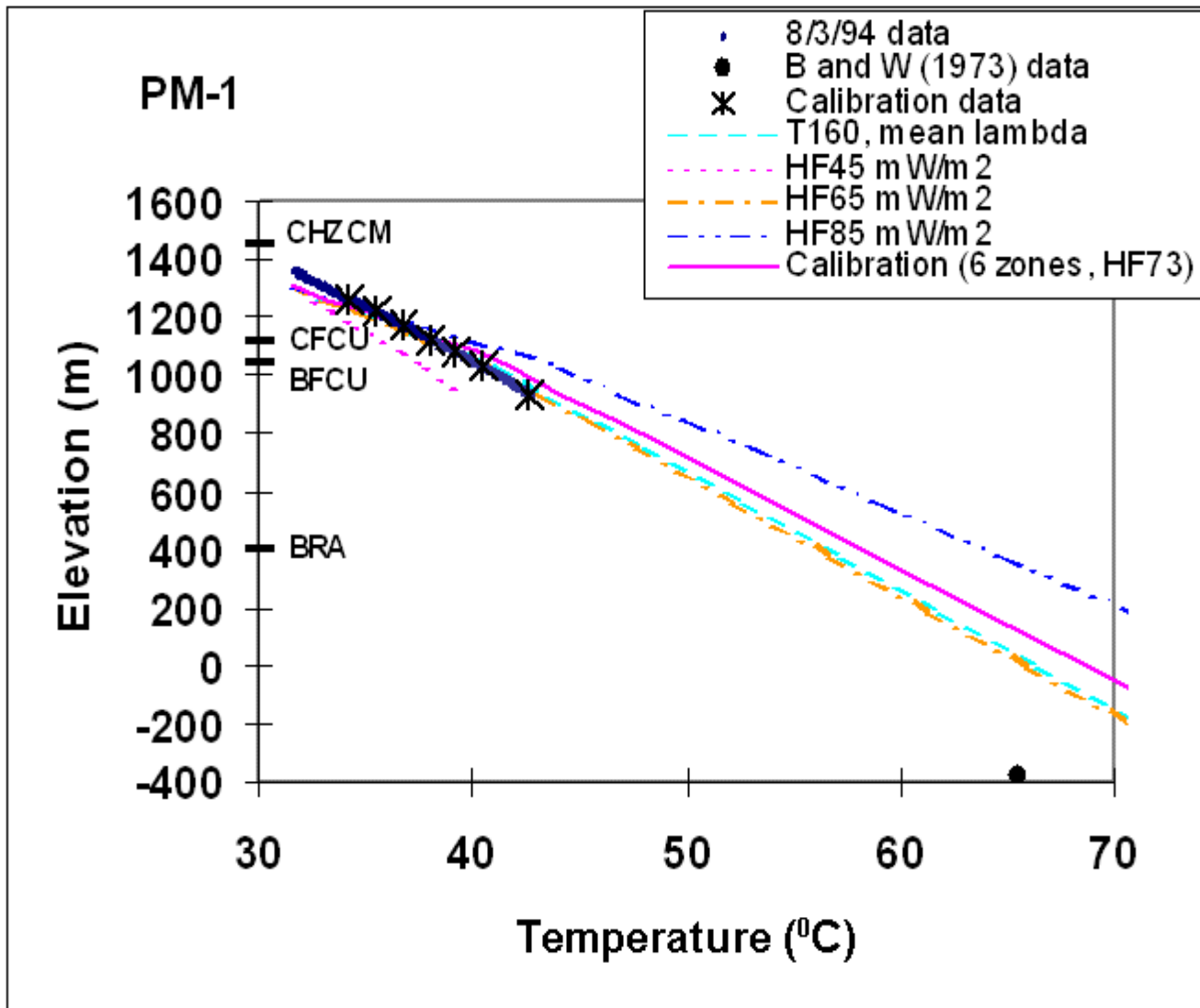


Figure C13

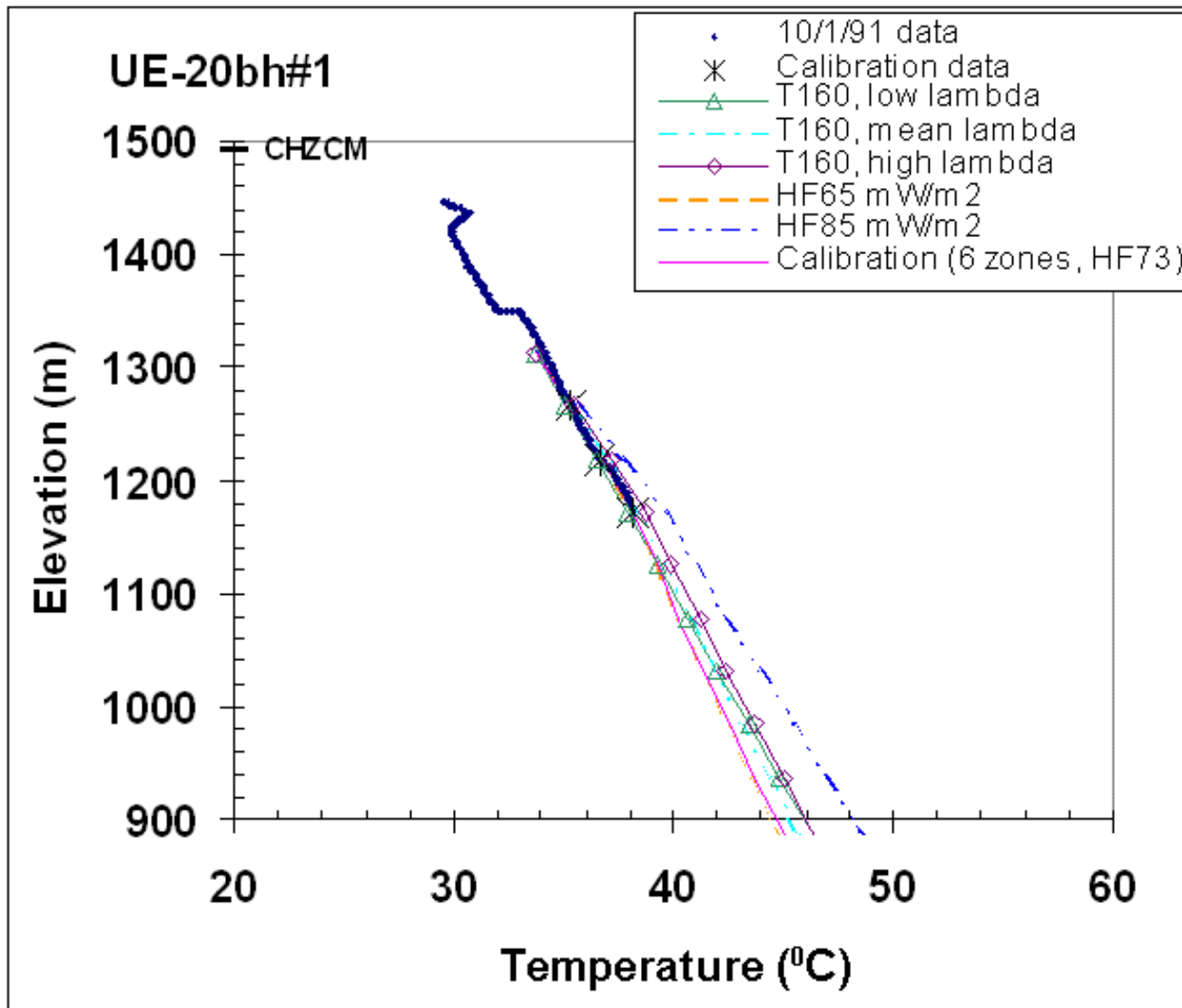


Figure C14

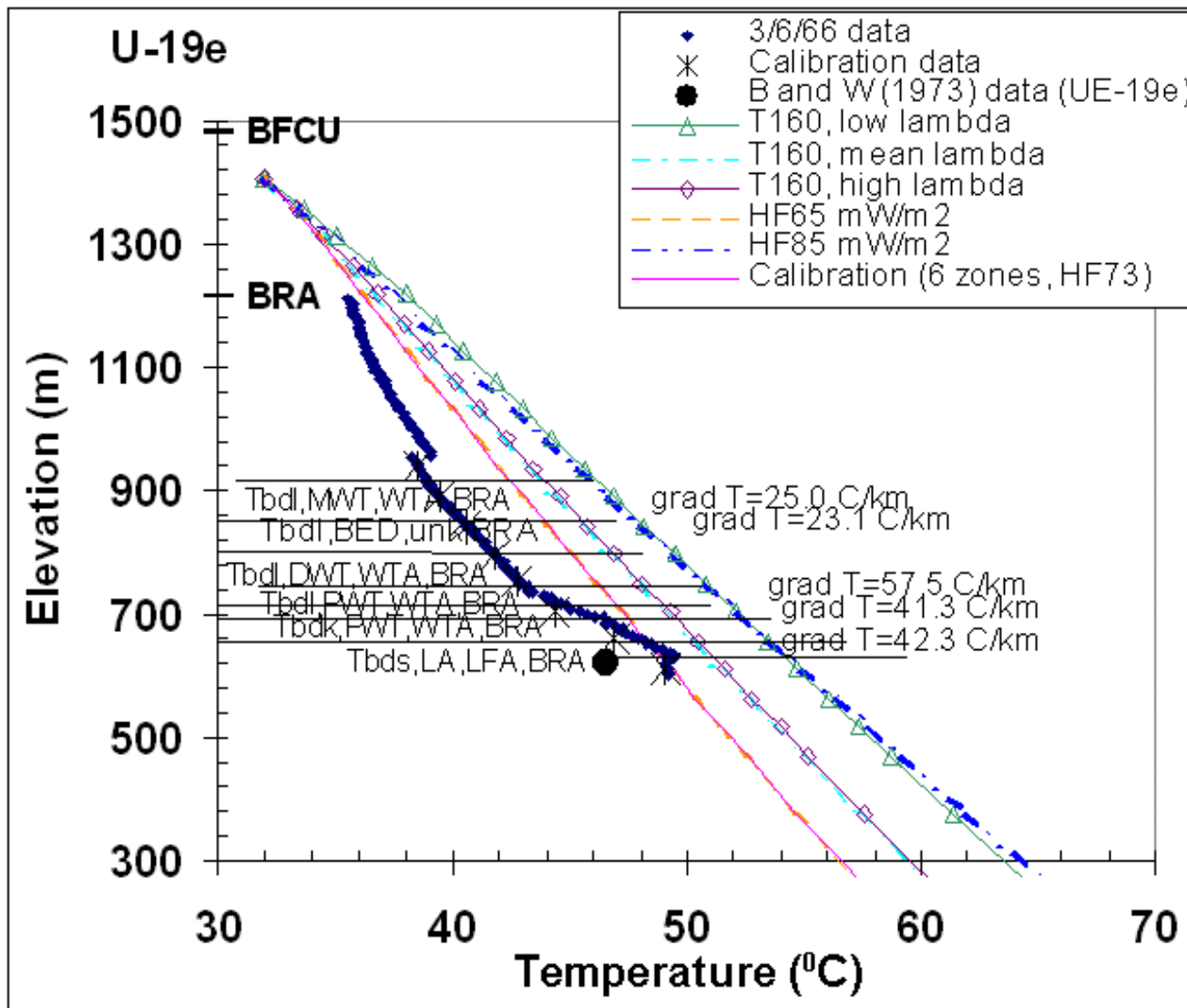


Figure C15

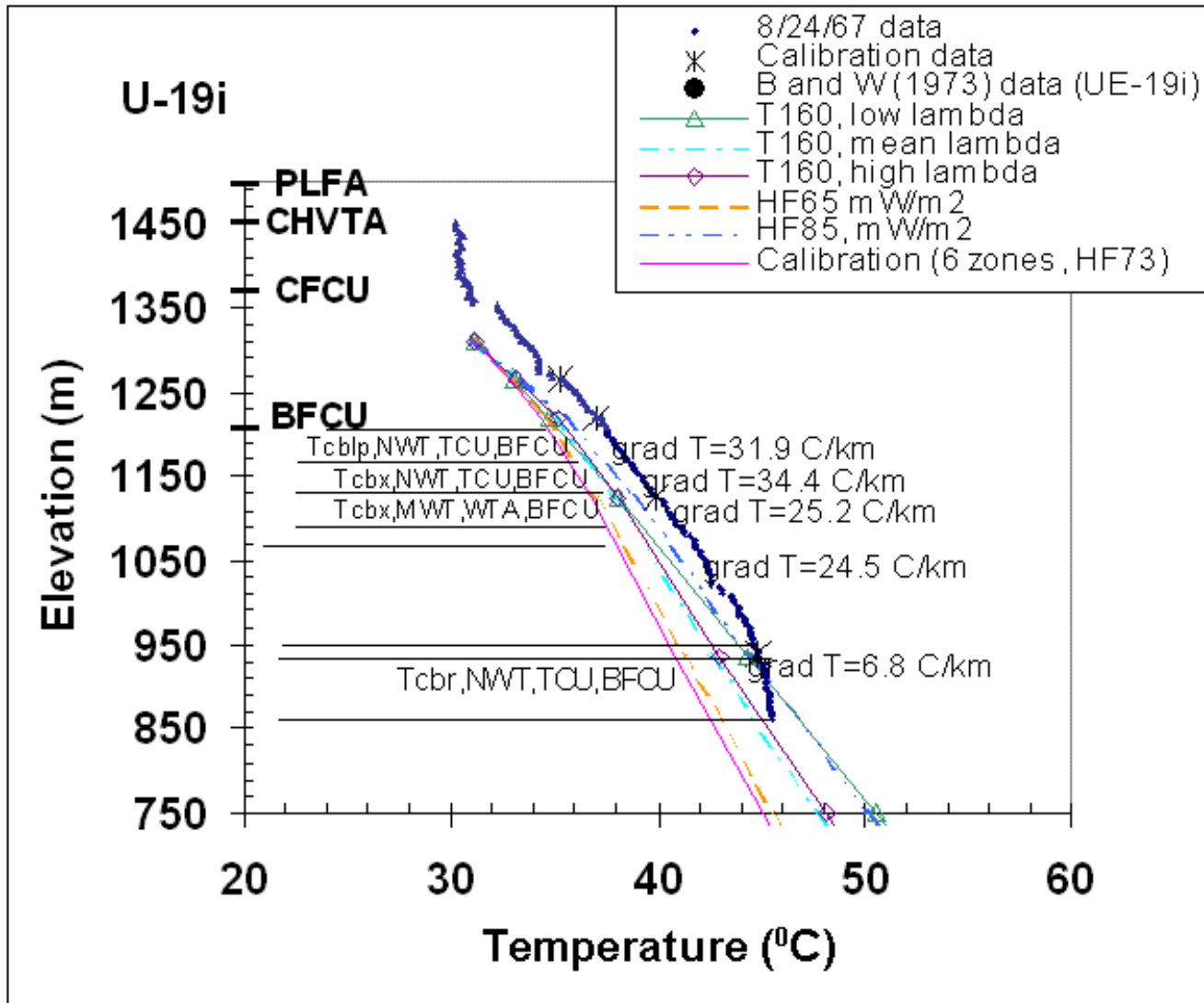


Figure C16

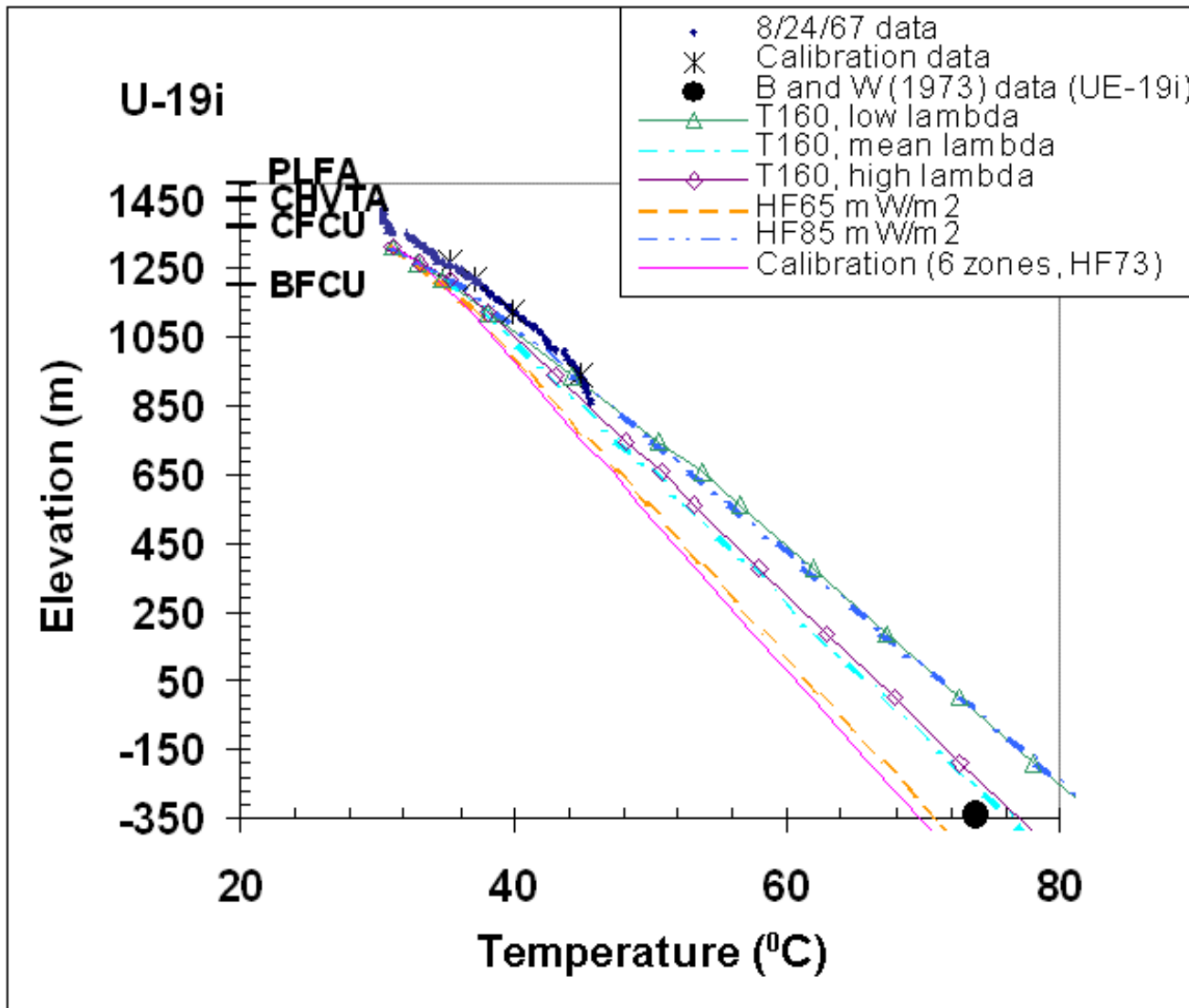


Figure C17

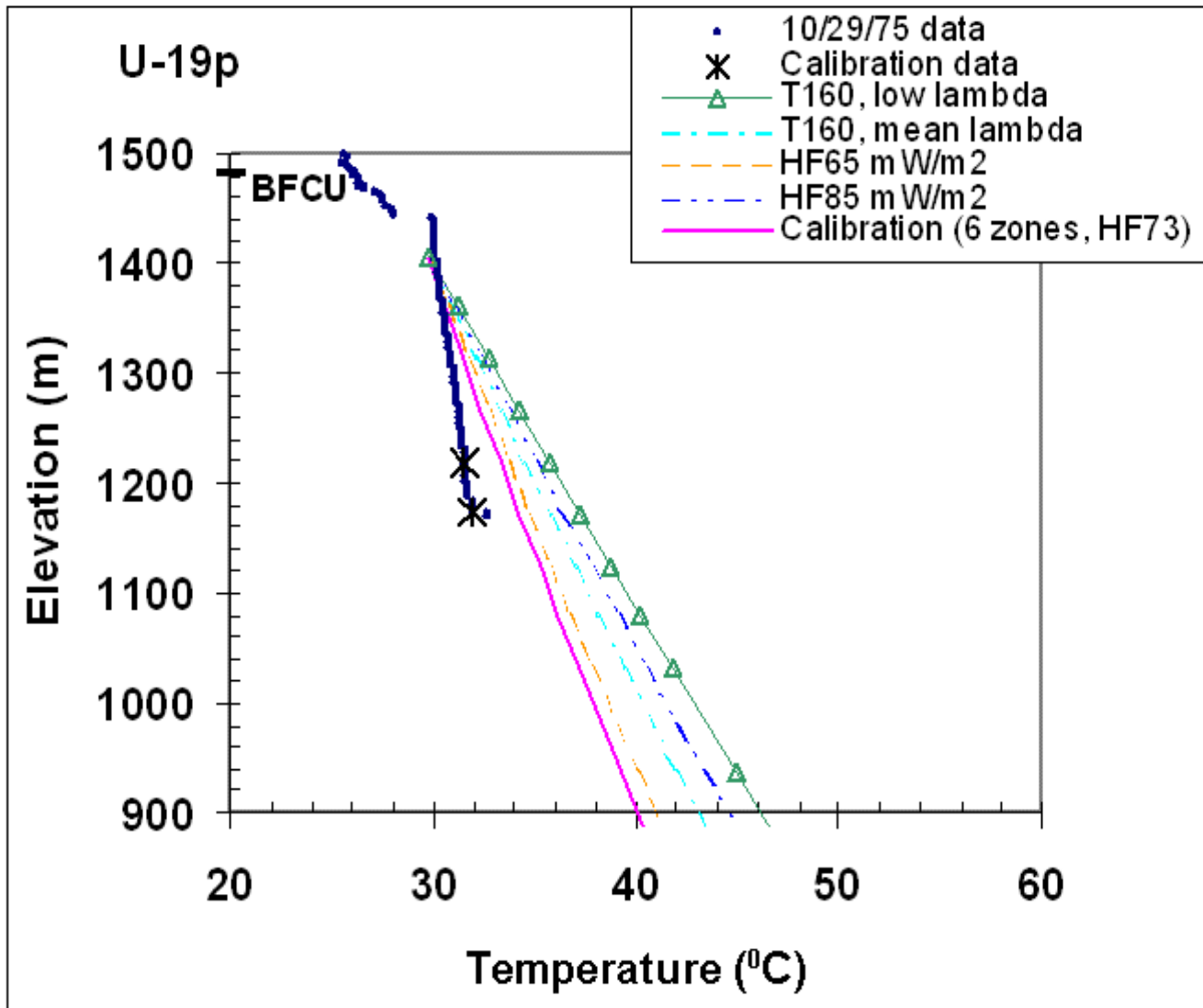


Figure C18

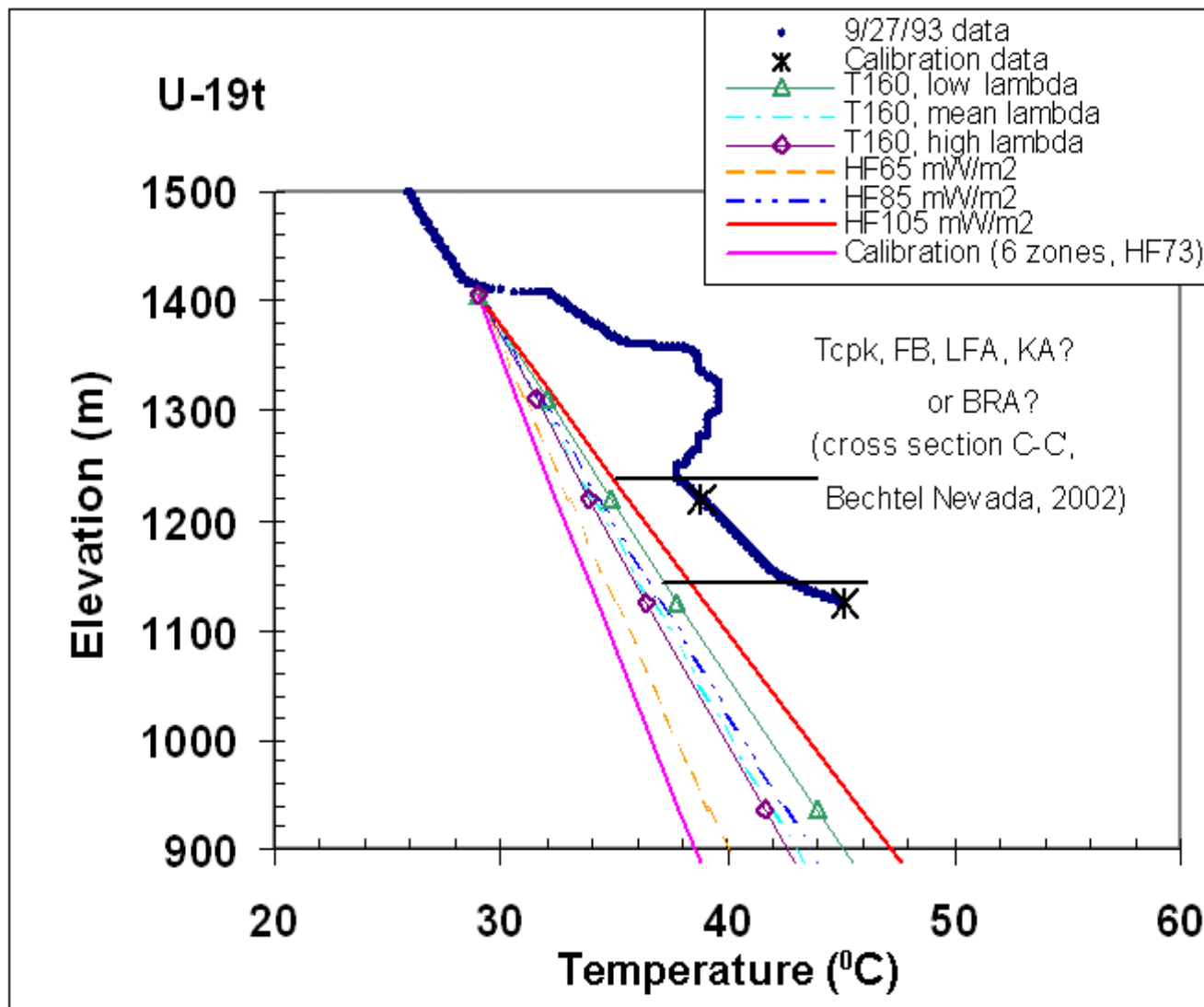


Figure C19

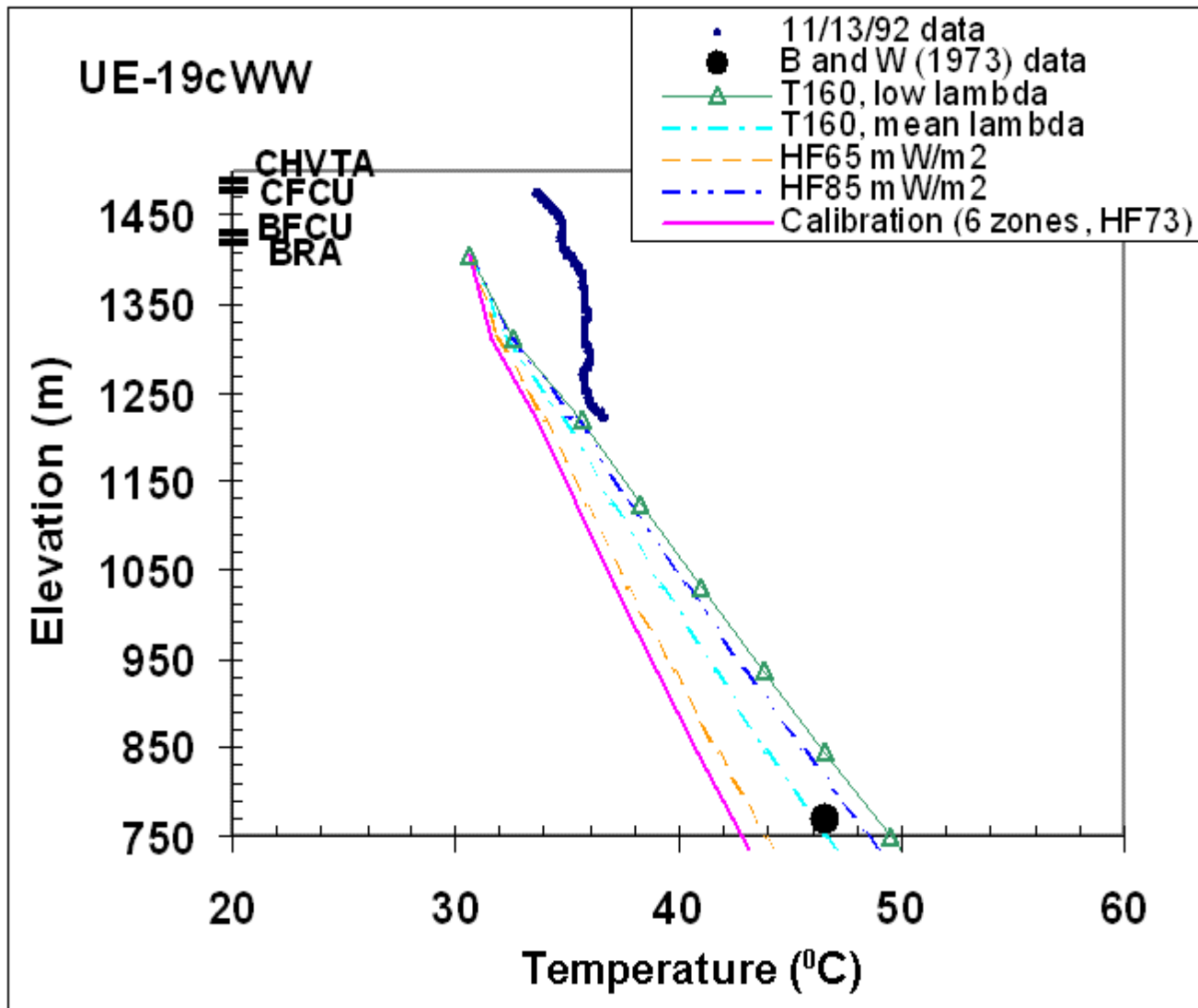


Figure C20

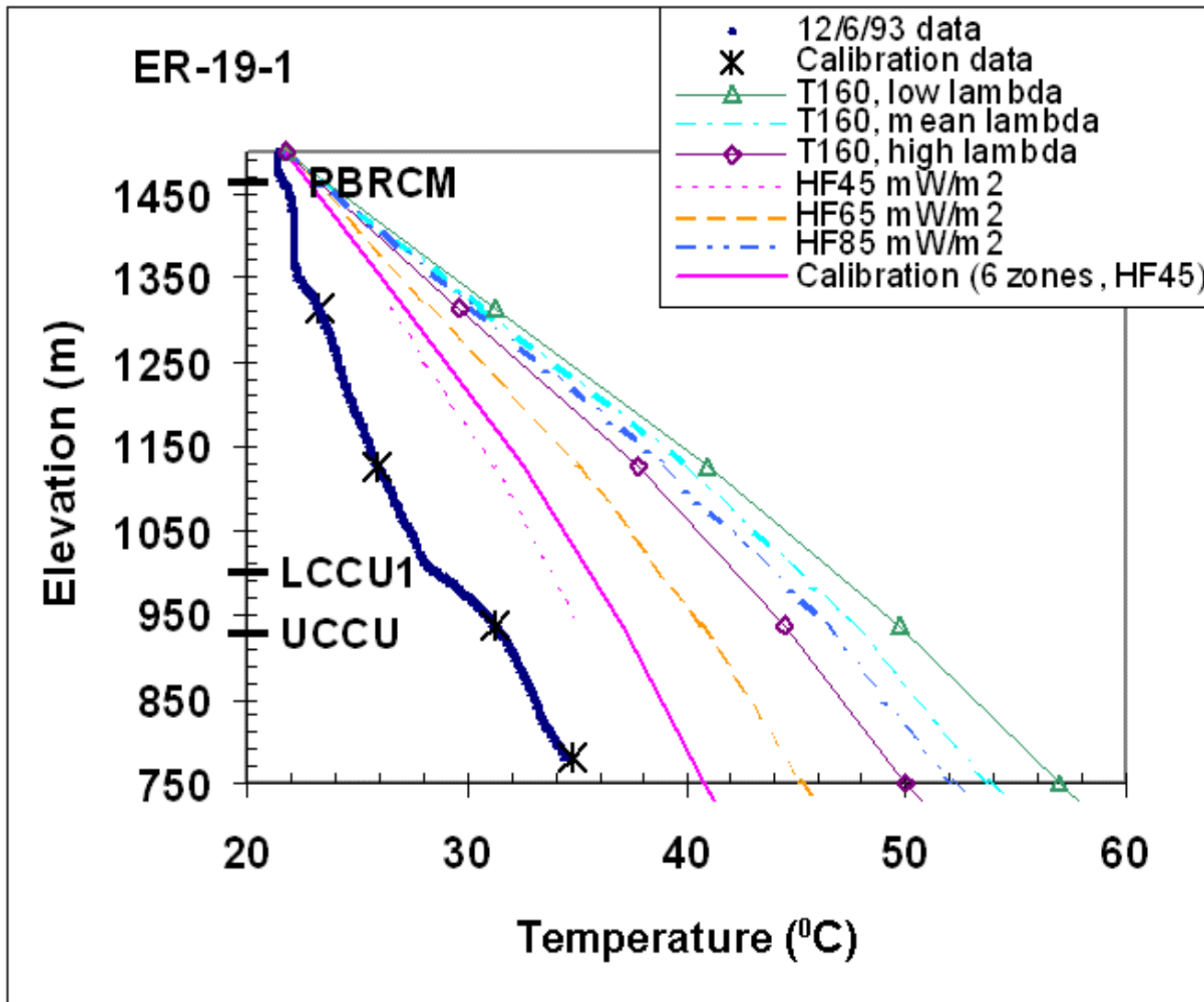


Figure C21

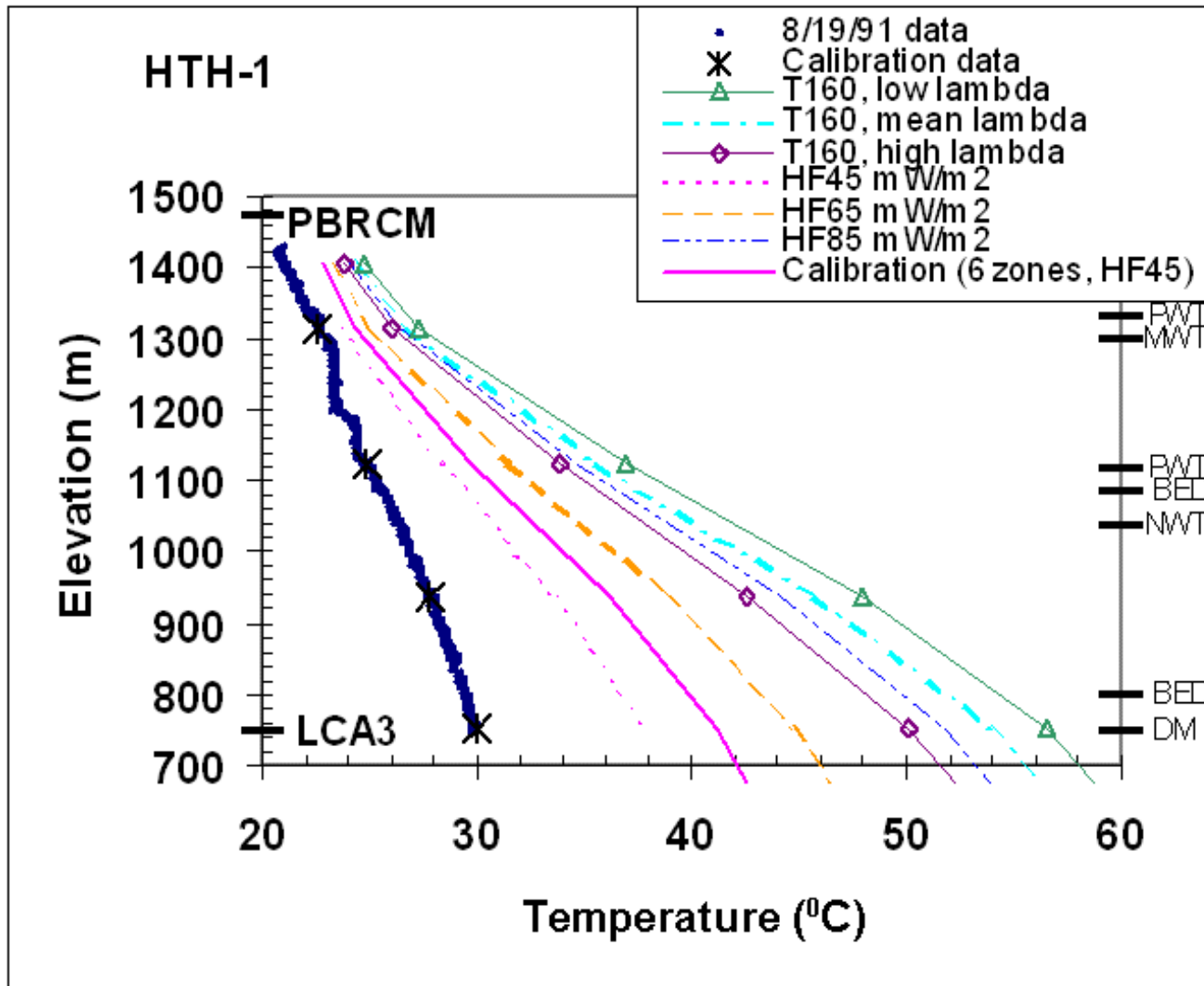


Figure C22

Uncontrolled When Printed

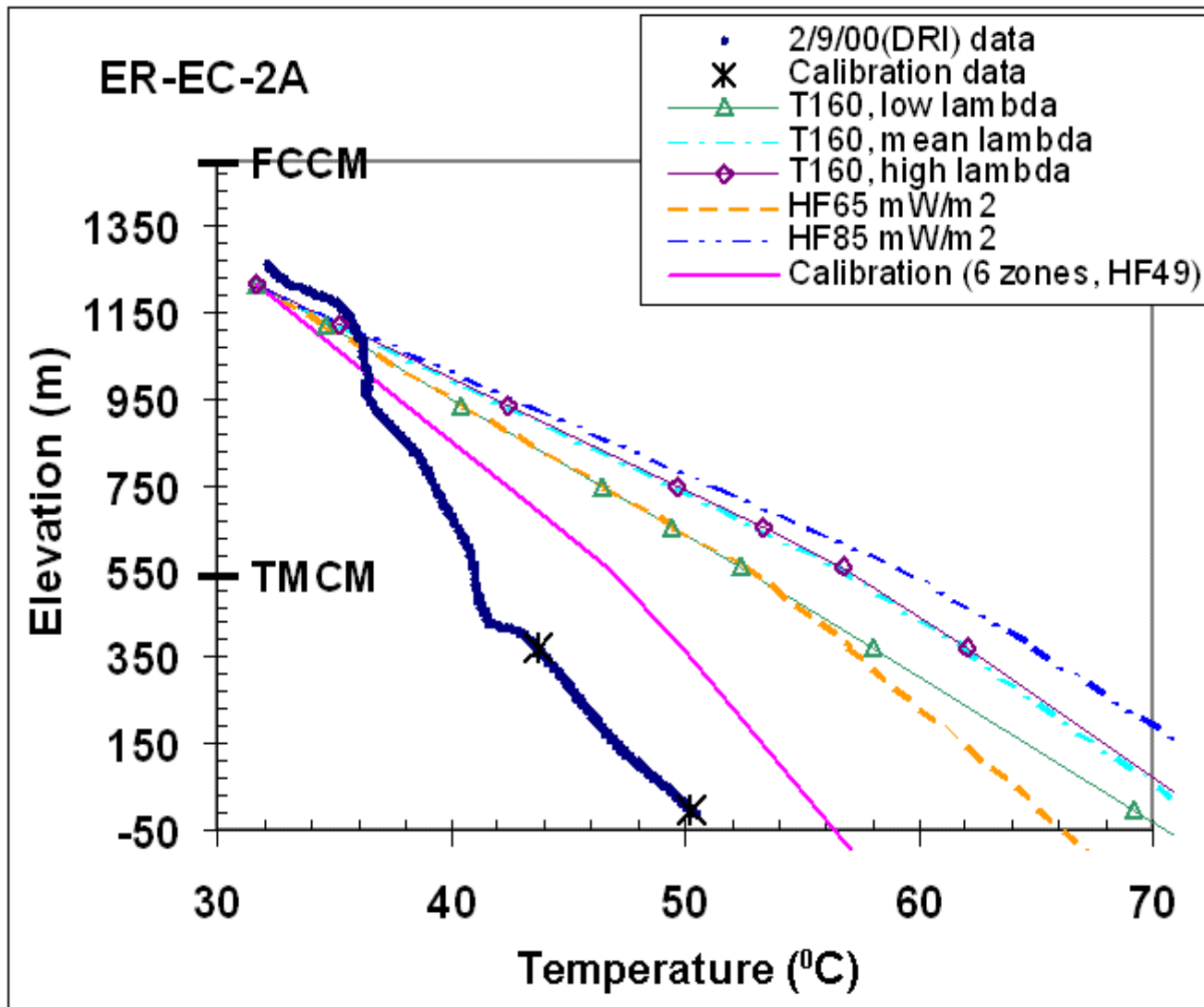


Figure C23

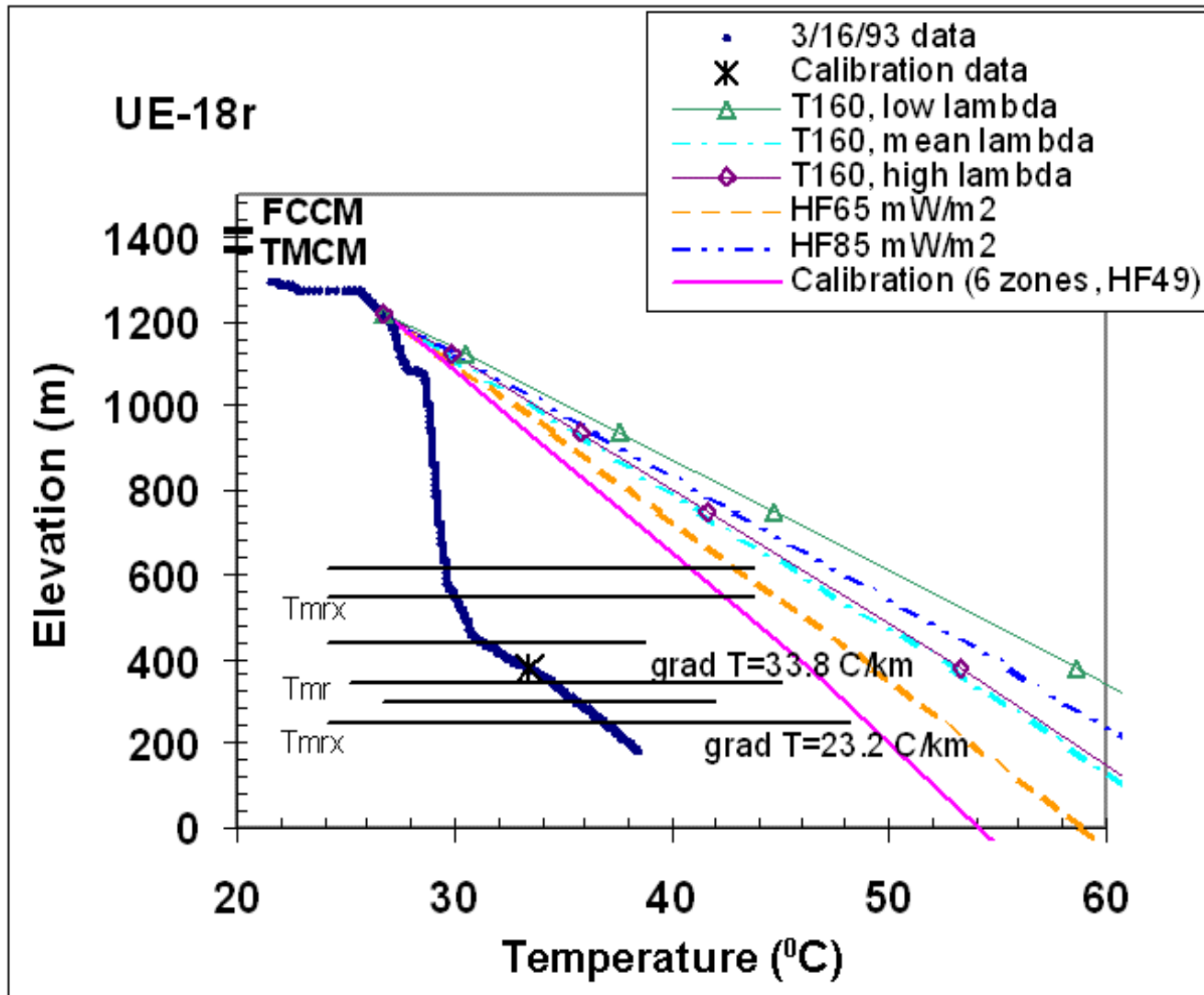


Figure C24

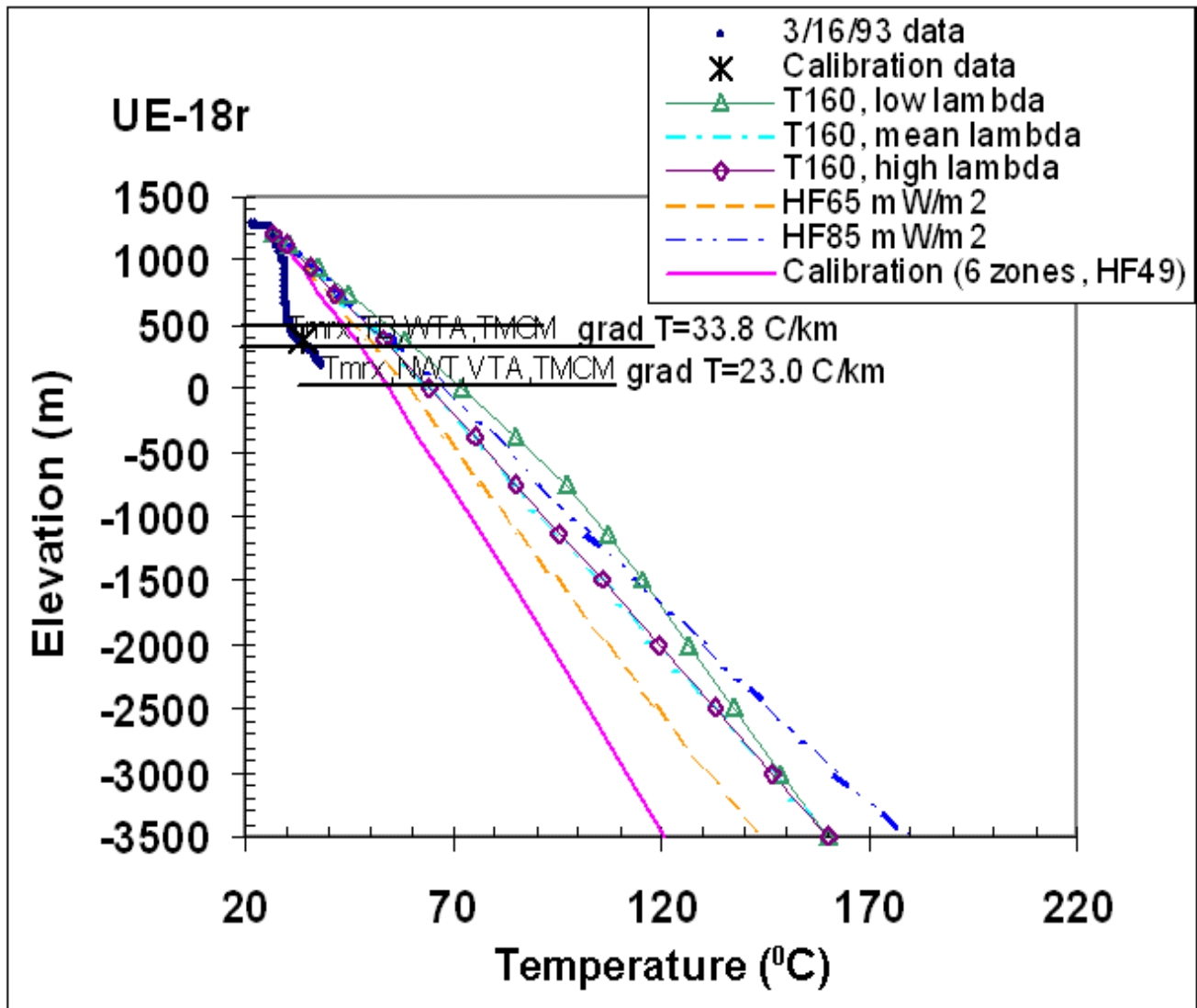


Figure C25

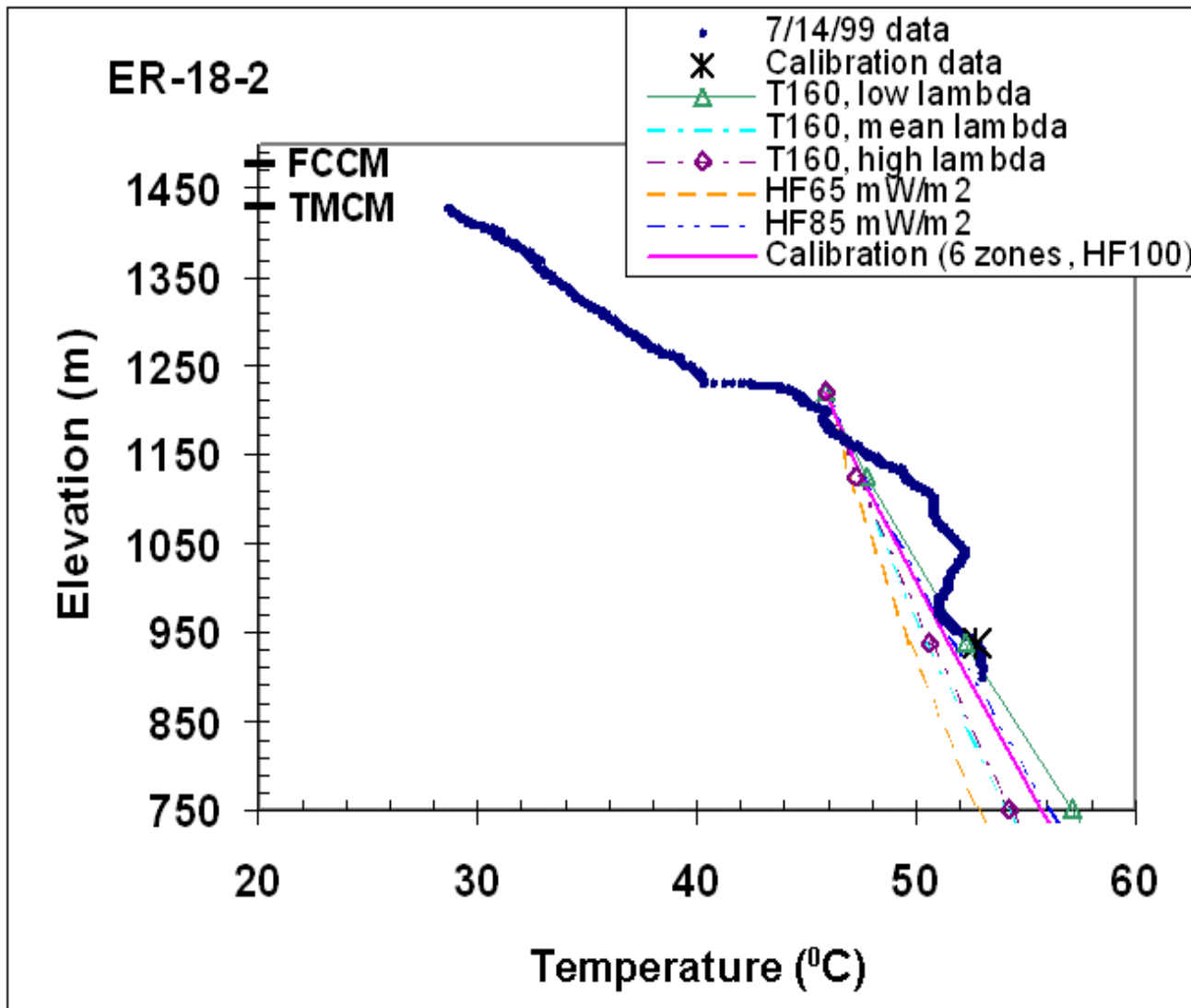


Figure C26

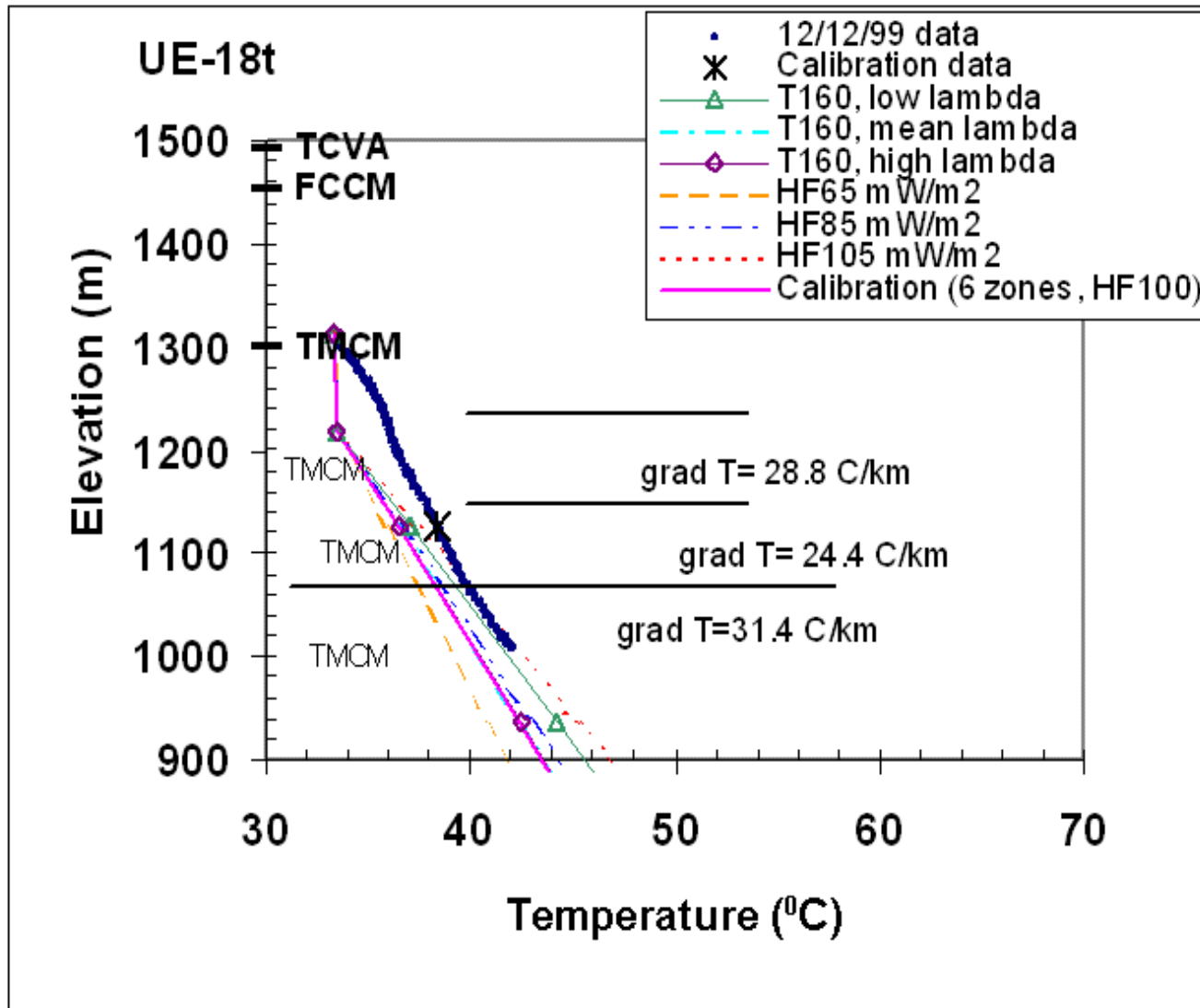


Figure C27

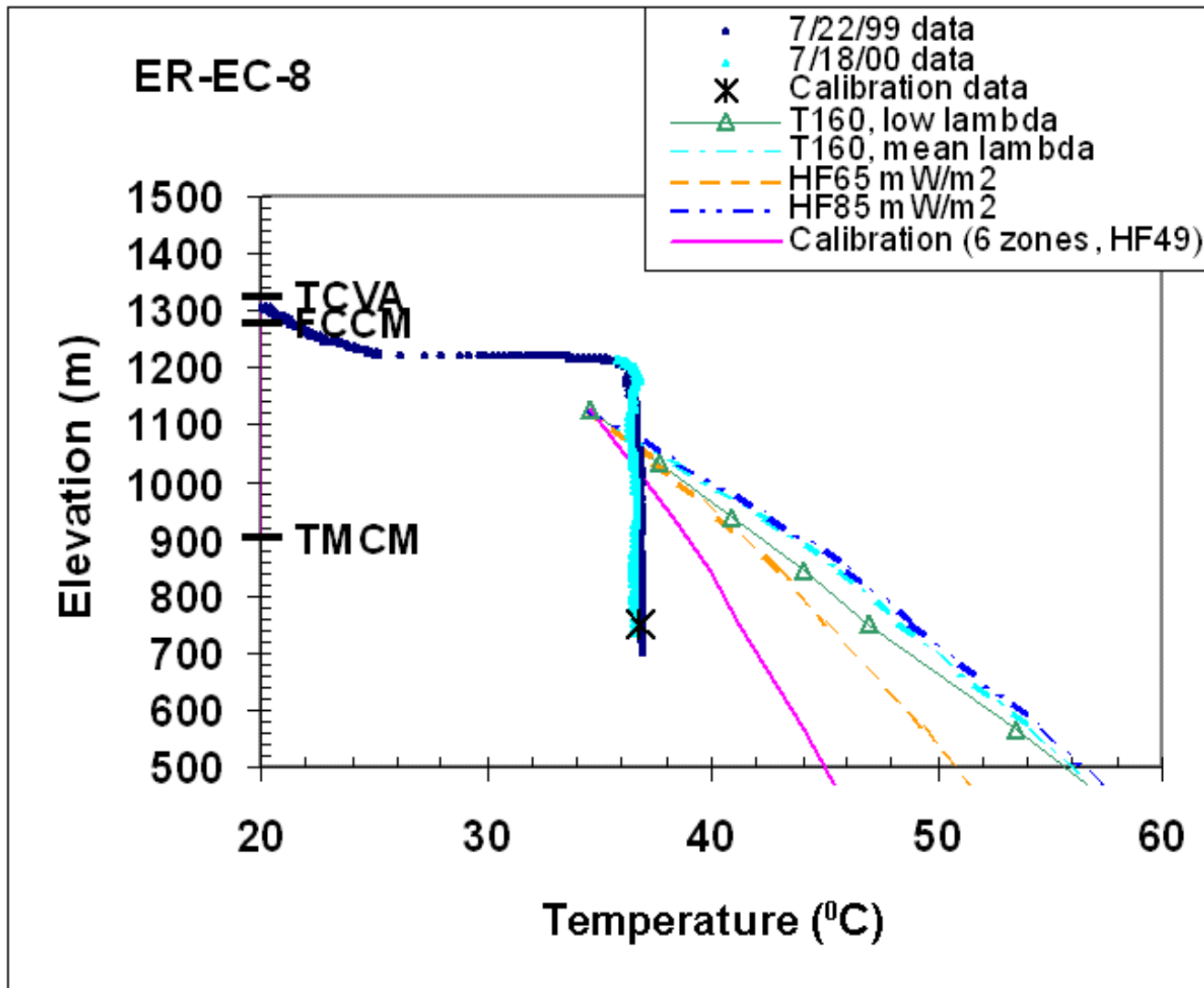


Figure C28

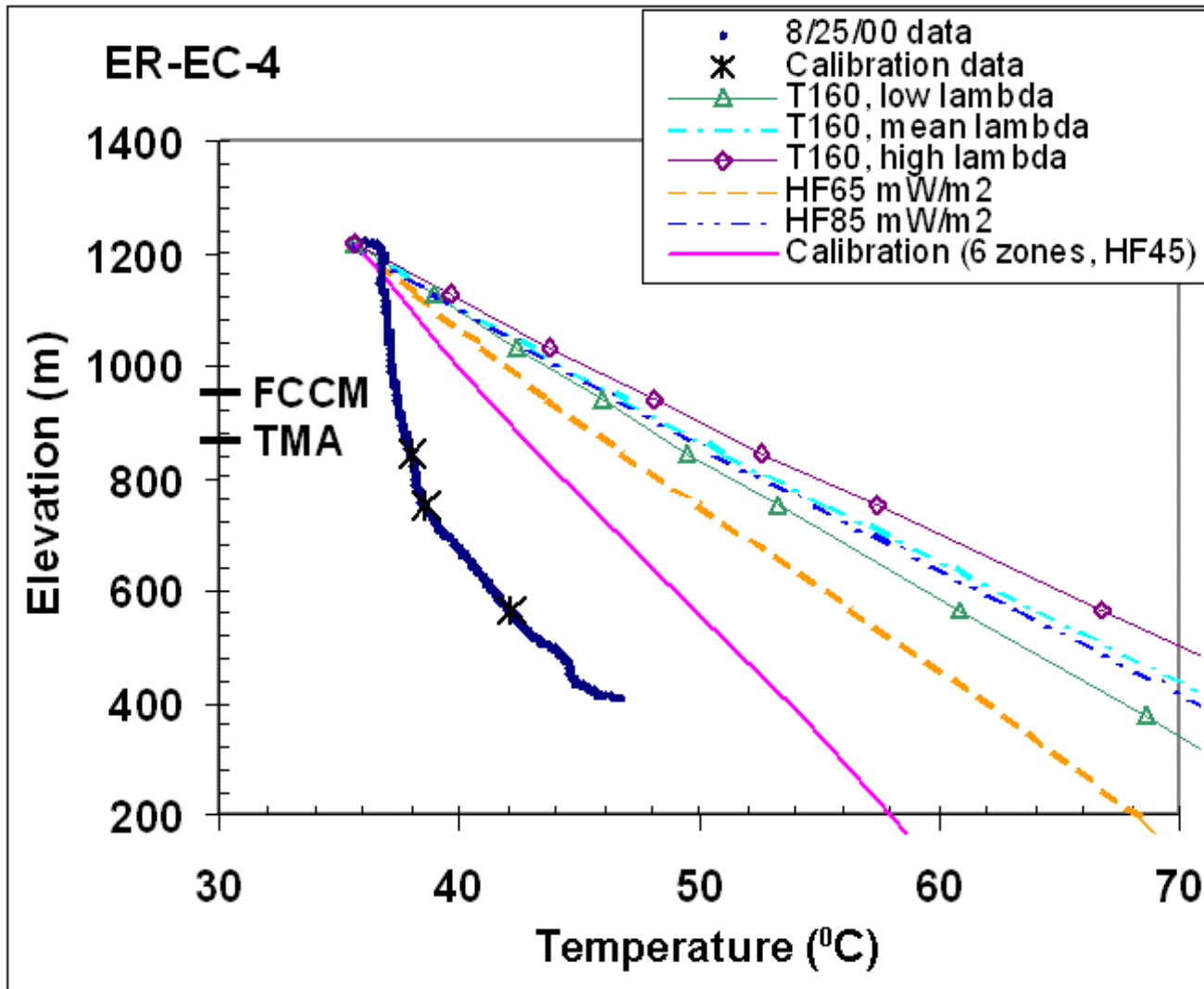


Figure C29

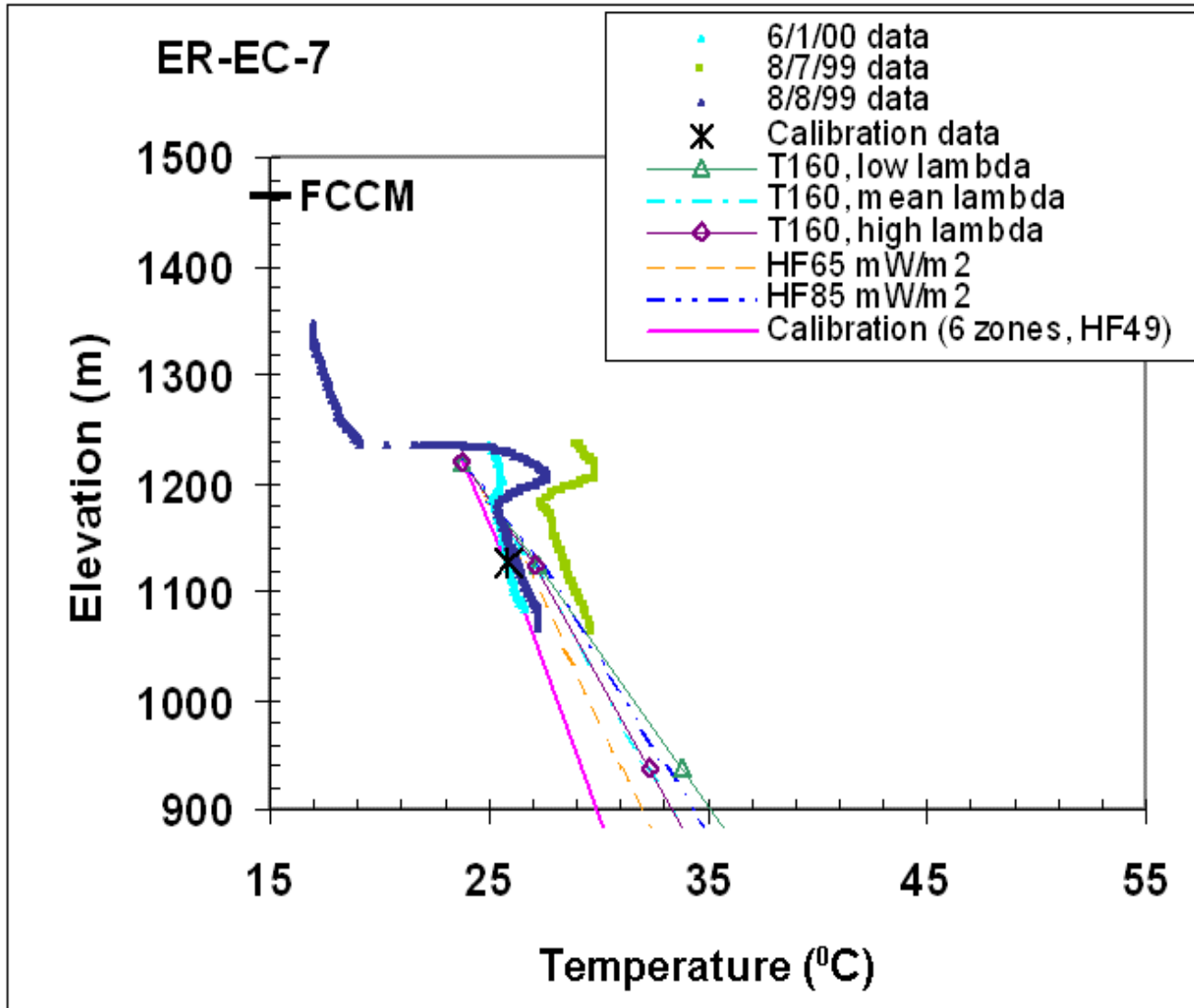


Figure C30

Explanation of stratigraphic symbols, rock types, alteration, and hydrogeologic units

Stratigraphy

unk = unknown
Tgs = Tertiary sediments
Tt = Thirsty Canyon Group
Ttr = Rocket Wash Tuff
Ttt = Trail Ridge Tuff
Ttp = Pahute Mesa and Rocket Wash Tuffs
Tf = Volcanics of Fortymile Canyon
Tfb = Beatty Wash Formation
Tfbr = Rhyolite of Chukar Canyon
Tfbw = Rhyolite of Beatty Wash
Tm = Timber Mountain Group
Tma = Ammonia Tanks Tuff
Tmab = bedded Ammonia Tanks Tuff
Tmap = mafic-poor Ammonia Tanks Tuff
Tmat = Rhyolite of Tannebaum Hill
Tmt = Basalt Rhyolite of Tannebaum Hill
Tmr = Rainier Mesa Tuff
TmrB = Bedded Rainier Mesa Tuff
TmrF = Rhyolite of Fluorspar Canyon
TmrR = mafic-rich Rainer Mesa Tuff
TmrP = mafic-poor Rainer Mesa Tuff
TmrH = Tuff of Holmes Road
TmrX = Landslide or eruptive breccia
Tmaw = Tuff of Buttonhook Wash
Tmw = Rhyolite of Windy Wash

Tp = Paintbrush Group
Tpb = Rhyolite of Benham
Tpc = Tiva Canyon Tuff
Tpd = Rhyolite of Delirium Canyon
Tpe = Rhyolite of Echo Peak
Tpr = Rhyolite of Silent Canyon
Tpt = Topopah Spring Tuff
Th = Calico Hills Formation
Tc = Crater Flat Group
Tcp = Prow Pass Tuff
Tci = Rhyolite of Inlet
Tcj = Andesite of Grimy Gulch
TcPk = Rhyolite of Kearsarge
Tcb = Bullfrog Tuff
Tct = Tram Tuff
Tb = Belted Range Group
Tbd = Deadhorse Flat Formation
Tq = Volcanics of Quartz Mountain
To = Volcanics of Oak Spring Butte
Ton = Older tunnel beds
Tor = Redrock Valley Tuff
Tot = Tuff of Twin Peaks

Lithology/Rock type

AL = alluvium
BD = basaltic dike
BS = basalt
BED = bedded tuff
DM = dolomite
DWT = densely welded tuff
FB = flow breccia
IN = intrusive
ITL = intermediate to trachytic lava
LA = lava
MWT = moderately welded tuff
NWT = nonwelded tuff

Major Alteration

KA = kaolinitic
KF = potassic
MP = microporphyratic (holocrystalline)
OP = opalline
PI = pilotaxitic (holocrystalline)
PY = pyritic
QC = silicic (chalcedony)
QF = quartzo-feldspathic

Hydrogeologic Units

AA = Alluvial aquifer
WTA = Welded tuff aquifer
VTA = Vitric Tuff aquifer
LFA = Lava flow aquifer
TCU = Tuff confining unit
CCU = Clastic confining unit

PL = pumiceous (frothy) lava
PWT = partially welded tuff
QTZ = quartzite or sandstone
RWT = reworked tuff
SLT = siltstone
TS = tuffaceous sandstone
TUF = tuff
TB = tuff breccia
unk = unknown
VT = vitrophyric tuff, vitric bedded
WBE = welded bedded tuff
WT = welded tuff

QZ = silicic
SE = seriate (holocrystalline)
unk = unknown
VP = devitrified (vapor phase)
ZA = zeolitic (analcime)
ZC = zeolitic (clinoptilolite)
ZE = zeolitic
ZM = zeolitic (mordenite)



Appendix D

Perturbation Sensitivity Analysis Plots

D.1.0 INTRODUCTION

This appendix contains perturbation sensitivity analysis plots for the Pahute Mesa Oasis Valley area. Included are figures for Base HFM with Depth Decay and Anisotropy, Base HFM with Selected Depth Decay and Selected Anisotropy, and Silent Canyon Caldera Complex Selected Depth Decay and Selected Anisotropy.

D.2.0 DATA PRESENTATION

The data are presented in individual figures. These figures present the change in some model metric as a function of model parameters. The model metrics in each file are as follows:

- Average Head – change in calibration target head as defined in [Section 6.1.1](#).
- Lateral Boundary west, south, east, and north – change in respective model edge flow objective function
- Lateral Boundary – Oasis Valley – change in objective function for each discharge zone in Oasis Valley
- Oasis Valley Discharge – change in objective function for entire Oasis Valley
- Boundary Flow Goodness of Fit – change in objective function for all boundary flows
- Total objective function – change in PHI, overall model goodness of fit
- Spring head – change in spring head component of model goodness of fit
- Observation well goodness of fit – change in observation well component of model goodness of fit

Model parameters are referred to in a shorthand that incorporates both the index number as given in [Section 4.0](#) and the HSU name abbreviation (also given in [Section 4.0](#)). For instance, hsu01lccu is HSU index number 1, which is also the LCCU. Depth decay is referred to by “dd” to identify the parameter, by HSU type via “ca” for carbonate and “va” for volcanic, and by HSU number. Thus, ddca02 is for a carbonate that is also HSU 2 (the LCA proper). DDVA32 is depth decay for volcanic HSU number 32, which is the PCM. Faults are referred to by number and a brief abbreviation of the name.

D.3.0 ACCESS TO DATA

The perturbation sensitivity analysis plots can be found on the accompanying CD in pdf format. The data files are listed below.

D.3.1 Base HFM with Depth Decay and Anisotropy with MME Recharge

- Average Head.pdf
- Lateral Boundary – West Face Model Flow.pdf
- Lateral Boundary – South Face Model Flow.pdf
- Lateral Boundary – East Face Model Flow.pdf
- Lateral Boundary – North Face Model Flow.pdf
- Lateral Boundary – Oasis Valley Discharge Region 1 Flow.pdf
- Lateral Boundary – Oasis Valley Discharge Region 2 Flow.pdf
- Lateral Boundary – Oasis Valley Discharge Region 3 Flow.pdf
- Lateral Boundary – Oasis Valley Discharge Region 4 Flow.pdf
- Lateral Boundary – Oasis Valley Discharge Region 5 Flow.pdf
- Lateral Boundary – Oasis Valley Discharge Region 6 Flow.pdf
- Lateral Boundary – Oasis Valley Discharge Region 8 Flow.pdf
- Oasis Valley Discharge.pdf
- Boundary Flow Goodness of Fit.pdf
- Total Objective Function.pdf
- Spring Head.pdf
- Observation Well Goodness of Fit.pdf

D.3.2 Base HFM with Selected Depth Decay and Selected Anisotropy with MME Recharge

- Average Head.pdf
- Lateral Boundary – West Face Model Flow.pdf
- Lateral Boundary – South Face Model Flow.pdf
- Lateral Boundary – East Face Model Flow.pdf
- Lateral Boundary – North Face Model Flow.pdf
- Lateral Boundary – Oasis Valley Discharge Region 1 Flow.pdf
- Lateral Boundary – Oasis Valley Discharge Region 2 Flow.pdf
- Lateral Boundary – Oasis Valley Discharge Region 3 Flow.pdf
- Lateral Boundary – Oasis Valley Discharge Region 4 Flow.pdf
- Lateral Boundary – Oasis Valley Discharge Region 5 Flow.pdf

- Lateral Boundary – Oasis Valley Discharge Region 6 Flow.pdf
- Lateral Boundary – Oasis Valley Discharge Region 8 Flow.pdf
- Oasis Valley Discharge.pdf
- Boundary Flow Goodness of Fit.pdf
- Total Objective Function.pdf
- Spring Head.pdf
- Observation Well Goodness of Fit.pdf

D.3.3 Silent Canyon Caldera Complex Selected Depth Decay and Anisotropy with MME Recharge

- Average Head.pdf
- Lateral Boundary – West Face Model Flow.pdf
- Lateral Boundary – South Face Model Flow.pdf
- Lateral Boundary – East Face Model Flow.pdf
- Lateral Boundary – North Face Model Flow.pdf
- Lateral Boundary – Oasis Valley Discharge Region 1 Flow.pdf
- Lateral Boundary – Oasis Valley Discharge Region 2 Flow.pdf
- Lateral Boundary – Oasis Valley Discharge Region 3 Flow.pdf
- Lateral Boundary – Oasis Valley Discharge Region 4 Flow.pdf
- Lateral Boundary – Oasis Valley Discharge Region 5 Flow.pdf
- Lateral Boundary – Oasis Valley Discharge Region 6 Flow.pdf
- Lateral Boundary – Oasis Valley Discharge Region 8 Flow.pdf
- Oasis Valley Discharge.pdf
- Boundary Flow Goodness of Fit.pdf
- Total Objective Function.pdf
- Spring Head.pdf
- Observation Well Goodness of Fit.pdf



Appendix E

CAU Model Permeability Along Geologic Model Cross Sections

E.1.0 CAU MODEL PERMEABILITY ALONG GEOLOGIC MODEL CROSS SECTIONS

This appendix presents the CAU model intrinsic permeability along geologic cross sections A through J as described in BN (2002) for the base HFM (selected and all HSU depth decay and anisotropy), the SCCC HFM, and the RIDGE, TCL, PZUP, SEPZ, and DRT alternatives (see Section 2.0 for a description, and Sections 5.0 and 6.0 for calibration results). The sections for PZUP with DRI-A recharge, PZUP with USGS-D recharge, DRT with DRI-A recharge, and DRT with USGS-D recharge are also presented. Figure E.1-1 shows the location and names of the sections.

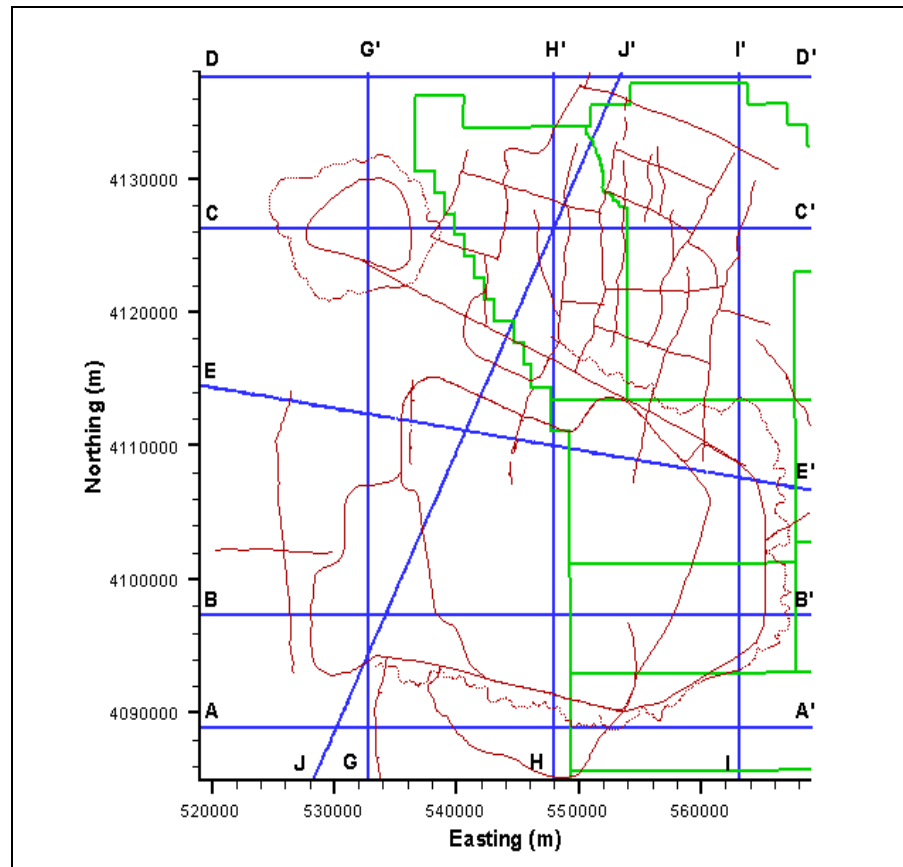
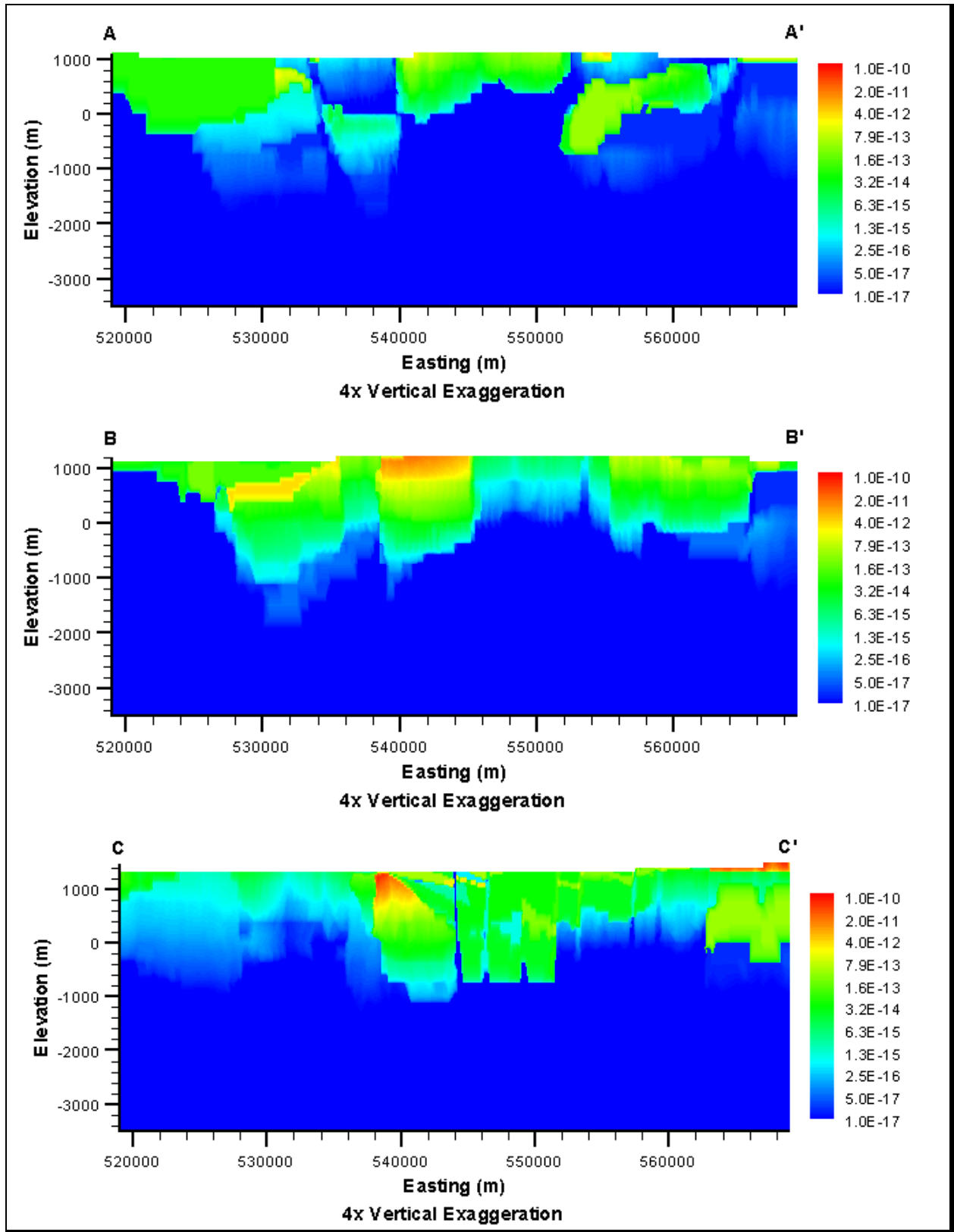
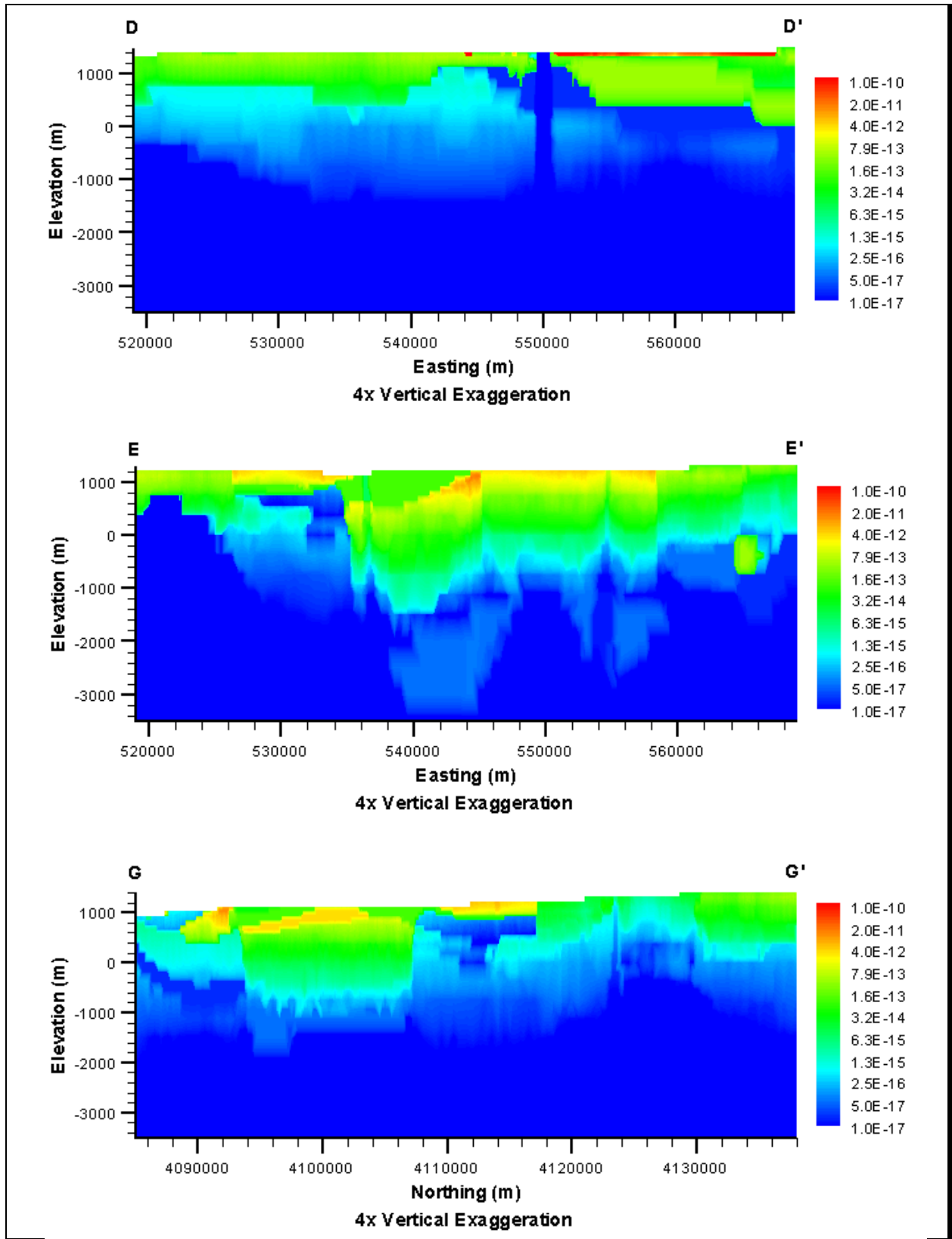
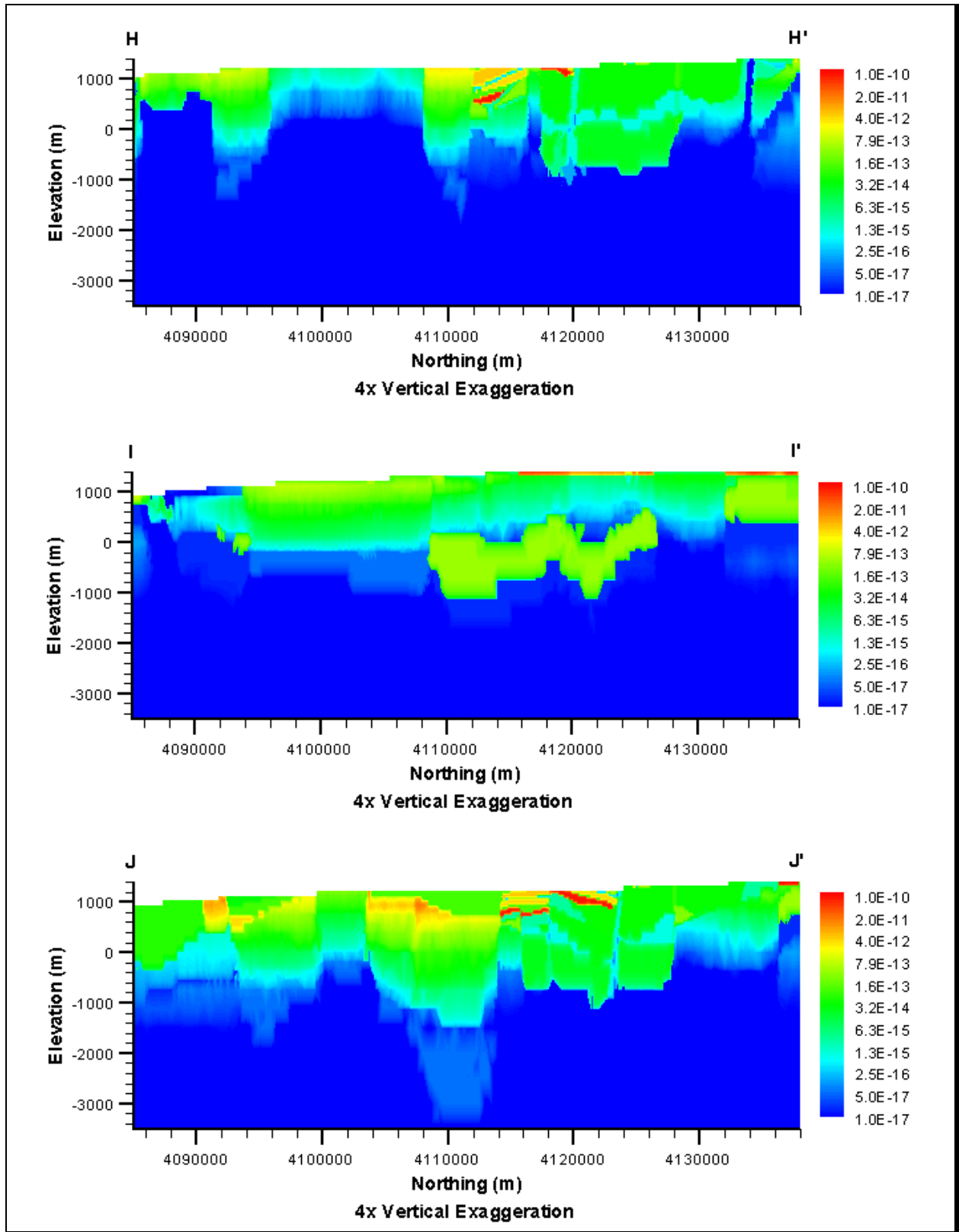


Figure E.1-1
Geologic Cross-Section Key

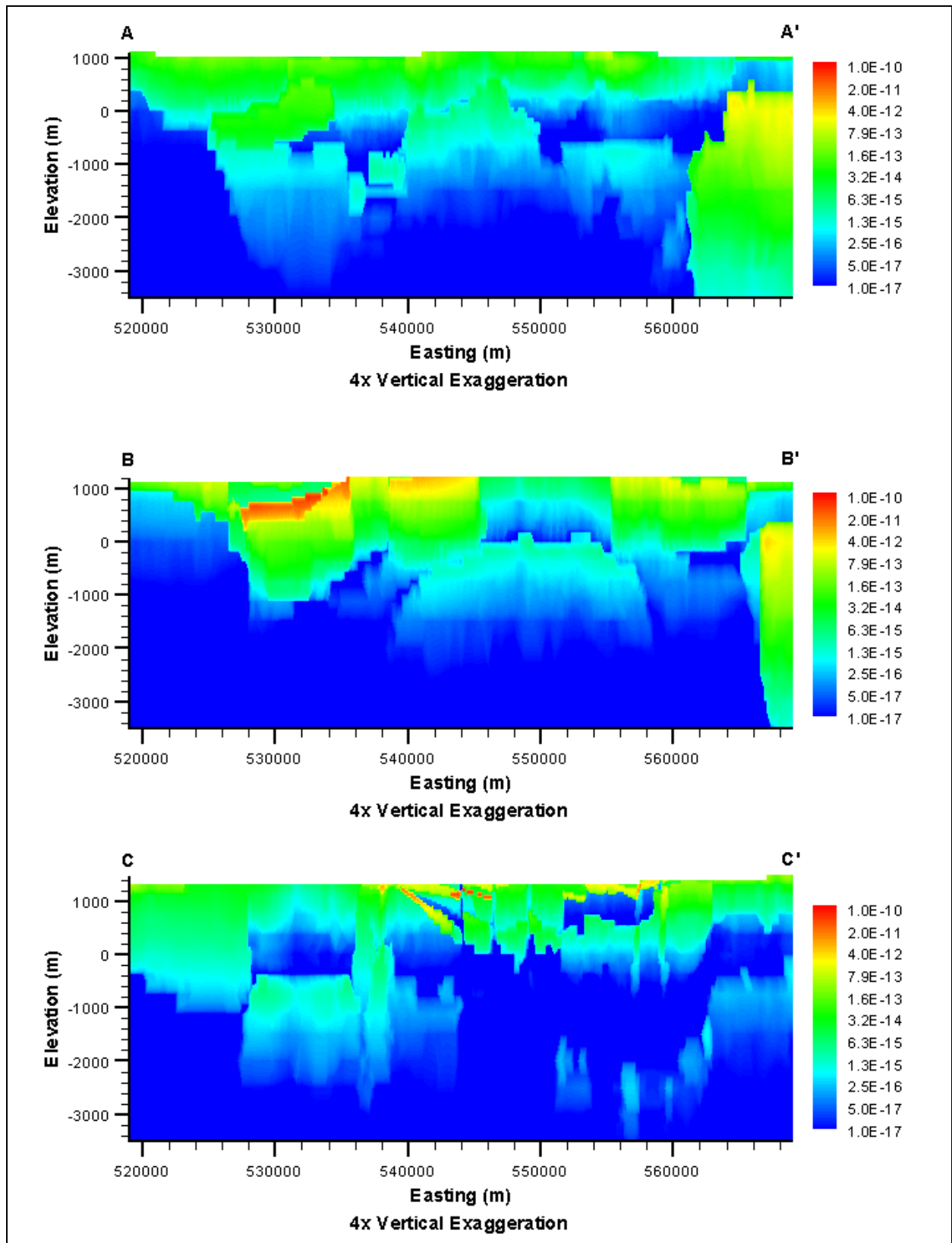
***Base HFM - Selected HSU Depth Decay and Anisotropy
(BN-MME-SDA)***

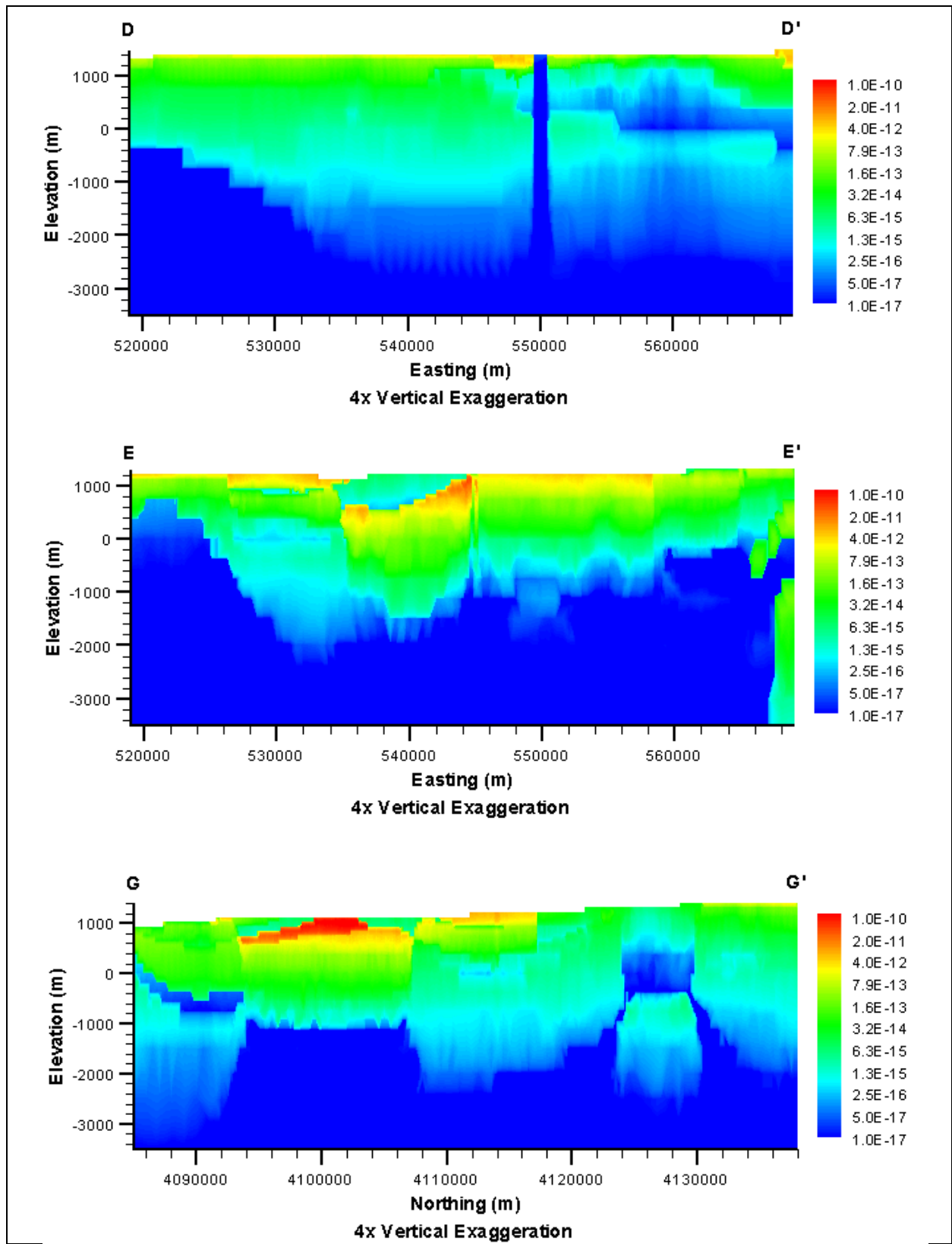


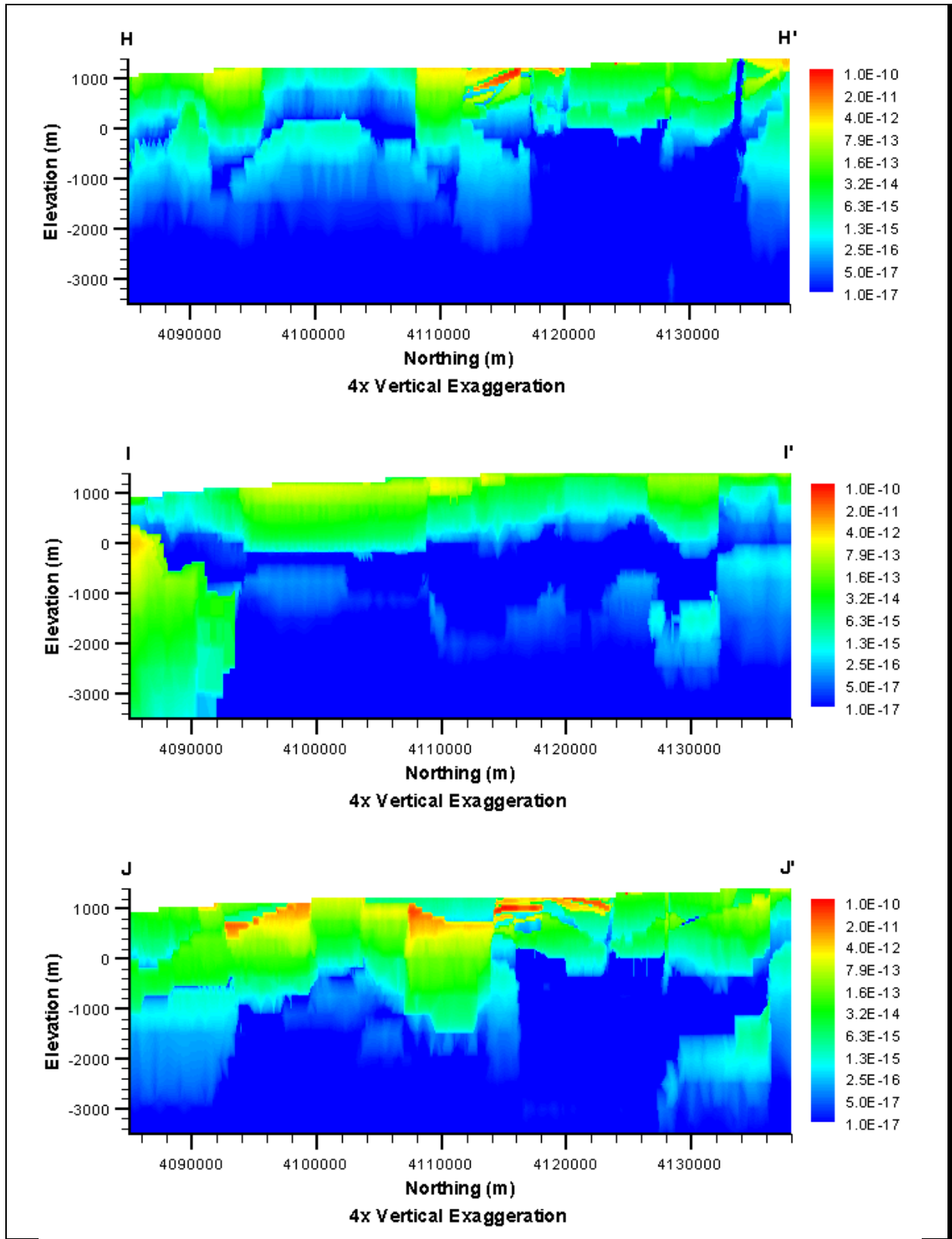




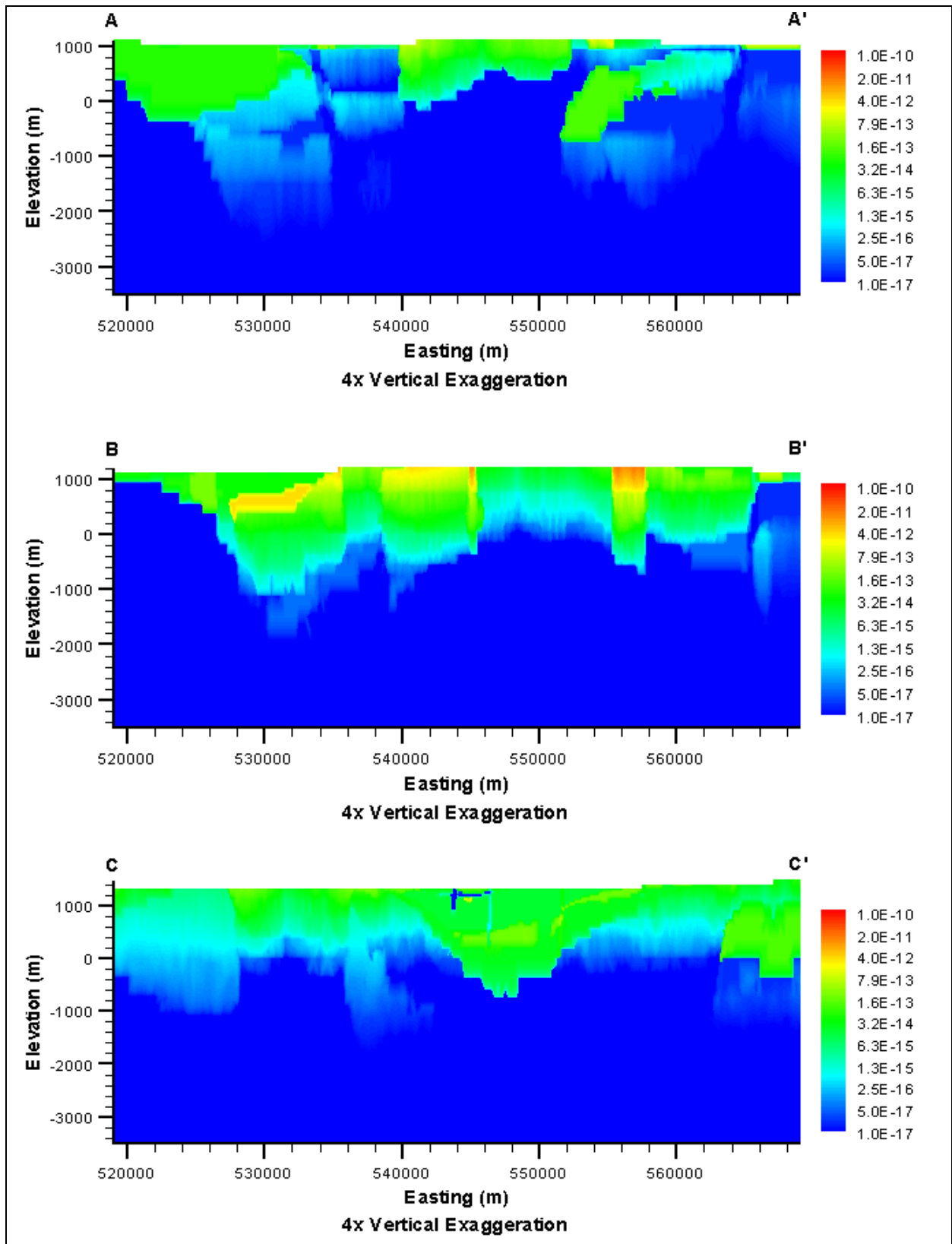
***Base HFM - All HSU Depth Decay and Anisotropy
(BN-MME-ADA)***

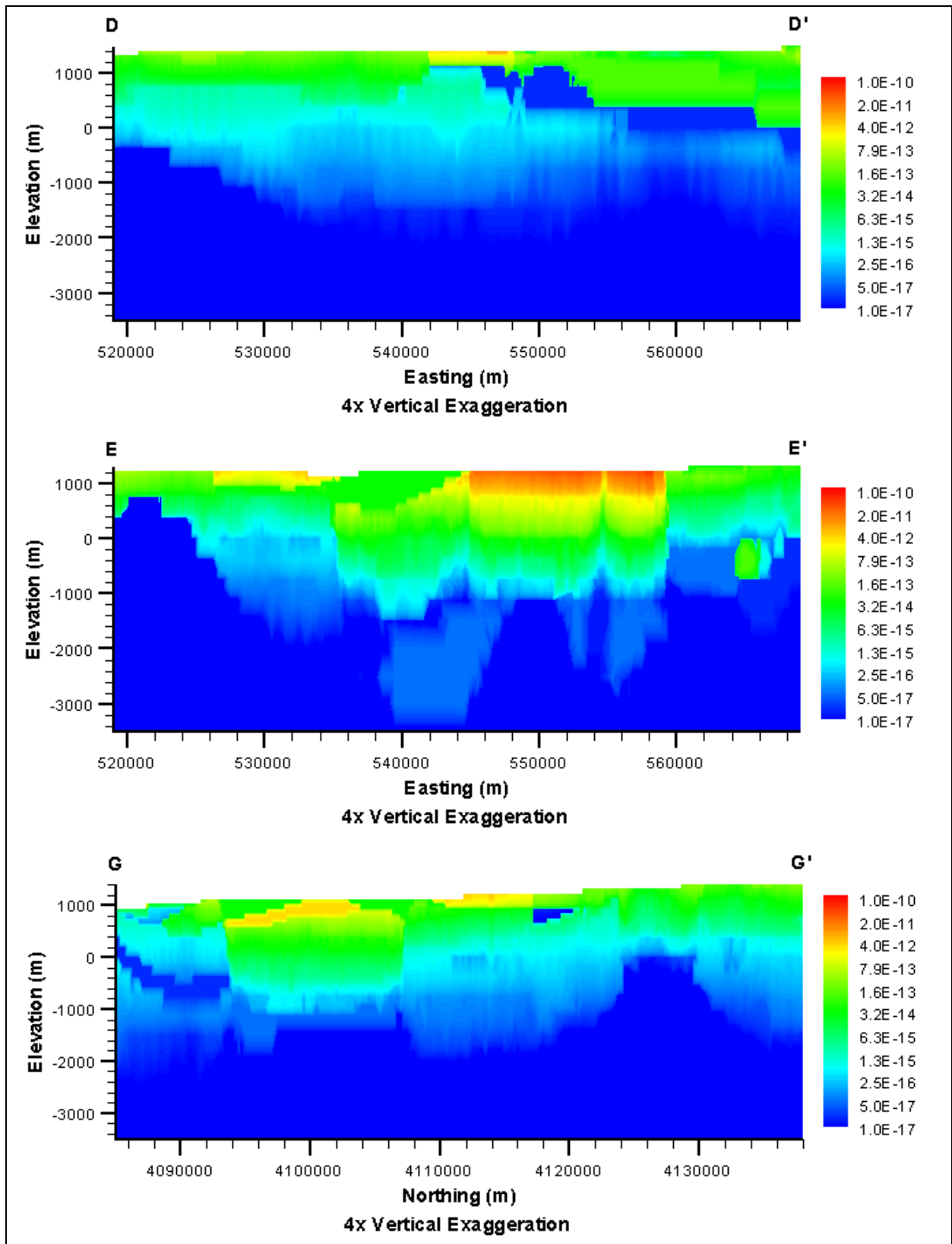


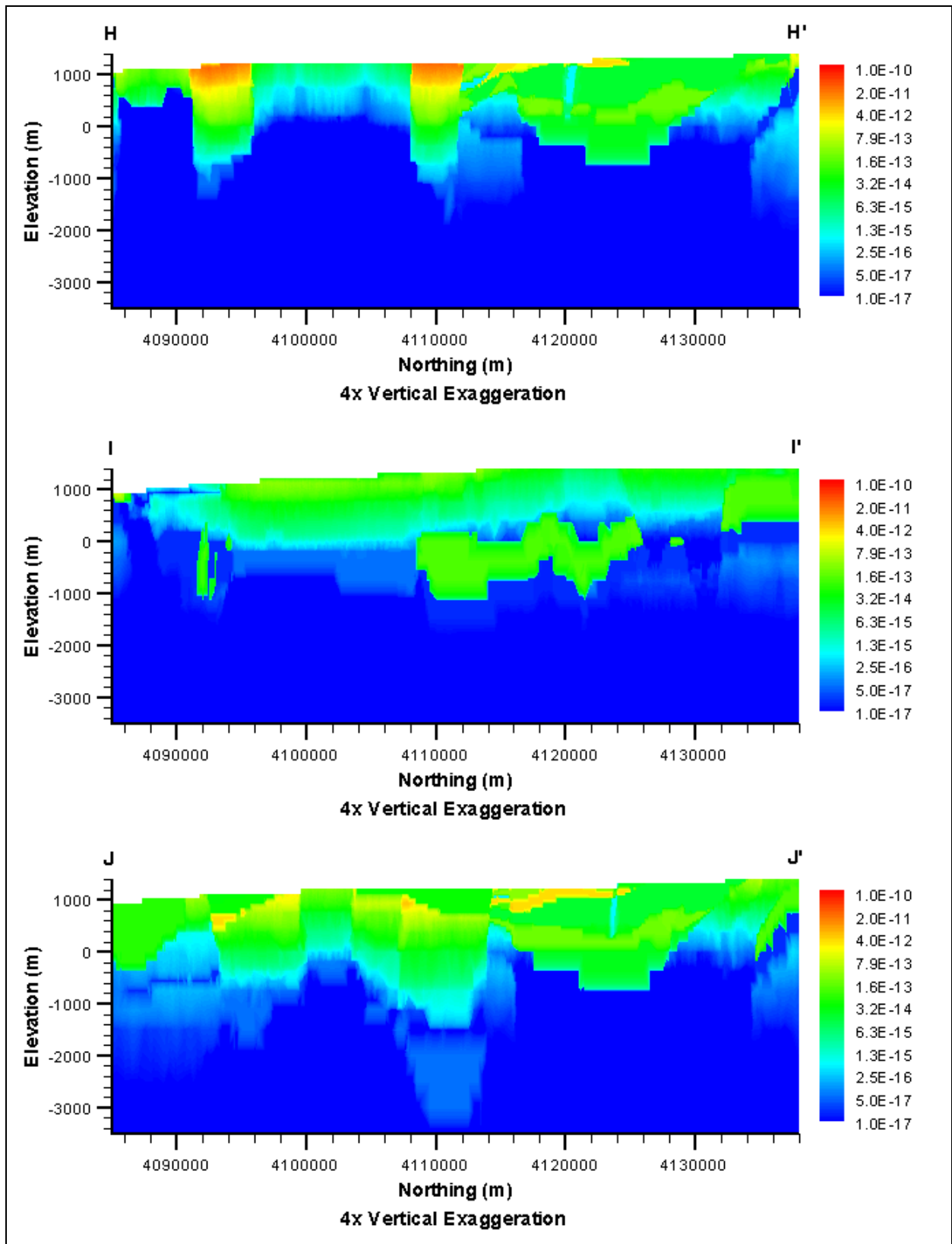




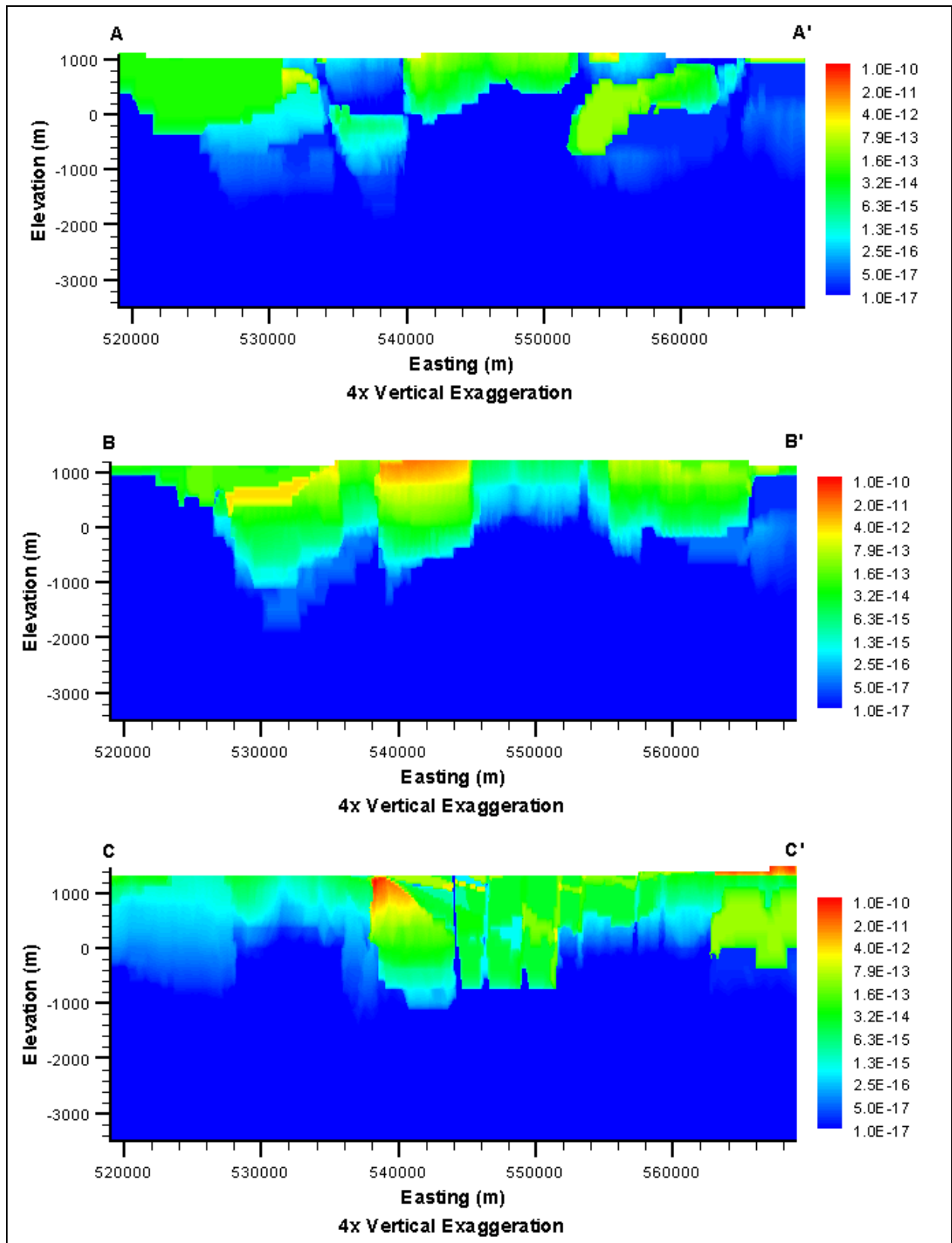
***SCCC HFM - Selected HSU Depth Decay and Anisotropy
(SCCC-MME-SDA)***

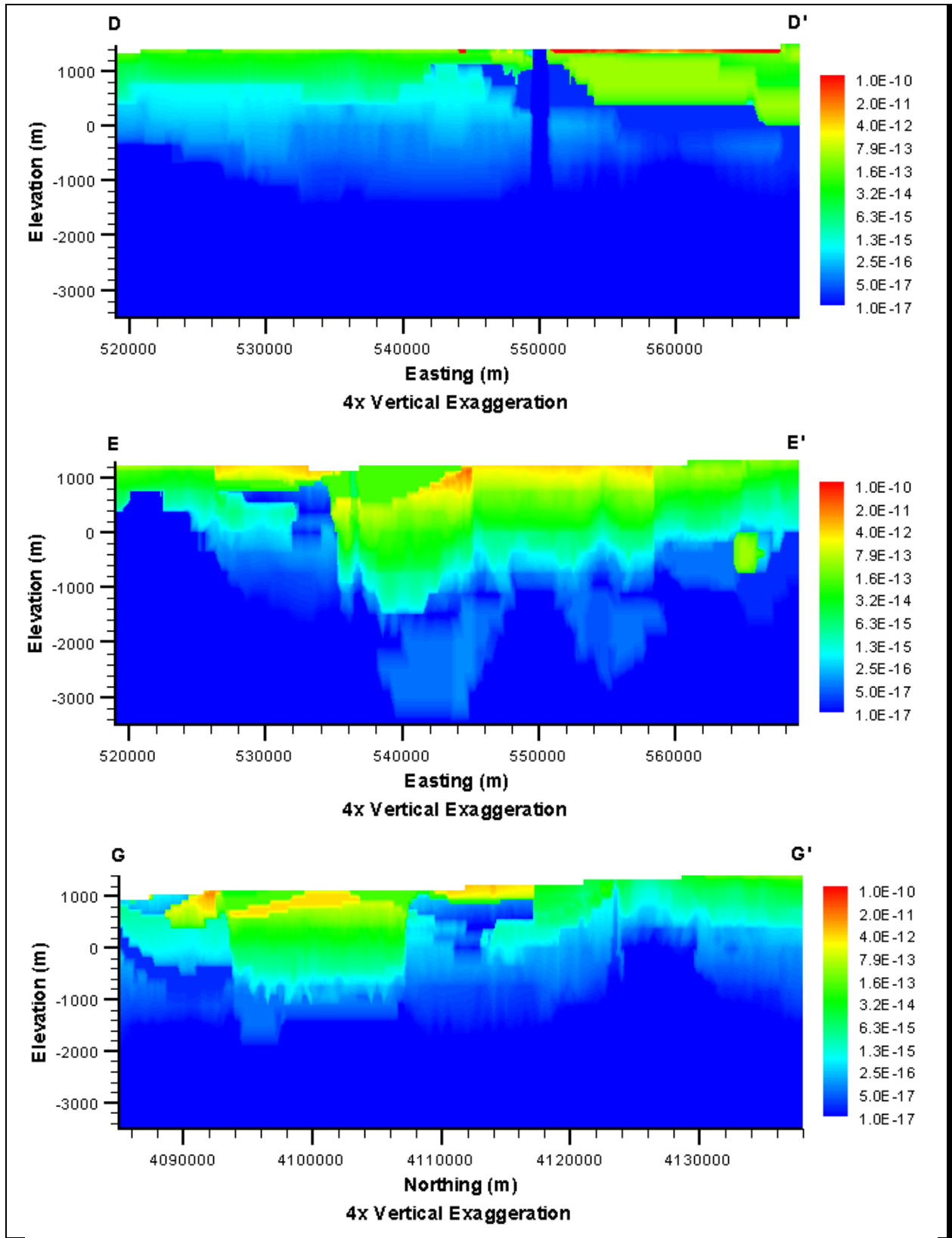


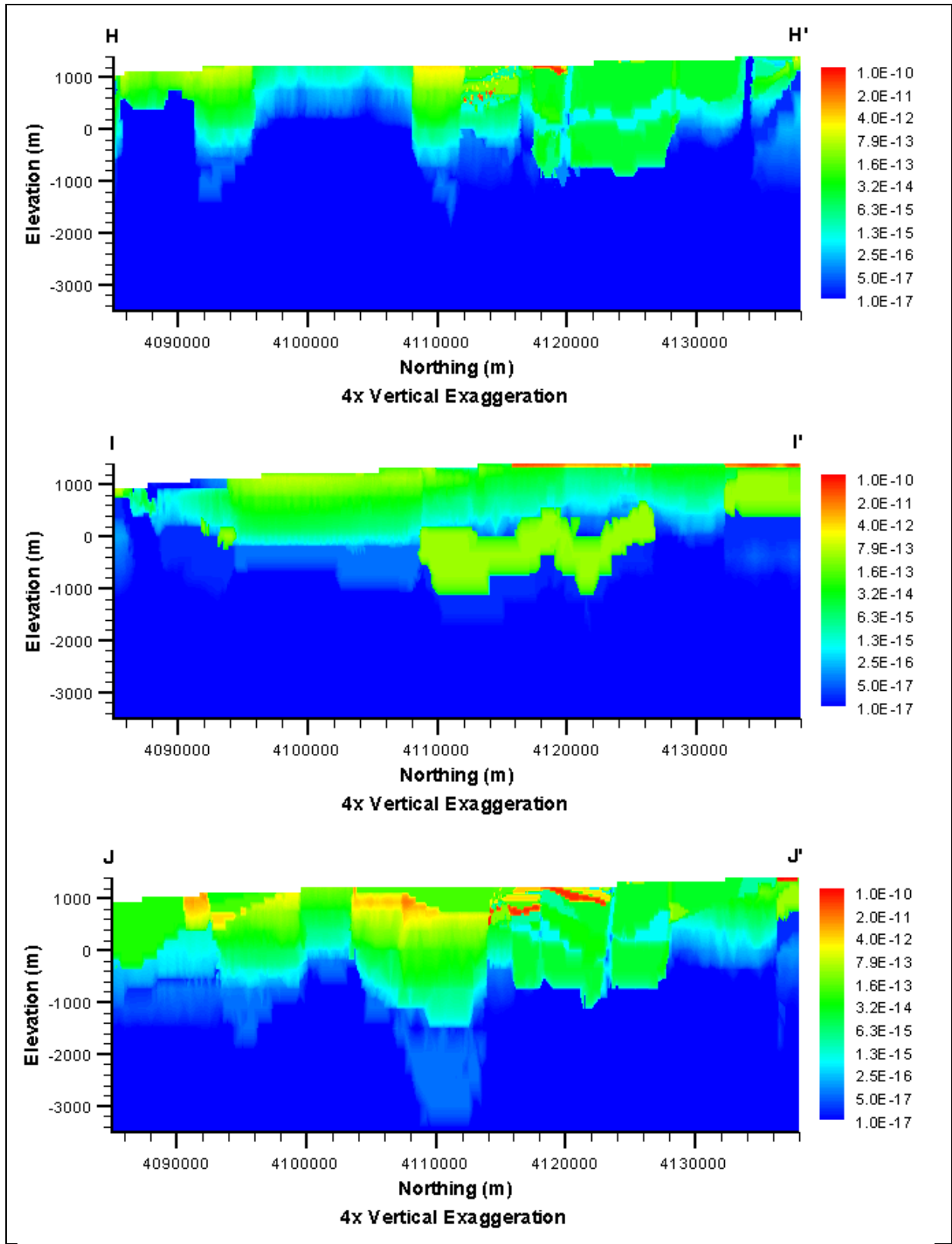




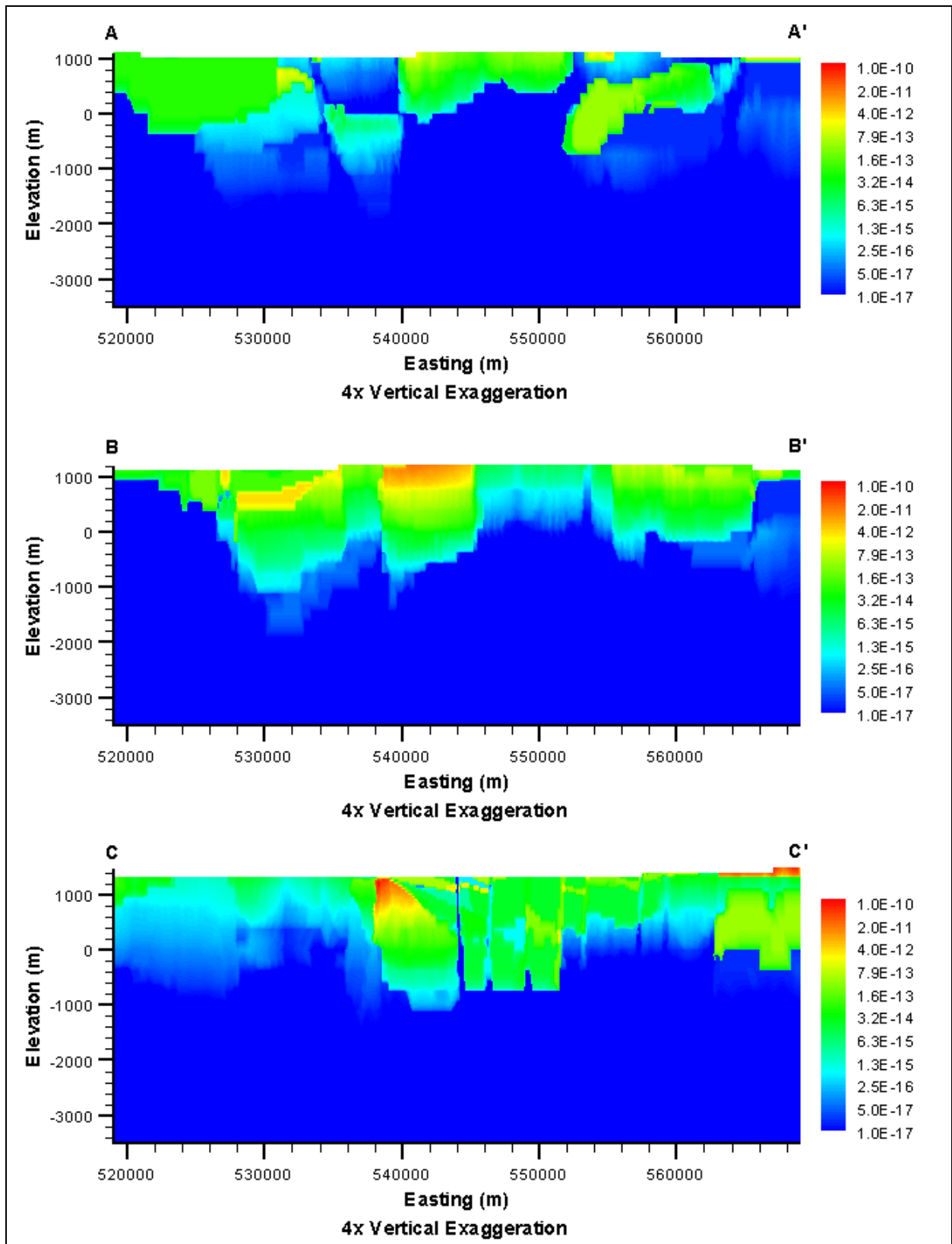
***Basement Ridge Model
(RIDGE-MME-SDA)***

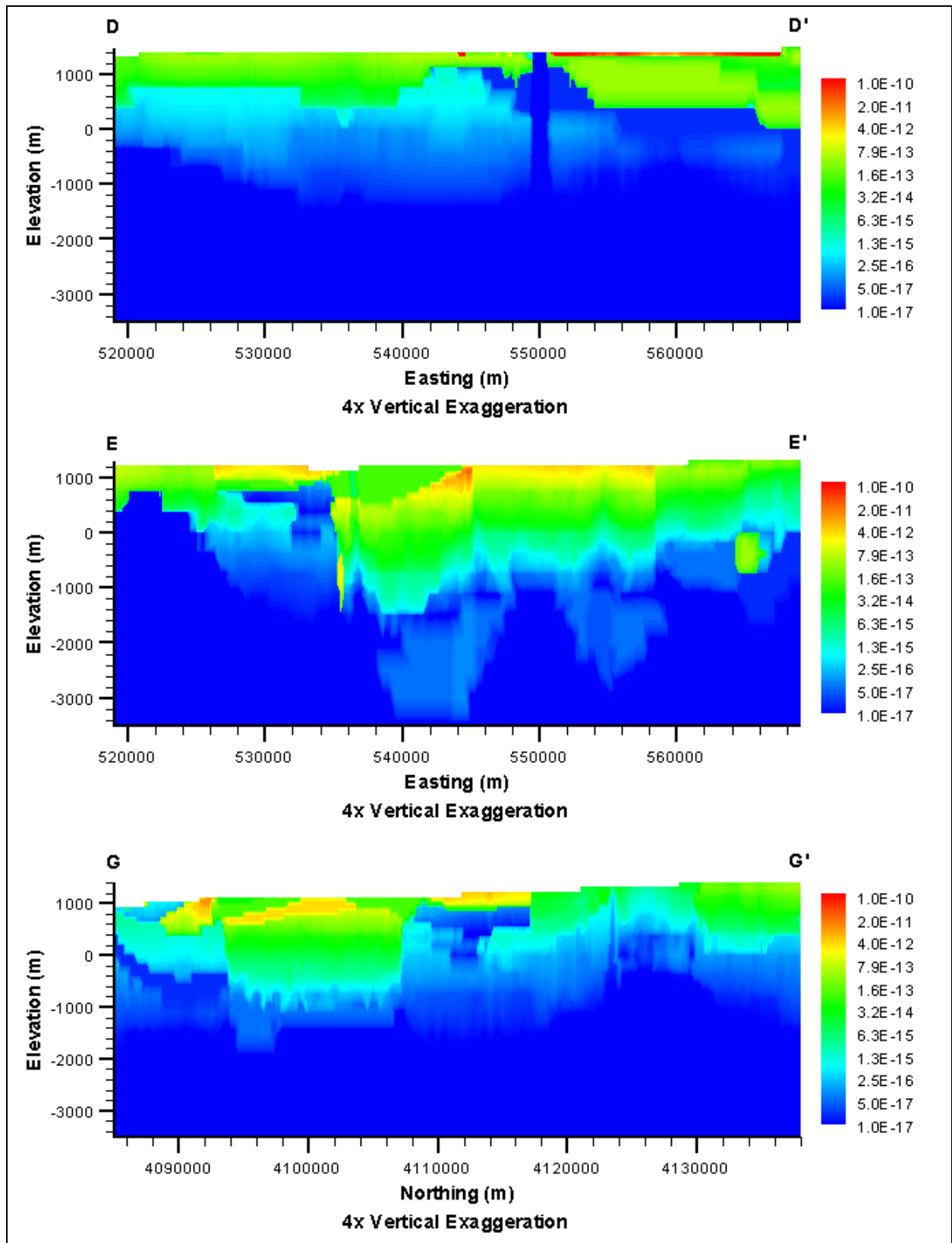


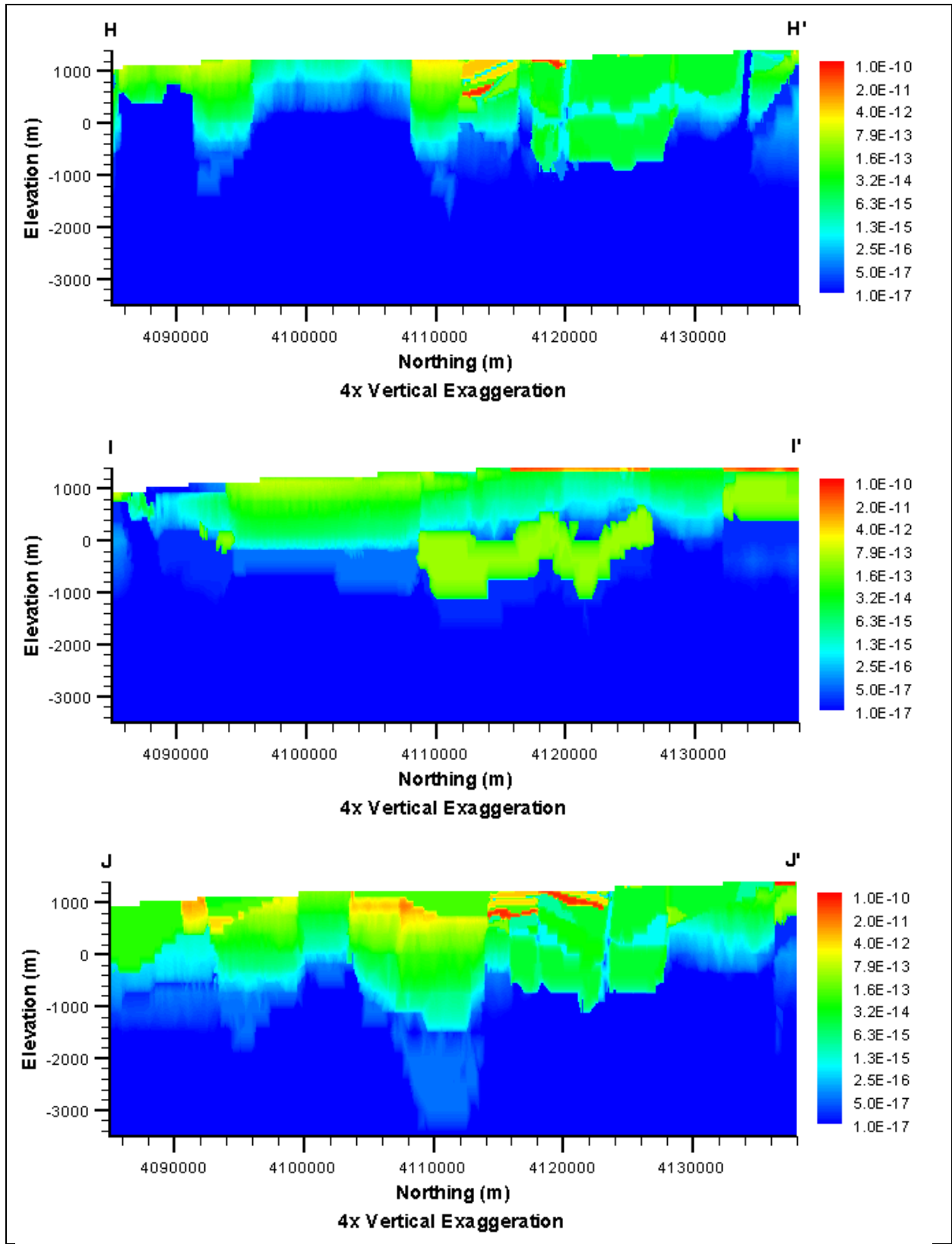




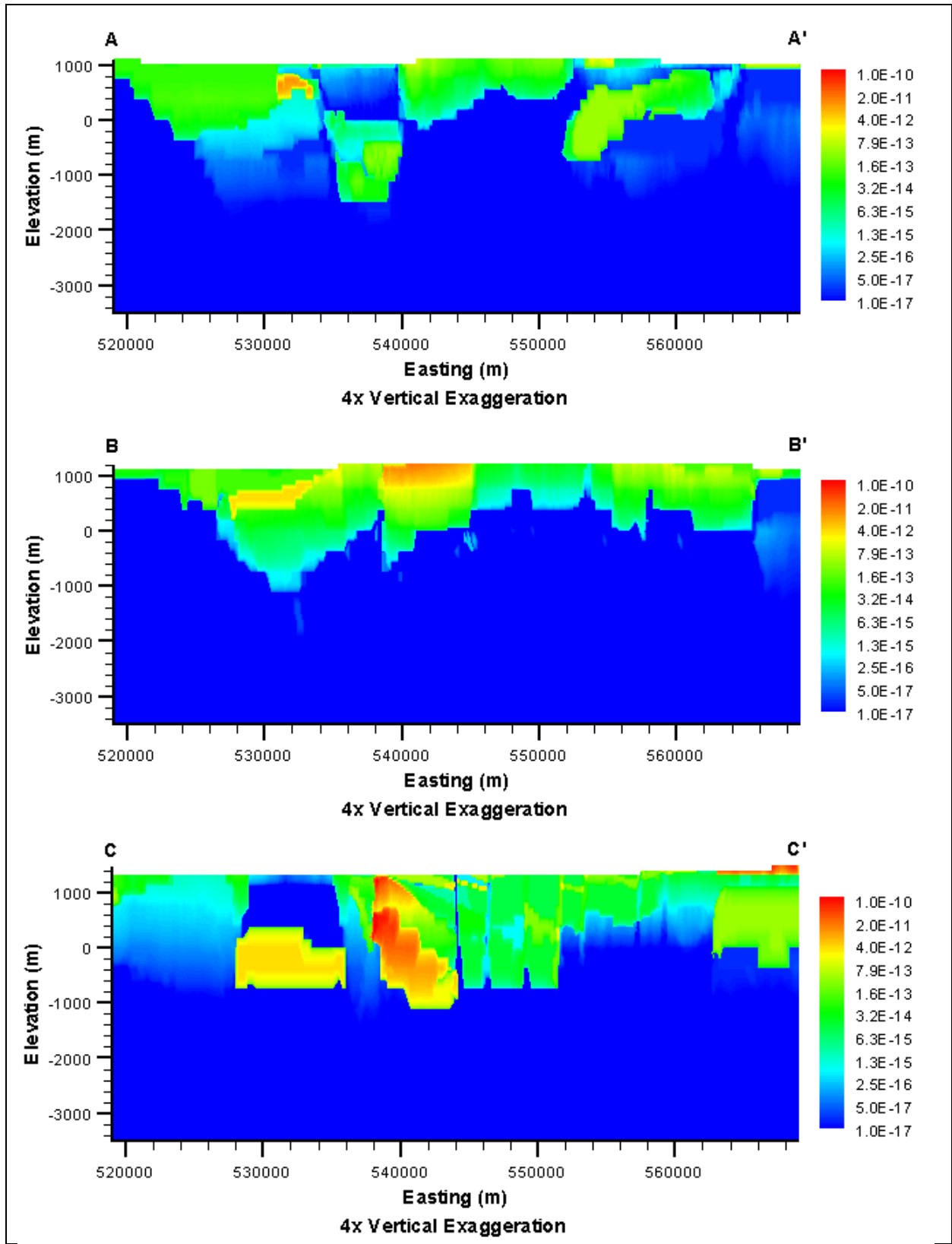
***Thirsty Canyon Lineament
(TCL-MME-SDA)***

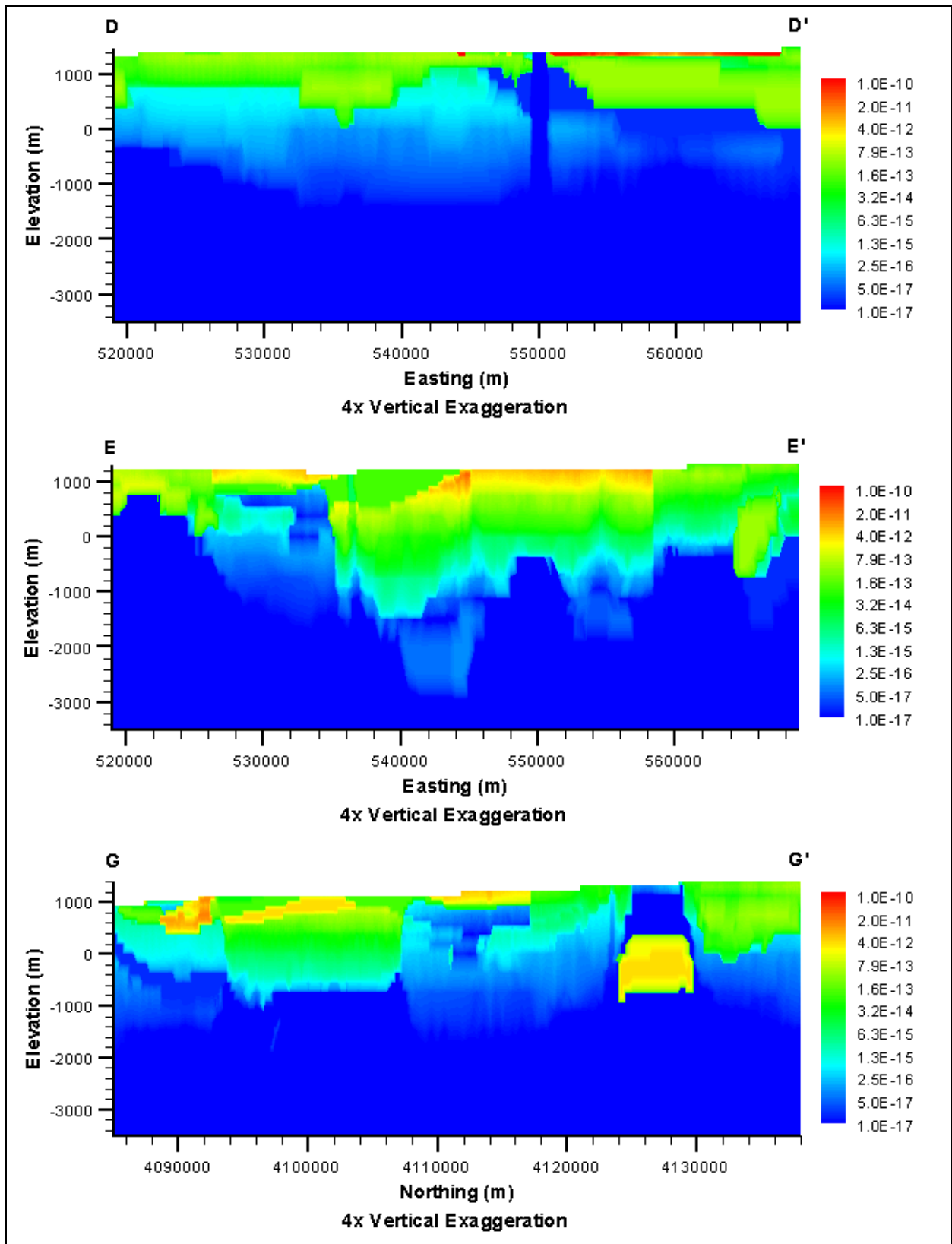


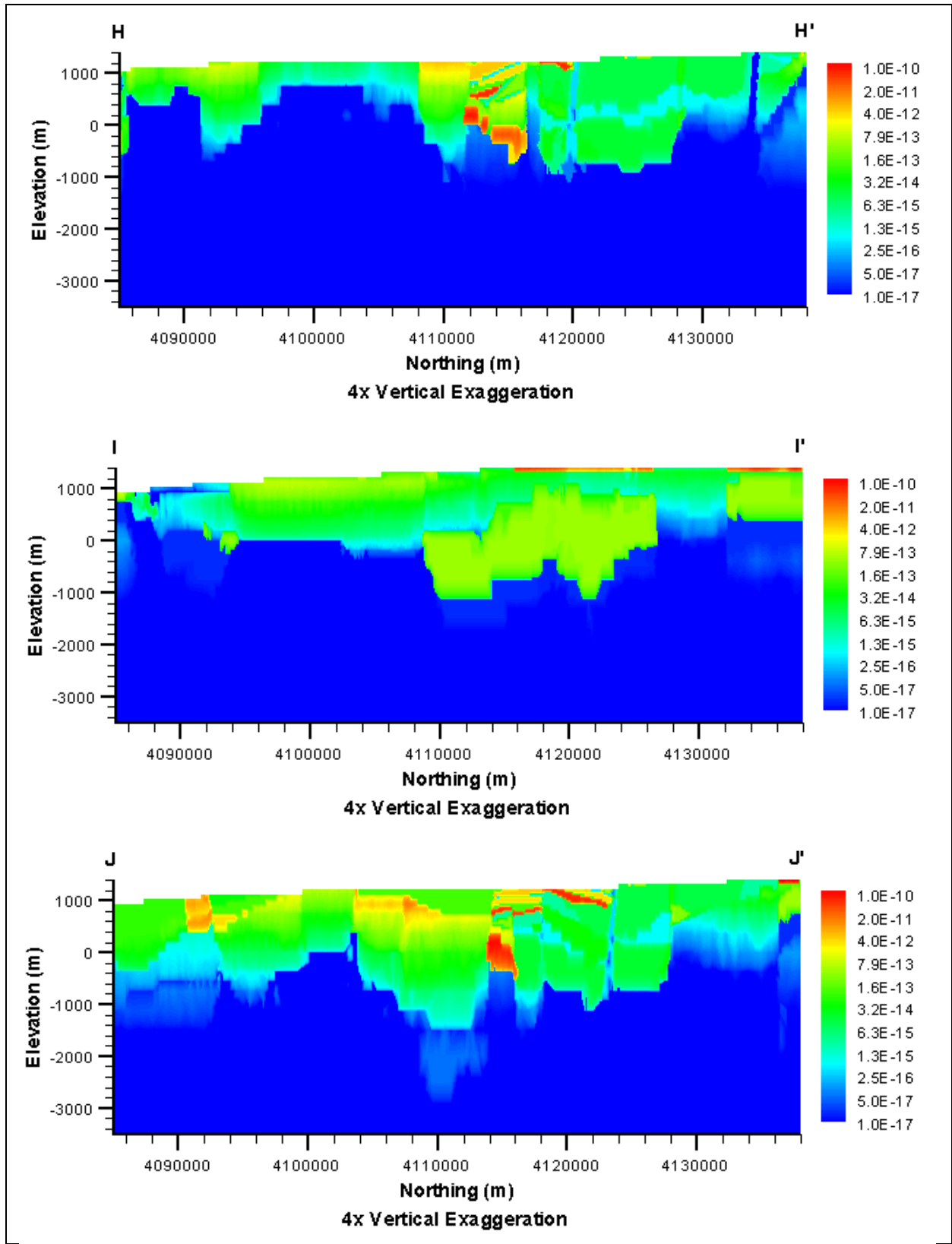




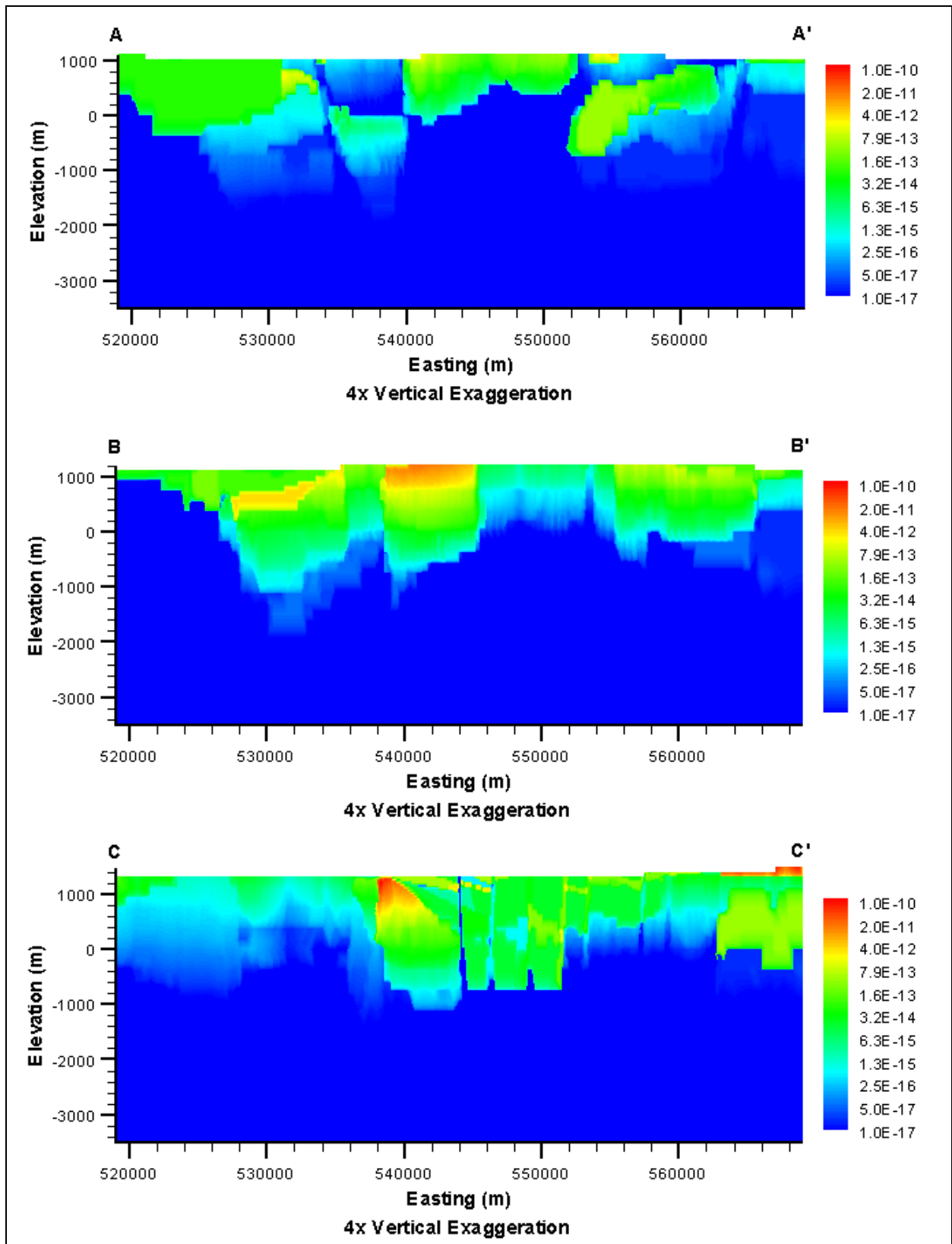
***Raised Pre-Tertiary Surface
(PZUP-MME-SDA)***

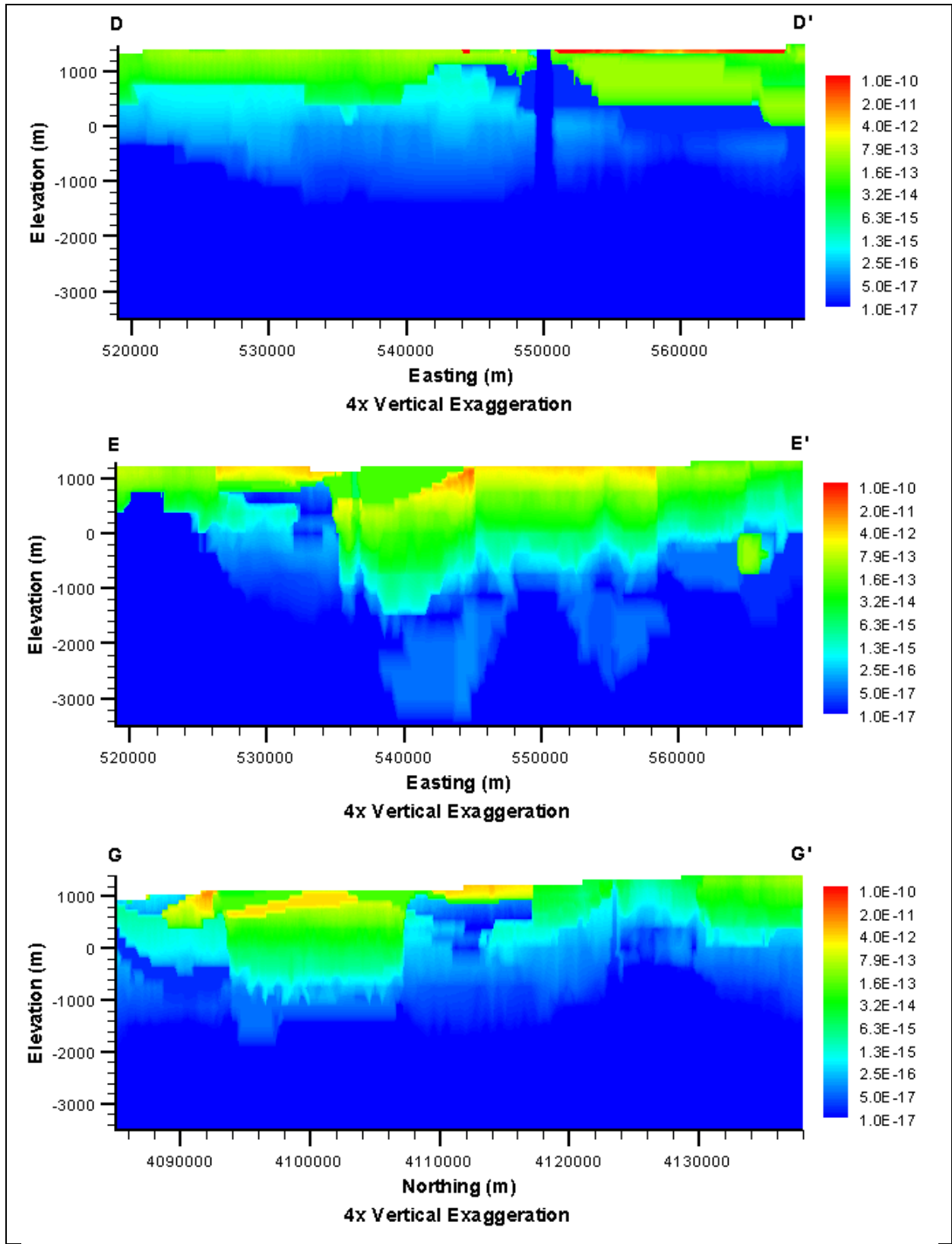


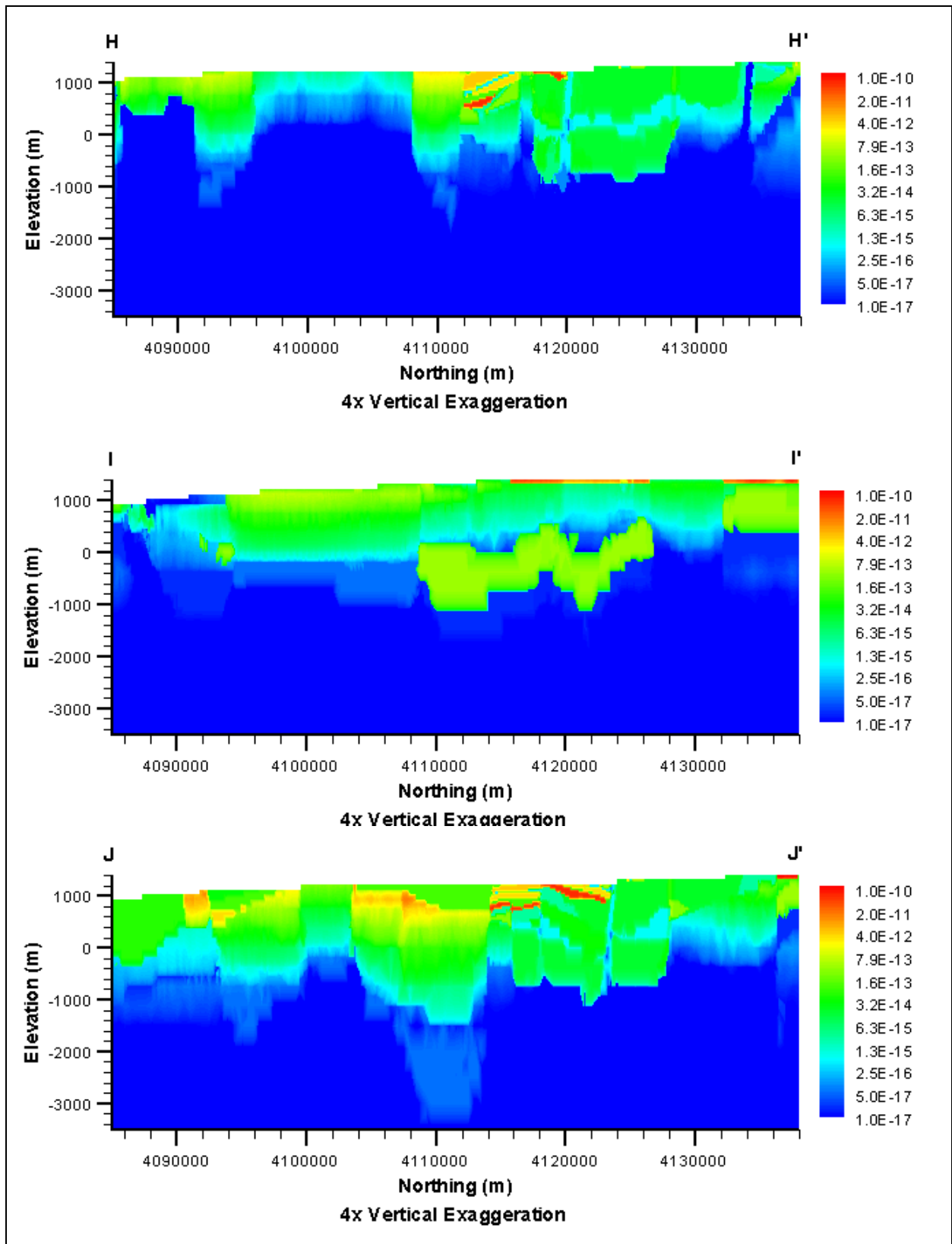




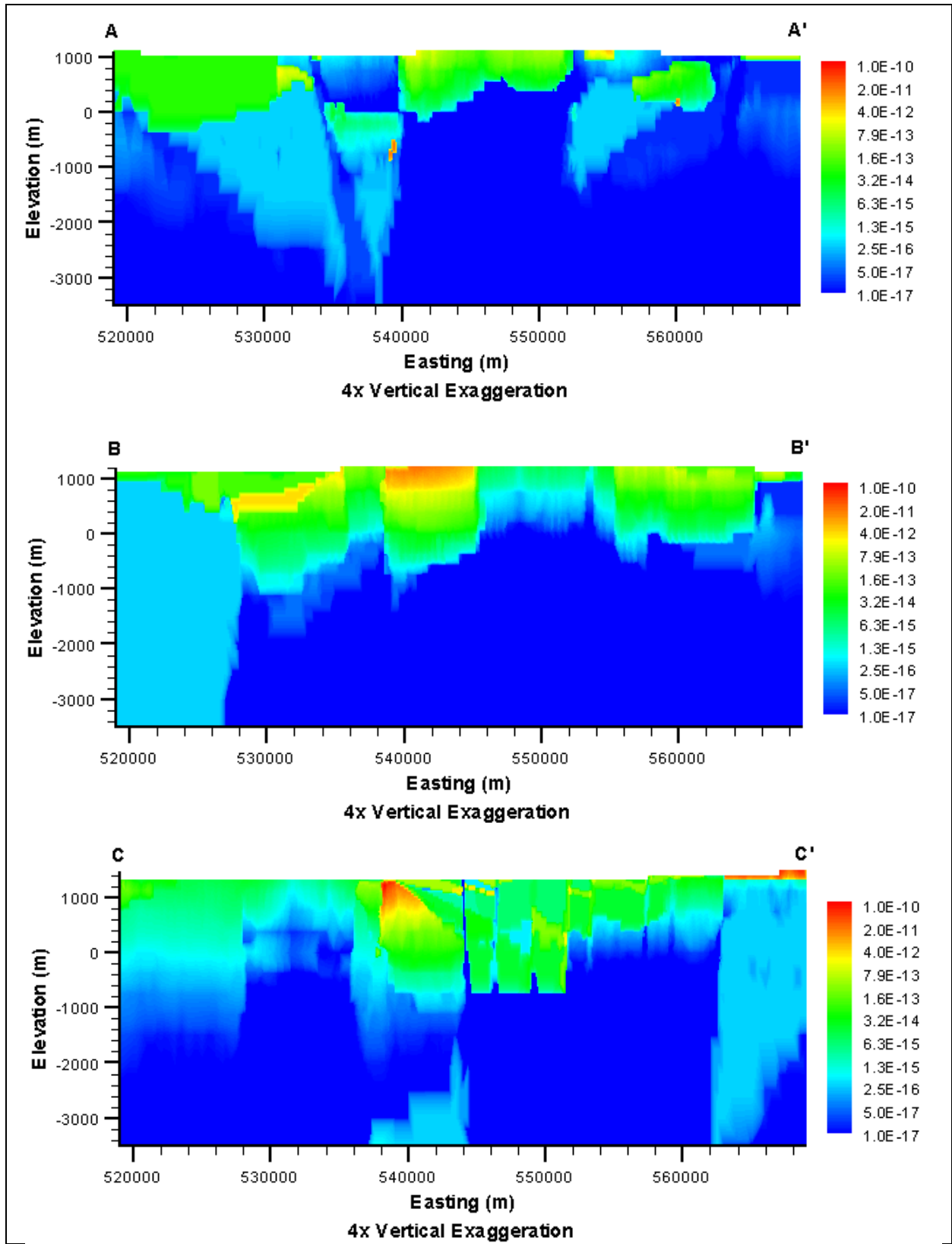
***Contiguous Imbricate Thrust Sheet
(SEPZ-MME-SDA)***

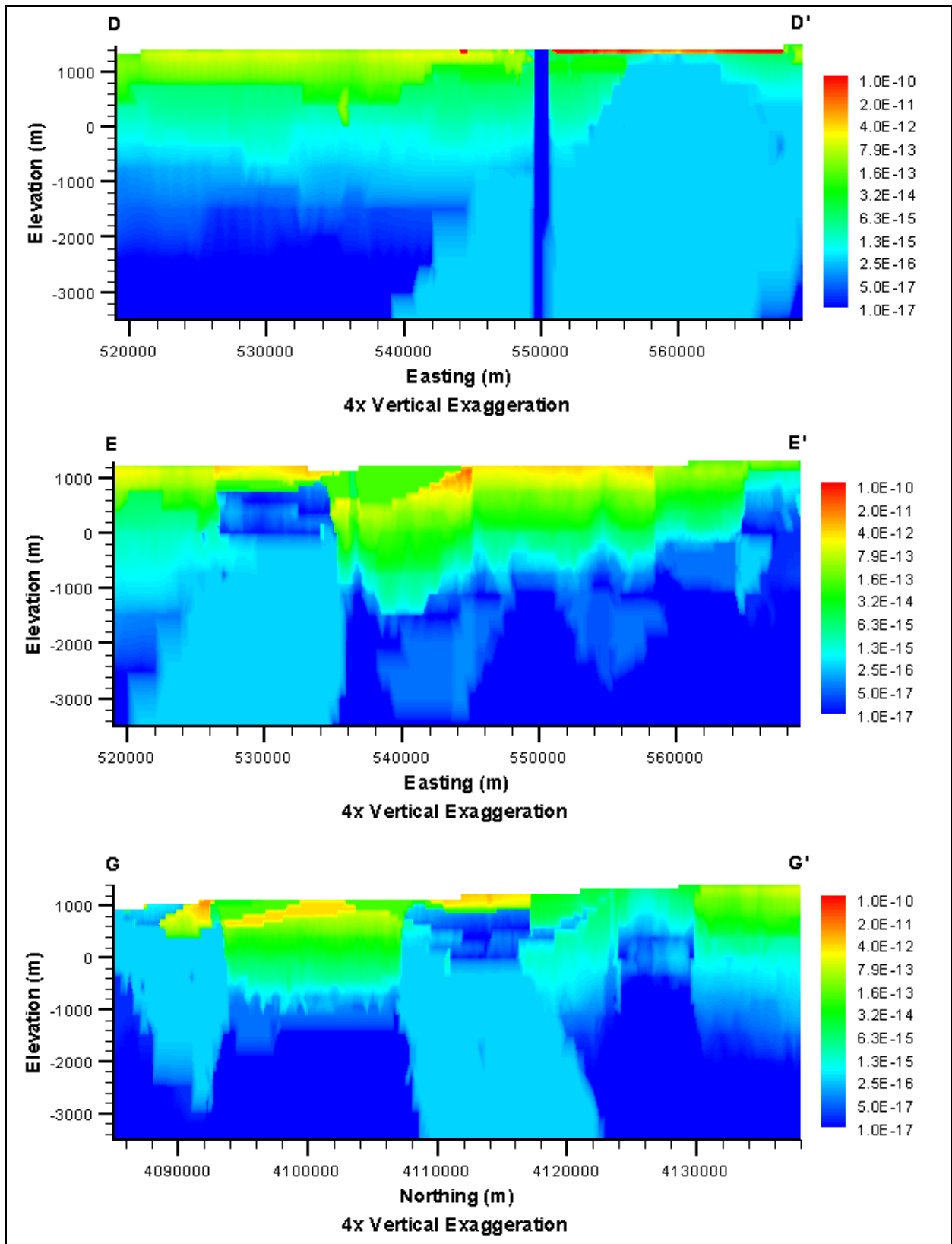


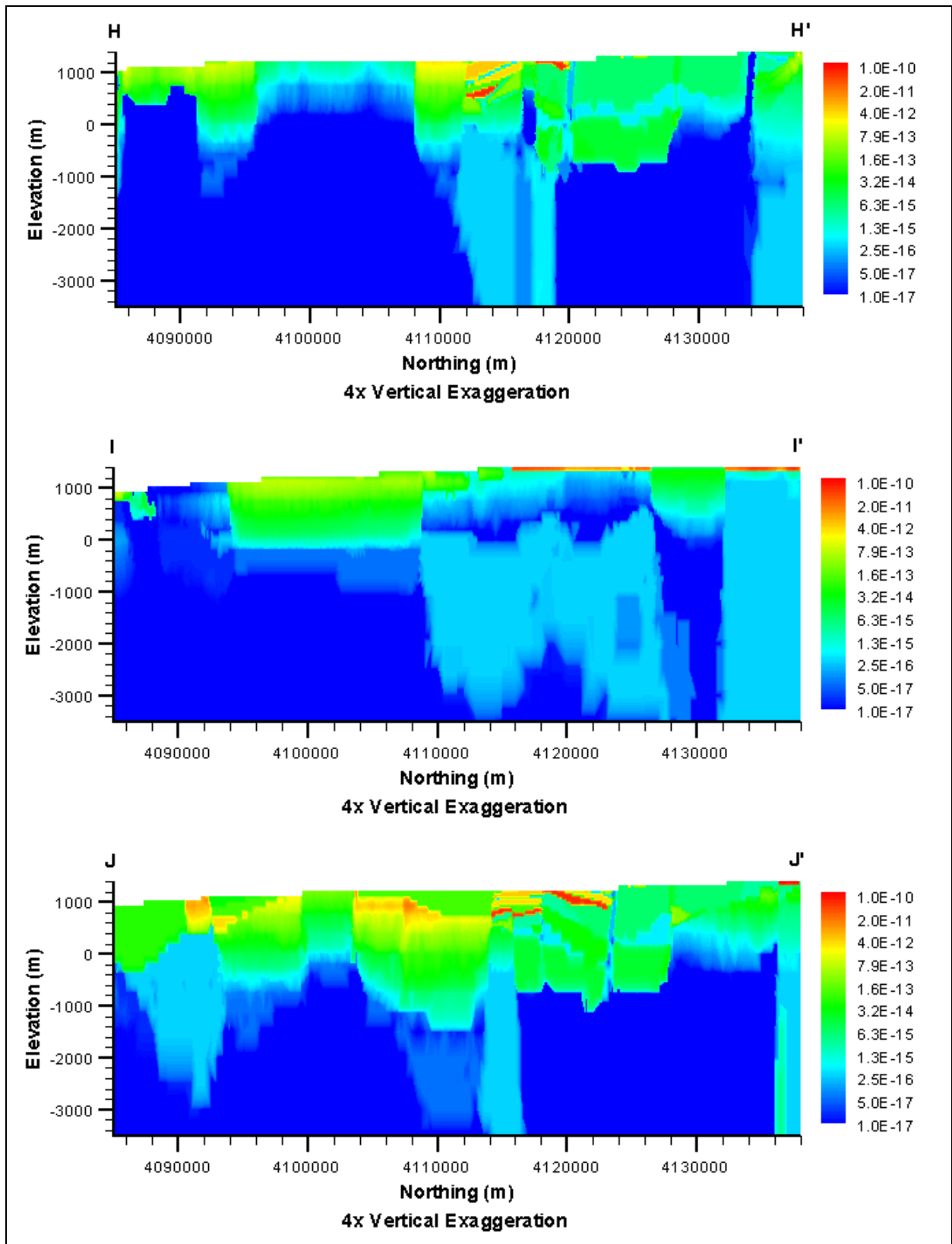




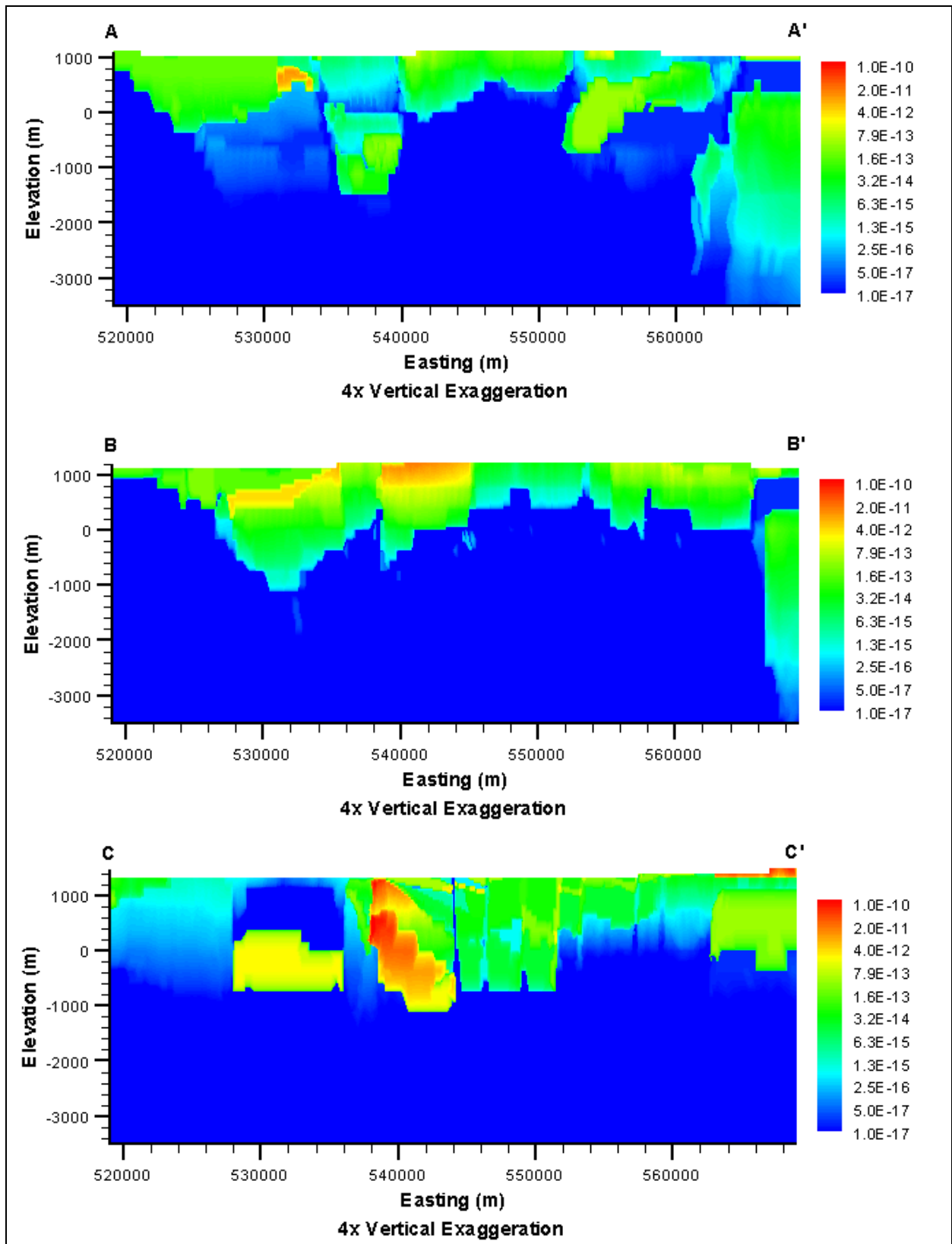
***Deeply Rooted Belted Range Fault Thrust
(DRT-MME-SDA)***

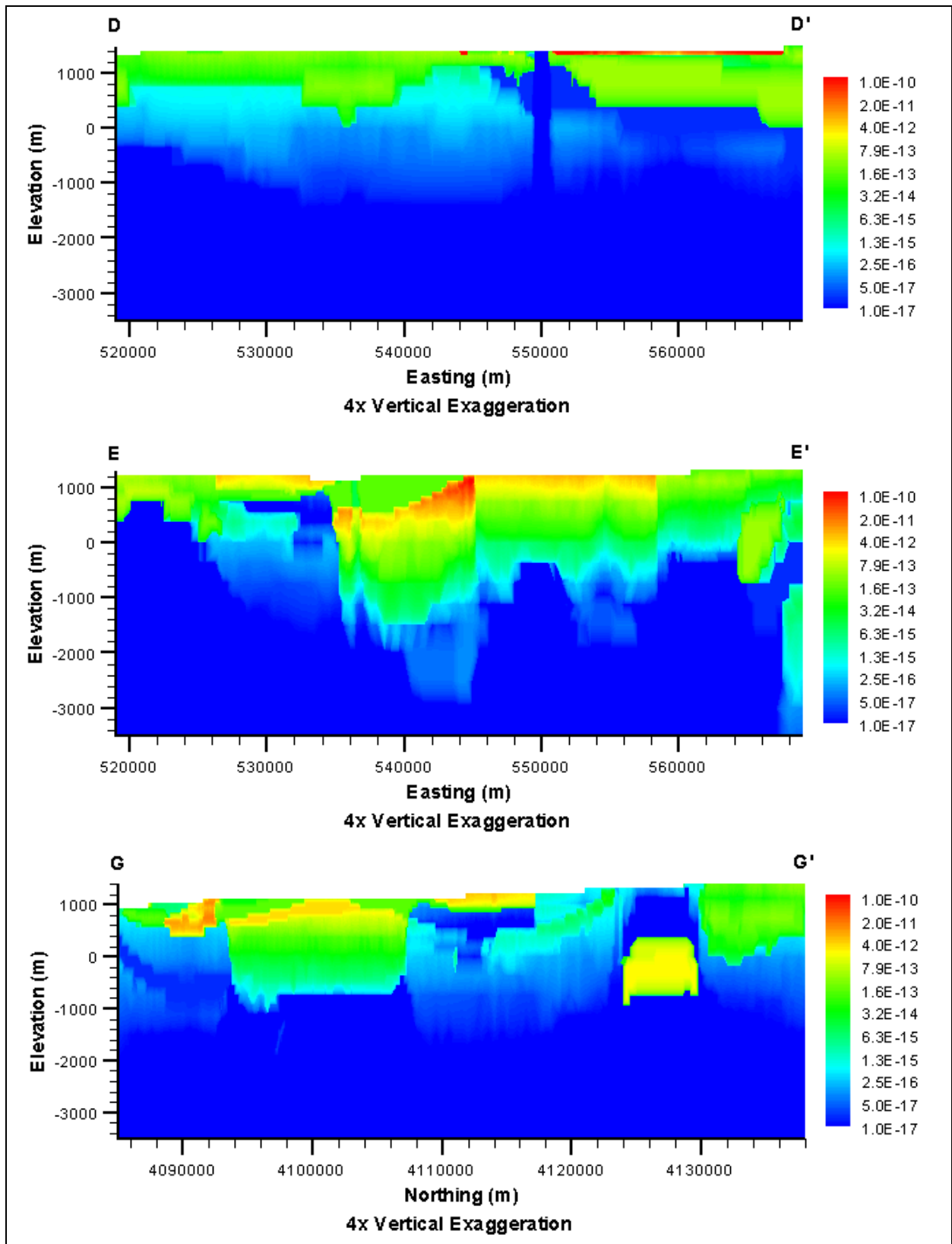


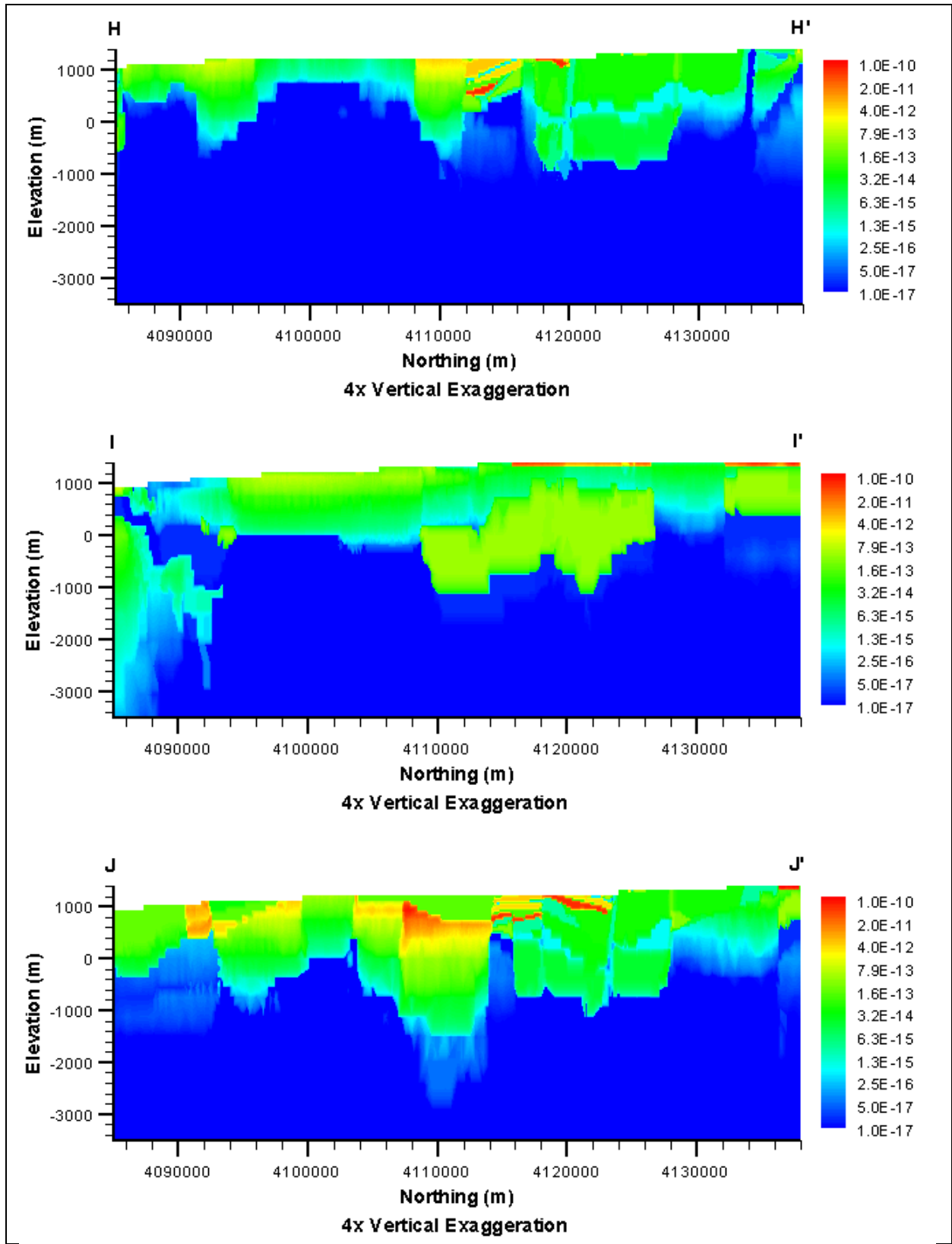




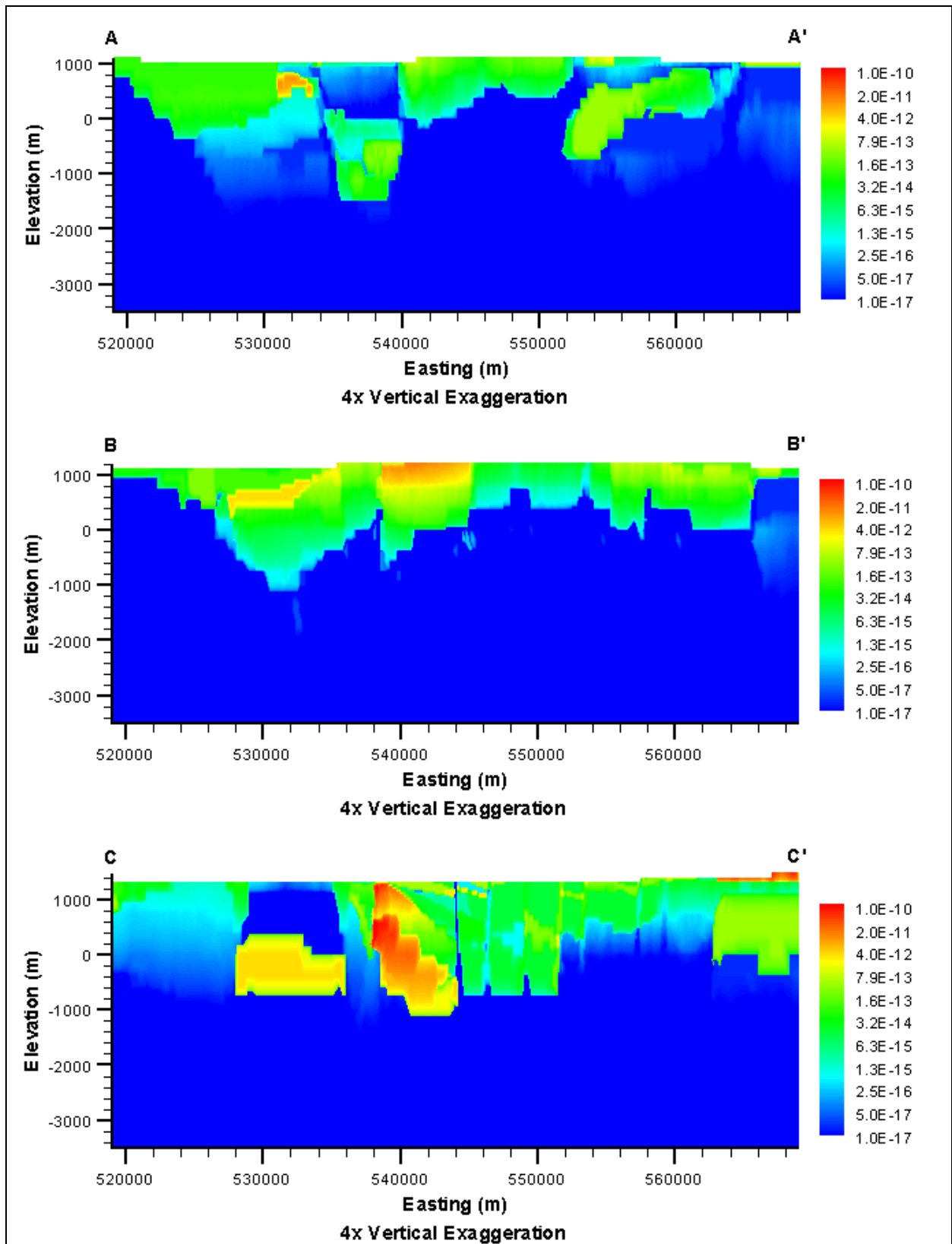
***Raised Pre-Tertiary Surface
(PZUP-DRIA-SDA)***

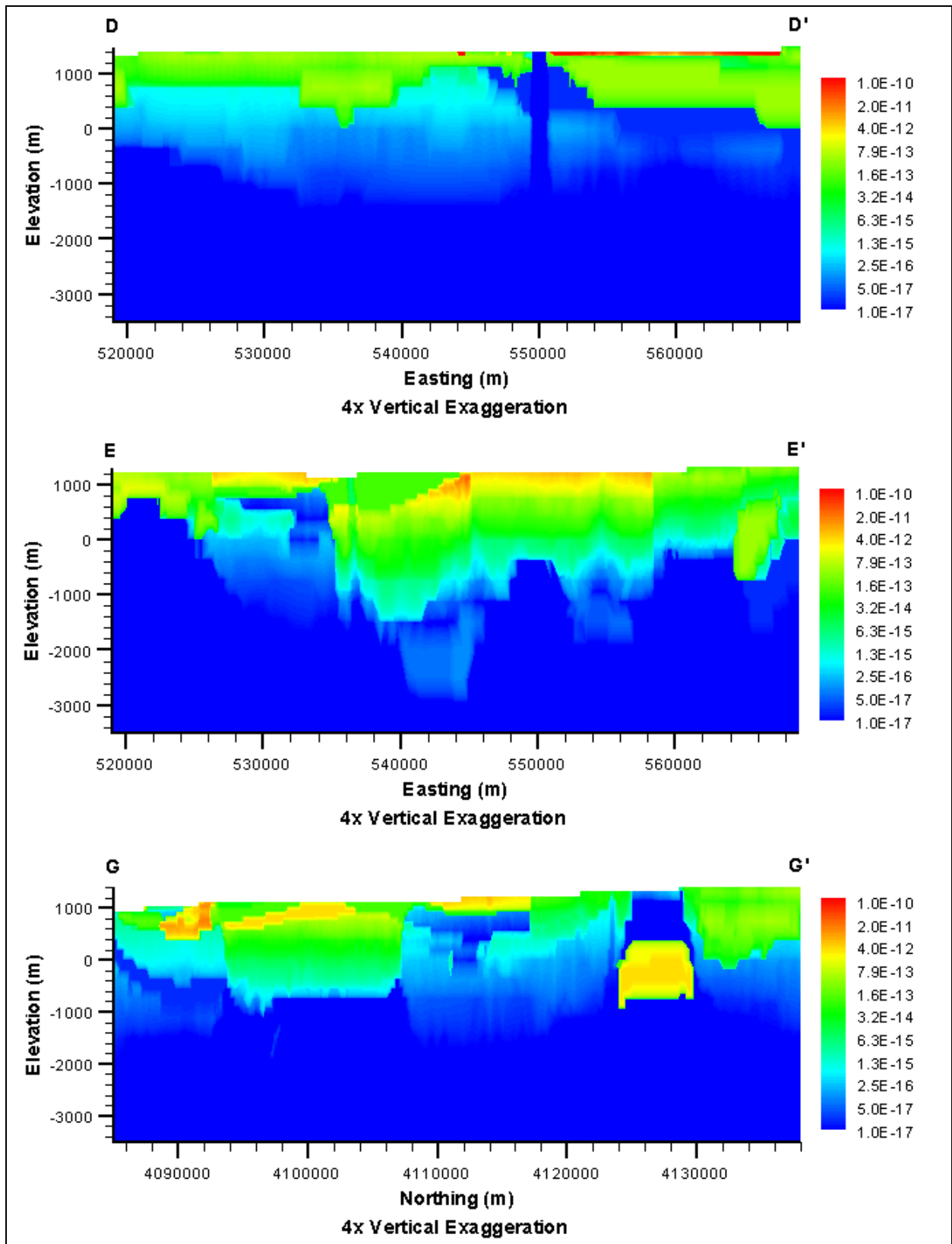


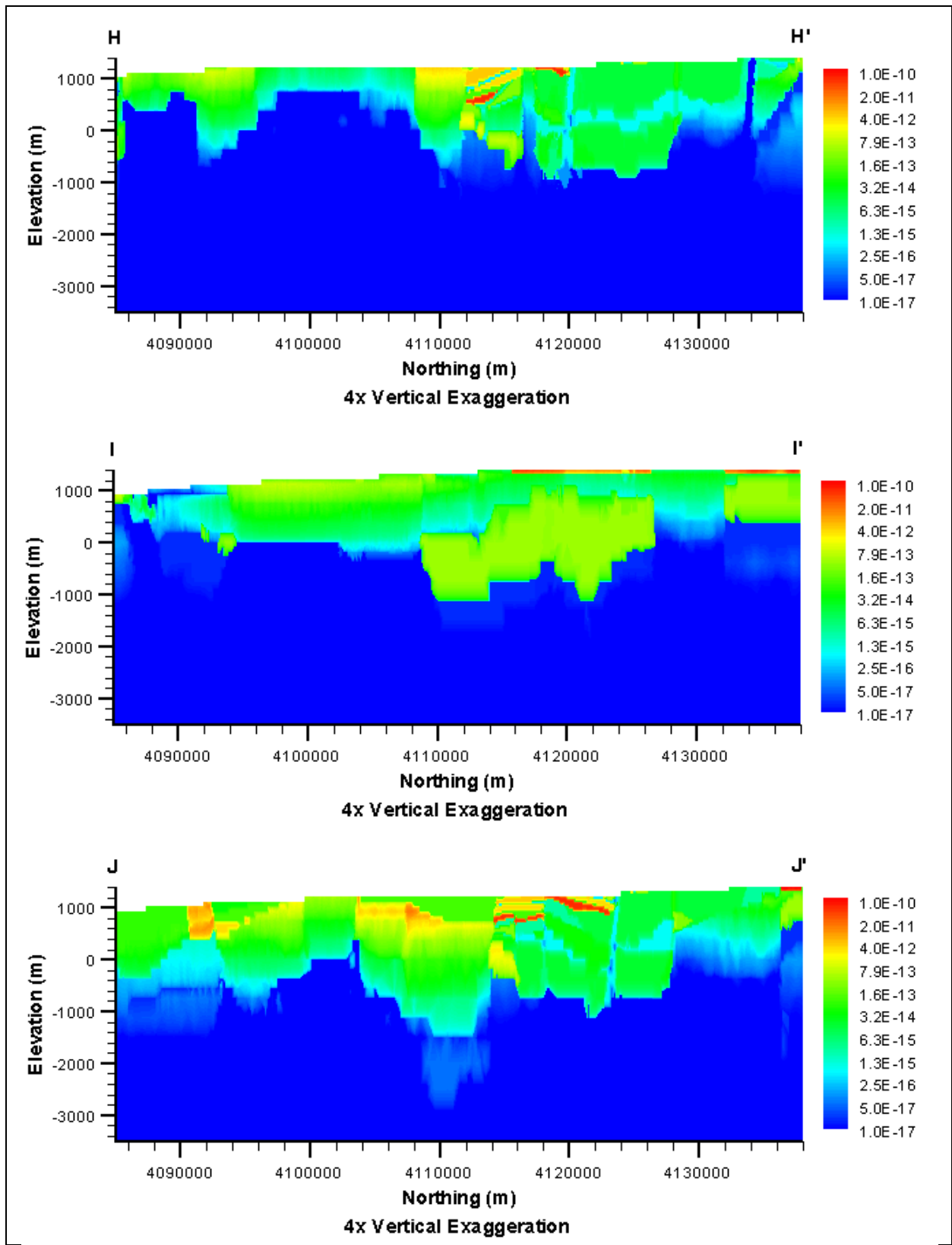




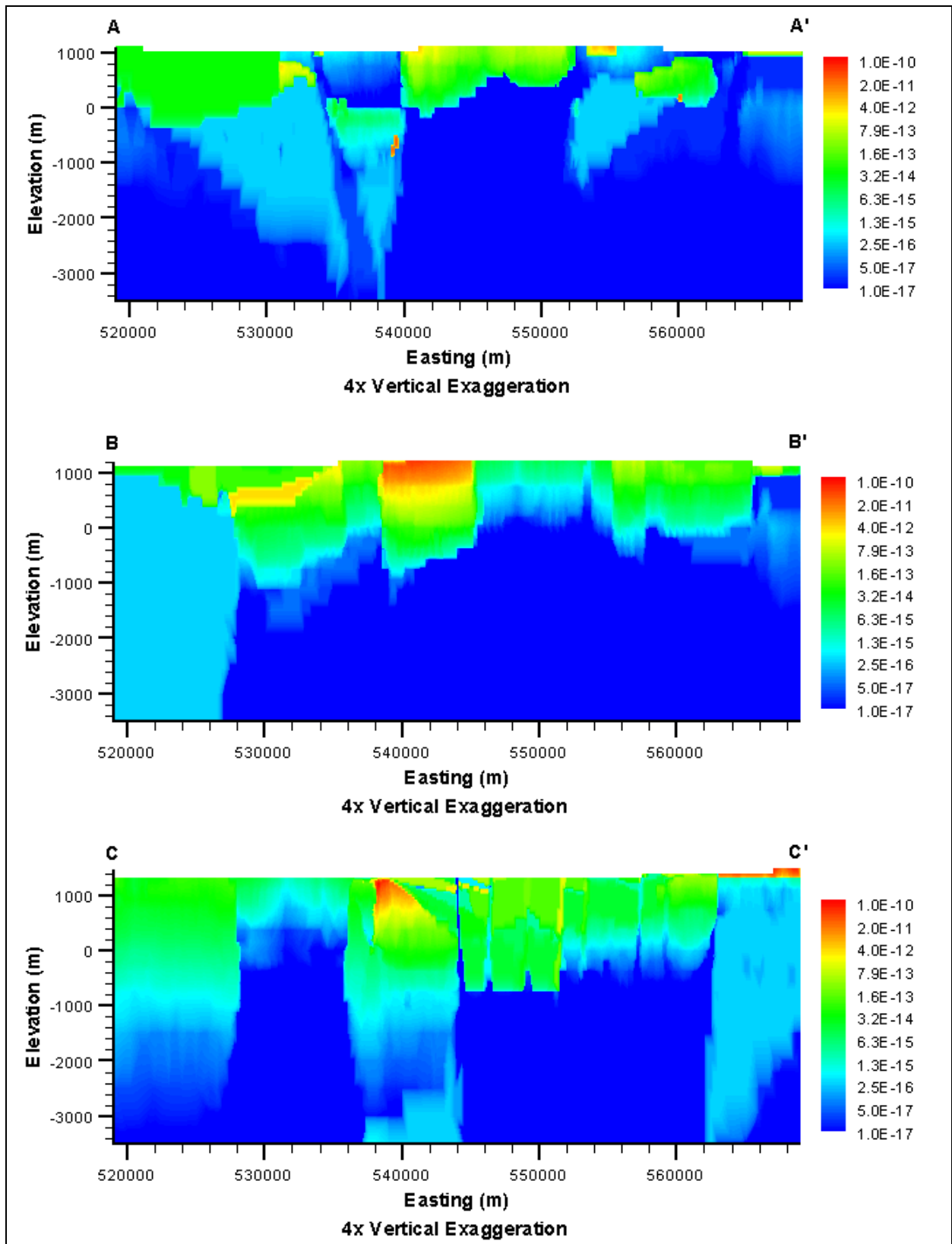
***Raised Pre-Tertiary Surface
(PZUP-USGSD-SDA)***

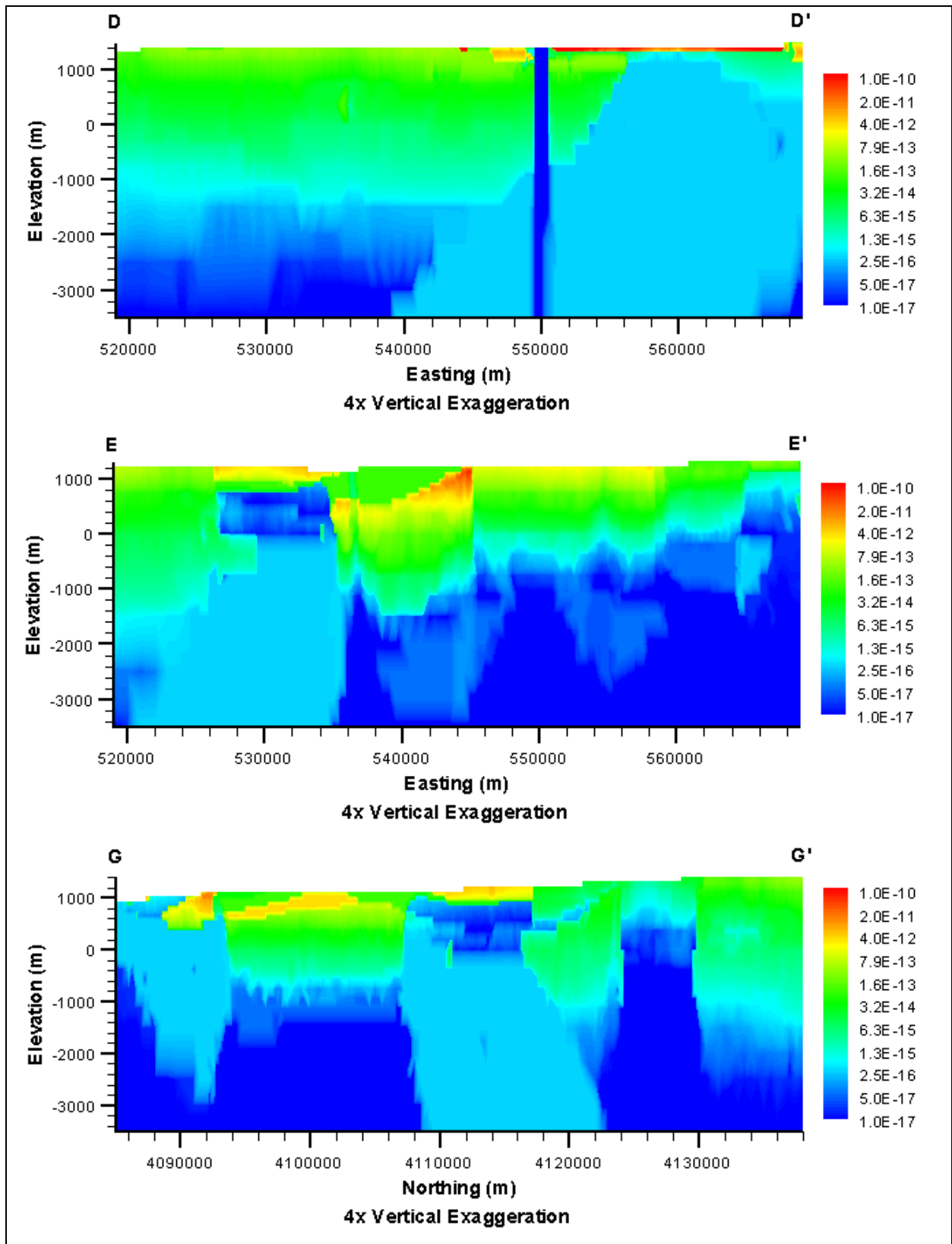


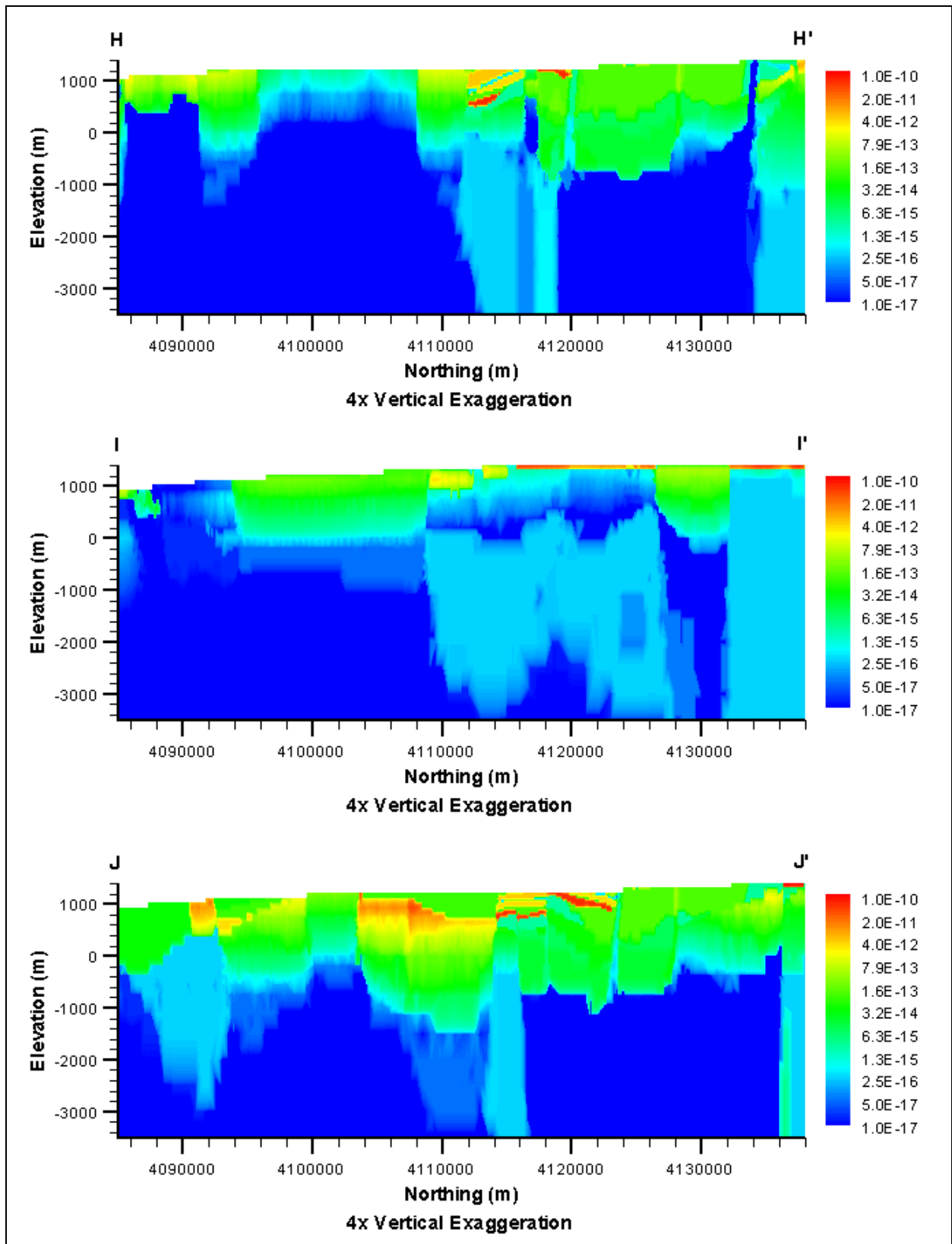




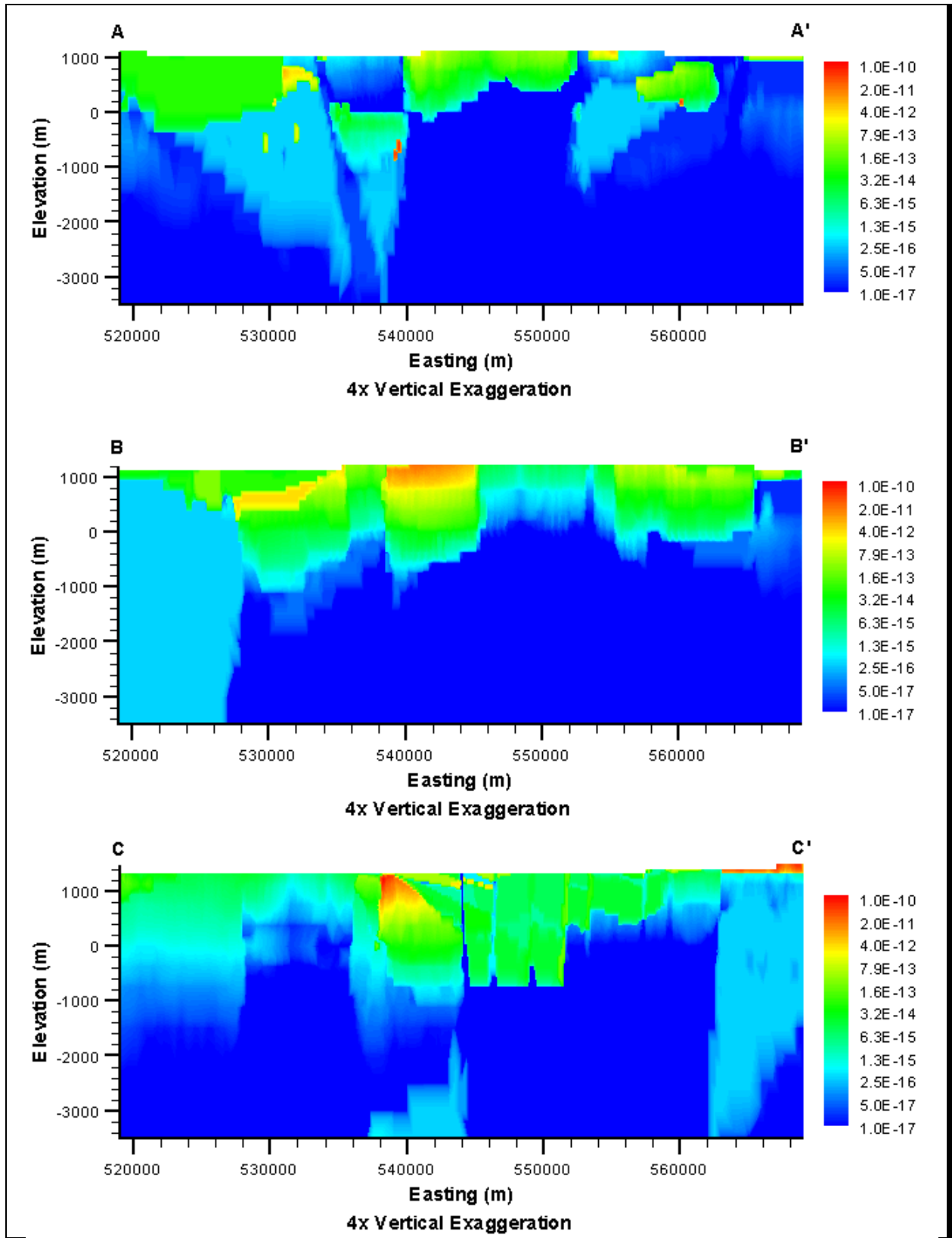
***Deeply Rooted Belted Range Fault Thrust
(DRT-DRIA-SDA)***

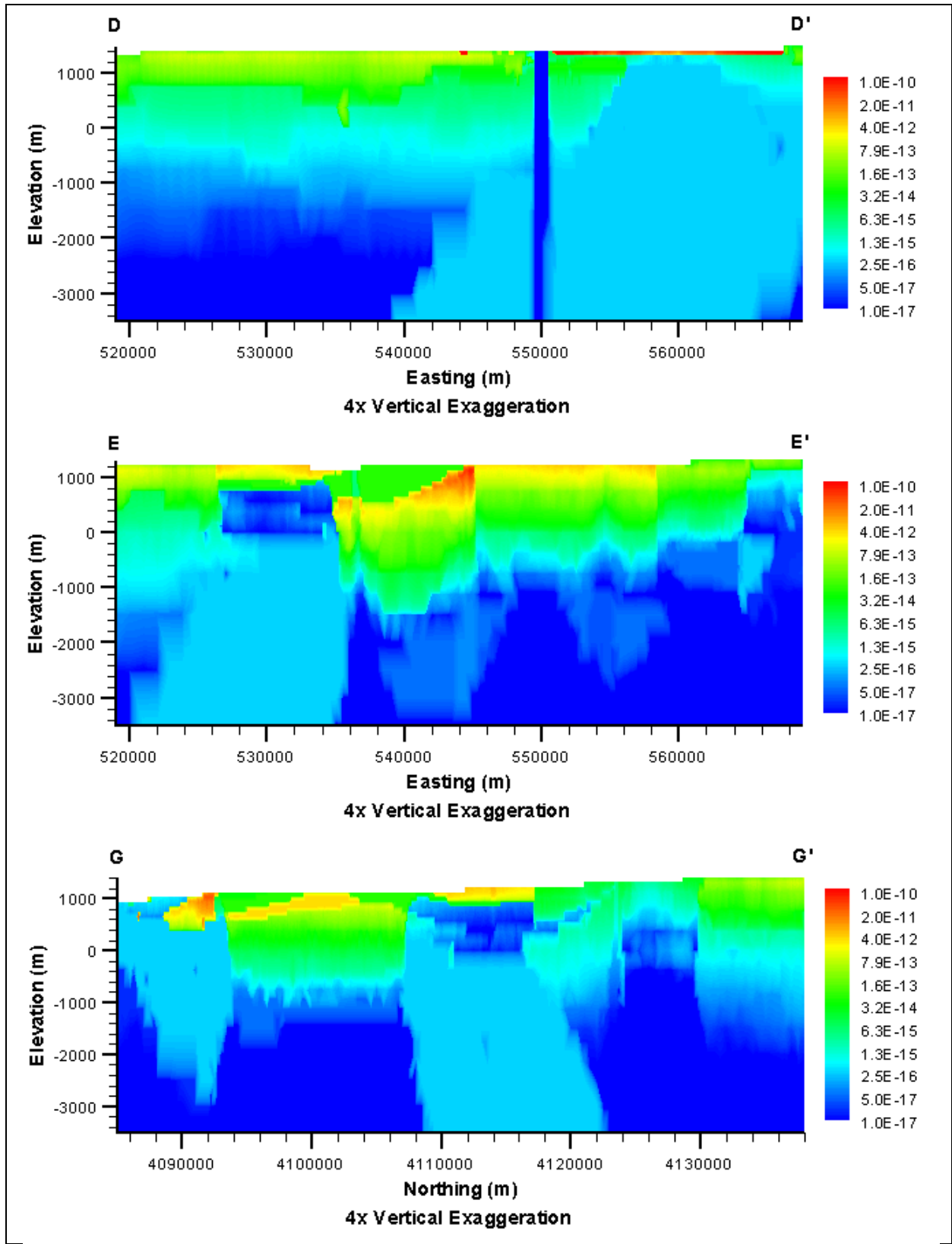


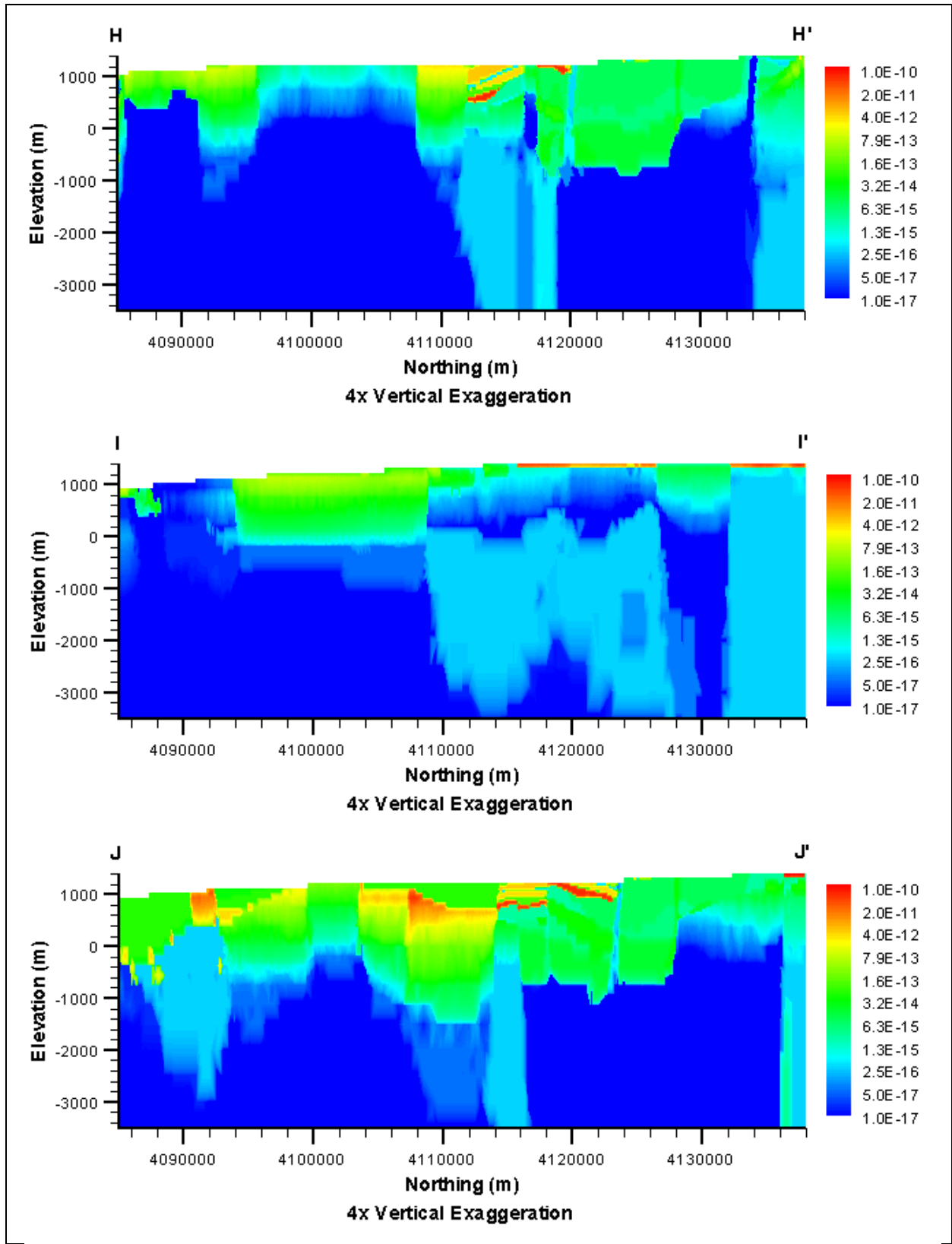




***Deeply Rooted Belted Range Fault Thrust
(DRT-USGSD-SDA)***









Appendix F

Well and Spring Head Calibration Data

F.1.0 INTRODUCTION

This appendix contains summary information on the hydraulic heads, the complete water elevations dataset, and the hydrograph analysis documentation.

F.1.1 Hydraulic Head Summary Data

The hydraulic head summary data discussed in the main text of this document is shown in [Table F.1-1](#). The mean water level elevations shown in [Table F.1-1](#) are the suggested target heads for flow model calibration.

Table F.1-1
Summary of Hydraulic Heads at Selected Sites within the
Pahute Mesa/Oasis Valley Area and Vicinity
 (Page 1 of 11)

Site Name	Mean Hydraulic Head (m amsl) ^a	Minimum Hydraulic Head (m amsl) ^b	Maximum Hydraulic Head (m amsl) ^b	Standard Deviation ^c	Variance on the Mean ^d	Total Uncertainty ^e	Data Points Used	First Measurement ^f	Last Measurement ^g	Comments ^h
Beatty Wash Terrace Well	1,048.77	1,044.85	1,049.44	0.35	0.10	9.39	48	10/13/1984	09/27/2001	—
Beatty Well No 1	996.70	—	—	—	—	—	1	10/26/1962	—	—
Boiling Pot Road Well	1,102.77	1,102.39	1,103.25	0.28	0.09	9.38	42	05/08/1997	06/26/2001	—
Coffer Dune Well	1,181.47	1,181.26	1,181.69	0.12	0.04	2.36	37	04/13/1998	06/26/2001	—
Coffer Lower ET Well	1,175.36	1,174.96	1,176.02	0.31	0.11	2.43	31	08/03/1998	06/26/2001	—
Coffer Middle ET Well	1,174.46	1,173.92	1,175.03	0.36	0.14	2.46	26	01/07/1999	06/26/2001	—
Coffer Windmill Well	1,231.39	—	—	—	—	—	1	07/30/1970	—	—
ER-18-2	1,287.90	1,283.98	1,287.90	—	—	—	1	05/24/1999	06/06/2001	—
ER-19-1-1 (deep)	1,326.01	1,324.55	1,338.67	0.95	0.35	0.35	29	02/03/1994	09/25/2001	—
ER-19-1-2 (middle)	1,498.92	1,468.87	1,533.33	15.75	5.25	5.25	36	02/15/1994	09/25/2001	—
ER-19-1-3 (shallow)	1,564.44	1,564.06	1,566.70	0.2	0.10	0.10	17	02/03/1994	04/11/2001	—
ER-20-1	1,277.68	1,277.55	1,278.94	0.1	0.04	0.04	28	09/18/1992	09/24/2001	—
ER-20-2-1	1,341.04	1,340.42	1,350.20	0.34	0.13	9.42	29	08/03/1993	09/25/2001	—
ER-20-5-1 (3-in. string)	1,275.54	1,275.13	1,276.43	0.38	0.18	0.18	17	11/17/1995	05/14/1996	—
ER-20-6-1 (3-in. string)	1,356.61	1,354.78	1,359.25	0.07	0.04	0.04	10	03/21/1996	03/20/2001	—
ER-20-6-2 (3-in. string)	1,356.62	1,354.29	1,356.64	0.03	0.03	0.03	4	04/01/1996	03/20/2001	—
ER-20-6-3 (3-in. string)	1,356.50	1,355.25	1,356.58	0.08	0.05	0.05	11	04/16/1996	09/24/2001	—
ER-30-1	1,280.06	1,280.01	1,280.13	0.05	0.03	0.03	9	06/21/1994	06/24/1994	—

Table F.1-1
Summary of Hydraulic Heads at Selected Sites within the
Pahute Mesa/Oasis Valley Area and Vicinity
 (Page 2 of 11)

Site Name	Mean Hydraulic Head (m amsl) ^a	Minimum Hydraulic Head (m amsl) ^b	Maximum Hydraulic Head (m amsl) ^b	Standard Deviation ^c	Variance on the Mean ^d	Total Uncertainty ^e	Data Points Used	First Measurement ^f	Last Measurement ^g	Comments ^h
ER-EC-1	1,271.08	1,270.98	1,271.81	0.02	0.01	0.04	8	05/10/1999	09/24/2001	—
ER-EC-2A (498.3-681.5 m)	1,264.22	1,263.06	1,264.24	0.03	0.04	0.07	2	02/18/2000	03/26/2001	—
ER-EC-2A (498.35-1515.8 m)	1,266.26	1,260.14	1,266.36	0.10	0.12	0.14	3	02/18/2000	08/07/2000	—
ER-EC-4 (290.2-1062.8 m)	1,222.46	1,222.40	1,222.48	0.02	0.02	0.04	4	07/18/1999	08/24/2000	—
ER-EC-4 (290.2-699.5 m)	1,222.50	1,222.49	1,222.53	0.02	0.02	0.04	5	10/05/2000	10/03/2001	—
ER-EC-4 (Lower Interval)	1,220.17	—	—	—	—	—	1	02/16/2000	—	—
ER-EC-5	1,237.55	1,237.34	1,237.62	0.05	0.04	0.06	7	07/19/1999	03/26/2001	—
ER-EC-6 (481.9-1164.3 m)	1,273.53	1,273.50	1,273.55	0.02	0.02	0.04	6	06/06/2000	09/24/2001	—
ER-EC-6 (481.9-1524 m)	1,273.60	1,273.58	1,274.25	0.01	0.01	0.03	4	04/20/1999	03/13/2000	—
ER-EC-7	1,236.67	1,236.46	1,236.76	0.1	0.08	0.10	7	08/30/1999	03/26/2001	—
ER-EC-8	1,222.36	1,222.24	1,222.43	0.05	0.04	0.06	8	08/04/1999	10/03/2001	—
ER-OV-01	1,235.86	1,235.61	1,236.48	0.02	0.01	0.03	17	10/02/1997	09/13/2001	—
ER-OV-02	1,174.04	1,173.67	1,174.10	0.05	0.02	0.05	17	10/02/1997	09/13/2001	—
ER-OV-03a	1,154.35	1,154.13	1,154.54	0.13	0.07	0.09	16	10/02/1997	09/13/2001	—
ER-OV-03a2	1,122.86	1,122.48	1,123.01	0.09	0.04	0.07	17	10/02/1997	09/13/2001	—
ER-OV-03a3	1,154.24	1,154.08	1,154.44	0.13	0.06	0.09	17	10/02/1997	09/13/2001	—
ER-OV-03b	1,184.52	1,184.29	1,184.61	0.07	0.03	0.06	17	10/02/1997	09/13/2001	—
ER-OV-03c	1,212.28	1,211.97	1,212.33	0.04	0.02	0.04	17	10/02/1997	09/13/2001	—

Table F.1-1
Summary of Hydraulic Heads at Selected Sites within the
Pahute Mesa/Oasis Valley Area and Vicinity
 (Page 3 of 11)

Site Name	Mean Hydraulic Head (m amsl) ^a	Minimum Hydraulic Head (m amsl) ^b	Maximum Hydraulic Head (m amsl) ^b	Standard Deviation ^c	Variance on the Mean ^d	Total Uncertainty ^e	Data Points Used	First Measurement ^f	Last Measurement ^g	Comments ^h
ER-OV-03c2	1,212.31	1,211.98	1,212.41	0.04	0.02	0.04	23	10/02/1997	09/13/2001	—
ER-OV-04a	1,056.85	1,056.36	1,057.02	0.12	0.06	0.08	17	10/02/1997	09/13/2001	—
ER-OV-05	1,190.50	1,190.19	1,190.52	0.02	0.01	0.03	17	10/02/1997	09/13/2001	—
ER-OV-06a	1,236.82	1,236.76	1,236.99	0.03	0.01	0.03	27	10/02/1997	09/13/2001	—
ER-OV-06a2	1,235.64	1,235.41	1,235.67	0.03	0.01	0.04	17	10/02/1997	09/13/2001	—
Gexa Well 4	1,010.05	954.99	1,010.10	—	—	—	1	09/01/1989	03/14/1996	—
Hagestad 1	1,841.84	1,802.13	1,843.77	1.48	0.53	0.53	31	01/24/1958	12/05/1963	—
Matheny Well	1,039.12	1,037.54	1,039.12	—	—	—	1	04/12/1988	03/21/1997	—
MOV ET Well	1,123.26	1,122.76	1,124.04	0.37	0.11	2.43	46	05/08/1997	06/26/2001	—
Pioneer Road Seep Well	1,112.22	1,111.73	1,112.61	0.25	0.08	9.37	43	05/22/1997	06/26/2001	—
PM-1 (2356.408 m)	1,359.49	1,355.14	1,360.53	0.5	0.13	0.13	61	01/01/1969	06/06/2001	—
PM-2	1,442.76	1,439.27	1,447.37	0.13	0.04	0.04	54	01/01/1969	09/24/2001	—
PM-3 (Upper Borehole)	1,330.42	1,331.00	1,331.61	—	—	—	1	09/09/1988	09/13/1988	—
PM-3 (Lower Borehole)	1,330.35	1,329.57	1,331.00	0.41	0.18	0.18	21	09/21/88	09/30/91	—
PM-3-1 (Piez 1)	1,330.58	1,329.72	1,330.58	—	—	—	1	04/10/1992	06/05/2001	—
PM-3-2 (Piez 2)	1,331.18	1,330.42	1,331.18	—	—	—	1	04/10/1992	06/05/2001	—
Springdale ET Deep Well	1,131.67	1,131.18	1,132.12	0.28	0.07	2.39	60	06/20/1996	06/26/2001	—
Springdale ET Shallow Well	1,131.13	1,130.56	1,131.50	0.36	0.10	2.42	57	08/14/1996	06/26/2001	—

Table F.1-1
Summary of Hydraulic Heads at Selected Sites within the
Pahute Mesa/Oasis Valley Area and Vicinity
 (Page 4 of 11)

Site Name	Mean Hydraulic Head (m amsl) ^a	Minimum Hydraulic Head (m amsl) ^b	Maximum Hydraulic Head (m amsl) ^b	Standard Deviation ^c	Variance on the Mean ^d	Total Uncertainty ^e	Data Points Used	First Measurement ^f	Last Measurement ^g	Comments ^h
Springdale Lower Well	1,129.70	1,128.33	1,130.82	0.81	0.21	9.50	58	06/20/1996	06/26/2001	—
Springdale Upper Well	1,143.29	1,143.13	1,143.45	0.09	0.02	2.35	60	06/06/1996	09/27/2001	—
Springdale Windmill Well	1,175.24	1,174.39	1,175.43	0.09	0.03	2.35	44	04/01/1941	09/25/2000	—
TW-1 (1125 m)	1,430.40	1,428.93	1,430.49	0.02	0.02	0.02	5	04/07/1980	07/26/2001	—
TW-1 (1127-1137 m)	1,271.57	—	—	—	—	—	1	06/09/1961	—	—
TW-1 (170 m)	1,751.17	—	—	—	—	—	1	09/30/1960	—	—
TW-1 (492 m)	1,749.67	1,749.61	1,749.67	—	—	—	1	11/10/1960	11/18/1960	—
TW-1 (560 m)	1,564.20	1,564.20	1,564.36	—	—	—	1	02/17/1961	02/21/1961	—
TW-1 (826 m)	1,437.07	1,437.07	1,437.16	—	—	—	1	08/14/1962	08/16/1962	—
TW-1 (839 m)	1,437.31	1,437.01	1,437.71	0.26	0.17	0.17	9	09/25/1963	10/17/1963	—
TW-1 (839-1279 m)	1,277.25	1,276.41	1,277.33	0.06	0.05	0.05	6	09/25/1963	12/05/1963	—
U-12s (451.1 m)	1,784.75	1,778.87	1,791.00	1.92	0.51	0.51	57	08/06/1966	07/25/2001	—
U-19ab	1,494.97	1,494.74	1,495.35	0.29	0.29	0.29	4	07/17/1980	06/30/1985	—
U-19ab 2	1,497.89	1,497.48	1,498.11	0.36	0.42	0.42	3	12/03/1984	12/12/1984	—
U-19ad	1,372.21	—	—	—	—	—	1	06/16/1979	—	—
U-19ae	1,369.77	1,369.47	1,370.08	0.43	0.61	0.61	2	01/24/1982	02/23/1982	—
U-19ai	1,428.99	1,428.29	1,429.82	0.46	0.29	0.29	10	06/30/1980	10/11/1980	—
U-19aj	1,432.38	—	—	—	—	0.58	1	02/23/1981	—	—

Table F.1-1
Summary of Hydraulic Heads at Selected Sites within the
Pahute Mesa/Oasis Valley Area and Vicinity
 (Page 5 of 11)

Site Name	Mean Hydraulic Head (m amsl) ^a	Minimum Hydraulic Head (m amsl) ^b	Maximum Hydraulic Head (m amsl) ^b	Standard Deviation ^c	Variance on the Mean ^d	Total Uncertainty ^e	Data Points Used	First Measurement ^f	Last Measurement ^g	Comments ^h
U-19aq	1,428.95	1,428.45	1,429.36	0.47	0.54	0.54	3	01/10/1987	06/17/1987	—
U-19ar	1,398.93	1,398.12	1,399.64	0.77	0.89	—	3	11/05/1985	03/28/1986	—
U-19aS (857 m)	1,392.69	—	—	—	—	—	1	07/27/1964	—	—
U-19au	1,358.57	1,358.28	1,360.02	0.14	0.09	0.09	9	06/05/1987	06/30/1988	—
U-19au 1	1,358.78	1,358.62	1,359.10	0.28	0.32	0.35	3	02/22/1988	03/02/1988	—
U-19ay	1,396.93	1,396.87	1,399.15	0.05	0.06	0.06	3	12/22/1987	01/09/1989	—
U-19az	1,424.58	1,417.08	1,425.06	0.18	0.07	0.07	26	12/16/1988	07/02/1990	—
U-19ba	1,488.78	1,484.44	1,488.89	0.05	0.03	0.03	10	09/15/1989	12/11/1990	—
U-19bg 1	1,394.52	1,394.34	1,394.70	0.14	0.13	0.13	5	08/20/1991	11/18/1991	—
U-19bh	1,425.93	1,410.52	1,426.06	0.08	0.06	0.06	7	06/24/1991	06/12/2001	—
U-19bj	1,493.23	1,493.23	1,495.90	—	—	—	1	09/24/1992	06/12/2001	—
U-19bk	1,427.93	1,427.67	1,428.14	0.14	0.06	0.06	24	09/24/1992	06/11/2001	—
U-19d 2	1,427.59	1,417.59	1,428.45	—	—	—	1	06/23/1964	01/13/1965	—
U-19e	1,432.87	1,425.46	1,432.87	—	—	—	1	09/06/1966	01/01/1969	—
U-19g	1,424.23	1,422.81	1,425.25	0.98	0.80	0.80	6	09/27/1965	01/04/1976	—
U-19x	1,392.02	—	—	0	0	—	2	08/21/1976	06/30/1978	—
U-20 WW (Open)	1,351.54	1,351.48	1,351.61	0.09	0.13	0.13	2	07/01/1982	07/16/1985	—
U-20a	1,328.66	1,328.66	1,328.93	—	—	—	1	02/13/1964	01/01/1969	—

Table F.1-1
Summary of Hydraulic Heads at Selected Sites within the
Pahute Mesa/Oasis Valley Area and Vicinity
 (Page 6 of 11)

Site Name	Mean Hydraulic Head (m amsl) ^a	Minimum Hydraulic Head (m amsl) ^b	Maximum Hydraulic Head (m amsl) ^b	Standard Deviation ^c	Variance on the Mean ^d	Total Uncertainty ^e	Data Points Used	First Measurement ^f	Last Measurement ^g	Comments ^h
U-20a 2 WW	1,343.25	1,342.95	1,345.39	—	—	—	1	03/30/1964	10/23/1975	—
U-20ah	1,354.02	1,352.40	1,355.75	1.02	0.59	0.59	12	12/15/1980	04/01/1981	—
U-20ai	1,356.20	1,355.14	1,357.27	0.67	0.51	0.51	7	09/26/1981	10/30/1985	—
U-20ak	1,278.46	1,277.72	1,279.25	0.54	0.41	0.41	7	07/11/1982	11/30/1985	—
U-20am	1,356.97	1,356.67	1,357.27	0.43	0.61	0.61	2	10/13/1983	02/01/1984	—
U-20an	1,363.10	1,362.88	1,363.37	0.25	0.29	0.29	3	10/10/1984	03/12/1985	—
U-20ao	1,317.29	—	—	—	—	—	1	05/17/1985	—	—
U-20ar 1	1,364.42	1,363.50	1,366.17	0.49	0.35	0.37	8	02/09/1987	05/08/1987	—
U-20as	1,284.43	1,284.41	1,284.70	0.03	0.03	0.03	4	04/22/1986	06/06/1986	—
U-20at 1	1,284.41	1,284.03	1,284.64	0.29	0.29	0.29	4	12/09/1986	02/13/1987	—
U-20av	1,338.00	1,336.20	1,338.38	0.53	0.75	0.77	2	08/04/1986	12/08/1986	—
U-20aw	1,371.43	1,371.30	1,371.60	0.1	0.06	0.06	10	12/10/1986	11/04/1988	—
U-20ax	1,329.93	1,328.87	1,367.12	0.24	0.08	0.08	37	08/31/1987	05/26/1993	—
U-20ay	1,360.98	1,357.82	1,363.89	0.06	0.04	0.04	9	06/22/1987	01/11/1988	—
U-20az	1,345.05	1,334.48	1,345.05	—	—	—	1	12/12/1988	08/31/1989	+1 to 5 m
U-20bb (579.12 m)	1,367.70	1,341.03	1,367.70	—	—	—	1	07/15/1988	12/18/1989	+10 to 20 m
U-20bb (676.66 m)	1,272.94	1,272.94	1,298.11	—	—	—	1	02/13/1990	04/19/1990	-1 to 5 m
U-20bb 1	1,280.00	1,279.71	1,280.23	0.16	0.08	2.40	17	05/15/1990	07/09/1990	—

Table F.1-1
Summary of Hydraulic Heads at Selected Sites within the
Pahute Mesa/Oasis Valley Area and Vicinity
 (Page 7 of 11)

Site Name	Mean Hydraulic Head (m amsl) ^a	Minimum Hydraulic Head (m amsl) ^b	Maximum Hydraulic Head (m amsl) ^b	Standard Deviation ^c	Variance on the Mean ^d	Total Uncertainty ^e	Data Points Used	First Measurement ^f	Last Measurement ^g	Comments ^h
U-20bc	1,303.07	1,299.70	1,303.87	0.13	0.05	0.05	23	07/07/1988	08/02/1989	—
U-20bd (689.15 m)	1,355.79	1,355.72	1,355.87	0.05	0.04	0.04	7	04/28/1989	05/16/1989	—
U-20bd 1	1,355.50	1,355.35	1,355.68	0.14	0.13	0.13	5	01/09/1990	03/14/1990	—
U-20bd 2	1,355.86	1,355.58	1,356.21	0.24	0.21	0.24	5	01/09/1990	03/14/1990	—
U-20be	1,303.78	1,303.48	1,319.39	0.2	0.10	0.10	15	06/14/1989	06/05/1991	—
U-20bf	1,338.18	1,332.77	1,353.98	0.43	0.15	0.15	31	08/28/1989	01/30/1991	—
U-20bg	1,352.49	1,350.07	1,352.98	—	—	—	1	01/08/1991	09/25/2001	+5 m
U-20c	1,275.28	1,273.15	1,275.28	—	—	—	1	02/25/1965	11/13/2000	—
U-20e	1,360.32	—	—	—	—	—	1	02/07/1969	—	—
U-20g	1,357.27	—	—	—	—	—	1	10/30/1964	—	—
U-20i	1,361.24	—	—	—	—	—	1	08/30/1967	—	—
U-20m	1,412.14	—	—	—	—	—	1	10/04/1968	—	—
U-20n PS 1DD-H (922 m)	1,350.32	1,345.84	1,350.32	—	—	—	1	05/17/1985	07/09/1998	—
U-20y	1,276.94	1,275.28	1,278.03	0.76	0.51	0.51	9	12/18/1974	02/18/1975	—
UE-12n 15a	1,841.00	1,840.44	1,841.97	0.64	0.57	0.57	5	05/31/1988	06/20/1988	—
UE-18r	1,271.89	1,269.74	1,272.34	0.61	0.21	0.21	35	01/29/1968	06/06/2001	—
UE-18t	1,306.27	1,305.73	1,307.35	0.22	0.07	0.09	43	10/06/1978	06/06/2001	—
UE-19b 1 WW	1,427.93	1,427.90	1,427.96	0.04	0.06	0.08	2	06/19/1964	01/13/1965	—

Table F.1-1
Summary of Hydraulic Heads at Selected Sites within the
Pahute Mesa/Oasis Valley Area and Vicinity
 (Page 8 of 11)

Site Name	Mean Hydraulic Head (m amsl) ^a	Minimum Hydraulic Head (m amsl) ^b	Maximum Hydraulic Head (m amsl) ^b	Standard Deviation ^c	Variance on the Mean ^d	Total Uncertainty ^e	Data Points Used	First Measurement ^f	Last Measurement ^g	Comments ^h
UE-19c WW	1,430.50	1,428.32	1,438.38	0.47	0.18	0.18	26	04/30/1964	06/12/2001	—
UE-19e WW	1,432.03	1,429.70	1,433.02	1.56	1.56	1.56	4	09/03/1964	06/26/1975	—
UE-19fs	1,350.02	1,349.11	1,351.24	—	—	—	1	08/17/1965	—	—
UE-19gS	1,424.76	1,423.11	1,425.25	—	—	—	1	05/06/1965	—	—
UE-19gS WW	1,425.24	1,413.05	1,428.60	0	0	0.02	3	03/24/1965	01/13/1976	—
UE-19h	1,423.14	1,422.84	1,472.70	0.11	0.04	0.04	35	08/09/1965	06/11/2001	—
UE-19i	1,396.26	1,396.26	1,408.45	—	—	—	1	09/01/1965	01/01/1969	—
UE-19z	1,429.66	1,429.21	1,429.82	0.26	0.21	—	6	07/12/1977	09/24/1977	—
UE-20ab	1,357.88	1,355.75	1,357.88	—	—	—	1	06/02/1978	10/30/1978	—
UE-20av	1,319.66	1,319.32	1,319.66	—	—	—	1	12/15/1986	01/15/1987	—
UE-20bh 1	1,348.55	1,347.63	1,349.47	0.54	0.20	0.20	30	10/29/1991	09/25/2001	—
UE-20c	1,267.05	—	—	—	—	—	1	02/28/1964	11/13/2000	—
UE-20d	1,273.90	1,272.54	1,292.35	0.67	0.95	0.97	2	08/19/1964	01/14/1965	—
UE-20e 1	1,365.47	1,359.49	1,365.50	—	—	—	1	06/04/1964	04/05/1975	—
UE-20f (1384.7 m)	1,268.62	1,268.58	1,268.67	0.06	0.08	0.09	2	04/07/1964	11/13/2000	—
UE-20f (4171 m)	1,322.86	1,269.19	1,337.55	1.22	1.41	1.41	3	01/13/1965	11/24/1974	—
UE-20h WW	1,356.48	1,353.50	1,356.97	0.69	0.98	0.98	2	08/20/1964	01/01/1969	—
UE-20j WW	1,411.96	—	—	—	—	—	1	10/23/1964	—	—

Table F.1-1
Summary of Hydraulic Heads at Selected Sites within the
Pahute Mesa/Oasis Valley Area and Vicinity
 (Page 9 of 11)

Site Name	Mean Hydraulic Head (m amsl) ^a	Minimum Hydraulic Head (m amsl) ^b	Maximum Hydraulic Head (m amsl) ^b	Standard Deviation ^c	Variance on the Mean ^d	Total Uncertainty ^e	Data Points Used	First Measurement ^f	Last Measurement ^g	Comments ^h
UE-20n 1 (1005.84 m)	1,318.78	—	—	—	—	—	1	06/01/1987	—	—
UE-20n 1 (863.8 m)	1,349.75	1,346.16	1,349.75	0	0	—	2	06/12/1987	10/16/2000	—
UE-20p	1,423.11	1,412.29	1,423.11	—	—	—	1	10/01/1968	09/27/1970	—
UE-29a 1 HTH	1,189.97	1,188.12	1,194.45	1.42	0.19	0.19	219	06/21/1982	09/26/1997	—
UE-29a 2 HTH	1,187.62	1,186.24	1,191.31	1.1	0.15	0.15	219	06/21/1982	09/26/1997	—
USW UZ-N91	1,186.72	1,185.59	1,191.34	1.1	0.15	0.17	217	01/21/1986	09/26/1997	—
Ute Spr Drainage Well	1,066.02	1,065.00	1,066.82	0.63	0.19	9.48	43	05/22/1997	06/26/2001	—
WW-8	1,410.46	1,404.21	1,410.46	—	—	—	1	01/03/1963	09/13/2000	—
Spring	1,171.96	—	—	—	—	2.32	1	—	—	—
Crystal Springs Area	1,188.72	—	—	—	—	9.29	1	—	—	—
Revert Springs Channel	1,018.03	—	—	—	—	9.29	1	—	—	—
Revert Springs Area	1,027.18	—	—	—	—	14.52	1	—	—	—
Revert Springs Area	1,027.18	—	—	—	—	æ	1	—	—	—
Spring (Report R10)	1,127.76	—	—	—	—	9.29	1	—	—	—
Spring	1,057.66	—	—	—	—	9.29	1	—	—	—
Springdale Culvert	1,126.24	—	—	—	—	2.32	1	—	—	—
Torrance Spring	1,121.66	—	—	—	—	2.32	1	—	—	—
Ute Springs Area	1,083.56	—	—	—	—	0.58	1	—	—	—

Table F.1-1
Summary of Hydraulic Heads at Selected Sites within the
Pahute Mesa/Oasis Valley Area and Vicinity
 (Page 10 of 11)

Site Name	Mean Hydraulic Head (m amsl) ^a	Minimum Hydraulic Head (m amsl) ^b	Maximum Hydraulic Head (m amsl) ^b	Standard Deviation ^c	Variance on the Mean ^d	Total Uncertainty ^e	Data Points Used	First Measurement ^f	Last Measurement ^f	Comments ⁱ
Spring	1,097.28	—	—	—	—	—	1	—	—	—
OVU Culvert Spring	1,149.10	—	—	—	—	2.32	1	—	—	—
Hot Springs Area	1,097.28	—	—	—	—	9.29	1	—	—	—
Hot Springs Pump House	1,094.23	—	—	—	—	9.29	1	—	—	—
Hot Springs Bath House 1	1,094.23	—	—	—	—	9.29	1	—	—	—
Hot Springs Bath House 2	1,094.23	—	—	—	—	9.29	1	—	—	—
Hot Springs blw Culvert 1	1,094.23	—	—	—	—	9.29	1	—	—	—
Hot Springs Culvert 2	1,092.71	—	—	—	—	9.29	1	—	—	—
Hot Springs abv Culvert 2	1,092.71	—	—	—	—	9.29	1	—	—	—
Ute Springs Area	1,085.09	—	—	—	—	14.52	1	—	—	—
Spring	1,097.28	—	—	—	—	—	1	—	—	—
Ute Springs Culvert	1,051.56	—	—	—	—	9.29	1	—	—	—
Ute Springs	1,085.09	—	—	—	—	14.52	1	—	—	—
Oleo Road Spring	1,167.38	—	—	—	—	2.32	1	—	—	—
Goss Springs - North	1,139.34	—	—	—	—	9.29	1	—	—	—
Goss Springs	1,139.34	—	—	—	—	9.29	1	—	—	—
Spring id 179	1,139.35	—	—	—	—	—	—	—	—	—
Spring	1,158.24	—	—	—	—	—	1	—	—	—

Table F.1-1
Summary of Hydraulic Heads at Selected Sites within the
Pahute Mesa/Oasis Valley Area and Vicinity
 (Page 11 of 11)

Site Name	Mean Hydraulic Head (m amsl) ^a	Minimum Hydraulic Head (m amsl) ^b	Maximum Hydraulic Head (m amsl) ^b	Standard Deviation ^c	Variance on the Mean ^d	Total Uncertainty ^e	Data Points Used	First Measurement ^f	Last Measurement ^f	Comments ^f
Spring	1,211.58	—	—	—	—	2.32	1	—	—	—

Source: SNJV, 2004

^aMeters above mean sea level

^bApplies to all data available

^cApplies only to data used

^d $(2 \times \text{Standard Deviation}) / \text{Square Root (Number of Data Points Used)}$

^eTotal uncertainty is the variance on the mean plus variance associated with the land surface elevation

^fShows sites that should be used with caution with a positive or negative error associated with the hydraulic head

— Not Applicable or Not Available

F.2.0 REFERENCES

Stoller-Navarro Joint Venture. 2004. *Hydrologic Data for the Groundwater Flow and Contaminant Transport Model of Corrective Action Units 101 and 102: Central and Western Pahute Mesa, Nye County, Nevada*. Las Vegas, NV.

DISTRIBUTION

Tim Murphy 2 HC/2CD
State of Nevada
Division of Environmental Protection
1771 E. Flamingo Road, Suite 121A
Las Vegas, NV 89119

Bill R. Wilborn 2 HC/2CD
Environmental Restoration Project
U.S. Department of Energy
National Nuclear Security Administration
Nevada Site Office
P.O. Box 98518, MS/505
Las Vegas, NV 89193-8518

Alicia Tauber 1 CD
Environmental Management Records
U.S. Department of Energy
National Nuclear Security Administration
Nevada Site Office
P.O. Box 98518, MS/505
Las Vegas, NV 89193-8518

U.S. Department of Energy 1 HC
National Nuclear Security Administration
Nevada Site Office
Technical Library
P.O. Box 98518, M/S 505
Las Vegas, NV 89193-8518

U.S. Department of Energy 1 CD
Office of Scientific and Technical Information
P.O. Box 62
Oak Ridge, TN 37831-0062

Southern Nevada Public Reading Facility 1 HC
c/o Nuclear Testing Archive
P.O. Box 98521, M/S 400
Las Vegas, NV 89193-8521

Manager, Northern Nevada FFACO 1 HC
Public Reading Facility
c/o Nevada State Library & Archives
100 N Stewart Street
Carson City, NV 89701-4285

Edward M. Kwicklis 1 CD
Los Alamos National Laboratory
Hydrology, Geochemistry, and Geology Group, EES-6
Earth and Environmental Sciences Division
Bikini Atoll Rd., SM-30
Los Alamos, NM 87545

Andrew V. Wolfsberg 1 CD
Los Alamos National Laboratory
Hydrology, Geochemistry, and Geology Group, EES-6
Earth and Environmental Sciences Division
Bikini Atoll Rd., SM-30
Los Alamos, NM 87545

Naomi Becker 1 CD
Los Alamos National Laboratory, M/S F665
Bikini Atoll Rd., SM30
Los Alamos, NM 87545

Gayle Pawloski 1 CD
Lawrence Livermore National Laboratory
7000 East Avenue, L-221
Livermore, CA 94550-9234

Mavrik Zavarin 1 CD
Lawrence Livermore National Laboratory
7000 East Avenue, L-221
Livermore, CA 94550-9234

Bonnie Thompson 1 CD
USGS WRD
160 North Stephanie Street
Henderson, NV 89074

Chuck E. Russell 1 CD
Desert Research Institute
755 E. Flamingo
Las Vegas, NV 89119

Ken Ortego 1 CD
Bechtel Nevada
P.O. Box 98521, M/S NLV 082
Las Vegas, NV 89193-8521

John P. McCord 1 CD
Stoller-Navarro Joint Venture
7710 W. Cheyenne, Bldg. 3
Las Vegas, NV 89129

Greg Ruskauff 1 CD
Stoller-Navarro Joint Venture
7710 W. Cheyenne, Bldg. 3
Las Vegas, NV 89129

Stoller-Navarro Joint Venture 1 HC/1 CD
FFACO Support Office
7710 W. Cheyenne Ave., Bldg. 3
Las Vegas, NV 89129

Stoller-Navarro Joint Venture 1 HC/1 CD
Central Files
7710 W. Cheyenne, Bldg. 3
Las Vegas, NV 89129

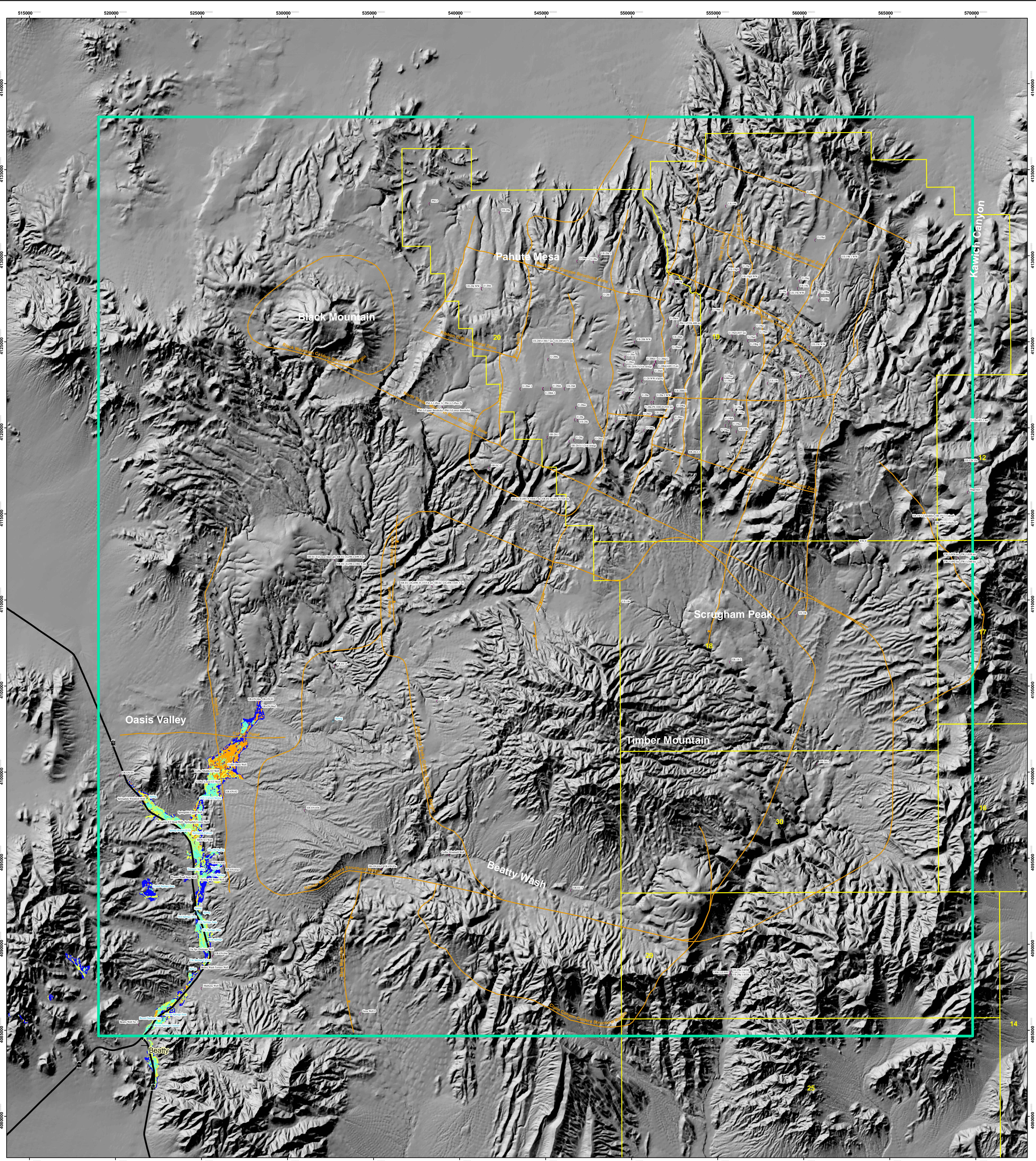
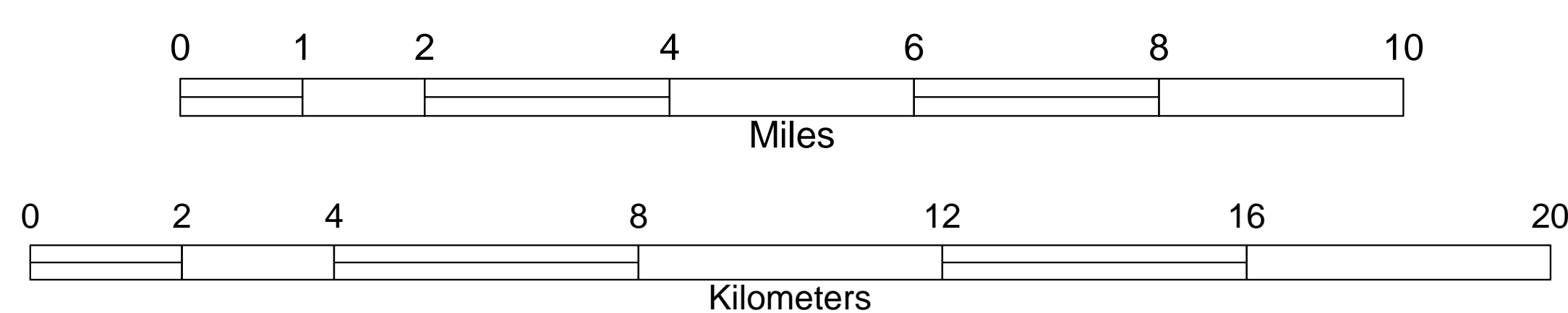


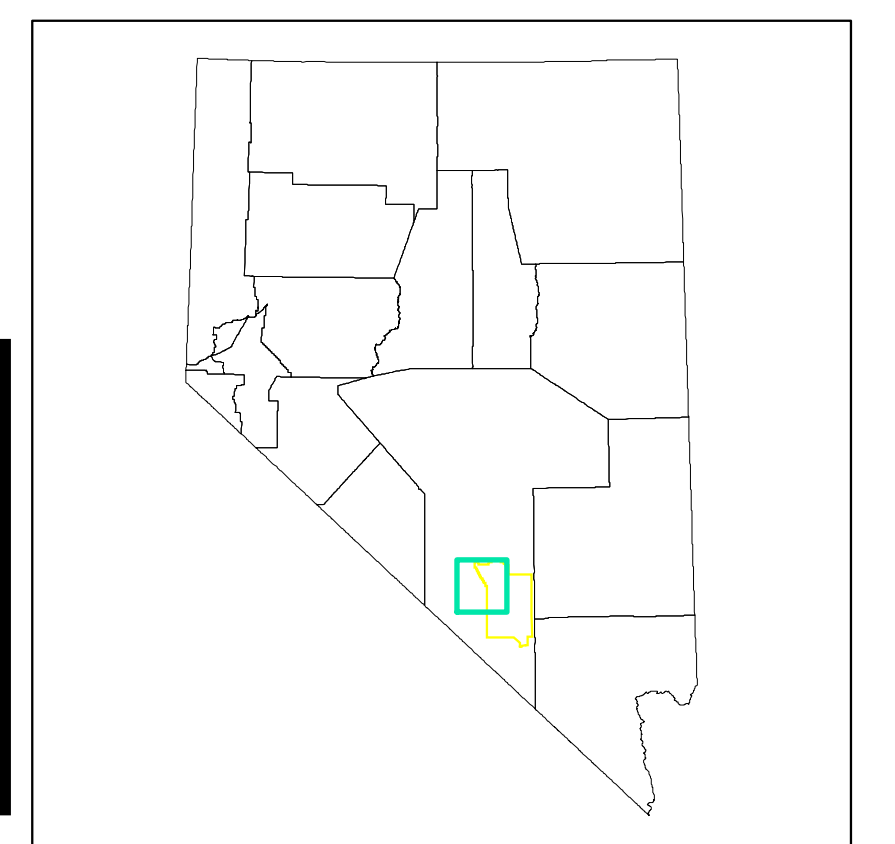
Plate 1 - Pahute Mesa Model Area Showing Topography, Selected Geographic Features, and Wells and Springs Used in Calibration of the Flow Model

EXPLANATION

- Calibration Data Points
- Spring
- Well
- City
- Pahute Mesa Model Area
- NTS Area Boundaries
- NTS Area Numbers
- Faults in Numerical Model
- Nevada Highways



Projection and Grid: Universal Transverse Mercator Zone 11, 1927 North American Datum Meters



9